SWAMI DAYANANDA COLLEGE OF ARTS & SCIENCE, MANJAKKUDI – 612 610

Name : **K.Sathish**

Subject : **Nuclear physics**

Department : **Physics**

Constituents and General Properties of Nuclei

The α-ray scattering experiments of Rutherford established the existence of the atomic *nucleus*. We shall in this chapter make a general review of the constitutents and general properties of nuclei. Like the atom, the nucleus may also exist in different *quantum states* based on energies and angular momenta. The state corresponding to the lowest energy is termed the *ground state* in which a nucleus normally exists. In surveying the general properties of the nuclei, we shall assume that they are in the ground states and properties in such states are usually known as *static characteristics* of the nuclei. The so-called *dynamic characteristics* are shown during nuclear reactions, nuclear excitations and nuclear decays. The important static properties are : nuclear charge, nuclear mass, size, shape, binding energy, angular momentum, magnetic moment, statistics, parity, isospin etc.

1.1 Constituents of nuclei

With the discovery of neutron by Chadwick in 1932, it was recognised that the atomic nuclei are composed of two different types of elementary particles – *protons* and *neutrons*. Collectively, the neutrons and protons are referred to as *nucleons*. The nucleons are fundamental particles in the same sense as electrons are. Any particular type of nucleus, a species of nucleus, is called a *nuclide*.

The proton is identified as the nucleus of the lightest and the commonest isotope of hydrogen, that is, a hydrogen atom from which the single orbital electron has been removed. It carries one electronic but positive charge, $+e$ and has a mass of about 1836 times the electronic mass, m_e : an electron is thus much much lighter than a proton.

The neutron, on the other hand, possesses no charge — electrically *neutral* — and hence the name. Its mass is almost equal to, but slightly more than, the mass of a proton. Compared to the mass of a proton or a neutron, the mass of an electron is thus negligibly small.

Scanned with CamScanner

The negatively charged electrons move around the nucleus and the orbits or *effects* of the electrons extend to about 10^{-10} m, the so-called *radius of the atom*. The *radius of a typical nucleus* however is about 10^{-14} m.

The atom is thus *electrically neutral* and has a *massive nucleus*. The distribution of mass in the atom is such that most of its space is *empty*. The clouds of extra-nuclear electrons again are arranged in layers or *shells*. The outermost or valence electrons dictate the chemical properties of the atom. The effect of the nucleus on chemical reactions is negligible.

According to Coulomb's law, the positively charged protons, closely spaced within the nucleus, should repel each other so strongly that they should fly apart. It is thus difficult to explain the ***stability of the nucleus*** unless one assumes that nucleons (protons and neutrons) are held together under the influence of a *very strong short range attractive force*. This force is different from the commonly known forces like gravitation or electromagnetic and is classified as *strong interactions*.

The number of protons in the nucleus determines the *atomic number* of the nuclide. It is also called the ***Z-value*** or the ***proton number***. The sum of the numbers of protons (Z) and neutrons (N) inside the nucleus, that is, the total number of nucleons in a nucleus, is known as its ***mass number*** A.

$$\therefore \quad \boxed{A = N + Z}$$

Obviously, the mass number A is an *integer* just as both N and Z are.

For a given Z, the ***neutron number*** N is therefore given by

$$N = A - Z$$

so that a change in neutron number causes a change in the nuclear masses.

A nucleus of an atom X of atomic number Z and a mass number A, that is, a nuclide is symbolically represented by ${}^{A}_{Z}\mathrm{X}$. For instance, ${}^{4}_{2}\mathrm{He}$ represents the nucleus of a helium atom of atomic number 2 and mass number 4 (an α-particle). The proton and neutron are symbolically writen as p and n. Since the chemical symbol itself gives uniquely the atomic number of the element, the subscript is often omitted and ${}^{A}_{Z}\mathrm{X}$ is simply written as ${}^{A}\mathrm{X}$. Thus ${}^{1}\mathrm{He}$, ${}^{7}\mathrm{Li}$, ${}^{12}\mathrm{C}$ are respectively the helium, lithium and carbon nuclei.

1.2 Isotopes, isobars, isotones and mirror nuclei

Isotopes : Nuclei with the ***same atomic number*** Z (i.e., same element), but ***different mass number*** A are called ***isotopes***. Thus, a given element of atomic number Z may have isotopes of different mass numbers. Their nuclei have the same number of protons but different number of neutrons. Thus ${}^{6}\mathrm{Li}$ and ${}^{7}\mathrm{Li}$ are two stable isotopes of lithium. The number of protons in the nucleus of each is 3 but their neutron numbers are $6 - 3 = 3$ and $7 - 3 = 4$ respectively.

Isotopes were first discovered in naturally radioactive elements. Thomson, while investigating positive rays by parabola method, found two stable isotopes of Neon — ${}^{20}\mathrm{Ne}$ and ${}^{22}\mathrm{Ne}$. Elements having stable isotopes contain in natural states a mixture of the isotopes in almost constant proportions — the so-called *relative abundances* (see Appendix 2). Hydrogen has two stable isotopes ${}^{1}\mathrm{H}$ and ${}^{2}\mathrm{H}$ of relative abundances 99.99% and 0.01% respectively. The isotope ${}^{2}\mathrm{H}$ is called ***heavy hydrogen*** or ***deuterium*** (${}^{2}\mathrm{D}$) and its nucleus ***deuteron***. Another isotope of hydrogen, which is unstable, ${}^{3}\mathrm{H}$ is called ***tritium*** and its nucleus ***triton***. Some elements like As, F, I and Au have a *single isotope* only. All the isotopes of an element have identical chemical properties but they slightly differ in physical properties.

Isobars : Nuclei with the ***same mass number*** A but ***different atomic number*** Z (i.e., different elements) are called ***isobars***. For instance, the two nuclides ${}^{15}_{8}\mathrm{O}$ and ${}^{15}_{7}\mathrm{N}$ are isobaric to each other. Both have the same mass number $A = 16$ but $Z = 8$ for ${}^{16}_{8}\mathrm{O}$ and $Z = 7$ for ${}^{16}_{7}\mathrm{N}$

Isotones : Nuclei with the ***same number of neutrons***, that is, having the same N (no matter what the Z-value is), are known as ***istones***. The nuclides ${}^{23}_{11}\mathrm{Na}$ and ${}^{24}_{12}\mathrm{Mg}$ are isotonic to each other, since both have $23 - 11 = 12$ or $24 - 12 = 12$ neutrons in the nucleus.

Mirror nuclei : The ***pairs of isobaric nuclei*** where the ***proton number*** Z and the ***neutron number*** N ***are interchanged*** and differ by ***one unit*** are known as ***mirror nuclei***. Examples are (${}^{11}_{6}\mathrm{C}$ and ${}^{11}_{5}\mathrm{B}$), (${}^{13}_{7}\mathrm{N}$ and ${}^{13}_{6}\mathrm{C}$), etc. Their mass number is $A = 2Z - 1$ where Z is the higher atomic number of the members of the pair, the other member of the pair has the atomic number $Z - 1$. The first member is usually β^+ active and changes into the second by β^+ transformation.

1.3 Nuclear mass and binding energy

The mass-spectroscopic measurements give *not* the masses of the nuclei but those of the atoms. The nuclear mass M_{nuc} is obtained from the *atomic mass* $M(A, Z)$ by subtracting the masses of Z orbital electrons.

$$\therefore \quad \boxed{M_{nuc} = M(A, Z) - Zm_e} \qquad (1.3.1)$$

The above expression however is *not exact* in that the binding energies of the electrons have not been taken into consideration. The error however is negligibly small.

The nuclei are very strongly bound and energies of $\sim$ few MeV are needed to break away a nucleon from the nucleus. In contrast, only a few eV is necessary to detach an orbital electron from an atom. So to break up a nucleus of Z protons and N neutrons completely into separate particles, a *minimum amount of energy* is to be supplied to the nucleus. This energy is called the ***binding energy***, E_B, of the nucleus. Conversely, to build, out of Z protons and N neutrons remaining at rest and separate from one

Scanned with CamScanner

another, a nucleus of mass number $A (= N + Z)$ and nuclear charge Z, an amount of energy equal to E_B will be evolved. But *what indeed is the source of this energy*?

According to special relativity, the energy equivalent E corresponding to a complete conversion of a mass m into energy is $E = mc^2$, where c is the velocity of light in free space. In forming a nucleus out of the constituent particles, a fraction of the total mass of the constituents disappears and the evolution of equivalent energy E_B occurs. If ΔM be the amount of *mass disappeared*, then the

$$\text{Binding energy, } E_B = \Delta M c^2 \tag{1.3.2}$$

If M_H, M_n be the masses of hydrogen atom and the neutron respectively,

$$\Delta M = ZM_H + NM_n - M(A, Z) \tag{1.3.3}$$

where $M(A, Z)$ is the mass of the atom of mass number A and atomic number Z.

$$\therefore \quad E_B = [ZM_H + NM_n - M(A, Z)]\, c^2$$
$$= [ZM_p + NM_n + Zm_e - M_{nuc} - Zm_e]\, c^2$$

$$\therefore \quad \boxed{E_B = [ZM_p + NM_n - M_{nuc}]\, c^2} \tag{1.3.4}$$

using (1.3.1), (1.3.2) and (1.3.3).

So, the mass-loss ΔM for the formation of nucleus is equal to the sum of the masses of Z protons, N-neutrons minus the nuclear mass of the atom.

In energy unit,

$$\Delta M = ZM_p + NM_n - M_{nuc}$$

dropping c^2 from the above equation (1.3.4).

The methods of determination of atomic masses have already been described in companion volume : *Physics of Atoms and Molecules* in Chapter : *Ions and Electrons*.

1.4 Unit of atomic mass

The unit of atomic mass is presently ***defined to be one-twelfth of the mass of the atom of carbon isotope*** ^{12}C ***taken to be exactly*** 12 ***units***, and is symbolised by **u**, the abbreviation for '*unified atomic mass unit*'. This comes to usage since 1961 by an international agreement. It is called 'unified' since prior to 1961 there was no unity among the physicists and the chemists in regard to atomic mass unit. While the physicists' unit was one-sixteenth of the mass of ^{16}O isotope (taken to be exactly 16 units), called the 'atomic mass unit' (amu), the chemists' atomic mass unit was one-sixteenth of the average atomic weight of the three isotopes of oxygen ^{16}O, ^{17}O and ^{18}O with relative abundances 99.76%, 0.04% and 0.20 % respectively. The conversion factor from one scale to the other is

$$1 \text{ u} : 1 \text{ amu} = 1.0003172 : 1$$

The unit of atomic mass in ^{12}C scale is therefore

$$1 \text{ u} = \frac{1}{12} \times \frac{12 \times 10^{-3}}{N_A} = \frac{10^{-3}}{6.02205 \times 10^{23}} \text{ kg}, \quad (N_A = \text{Avogadro number})$$
$$= 1.660566 \times 10^{-27} \text{ kg}$$

The **energy-equivalent of 1 u** is thus

$$1 \text{ u} = 1.660566 \times 10^{-27} \times c^2 = 1.660566 \times 10^{-27} \times 8.98755 \times 10^{16}$$
$$= 14.924419 \times 10^{-11} \text{ J} = \frac{14.924419 \times 10^{-11}}{1.60219 \times 10^{-13}} \text{ MeV}$$
$$= \mathbf{931.501 \text{ MeV}}$$

The energy-equivalents of the rest mass of **electron, proton** and **neutron** are respectively given as under :

Electron (m_e) = 9.10953×10^{-31} kg = 5.48580×10^{-4} u
Proton (m_p) = 1.677265×10^{-27} kg = 1.0072765 u
Neutron (m_n) = 1.67495×10^{-27} kg = 1.0086650 u

• Modern mass spectroscopes can measure atomic masses accurately up to one part in a million or still better. Such accuracies are of great *importance* in correctly determining the nuclear *binding energies* and nuclear *disintegration energies*. A simple calculation on the α-disintegration of a heavy element like Ra-226 would indicate that the disintegration energy is less than one part in 40,000 of the mass of the disintegrating nucleus. So, if the atomic masses are not measured more accurately than that order, correlation of the measured disintegration energy with the change in mass due to disintegration would be a far cry.

1.5 Binding energy and stability of nucleus

If $E_B > 0$, *i.e. positive, the nucleus is stable* and energy from outside is to be supplied to disrupt the nucleus into its constituents separately. If, however, $E_B < 0$, *i.e. negative, the nucleus is unstable* and will disintegrate of itself. The E_B*-value is a measure of the stability of the nucleus*. More the E_B, more is the *stability*.

As an example, let us compute the binding energy E_B for an α-particle, i.e. ^4_2He. The helium nucleus is made up of 2 protons and 2 neutrons.

$$\therefore \quad ZM_p = 2 \times 1.007276 = 2.014552 \text{ u}$$
$$NM_n = 2 \times 1.008665 = 2.017330 \text{ u}$$
$$\text{Total} = 4.031882 \text{ u}$$
$$\text{Atomic mass of } ^4_2He = 4.002603 \text{ u}$$
$$\text{Difference} = +0.029279 \text{ u}$$

Scanned with CamScanner

The plus sign indicates that the nucleus is *stable*. And since 1 u $\simeq$ 931 MeV, the binding energy in MeV is $E_B = 0.029279 \times 931 = 27.16$ MeV.

The **binding energy of He-nucleus is 27.16 MeV** and this explains why it is a **very stable** structure, coming out as it does as α-particle in radioactive decay.

Every nuclide has a fixed binding energy meaning that the same amount of energy would always be required to pull all the nucleons completely apart. This binding energy divided by the number of nucleons is called the (average) **binding energy per nucleon**, or **binding fraction**, $f_B = E_B/A$

1.6 Mass defect and packing fraction

Accurate determination of the atomic masses indicates that they are not exactly whole numbers, although the difference is small. For instance, the atomic mass of ^{12}C is exactly 12 u, but the masses of other atoms, although very close to, are not exactly whole numbers (integral). For instance,

$$^1H = 1.007825 \text{ u}; \quad ^2H = 2.014102 \text{ u}$$

$$^4He = 4.002603 \text{ u}; \quad ^{16}O = 15.994915 \text{ u}; \quad ^{226}Ra = 226.02543 \text{ u}$$

and so on and so forth.

Mass defect — The difference between the measured atomic mass $M(A, Z)$ in u, and the mass number A of a nuclide is called the **mass defect**, $\Delta M'$

$$\therefore \quad \boxed{\Delta M' = M(A, Z) - A}$$

The mass defect of $^4He = 4.002603 - 4 = +0.002603$ u and that of $^{16}O = 15.994915 - 16 = -0.005085$ u. The mass defect can therefore be both positive and negative. It is found that the mass defect is positive for *very light* and *very heavy* atoms, and it is negative for atoms in the *intermediate range*.

Packing fraction — Aston expressed the departure of atomic masses from their mass numbers in terms of *packing fraction* for each nuclide.

The **packing fraction** f is defined as the *mass defect per nucleon* in the nucleus, that is, the mass defect of an atom divided by its mass number. So,

$$f = \frac{\Delta M'}{A} = \frac{M(A, Z) - A}{A}$$

$$= \frac{M(A, Z)}{A} - 1$$

$$\text{or,} \quad \boxed{M(A, Z) = A(1 + f)} \qquad (1.6.1)$$

Note that the f has the same sign as the mass defect $\Delta M'$.

It is found that the packing fraction f varies with the mass number in a systematic fashion (*packing fraction curve*) as represented graphically in Fig. 1.1. It is observed that the packing fraction is positive for very light nuclei and as A increases, f decreases rapidly, becoming negative for $A > 20$. It attains a minimum value (negative) at $A \sim 60$, whence it starts increasing again but rather slowly. For $A \sim 180$, it becomes positive again.

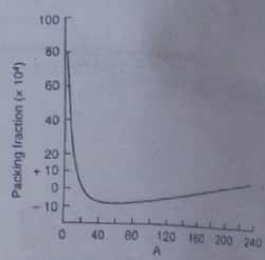

Fig. 1.1 Packing fraction curve

This variation of f with A can be explained from the consideration of nuclear binding energy. We have,

$$f_B = \frac{E_B}{A} = \frac{ZM_p + NM_n - M(A, Z)}{A} \qquad (1.6.2)$$

expressed in energy unit.

Computation of f_B's for different nuclides shows that they are highly variable. For instance, it is 1.112 MeV for deuteron, 7.07 MeV for α-particle (^4He) and 7.98 MeV for ^{16}O. These differences reflect the relative strengths of their binding. While ^2H is weakly bound, ^4He or ^{16}O are relatively more strongly bound.

1.7 Binding fraction *vs* mass number curve

The nature of variation of f_B with A, for different nuclei is represented graphically in Fig. 1.2 and is called the *binding fraction curve*.

A critical survey of the curve will readily bring out the following points of immense physical importance :

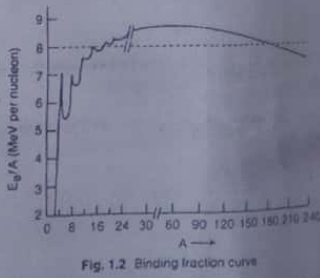

Fig. 1.2 Binding fraction curve

1. f_B is very small for very light nuclei and goes on increasing rapidly with increasing A and reaches a value $\sim$ **8 MeV** for the mass number $A \sim 20$. Thereafter, the rise of the curve is much slower, reaching a maximum value of 8.7 MeV for $A = 56$. If A is increased still further, the curve again decreases but slowly.

2. The variation in f_B is very slight in the range of mass number $20 < A < 180$ and in this region f_B may be considered to remain virtually constant having a mean value $\sim$ 8.5 MeV.

Scanned with CamScanner

3. For $A > 180$, that is, for heavy nuclei, the f_B-value decreases monotonically with increasing A and is ~ 7.5 MeV for heaviest nuclei.

4. A rapid fluctuation in f_B is noted for very light nuclei with some peaks in the curve in this region, corresponding to the even–even nuclei, such as ^{4}He, ^{8}Be, ^{12}C, ^{16}O etc. i.e. with mass number $A = 4n$, where $n = 1, 2, 3, 4 \cdots$ etc. Peaks in the curve are also seen at Z or N equal to 20, 28, 50, 82, 126. These are called **magic numbers** (to be discussed, in more details, in Chapter : *Nuclear models*).

The significance of these peaks is that the corresponding nuclei are more stable relative to those in their neighbourhood.

• The phenomena like the energy release in *nuclear fission* and *fusion* and also the reason for *α-decay of heavy nuclei* can be qualitatively explained by the binding fraction curve and we shall often refer to it later.

1.7.1 Complementarity of binding and packing fraction curves

It is easy to observe that the binding fraction curve (Fig. 1.2) is *complementary* to the packing fraction curve (Fig. 1.1) and it can be readily understood why it is so.

We have : $E_B = ZM_p + NM_n - M(A, Z)$

$= Z(1 + f_p) + N(1 + f_n) - A(1 + f)$, using (1.6.1)

$= (Z + N) + Zf_p + Nf_n - A - Af$

$= Zf_p + Nf_n - Af \quad (\because \ A = Z + N)$

$$\therefore \quad f_B = \frac{E_B}{A} = \frac{Zf_p + Nf_n}{A} - f \qquad (1.7.1)$$

Now, the first term on the right side of (1.7.1) is nearly constant, particularly for lower A-values when $Z \simeq N \simeq A/2$. Thus, f_B increases or decreases as f decreases or increases respectively. Thus, the curves representing the variation of f_B and f appear complementary in character. Where the (f-A) curve shows a minimum, the (f_B-A) curve shows a maximum. Further, for lower A, the region of negative slope in (f-A) curve corresponds to the region of positive slope in (f_B-A) curve; and for higher A, the region of positive slope in the first curve corresponds to the region of negative slope in the second.

1.8 Nuclear size

Nuclear radius : ***Experiments*** indicate that the majority of atomic nuclei are spherical, or nearly so, in shape. So, its volume is proportional to the total number of nucleons in it or its mass number A.

$$\therefore \quad \tfrac{4}{3}\pi R^3 \propto A$$

$$\text{or,} \quad R \propto A^{\frac{1}{3}}$$

$$\therefore \quad \boxed{R = r_0 A^{\frac{1}{3}}} \qquad (1.8.1)$$

where R is the radius of the nucleus and r_0, a constant, called ***nuclear radius parameter***. The value of r_0 ranges from $(1.1 - 1.5) \times 10^{-15}$ m, i.e. $(1.1 - 1.5)$ fm and can be evaluated by a number of different methods.

• The ***nuclear radius***, as discussed, is the *radius of nuclear mass distribution*. One may as well talk of the *radius of nuclear charge distribution*. Since nuclear charge parameter $Z \propto A$ i.e., is almost *linearly proportional* to the mass number, and the nuclear charge density ρ_e is nearly the same throughout the nuclear volume, the distribution of nuclear charge $+Ze$ follows the pattern of nuclear mass distribution. Hence *charge radius* $\simeq$ *mass radius*, of the nucleus.

• The size of the nucleus was first estimated from Rutherford's α-ray scattering using various atoms. The larger the angle of scattering of α-particle, closer is its approach to the nucleus. If the kinetic energy of α-particle be equal to the repulsive Coulomb energy between α-particle (of charge 2e, mass m and velocity v) and the nucleus (of charge Ze) it would come momentarily to rest such that the *distance of closest approach* R is given by

$$\frac{1}{2}mv^2 = \frac{2e \times Ze}{4\pi\varepsilon_0 R} \Rightarrow R = \frac{Ze^2}{\pi\varepsilon_0 mv^2}$$

Substituting for $m = 6.64 \times 10^{-27}$ kg, $e = 1.6 \times 10^{-19}$C and $v = 10^7$ m/s, the value of R for $Z = 20$ is $\sim 1.5 \times 10^{-14}$m.

The mean squared radius $\langle r^2 \rangle$ of *nuclear charge distribution* is given by

$$\langle r^2 \rangle = \frac{\int_0^R r^2 \cdot 4\pi r^2 \rho(r) dr}{\int_0^R 4\pi r^2 \rho(r) dr} = \frac{\int_0^R r^4 dr}{\int_0^R r^2 dr} = \frac{3}{5}R^2$$

for a uniformly charged sphere of radius R, ρ = constant and $\rho = 0$ for $r > R$

$$\therefore \quad \boxed{R^2 = \frac{5}{3}\langle r^2 \rangle} \qquad (1.8.2)$$

Estimation of nuclear radius — Of the different methods generally used to estimate the nuclear radius, we shall describe here only two of them : (i) the *mirror nuclei method* and (ii) the *muonic x-ray method*.

Mirror nuclei method — As already defined, the *mirror nuclei* are pairs of nuclei obtained from each other by the interchange of neutron with proton, e.g. ($^{13}_6$C, $^{13}_7$N). A mirror nucleus like $^{13}_7$N is unstable and is converted to $^{13}_6$C by positron (β^+) emission.

$$^{13}_7\text{N} \rightarrow {}^{13}_6\text{C} + \beta^+ + \nu$$

where ν is the *neutrino*, a neutral particle of negligible mass.

Scanned with CamScanner

If Z be the atomic number of the daughter nucleus, then it can be shown that the difference in Coulomb energies of mirror nucleus is

$$\frac{1}{4\pi\varepsilon_0}\left(\frac{6Ze^2}{5R}\right)$$

where R = the radius of the daughter nucleus.

The above energy is spent in providing (i) the rest mass energy $m_e c^2$ to produce positron, (ii) the kinetic energy E_{β^+} of the β^+ particle and (iii) the rest mass $(m_n - m_p)c^2$ required for conversion of a neutron of larger mass m_n into a proton of smaller mass m_p

$$\therefore \quad \frac{1}{4\pi\varepsilon_0}\left(\frac{6Ze^2}{5R}\right) = m_e c^2 + E_{\beta^+} + (m_n - m_p)c^2$$

whence R could be readily estimated.

The average value of R estimated by this method is $(1.23 \pm 0.03)A^{\frac{1}{3}} \times 10^{-15}$ m.

Muonic x-rays – The energies of x-rays emitted by muons are called *muonic x-rays*. When a beam of muons, whose mass is $207\,m_e$ and charge equal to e, is incident on nuclei like graphite, the muons move in Bohr's quantized orbits. Naturally, the orbit has a radius 207 times smaller and energy 207 times greater than that of an electron. Muonic x-rays are produced when such μ-mesons are excited and de-excited; the energies of such x-rays depend on the value of R, the nuclear radius and may be used to estimate the size of the nucleus.

The average value of R obtained by this method is $(1.20 \pm 0.03)A^{\frac{1}{3}} \times 10^{-15}$ m.

• The other important method for estimating R is the *electron scattering method* into which we are not entering here. We shall highlight some of the important conclusions arrived at by a comparison of these methods in respect of atomic nucleus. These are (i) the *distribution of density of protons* in the nucleus is *slightly different from that of all the nucleons* within the nucleus, (ii) the *nuclear charge distribution* is *not spherically symmetric* in some nuclei which possess electric quadrupole moment and (iii) the *charge radius* of a nucleus is not significantly less than the radius of nuclear matter consisting of all the nucleons.

Nuclear density — The *nuclear density*, ρ_N can be estimated from the relation

$$\rho_N = \frac{\text{nuclear mass}}{\text{nuclear volume}}$$

But the *nuclear mass* M_N is approximately equal to Am_N where A is the mass number and m_N the mass of the nucleon $\simeq 1.67 \times 10^{-27}$ kg

The **nuclear volume**, $V_N = \frac{4}{3}\pi R^3 = \frac{4}{3}\pi(r_0 A^{\frac{1}{3}})^3 = \frac{4}{3}\pi r_0^3 A$.

$$\therefore \quad \rho_N = \frac{Am_N}{\frac{4}{3}\pi r_0^3 A} = \frac{m_N}{\frac{4}{3}\pi r_0^3} = \frac{1.67 \times 10^{-27}}{\frac{4}{3}\pi(1.3 \times 10^{-15})^3} \qquad (1.8.3)$$

Using the relation (1.8.3) above, we have

$$\rho_N \simeq 1.816 \times 10^{17}\ \text{kg/m}^3,$$

an *unusually large number*. So the nuclear matter is in a highly compressed state and the *nuclear density is extremely high* being comparable to that of some stars like the white dwarfs

• Since the atomic radius = $10^4\times$ nuclear radius, the **atomic density**, $\rho_A \simeq 2 \times 10^{17}/(10^4)^3 \simeq 2 \times 10^5$ kg/m^3 which is *much smaller* compared to ρ_N. The density of water, $\rho_w = 10^3$ kg/m^3 which is much smaller compared to ρ_A.

• *As the density of nucleus is independent of A* (Eq. 1.8.3), *its value is almost the same for all nuclei.*

1.9 Nuclear spin

While studying Bohr's theory of atom, we observed that the corresponding atomic states of the isotopic nuclides do not possess the same energy. This is because the *reduced mass* of the electron depends on the nuclear mass. This *isotopic shift* apart, each atomic energy level with a given value of J shows a splitting even when a single isotope of an element or a mono-isotopic element is taken. This splitting, which is finer than the fine structure splitting, is referred to as *hyperfine structure* of the level. The hyperfine components are observed only when a high resolution interferometer is used. The spinning property of an electron, it might be recalled, was first proposed by Uhlenbeck and Goudsmit to explain the doublet structure of the alkali spectra. In a like fashion, Pauli suggested in 1924 that the hyperfine structure could be explained if we assume that the nucleus of the atom possesses an *angular momentum of spin* with an associated *magnetic moment*.

The methods employed to study the angular momentum of spin and the magnetic moment of nuclei are based on (i) the hyperfine structure of spectral lines, (ii) alternating intensities in homonuclear molecular spectra, (iii) microwave spectra, (iv) magnetic resonance and the deflection of atomic and molecular beams, (v) nuclear magnetic resonance (NMR) in bulk and (vi) optical detection of NMR.

The *spin of a nucleus is the resultant of the spins* of its constituent nucleons — *protons and neutrons*. It turns out that the spins of protons and neutrons can be represented, like that of an electron, by the same quantum number $\frac{1}{2}$. They have an *angular momentum* $\frac{1}{2}(h/2\pi)$ or $\frac{1}{2}h$ *due to spin*. The orientation of spin vector, according to wave mechanics, is such that the component of spin can have its axis either parallel or antiparallel to a specific direction with spin angular momentum $\frac{1}{2}(h/2\pi)$ or $-\frac{1}{2}(h/2\pi)$ respectively.

In addition to the spin angular momentum, the protons and neutrons in the nucleus have *orbital angular momentum* such that its magnitude in specific Z-direction is an integral multiple of $h/2\pi$. Thus the *intrinsic angular momentum* of a nucleus is a *vector*

Scanned with CamScanner

$\vec{I}$ such that

$$\vec{I} = \sum_n \vec{l}_n + \sum_s \vec{l}_s = \vec{L} + \vec{S}$$

where $\sum_s \vec{l}_s$ is the contribution of the spin and $\sum_n \vec{l}_n$ is the contribution of orbital angular momentum of all the nucleons inside the nucleus.

The magnitude of the total angular momentum vector $\vec{I}$ is given by

$$\vec{I} = \sqrt{I(I+1)}\,(h/2\pi)$$

where I is a quantum number that gives the maximum value of $\vec{I}$ along the specific Z-direction. I may be zero, half integral or an integral multiple of $h/2\pi$.

Now, the orbital angular momentum $\vec{L}$ is an integral multiple of $h/2\pi$. The spin angular momentum $\vec{S}$ is either a half-integral multiple or an integral multiple of $h/2\pi$, depending on whether the number of nucleons is odd or even. The nuclei in the ground state with *even* Z and *even* N nucleons have *zero* angular momentum *without exception*. So for *even A-type nuclei* having either *odd Z*, *odd N* or *even Z*, *even N* nucleons, the vector $\vec{I}$ will be zero or an integral multiple of $h/2\pi$. And for *odd A*-type *nuclei* having either *odd Z*, *even N* or *even Z*, *odd N* nucleons, $\vec{I}$ will be an odd half-integral multiple of $h/2\pi$.

$$\therefore \quad \vec{I} = \tfrac{1}{2}, \tfrac{3}{2}, \tfrac{5}{2}, \tfrac{7}{2}, \quad \cdots \quad \text{for odd } A\text{-type nuclei}$$

$$\text{and} \quad \vec{I} = 0, 1, 2, 3 \quad \cdots \quad \text{for even } A\text{-type nuclei.}$$

The *total angular momentum* $\vec{I}$ of a nucleus is loosely but usually called the *spin of the nucleus* or *nuclear spin*, but it is different from the spin angular quantum number. The total angular momentum of a nucleus can be computed from the multiplicity and relative spacings of spectral lines in an applied magnetic field. If a nucleus with total angular momentum $\vec{I}$ be placed in an externally applied magnetic field, the magnetic quantum number m_I have values ranging from $+I$ to $-I$ and thus split the energy levels into $2I+1$ sub-levels. The transitions between these sub-states may be used to estimate I from the multiplicity of spectral lines. We have already discussed earlier, in this section, the different methods used to determine $\vec{I}$.

• The symbol J is also sometimes used to represent the total angular momentum of a nucleus and the reader must remain careful.

The cartesian components of spin angular momentum vector $\vec{S}$ of a spin $\frac{1}{2}$-particle are expressed as

$$S_x = \tfrac{1}{2}\hbar\sigma_x, \quad S_y = \tfrac{1}{2}\hbar\sigma_y, \quad S_z = \tfrac{1}{2}\hbar\sigma_z \tag{1.9.1}$$

where σ_x, σ_y and σ_z, known as **Pauli matrices** are given as

$$\sigma_x = \begin{pmatrix} 0 & 1 \\ 1 & 0 \end{pmatrix}, \quad \sigma_y = \begin{pmatrix} 0 & -i \\ i & 0 \end{pmatrix}, \quad \sigma_z = \begin{pmatrix} 1 & 0 \\ 0 & -1 \end{pmatrix} \tag{1.9.2}$$

$$\sigma_x^2 = \sigma_y^2 = \sigma_z^2 = 1 \text{ (a } 2 \times 2 \text{ unit-matrix)}$$

From (1.9.1) and (1.9.2) we have

$$S_x^2 + S_y^2 + S_z^2 = \tfrac{3}{4}\hbar^2 \cdot 1 = S^2 \tag{1.9.3}$$

S^2 is an operator representing the square of the spin angular momentum of the particle.

The magnitude of the spin S is $\frac{\sqrt{3}}{2}\hbar$ and the projection of the spin along z-axis (say) is $\pm\frac{1}{2}\hbar$. In the above representation, $S_z = \frac{1}{2}\hbar\sigma_z$ has eigen values $\pm\frac{1}{2}\hbar$ corresponding to eigen-states $\alpha = \begin{pmatrix} 1 \\ 0 \end{pmatrix}$ and $\beta = \begin{pmatrix} 0 \\ 1 \end{pmatrix}$ respectively. Any general spin function (state) of the particle can be represented by

$$\chi = \phi_+\alpha + \phi_-\beta \tag{1.9.4}$$

where $|\phi_+|^2$ and $|\phi_-|^2$ are the probabilities that the particle in the state χ has its spin up ($\uparrow$) and down ($\downarrow$) respectively; ϕ_+ and ϕ_- satisfy the equation

$$|\phi_+|^2 + |\phi_-|^2 = 1 \tag{1.9.5}$$

α and β form the basis vectors of a two-dimensional vector space (called *spin space*), so that (1.9.4) can be written as

$$\chi = \begin{bmatrix} \phi_+ \\ \phi_- \end{bmatrix}$$

χ is called a **spinor**; α and β are known as Pauli's *fundamental spinors*.

1.10 Nuclear energy levels

Studies of inelastic scattering and nuclear reactions indicate that nuclei possess a discrete spectrum of excited states — the ***nuclear energy levels***. As suggested in Bohr's theory, here also, when the nucleus is in an excited state it may give up the energy and come back to the ground state by an emission of photon of energy exactly equal to the difference of the energies of the two states involved. This magnitude of energy however is such that the photon is a γ-radiation.

There are definite minimum energies needed to disrupt the nucleus into various components. For instance, the light nucleus ^{12}C may break up into

(i) $^{8}Be + {}^{4}He$ (ii) $^{11}B + {}^{1}H$

(iii) $^{11}C + {}^{1}n$ (iv) $^{10}B + {}^{2}H$ etc.

The minimum energy values for the above disruptions of ^{12}C nucleus are all above the ground state energy. It implies that the nucleus in the ground state is stable against these decays. But those excited states which are above the thresholds can break up in various ways indicating that the nucleus does not remain in an excited state indefinitely. The *life time of an excited state is finite* and may be short or long depending on such

Scanned with CamScanner

factors as the probability of decay, the number of possible decay modes, selection rules, etc. From the uncertainty relation $\Delta E \cdot \Delta t \sim \hbar$, it follows that if the *life time* is *finite*, the energy of the state cannot be *ideally sharp* but would show a *width* or *energy spread*, $\Delta E = \hbar/\Delta t$.

1.11 Nuclear magnetic moment : Nuclear magneton

The magnetic dipole moment associated with a spinning electron is given by 1 Bohr magneton, μ_B where

$$\mu_B = \frac{e\hbar}{2m_e} = \frac{eh}{4\pi m_e} \quad (\because \hbar = h/2\pi)$$

$$= 9.27 \times 10^{-24} \text{ J/Tesla}$$

In analogy, the magnetic dipole moment associated with nuclear spin is given by what is called a *nuclear magneton*, β_N.

$$\beta_N = \frac{e\hbar}{2m_p} = \frac{eh}{4\pi m_p} = 5.05 \times 10^{-27} \text{ J/Tesla}$$

where $m_p = 1836\, m_e$, is the mass of a proton.

The ratio of a nuclear magneton to a Bohr magneton

$$\frac{\beta_N}{\mu_B} = \frac{m_e}{m_p} = \frac{1}{1836}$$

The nuclear magneton is thus 1836 times smaller than the Bohr magneton and is also called *Rabi magneton*.

For all nuclei, the magnetic moment μ_I is given by

$$\mu_I = g\beta_N = g\frac{eh}{2m_p}$$

where g-factor (also called *gyromagnetic ratio*) varies from nucleus to nucleus.

For proton, $g = 2.792$ so that $\mu_{\text{proton}} = 2.7927\beta_N$

For neutron, $g = -1.913$ so that $\mu_{\text{neutron}} = -1.9131\beta_N$

• The magnetic moment of a proton is not 1 nuclear magneton; it has instead a moment $+2.7927\beta_N$. The positive sign indicates that the direction of the magnetic moment vector, $\vec{\mu}$, coincides with that of the angular momentum vector $\vec{I}$, as if there were circulation of positive charge.

• The neutron has no net electric charge. But it has also a magnetic moment equal to $-1.9131\beta_N$. The negative sign points out that the direction of angular momentum vector $\vec{I}$ is opposite to that of the magnetic moment vector $\vec{\mu}$.

Note 1. Nuclei possess magnetic dipole moments because of the magnetic moments of individual nucleons. In even-even nuclei, the resultant spin is zero and the magnetic moment is also zero. In case it is not zero, it is measured in terms of nuclear magneton.

Note 2. It is rather hard to understand how the neutral particle, neutron, can have a magnetic moment. It can be attributed to the *internal structure of neutron* which can be looked upon as *a combination of a proton and an electron*. These particles, spinning in different directions, have different values for magnetic moments which when vectorially added give a negative magnetic moment. Further, the fractional values of dipole moments of neutrons and protons show that they are *not simple in structure*.

Table 1.1 : *Magnetic dipole moment of some nuclides*

Nuclide	Spin	Magnetic dipole moment (in unit of β_N)
$^1_0$n	$\frac{1}{2}$	−1.9131
$^1_1$H	$\frac{1}{2}$	2.7927
$^2_1$H	1	0.8574
$^3_2$He	$\frac{1}{2}$	−2.1275
$^3_1$H	$\frac{1}{2}$	2.9789
$^4_2$He	0	0

The net magnetic moment $\vec{\mu}$ of a nucleus depends on the resultant total angular momentum of the nucleus, $\vec{I}$ and is given by

$$\vec{\mu} = g\beta_N\vec{I} = \gamma\vec{I}$$

where γ is the product of the gyromagnetic ratio g and the nuclear magneton β_N.

The values of nuclear magnetic moments can be estimated by nuclear magnetic resonance (NMR) spectrometers, microwave spectrometers, molecular beam magnetic deflection method etc.

1.11.1 Determination of nuclear magnetic moment Nuclear magnetic resonance (NMR)

The nuclear magnetic moment may be directly determined experimentally by the methods of *magnetic resonance* and *nuclear resonance absorption*.

Rabi's method — The first accurate measurement of nuclear magnetic moments by magnetic resonance was made by Rabi and co-workers. The method is known as *molecular beam magnetic resonance* and closely resembles the Stern-Gerlach experiment.

It consists essentially in allowing a beam of molecules from an oven (source) into the region of a *non-uniform* magnetic field of a magnet A. The beam follows a curved path, as shown in Fig. 1.3, and passes through the slit S_1. The magnet B produces however a *uniform* magnetic field and as such would exert a net zero deflecting force. But in the region of this uniform field, another magnetic field is created (dotted circle) at right angles to the previous field by a high-frequency (hf) electric current. Next, the magnet C produces a *non-uniform* field that bends back the molecular beam such

Scanned with CamScanner

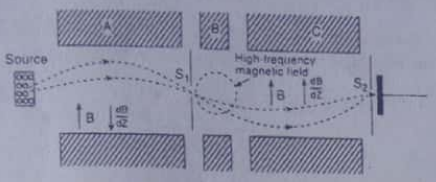

Fig. 1.3 Rabi's method of determining nuclear magnetic moment

that the beam passes through the slit S_2 and is detected by the *detector*. Note that the magnets A and C give ***non-uniform fields*** in the same direction but with opposite gradients $d\vec{B}/dZ$.

The molecules, on passing through the uniform field, are spatially quantized and precess like a spinning top about the field direction. As the frequency of electric current is varied and made equal to that of precession, energy would be absorbed and the molecules take up a different quantized space-orientation. The magnet C deflects them to pass through the slit S_2. The decrease in the number of molecules through S_2 can then be used to find the precessional frequency which depends on the magnetic moment and the intensity of the central uniform field. The method thus gives the value of the magnetic moment.

Nuclear resonance absorption — Purcell, Torrey and others developed another method of finding the magnetic moment. This method, known as *magnetic nuclear resonance absorption*, uses no molecular beam.

Here the solid or the liquid sample is placed in a uniform magnetic field and on it is superposed at right angles a hf-alternating field. Protons and other simple nuclei precessing round the direction of the uniform field will get their quantized angles of space-orientation abruptly changed by absorption of energy when the alternating field is tuned to resonance with the frequency of precession. This absorption can be detected and magnetic moments computed.

1.12 Parity of nuclei

Parity is purely a ***quantum mechanical concept*** having no classical analogue.

It was first proposed by Eugene Wigner and describes the kind of spatial symmetry of physical phenomena. A particle moving with a large velocity can be quantum mechanically associated with a wave and the wave motion can be described by a wave function $\psi(x, y, z)$ which depends on the space coordinates (x, y, z). Also, if ψ^* be the complex conjugate of ψ, $\psi^*\psi = |\psi|^2$ gives the *probability* of finding the particle at any given point. Parity is the property of such a wave function representing a quantum mechanical nuclear state, which may or may not change its sign on inversion of the space coordinates throughout from (x, y, z) to $(-x, -y, -z)$ i.e., on reflection of the coordinate system at the origin. The parity of a nucleus is thus related to the behaviour of nuclear wavefront as a result of reflection.

Definition : If the sign of the wave function ψ does not, as a whole, change with the change in sign of the space coordinates -- the so-called process of *reflection* of nuclear position *about the origin* of (x, y, z), system of axis -- the parity is said to be *even* or *positive*. If however the sign of spatial part of wave function changes with change in sign of space co-ordinates, the system is said to have *odd* or *negative* parity.

$$\boxed{\begin{aligned} \psi(-x,-y,-z) &= +\psi(x,y,z) \quad \text{even } (+) \text{ parity} \\ \psi(-x,-y,-z) &= -\psi(x,y,z) \quad \text{odd } (-) \text{ parity} \end{aligned}}$$

Parity, thus defined, depends on the quantum state of motion of the system and for a particle under a central force (i.e. hydrogen-like atoms), the parity P is determined by the orbital quantum number l : $P = (-1)^l$, so that for $l = 0$ or even, the parity is even and for l = odd, the parity is odd. In the case of a system of particles $P = (-1)^L$ where $L = \Sigma l$, the orbital angular momentum of the system.

Let us further investigate the consequence of this reflection of the coordinate system, called the **parity operation**, P. It is equivalent to changing from a right-handed frame of reference to a left-handed one.

Consider a system of n-particles so that

$$P\psi(\vec{r}_1, \vec{r}_2, \cdots, \vec{r}_n) = \psi(-\vec{r}_1, -\vec{r}_2, \cdots, -\vec{r}_n) \tag{1.12.1}$$

Assuming that the Hamiltonian H of the system remains invariant under inversion about the origin,

$$PH(\vec{r}_1, \vec{r}_2, \cdots) = H(\vec{r}_1, \vec{r}_2, \cdots) \tag{1.12.2}$$

But, Schrödinger's wave equation gives

$$H\psi(\vec{r}_1, \vec{r}_2, \cdots, \vec{r}_n) = E\psi(\vec{r}_1, \vec{r}_2, \cdots, \vec{r}_n) \tag{1.12.3}$$

$$\therefore \quad PH\psi(\vec{r}_1, \vec{r}_2, \cdots) = PE\psi(\vec{r}_1, \vec{r}_2, \cdots) = E\psi(-\vec{r}_1, -\vec{r}_2, \cdots) \tag{1.12.4}$$

using (1.12.1).

$$\therefore \quad H\psi(-\vec{r}_1, -\vec{r}_2, \cdots) = E\psi(-\vec{r}_1, -\vec{r}_2 \cdots) \tag{1.12.5}$$

by virtue of (1.12.4).

$\psi(-\vec{r}_1, -\vec{r}_2, \cdots)$ thus *satisfies the same differential equation as* $\psi(\vec{r}_1, \vec{r}_2, \cdots)$. Assuming *non-degeneracy*, the two solutions of Schrödinger's equation must be connected by a *phase factor* (constant), so that

$$\psi(-\vec{r}_1, -\vec{r}_2, \cdots) = k\psi(\vec{r}_1, \vec{r}_2, \cdots) \tag{1.12.6}$$

$$\therefore \quad P\psi(-\vec{r}_1, -\vec{r}_2, \cdots) = \psi(\vec{r}_1, \vec{r}_2, \cdots) = kP\psi(\vec{r}_1, \cdots \vec{r}_2, \cdots)$$

$$= k\psi(-\vec{r}_1, -\vec{r}_2, \cdots) = kk\psi(\vec{r}_1, \cdots \vec{r}_2, \cdots) \tag{1.12.7}$$

by virtue of (1.12.6).

$$\therefore \quad \boxed{k^2 = 1 \;\Rightarrow\; k = \pm 1} \tag{1.12.8}$$

Scanned with CamScanner

Thus, according to (1.12.6) and (1.12.8), *parity is a quantum number implying that all wave functions are either odd or even under space inversion or P-opertion.*

• Apart from *orbital parity*, elementary particles may also have what is called *intrinsic parity* referring to inversion of some internal axis of the particle. It is defined in a relative manner. The *nucleons* are taken to have *even parity*, purely *by convention*, and it is then fixed for other particles such that the total parity, defined as the product of orbital and intrinsic parity, is conserved in nuclear reactions involving strong and electromagnetic interactions between the particles.

It was believed, till 1956, that in all nuclear reactions, the parity was conserved. But in 1956, direct experimental evidence was obtained that ***parity is not conserved in nuclear phenomena involving weak interaction forces***. The non-conservation of parity was first suspected theoretically by Li and Yang and was subsequently confirmed experimentally by Wu in 1956.

The weak interaction in β-decay provides an example of non-conservation of parity. The conservation of parity leads to some important selection rules in nuclear, atomic and molecular processes and in the production and decay of elementary particles. Parity is thus an important *characteristic of a state* describing quantum mechanical systems.

• An interesting consequence of the fact that parity P is a good quantum number is that ***nuclei can have no permanent electric dipole moment.***

While we are familiar with the classical definition of electric dipole moment of a charge distribution, quantum mechanically it is defined as

$$\langle D \rangle = \int \sum_j e_j \vec{r}_j \; \psi^*(\vec{r}_1, \vec{r}_2, \cdots, \vec{r}_n)|^2 \, d\vec{r}_1 d\vec{r}_2 \cdots d\vec{r}_n \qquad (1.12.9)$$

If now we replace $\vec{r}_1$ by $-\vec{r}_1, \vec{r}_2$ by $-\vec{r}_2$, etc., the first factor $\vec{r}_j$ changes sign, but not $|\psi|^2$ because of parity.

$$\therefore \quad \boxed{\langle D \rangle = -\langle D \rangle \;\Rightarrow\; \langle D \rangle = 0}$$

We thus obtain the important result that ***the electric dipole moment of a nucleus in its ground state vanishes.*** This is also true for all *non-degenerate excited states* of the nucleus.

• Read also the Chapter : *Elementary Particles* in this very volume.

1.13 Electric multipole moments

If a localised charge distribution described by $\rho(\vec{r})$ be placed in an external potential $\phi(\vec{r})$, the electrostatic energy of the system is

$$W = \int \rho(\vec{r})\phi(\vec{r}) d^3r \qquad (1.13.1)$$

with origin $\vec{r} = 0$ as the centre of mass of the nucleus. Since $\rho(\vec{r})$ is confined to the small nuclear volume, $\phi(\vec{r})$ may be expanded in a Taylor series to get

$$\phi(\vec{r}) = \phi(0) + r\vec{\nabla}\phi(0) + \tfrac{1}{2}\sum\sum x_i x_j \frac{\partial^2\phi(0)}{\partial x_i \partial x_j} + \cdots \qquad (1.13.2)$$

$i, j = x_1, x_2, x_3$.

Now, the electric field $\vec{E} = -\vec{\nabla}\phi$. But since the field is source-free, $\vec{\nabla}\cdot\vec{E} = 0$.

$$\therefore \quad \vec{\nabla}\cdot\vec{E} = \vec{\nabla}\cdot(-\nabla\phi) = -\nabla^2\phi = -\frac{\partial^2\phi}{\partial x_i \partial x_j}\delta_{ij} = 0; \quad i, j \text{ being dummy indices.}$$

Subtracting $\frac{1}{6}r^2\frac{\partial^2\phi}{\partial x_i \partial x_j}\delta_{ij}$ from the third term of (1.13.2), we obtain

$$\phi(\vec{r}) = \phi(0) + r\vec{\nabla}\phi + \tfrac{1}{6}\sum_i\sum_j (3x_i x_j - r^2\delta_{ij})\frac{\partial^2\phi(0)}{\partial x_i \partial x_j} + \cdots$$

$$= \phi(0) - r\vec{E}(0) - \tfrac{1}{6}\sum_i\sum_j (3x_i x_j - r^2\delta_{ij})\frac{\partial E_j(0)}{\partial x_i} + \cdots \qquad (1.13.3)$$

Inserting (1.13.3) in (1.13.1), we obtain

$$W = q\phi(0) - pE(0) - \tfrac{1}{6}\sum Q_{ij}\frac{\partial E_j(0)}{\partial x_i} \qquad (1.13.4)$$

where $$q = \int \rho(\vec{r}) d^3r = \text{total charge of the nucleus} \qquad (1.13.5a)$$

$$p = \int \vec{r}\rho(\vec{r}) d^3r = \text{dipole moment of charge distribution} \qquad (1.13.5b)$$

$$Q_{ij} = \int (3x_i x_j - r^2\delta_{ij})\rho(\vec{r}) d^3r \qquad (1.13.5c)$$

$= (i\text{-}j)$ component of quadrupole moment tensor of the charge distribution inside the nucleus

$Q_{ij} = Q_{ji}$ implies that the tensor is *symmetric* and is of *rank* 2 in three dimensions.

It can be shown that

$$Q_{11} + Q_{22} + Q_{33} = 0 \qquad (1.13.6)$$

By a principal axis transformation, one obtains a diagonal representation of the tensor. As the tensor is, by (1.13.6), traceless it remains invariant under the above transformation. The number of independent components is *two*. For a nucleus in the shape of a spheroid (Fig. 1.4)-*a prolate* (the charge distribution stretched in the z-direction) or *an oblate* (the charge distribution is stretched perpendicular to z-direction), the axial symmetry gives

$$Q_{11} = Q_{22} \neq Q_{33} \;\Rightarrow\; Q_{33} = -2Q_{11} = -2Q_{22}$$

Scanned with CamScanner

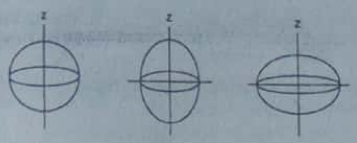

Fig. 1.4 Electric quadrupole moment (a) spherical charge distribution (Q = 0) (b) prolate spheroid (Q > 0), (c) oblate spheroid (Q < 0)

So, for such a system,

$$Q_{33} = \int \rho(\vec{r})(3z^2 - r^2)d^3\tau \qquad (1.13.7)$$

• 1. For a *prolate* spheroid,

$$\frac{x^2}{a^2} + \frac{y^2}{a^2} + \frac{z^2}{b^2} = 1 \quad (a > b)$$

Now, assuming a uniform charge density, we have

$$\rho(\vec{r}) = q/\tfrac{4}{3}\pi a^2 b$$

$$\text{and} \quad Q_{33} = \tfrac{2}{5}Z(a^2 - b^2)$$

where Z is the charge number of the nucleus.

• 2. For a *spherically symmetric* charge distribution,

$$Q_{11} = Q_{22} = Q_{33} = Q, \text{ say}$$

Then, by (1.13.6), $\quad Q_{11} = Q_{22} = Q_{33} = Q = 0$

Obviously, *the existence of quadrupole moment, Q implies deviation from the spherical symmetry.*

If R be the average nuclear radius and ΔR the deviation of R from the direction of symmetry axis, then

$$Q = \tfrac{6}{5}ZR^2(\Delta R/R)$$

Q is usually measured in unit, called **barn**, where 1 barn is given by

$$\boxed{\textbf{1 barn} = 10^{-28}\,\text{m}^2}$$

The magnitude of Q lies mostly in the range 10^{-28} to $10^{-30}\,\text{m}^2$ and depends on the radius and charge of the nucleus and the amount of its deviation from spherical symmetry. Quadrupole moment was first discovered in deuteron from the observations on the hyperfine structure of atomic spectral lines. For deuteron, $Q = +2.82$ milli-barn (mb) which shows that the charge distribution in ^{2}H nucleus has the shape of a prolate spheroid.

Q can also be estimated from the interaction of electric field gradient with the quadrupole moment of the nucleus from Mössbauer spectroscopy, microwave spectroscopy, paramagnetic resonance spectroscopy, nuclear quadrupole resonance spectroscopy and from optical hyperfine spectra.

While a nucleus like deuteron, ^{2}H, has the ratio $\Delta R/R = 4\%$, the value of this ratio may be as high as 25–30%. The largest positive and largest negative values of Q belong respectively to Lutecium nucleus, ^{176}Lu ($Z = 71$) and the Antimony nucleus, ^{123}Sb ($Z = 51$).

$$Q = +7 \times 10^{-28}\,\text{m}^2, \text{ for Lu}$$

$$\text{and} \quad Q = -1.2 \times 10^{-28}\,\text{m}^2, \text{ for Sb}$$

• The above discussion on quadrupole moment has been made from *classical considerations*. When however *quantum mechanics* is applied, it receives a *new definition*.

The charge distribution in a nucleus is treated *quantum mechanically* by defining quadrupole moment operator by

$$Q_{ij} = \sum_{p\,(\text{protons})} \left[3x_{p_i}x_{p_j} - \delta_{ij}r_p^2\right]$$

where x_p's are the coordinates of protons.

$$\therefore \quad \langle Q_{ij}\rangle = \int \sum_{\text{protons}} \left[3x_{p_i}x_{p_j} - \delta_{ij}r_p^2\right] |\phi(\vec{r})|^2 d^3\tau$$

$$= C\left\langle \left[\tfrac{3}{2}(J_iJ_j + J_jJ_i) - \delta_{ij}J^2\right]\right\rangle$$

where C is a constant and $\langle\ \rangle$ indicate any matrix element between $(2J+1)$-nuclear states of *angular momentum quantum number* J, labelled by J_z. Thus all the matrix elements of Q_{ij} are determined by a single quantity.

We usually take the expectation value of Q_{33} in the state with J_z equal to the maximum value of J, and define this as the ***nuclear electric quadrupole moment*** Q.

$$\therefore \quad Q = C\left[3J^2 - J(J+1)\right]_{-} = CJ(2J-1)$$

$$\Rightarrow \quad C = \frac{Q}{J(2J-1)}$$

Other matrix elements are determined in terms of Q; Q vanishes for $J = \frac{1}{2}$ or $J = 0$.

1.14 Statistics of nuclei

The statistical behaviour of nuclear particles such as protons, neutrons, electrons and other fundamental particles can only be described quantum mechanically as they are indistinguishable from each other. The wave function of a system of two identical particles, describing a particular property of the particle, can be either symmetric or

Scanned with CamScanner

antisymmetric by the interchange of spatial coordinates of the two particles. When the wave function does not change in sign by such an interchange, it is said to be symmetric. The corresponding quantum statistics is known as ***Bose-Einstein*** (B.E.) ***statistics***. If however the sign of the wave function changes by the interchange of coordinates, the wave function is said to be *antisymmetric* and the corresponding statistics is called ***Fermi-Dirac*** (F.D.) ***statistics***.

All fundamental particles or their assemblies obey either the B.E. statistics or the F.D. statistics. Those particles which have total angular momentum or spin equal to zero or an integral multiple of $h/2\pi$ follow the Bose-Einstein statistics and are called *bosons*. Such particles do not obey Pauli's exclusion principle so that any number of bosons can occupy the same quantum state. Particles such as photons, π-mesons, K-mesons, and all nuclei having even mass numbers such as ${}^{2}_{1}\mathrm{D}$, ${}^{4}_{2}\mathrm{He}$, ${}^{16}_{8}\mathrm{O}$, ··· and integral spin follow the Bose's statistics and are bosons.

Particles with an odd half integral spin $(\frac{1}{2}, \frac{3}{2}, \cdots)$, that is, having total angular momentum equal to an odd half integral multiple of $h/2\pi$ however follow the Fermi statistics and are called *fermions*. Fermions, unlike bosons, follow Pauli's exclusion principle so that no two identical particles can have all the quantum numbers the same barring them to occupy the same quantum state. Particles such as e^-, e^+, p, n, μ-meson and nuclei of odd mass number like ${}^{1}_{1}\mathrm{H}$, ${}^{7}_{3}\mathrm{Li}$, ${}^{19}_{9}\mathrm{F}$, ${}^{23}_{11}\mathrm{Na}$, ${}^{31}_{15}\mathrm{P}$, ${}^{35}_{17}\mathrm{Cl}$, ··· which possess half integral spin follow the Fermi-Dirac statistics and are fermions.

In nuclear reactions, the statistics of the particles is *conserved*. If F.D. statistics is represented by symbol -1 and B.E. by $+1$, the statistics of a group of particles is determined by the product of the symbols for each. For instance, let us take the case of annihilation of a positron and an electron. Before annihilation, the statistics of the system is $(-1) \times (-1) = +1$. After annihilation, the electron-positron pair gives rise to two photons which are bosons and they have the statistics $(+1) \times (+1) = +1$. So there is the conservation of statistics in nuclear phenomena.

1.15 Nuclear forces

According to Coulomb's law, the positively charged protons, closely spaced within the nucleus, should repel each other strongly and they should fly apart. It is therefore difficult to explain the stability of nucleus unless one assumes that nucleons are under the influence of some *very strong attractive type forces*. The forces inside the nucleus, binding neutron to neutrons, protons to protons and neutrons to protons, are classified as *strong interactions* and are represented as $n - n$, $p - p$ and $n - p$ forces respectively. These forces are essentially equal in magnitude as warranted by *experimental* evidence and were studied extensively over a long period by the Japanese scientist Hideki Yukawa. In 1935, he described the chief characteristics of ***nuclear forces*** and postulated a particle, a *pion* with a rest mass 270 m_e, that played an integral part in the explanation of nuclear forces. Yukawa was awarded Nobel Prize in physics in 1949 for his contributions to the understanding of nuclear forces.

According to Yukawa, the following are the ***characteristics*** of nuclear forces :

1. They are *short range* forces, i.e. effective only at short ranges.
2. They are *charge-independent*, i.e. they do not seem to depend on the charge of the particle.
3. They are the *strongest* known forces in nature.
4. They get readily *saturated* by the surrounding nucleons, and
5. They are *spin-dependent*.

We shall now discuss the above characteristics of nuclear forces in somewhat more details.

Short range — The results of scattering experiments : pp scattering, np scattering etc. show that nuclear forces operate over extremely short distances inside the nucleus. Between two nucleons, the distance is of the order of 1 *Fermi* (1F=10^{-15} m) or less. They are *not* like the inverse square law forces such as Coulomb force between electric charges. If a nucleus is bombarded with protons and if the range of nuclear force be of the same order of magnitude as Coulomb repulsion, they would be affected by both type of forces. But the scattering of protons will be different from the one corresponding to a pure Coulomb scattering.

The protons that pass not too close to the nucleus are scattered by electric repulsive forces. But if the energy of the incident protons be large enough to overcome Coulomb repulsion, they may pass very close to nucleus, within a distance r_0 from the centre of the nucleus, and fall in the range of attractive nuclear forces. They would then be captured and fall, as it were, into the *potential well* of the nucleus. The scattering of protons in this case is mainly due to strong and attractive nuclear forces and the distribution is distinctly different from Coulomb scattering.

There is however some evidence to suggest that at extremely short distances (0.5 F), the *attractive force turns into a repulsion* so that in a stable nucleus, the nucleons do not get too close together.

Charge independence — *Experimental* evidence indicates that the interaction between any two nucleons is ***independent of the charge***. Also the interactions among the nuclear forces between $n - n$, $p - p$ and $p - n$, exclusive of Coulomb forces, have been found to be the same to a high degree of accuracy.

Strong forces — The ***strong interactions***, the forces between the nucleons, are the strongest forces found in nature. The gravitational and the electromagnetic interaction were known to us long before the nuclear forces, as they were associated with macroscopic bodies, e.g. the gravitational forces between the planets and the sun and the electrical forces between charged bodies. But they are far weaker compared to the nuclear force. For instance, the gravitational force is only $\sim 10^{-40}$ of the strong interaction.

Saturation — Nuclear forces are the only ones in nature that show saturation effect. The ability of nuclear forces to act upon other particles attain a point of

Scanned with CamScanner

saturation when a nucleon gets completely surrounded by other nucleons. Those nucleons that are located outside the surrounding nucleons do not 'feel' the interaction of the surrounded nucleon.

Summarising : (i) the forces between nucleons are attractive in nature when they are 0.5 - 25 F apart; (ii) these forces are of short range having maximum value at about 2×10^{-15} m and fall off sharply with distance, becoming negligible beyond this range; (iii) they are charge-independent so that the nuclear force between a proton and a neutron or between a neutron and a neutron are almost the same; (iv) they have the property of saturation - a particular nucleon interacts with a limited number of nucleons around it and the other surrounding ones remain unaffected. So they become saturated over short distances; (v) the nuclear forces depend on the *mutual orientation of spins of various nucleons* and are *different in parallel and antiparallel spins*.

• In addition to the strong nuclear force which is far stronger than Coulomb interaction, there is, as indicated by *experimental evidence*, a third type of force which is also a short range force but much weaker than the nuclear force. This is termed *weak interaction*. It may be as small as 10^{-14} of strong nuclear force. It is also not of gravitational type.

Interestingly, the weaker the force, the larger must be the system in order that it might be of importance. For example, the strong interactions hold the nucleons, the electromagnetic force holds the larger systems of atoms and molecules, while the gravitational force becomes important only in astral systems.

The chief forces of nature are thus of the following four types : (i) the *strong nuclear force*, (ii) the *electromagnetic force*, (iii) the *weak interaction force* and (iv) the *gravitational force*.

• According to Yukawa's theory, protons and neutrons do not exist independently within a nucleus but constantly exchange charges by emission and absorption of π-mesons (pions) in themselves. This constant emission and absorption result in an exchange of virtual mesons by nucleons, within the nucleus, in ultra short intervals $\sim 10^{-23}$ to 10^{-24} s. As the exchange occurs in a very short time, the uncertainty principle requires that no visible change in nucleonic mass would be observed. This gives rise to rapid meson exchange or *meson field* between protons and neutrons in which meson acts as a quantum of nuclear force. The process is analogous to exchange of photons between charged particles in electromagnetic interactions.

• Read also the Chapter 9 : *Nuclear force*, for more details.

1.16 Rutherford's α-ray scattering

Rutherford and his co-workers Geiger and Marsden made a detailed systematic study of the scattering of α-particles obtained from radioactive sources by ultra-thin foils of elements of high atomic weight e.g., gold, platinum etc. The foil is so thin that only *single scattering* occurs. They observed that the majority of α-particles were scattered through small angles, as expected, but a few however deviated by 90° and

a still smaller number *surprisingly* turned back, being *deflected almost by* 180°. This *large angle scattering* was called **anomalous scattering** as Thomson's atom model could not explain it.

To explain the *large angle scattering* of α-particles, Rutherford proposed that inside the atom, *the positive charge and almost the whole of the atomic mass were concentrated in a very small central region, called the* **nucleus**, round which, in some sort of configuration, the electrons rotate in groups.

1.16.1 Rutherford's scattering formula

We shall now derive the Rutherford's scattering formula here after Max Born.

The nucleus of the atom with charge Ze and an α-particle with charge $E(= 2e)$, mass M and distant r, repel one another with a force $F = (Ze)E/4\pi\varepsilon_0 r^2$ where ε_0 is the permittivity of free space. Let the heavy nucleus be at rest. The α-particle would then describe under the central inverse square law of repulsion, one branch of a *hyperbola* PAP' with K, one of its foci (K, K'), as the nucleus.

Let b be the distance of the nucleus K from the asymptote of the hyperbola (Fig. 1.5) which would have been described if there were no repulsion. This b is called the **collision** (or **impact**) **parameter** which may be *defined as the minimum distance to which the α-particle would approach the nucleus if there were no force between them.*

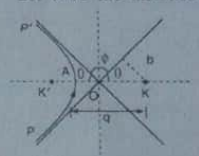

Fig. 1.5 Path of α-particles during scattering by a nucleus

Let q be the distance of K from the vertex A. Then, we have, from the equation of a conic (hyperbola)

$$q = \varepsilon(1 + \cos\theta)$$

where $\varepsilon = OK$, the linear eccentricity, O is the origin and θ the angle between the axis and the asymptote of the hyperbola.

$$\therefore \quad q = b\frac{1+\cos\theta}{\sin\theta} = b\cot\frac{\theta}{2} \quad (\because \sin\theta = b/\varepsilon) \qquad (1.16.1)$$

Step 1. First, we seek a relation between the *impact parameter* b and the *angle of scattering* ϕ, *defined as the angle between the asymptotic direction of approach of the α-particle and the asymptotic direction in which it moves back*, by applying the laws of conservation of energy and momentum. At a great distance from the nucleus, α-particles have only kinetic energy and let v be the velocity there.

From the *conservation of energy* when it passes the vertex A where the velocity is v_0, we obtain

$$\frac{1}{2}Mv_0^2 + \frac{ZeE}{4\pi\varepsilon_0 q} = \frac{1}{2}Mv^2, \quad \left(\frac{ZeE}{4\pi\varepsilon_0 q} = \text{potential energy}\right)$$

$$\therefore \quad \frac{v_0^2}{v^2} = 1 - \frac{2ZeE}{4\pi\varepsilon_0 qMv^2} = 1 - \frac{2k}{q} = 1 - \frac{2k\sin\theta}{b(1+\cos\theta)}. \qquad (1.16.2)$$

Scanned with CamScanner

the protons as Z increases. To counteract the repulsion and thereby attain stability, heavy nuclei tend to be composed of more neutrons than protons.

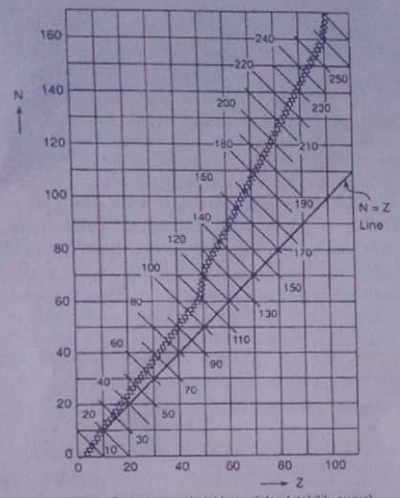

Fig. 8.1 Segre chart of stable nuclides (stability curve)

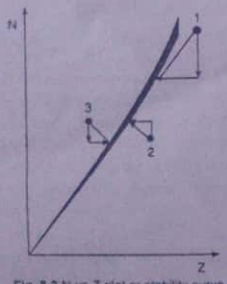

Fig. 8.2 N vs Z plot or stability curve

It is interesting to note that the isotopes lying above and below the stability curve are radioactive and spontaneously decay in such a way that eventually they reach a stable product that lies on the stability curve. This is shown in Fig. 8.2 which is a schematic display of Fig. 8.1. The point 1 shows α-decay where it is seen that to reach the stability curve, N decreases by 2 units and Z also decreases by 2 units. Similarly, the point 2 corresponds to β^+ decay where N increases by 1 unit and Z decreases by 1 unit to reach the stability curve. The point 3 represents β^- decay involving a decrease in N and an increase in Z, both by one unit, to reach the stability curve.

In course of our discussion of the liquid drop model of nucleus, we shall see how it can account for the stability curve.

• The results obtained from a study of two body system cannot be easily applied to many body system. To account for the complex interrelation between nucleons, several different nuclear models have been suggested, each however with its successes and limitations. There is *no one* complete model that can account for all the nuclear properties satisfactorily. Of these, two models are relatively more important : the *liquid drop model* and the *shell model*.

Of the other models, mention may be made of (i) Fermi gas model, (ii) Alpha particle model, and (iii) Collective model. We shall mainly discuss here in this chapter the liquid drop model and the shell model and give only a brief reference to some of the other nuclear models in bare outlines.

Liquid drop model

8.2 Essence of the liquid drop model

The liquid drop model is a very simple model of the nucleus and was first proposed by Niels Bohr and F. Kalcar in 1937. In spite of its simplicity, it could account for a good number of features of nuclear behaviour.

Bohr observed that there exists many similarities between the drop of a liquid and a nucleus. For instance, (i) both the liquid drop and the nucleus possess constant density, (ii) the constant binding energy per nucleon of a nucleus is similar to the latent heat of vaporization of liquid; (iii) the evaporation of a drop corresponds to the radioactive properties of the nucleus, and (iv) the condensation of drops bears semblance with the formation of the compound nucleus, etc. Guided by these observations, Bohr had suggested that this idea could be extended to a more quantitative description of the nucleus of the atom.

According to this model, the nucleus is supposed to be spherical in shape in the stable state with radius $R = r_0 A^{1/3}$, just as a liquid drop is spherical due to symmetrical surface tension forces. The *surface tension* effects are analogous to the *potential barrier* effects on the surface of the nucleus. The density of a liquid drop is *independent of the volume*, as is the case with the nucleus. But whereas the nuclear density is independent of the type of nucleus, the density of a liquid does depend on its nature. Like the nucleons inside the nucleus, the molecules in the liquid drop interact only with their immediate neighbours. The non-independence of the binding energy per nucleon on the *number* of nucleons is analogous to the non-independence of the heat of vaporisation of a liquid drop on the *size* of the drop. Molecules in a liquid drop *evaporate* from the surface when its temperature is raised due to their increased energy of thermal agitation. Analogously, therefore, if high energy nuclear projectiles bombard the nucleus, a *compound nucleus* is formed in which the nucleons quickly share the incident energy and the *emission of nucleons* occurs. The phenomenon of *nuclear fission* is easily explained (Chapter : *Neutron physics and Nuclear energy*) as

Scanned with CamScanner

the splitting of the liquid drop into two more or less equal parts when set into vibrations with sufficient amount energy.

8.21 Semi-empirical binding energy or mass formula

Since nuclear masses are accurately known experimentally, the nuclear binding energy $B.E$ is also known accurately. By using a semi-empirical approach, that is, an *approach based on experimental results*, Weizsäcker in 1935 proposed the following semi-empirical formula to achieve a quantitative and basic understanding of the nuclear binding energy, $B.E$ (in MeV) for the nucleus (Z, A).

$$B.E = a_v A - a_s A^{\frac{2}{3}} - a_c \frac{Z(Z-1)}{A^{1/3}} - a_n \frac{(A-2Z)^2}{A} \pm \frac{\delta}{A^{1/4}} \qquad (8.2.1)$$

with the constants or coefficients having typically the values all in MeV: $a_v = 14.0$, $a_s = 13.0$, $a_c = 0.60$, $a_n = 19$, and $\delta = 33.5$ for even-even or odd-odd nuclei and $\delta = 0$ for even-odd nuclei.

The mass formula has many applications, e.g., prediction of stability against β-decay for members of an isobaric family, explanation of fission by Bohr and Wheeler and calculation of stability limit against spontaneous fission etc.

We shall now describe the steps leading to the *mass formula*. The liquid drop analogy of a nucleus, suggests that like the volume energy and surface energy of a liquid drop, there will be various contributions to the nuclear binding energy.

1. Volume energy term — The first term, $B_v = a_v A$, is the *volume effect* representing the volume energy of all nucleons. The larger the total number of nucleons A, the more difficult it is to remove an individual nucleon from the nucleus. Since the nuclear density is nearly constant, the nuclear mass is proportional to the nuclear volume, which again is proportional, for spherical nucleus, to R^3. But $R \propto A^{1/3} \Rightarrow R^3 \propto A$. So the volume energy, $B_v \propto A$. Thus the main contribution to $B.E$ comes from the total number of nucleons A and, as a first approximation,

$$\boxed{B_v = a_v A}$$

where a_v is a constant, called the *volume coefficient*.

• **From liquid drop analogy** — The energy needed for a complete evaporation of a liquid drop is the product of latent heat L and the mass of the drop M and is used to overcome all the molecular bonds, i.e., it equals the binding energy B of the drop.

∴ For a liquid drop,

$$B = LM = LmA$$

where m = mass of a molecule, A = number of molecules in the drop.

$$\therefore \quad B/A = \text{constant} \Rightarrow B/A \text{ is } \textit{independent} \text{ of } A,$$

the total number of molecules in the drop—an *important feature* of any system (liquid drop or nucleus), where the range of interaction among the constituents is much less

$V = \frac{m}{A}$

than the dimension of the system. By analogy with liquid drop, therefore, we expect for a nucleus a volume energy term.

Since, B/A = constant, the volume energy term is given by

$$B_v = \text{constant} \times A = a_v A$$

In discussing B_v, we assumed that the size of the liquid drop was so large that all molecules are almost fully surrounded by neighbours and hence is more strongly bound. This however is *not correct* for the surface molecules, which has fewer neighbours. The situation becomes particularly more important for light nuclei and is represented in Fig. 8.3 where a medium nucleus and a light nucleus are shown. While in the medium nucleus the ratio of surface nucleons and the total number of nucleons $\simeq 0.63$ $(= 12/19)$, it is as high as 0.88 $(= 6/7)$ in light nuclei. So we have a second term in the mass formula—the *surface energy term* that follows.

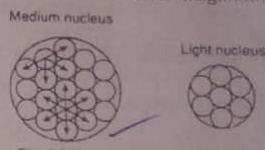

Fig. 8.3 Differences in surface energy of medium and light nuclei

2. Surface energy term — The second term, $B_s = a_s A^{2/3}$, is the *surface effect*, similar to the surface tension in liquids; like the molecules on the surface of a liquid, the nucleons at the surface of the nucleus are not completely surrounded by other nucleons. The total binding energy is thus reduced due to nucleons on the surface. This correction due to surface energy, B_s, is proportional to the surface area of the nucleus i.e. to $4\pi R^2$, for spherical nucleus of radius R. But $R \propto A^{1/3}$. So $B_s \propto A^{2/3}$.

$$\therefore \quad \boxed{B_s = a_s A^{2/3}}$$

where the constant, a_s is called the *surface coefficient*.

3. Coulomb energy term — The third term, B_c is the *Coulomb electrostatic repulsion* between the charged particles, protons, in the nucleus. Since each charged particle repulses all other charged particles, this term would be proportional to the possible number of combinations for a given proton number Z, which is $Z(Z-1)/2$. The energy of interaction between the protons is again inversely proportional to the distance of separation R. So the energy associated with Coulomb repulsion is

$$B_c = k\frac{Z(Z-1)}{R} = k\frac{Z(Z-1)}{r_0 A^{1/3}}$$

$$\text{or} \quad \boxed{B_c = a_c \frac{Z(Z-1)}{A^{1/3}}}$$

where R is replaced by $r_0 A^{1/3}$ and since this repulsive effect also dilutes the binding energy, it appears as a negative quantity in the semi-empirical mass formula.

4. Asymmetry energy term — The fourth term B_a, originates from the asymmetry between the number of protons and neutrons in the nucleus. For stable

Scanned with CamScanner

lighter nuclei, the number of protons is almost equal to that of neutrons : $N = Z$. As A increases, the symmetry of proton and neutron number is lost and the number of neutrons exceeds that of protons to maintain nuclear stability. This *neutron excess* i.e., excess of neutrons over protons, that is $N - Z$, is the measure of the *asymmetry* and it decreases the stability or $B.E$ of the medium or heavy nuclei.

The asymmetry energy, B_a, is directly proportional to (i) the *neutron excess*, $N - Z$ or $A - 2Z$ ($\because A = N + Z$), present in asymmetric nuclei and (ii) the *fraction of nuclear volume* in which the excess neutrons are present. As the nuclear volume is proportional to A, the fractional volume of the nucleus in which excess neutrons are present will be proportional to $(N - Z)/A$ i.e., neutron excess per nucleon.

$$\therefore \quad B_a \propto (N - Z), \text{ and also } \propto (N - Z)/A$$

$$\therefore \quad B_a = a_a \frac{(N - Z)^2}{A}$$

$$\boxed{B_a = a_n \frac{(A - 2Z)^2}{A}}$$

where a_a is a constant, called the *asymmetry coefficient*.

• Unlike in a liquid drop, there is in the nucleus the aspect of quantization of energy states of individual nucleons and the application of Pauli's principle.

If Z protons and N neutrons are put into a nucleus, the lowest Z-energy levels get filled up first. The *excess neutron* $(N - Z)$, by Pauli's principle, must go to higher unoccupied quantum states, as the first Z quantum states are already filled up with

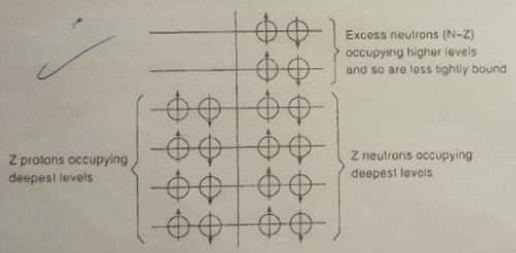

Fig. 8.4 Application of Pauli's principle to nucleon energy quantum states

protons and neutrons (Fig. 8.4). Consequently, the excess neutrons are less tighly bound than the first $2 \times Z$ nucleons, occupying the deepest energy levels. The asymmetry thus gives rise to a disruptive term B_a in nuclear binding energy — the *asymmetry term*.

By the incorporation of this purely quantum mechanical aspect in binding energy, the mass formula *goes beyond* the liquid drop analogy.

5. Pairing energy term — All the energy terms introduced so far involve a somewhat smooth variation of $B.E.$ with change in proton number Z or neutron number N. But $B.E./A$ vs. A plot shows a number of kinks and evidence of favoured pairings. For instance, nuclides with Z (or N) = 2, 4, 8, 20, 50, 82 and 126 (magic numbers) have larger $B.E.$-value. This fact is not taken into acount in a liquid drop model; intrinsic nucleonic spin and shell effects are disregarded. This omission demands a correction which is made in part by introducing the last term which is a pure corrective term, called the *pairing energy term*, B_p.

Nuclear data indicate that nuclei with ***even Z and even N are most stable***, whereas nuclei having ***odd Z and odd N are least stable***, and nuclei with odd N and even Z, or even N and odd Z lie in between. Each of the protons and neutrons having spin $\frac{1}{2}$ form pairs with parallel and anti-parallel spins in even N- even Z type nuclei giving them a stable configuration. But in odd Z- odd N type nuclei, one unpaired proton and one unpaired neutron are left to make the nuclei less stable. So the pairing of spins increases the $B.E$ of even Z- even N type nuclei and decreases it in odd Z- odd N nuclei. Thus, the correction term B_p of pairing energy which is proportional to $A^{-3/4}$ is given by

$$\boxed{B_p = \frac{\delta}{A^{3/4}}}$$

where δ is a constant. This relation was determined empirically by Fermi.

No correction term however is necessary if A is *odd*, i.e. for A odd, $\delta = 0$. The constant δ is selected according to the following table.

Table 8.1 : *Classification of Stable Nuclides*

Z	N	A	No. of stable nuclei	δ	B_p
even	even	even	165	−33.5	$-\delta/A^{3/4}$
even	odd	odd	55	0	0
odd	even	odd	50	0	0
odd	odd	even	4	+33.5	$+\delta/A^{3/4}$

The binding energy $B.E$ of a nucleus is thus finally given by

$$B.E = a_v A - a_s A^{2/3} - \frac{a_c Z(Z-1)}{A^{1/3}} - a_n \frac{(A-2Z)^2}{A} \pm \frac{\delta}{A^{3/4}}$$

$$\therefore \quad f_B = \frac{B.E}{A} = a_v - \frac{a_s}{A^{1/3}} - \frac{a_c Z(Z-1)}{A^{4/3}} - a_n \frac{(A-2Z)^2}{A^2} \pm \frac{\delta}{A^{7/4}} \qquad (8.22)$$

where f_B is the *binding fraction*, i.e., the binding energy per nucleon.

Scanned with CamScanner

The formula for the mass of the nucleus is given by

$$\begin{aligned} {}^{A}_{Z}M &= ZM_p + (A-Z)M_n - B.E/c^2 \\ &= ZM_p + (A-Z)M_n \\ &\quad - \frac{1}{c^2}\left[a_v A - a_s A^{\frac{2}{3}} - a_c \frac{Z(Z-1)}{A^{1/3}} - a_n \frac{(A-2Z)^2}{A} + \frac{\delta}{A^{1/4}}\right] \end{aligned} \quad (8.2.3)$$

The above formula (8.2.3) is known as the **semi-empirical mass formula** of Weizsäcker.

Discussion — The five empirical constants or coefficients are evaluated using information about the $B.E.$ of nuclei which again is obtained from the accurate nuclear masses. Once the five constants are evaluated from five nuclear masses, we can use them to predict hundreds of other masses and reactions. Thus, using some empirical data, much of the nuclear behaviour becomes predictable. Hence (8.2.3) is known as *semi-empirical mass formula*.

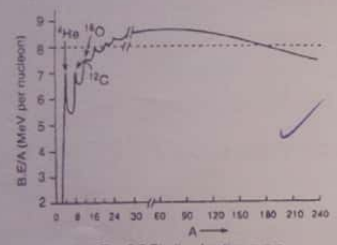

Fig. 8.5 Binding fraction curve

The $B.E/A$'s appear in Fig. 8.5 which is a plot of $B.E/A$ in MeV against the mass number A. With the exception of few irregularities such as ^{4}He, ^{12}C, ^{16}O etc, the curve is relatively smooth, rising sharply for small values of A. For values of $A \geq 30$, the binding energy is close to 8 MeV per nucleon.

The relative contributions of the various effects in Weizsäcker's formula are shown schematically in Fig. 8.6.

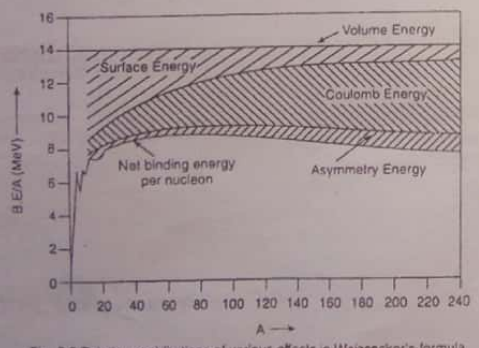

Fig. 8.6 Relative contributions of various effects in Weizsäcker's formula

Note that (8.2.3) is quadratic in Z and thus for each A-value, there is a particular Z-value for which M is minimum. A family of different nuclides with same A-value is called an *isobaric family*. The Z-value corresponding to minimum M is the *most stable member* of the isobaric family.

• Also note from Table 8.1 that while even-even nuclei are most stable and hence most abundant, the odd-odd nuclei are the least stable ones. Naturally, the odd-even nuclei are intermediate in respect of stability.

8.2.2 Applications of semi-empirical mass-formula

We give below a number of applications of the semi-empirical mass formula

1. Mass parabola : prediction of stability of nuclei against β-decay.

If $M(A, Z)$ be the atomic mass of an isotope of an element of atomic number Z and mass number A, then

$$M(A, Z) = ZM_p + NM_n - B.E. \quad (8.2.4)$$

where M_p, M_n are the masses of a proton and a neutron respectively.

Using (8.2.1), for $B.E$, the above equation becomes

$$M(A, Z) = ZM_p + (A-Z)M_n - a_v A + a_s A^{\frac{2}{3}} + a_c Z^2 A^{\frac{1}{3}} + a_n \frac{(A-2Z)^2}{A}, \quad (8.2.5)$$

neglecting δ and using Z^2 instead of $Z(Z-1)$ which appeared recently to be a better representation.

Introducing,
$$F_A = A(M_n - a_v + a_n) + a_s A^{\frac{2}{3}},$$
$$p = -4a_n - (M_n - M_p),$$
and
$$q = \frac{1}{A}(a_c A^{\frac{1}{3}} + 4a_n),$$

we obtain from equation (8.2.5) above

$$M(A, Z) = F_A + pZ + qZ^2 \quad (8.2.6)$$

which is an *equation to a parabola* for a given A (i.e., for a given isobaric line) and is known as the **mass parabola** (Fig. 8.7).

The lowest point of the parabola, $Z = Z_A$, is obtained by differentiating $M(A, Z)$ with respect to Z for a given A, and equating the same to zero.

$$\therefore \left(\frac{\partial M}{\partial Z}\right)_A = p + 2qZ = 0 \text{ at } Z = Z_A, \text{ whence,}$$

$$Z_A = -\frac{p}{2q} = \frac{(M_n - M_p + 4a_n)A}{2(a_c A^{\frac{2}{3}} + 4a_n)} \quad (8.2.7)$$

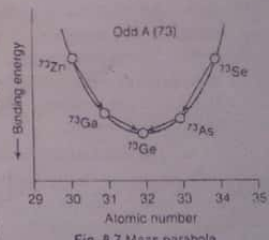

Fig. 8.7 Mass parabola

Scanned with CamScanner

Nucleon separation energy – A semi-empirical estimate of the nucleon *separation energy*, S_N may be easily made, for

$$S_N = B(A) - B(A-1) = \frac{dB}{dA}$$

But, $$\frac{d(B/A)}{dA} = \frac{1}{A}\frac{dB}{dA} - B\frac{1}{A^2}$$

$$\therefore \quad S_N = \frac{dB}{dA} = A\frac{d(B/A)}{dA} + \frac{B}{A} \qquad (8.2.18)$$

and can be evaluated directly by a measurement of the slope of B/A vs. A plot (Fig. 8.5).

The liquid drop model has other important applications: theory of compound nucleus and the phenomenon of nuclear fission, α-disintegration, β-disintegration energy of mirror nuclei.

Shell model

The large binding energy of He-nucleus (α-particle) suggests that 2 protons and 2 neutrons form a stable nuclear configuration. Taking the clue from the chemical stability of closed electron sub-shells and shells in atoms, the physicists enquired if nucleons too form similar closed sub-shells and shells in nuclei, i.e., if protons and neutrons in a nucleus are also arranged in some type of a shell structure. This idea of Elsasser eventually culminated in the development of the **nuclear shell model**.

8.3 Points in favour of the shell model

There exists a number of points in favour of the shell model of the nucleus and the following are worth noting.

1. Just as inert gases, with 2, 10, 18, 36, 54, ··· electrons, having closed shells show high chemical stability, nuclei with 2, 8, 20, 50, 82 and 126 nucleons—the so-called **magic numbers** — of the same kind (either proton or neutron) are particularly stable. The binding energy is found to be unusually high implying high stability which is reflected in high abundance of isotopes with these proton numbers and isotones with these neutron numbers. Nuclei both with Z and N = each a magic number, are said to be *doubly magic*.

2. The number of stable isotopes (Z = const.) and isotones (N = const.) is larger with respective number of protons and neutrons equal to either of the magic numbers : e.g., Sn ($Z = 50$) has 10 stable isotopes, Ca ($Z = 20$) has 6; the biggest group of isotone is at $N = 82$, then at $N = 50$ and $N = 20$.

3. The three naturally occurring radioactive series decay to the stable end product $^{208}_{82}$Pb with $Z = 82$ and $N = 126$ indicating extra stable configuration of magic nuclei.

4. The neutron absorption cross-section is low for nuclei with N = magic numbers like 50, 82 and 126, indicating reluctance of magic nuclei to accept extra neutrons in their completely filled shells.

5. Isotopes like $^{17}_{8}$O, $^{37}_{36}$K and $^{137}_{54}$Xe are spontaneous neutron emitters when excited by preceding β-decay. The isotopes have $N = 9$, 51 and 83 respectively, i.e., $N = (8+1)$, $(50+1)$ and $(82+1)$. One can interpret this loosely bound neutron as a *valence neutron* which the isotopes emit to assume some magic N-value for their stability.

6. Electric quadrupole moment Q of magic nuclei is zero indicating spherical symmetry of the nucleus for closed shells. When Z-value or N-value is gradually increased from one magic number to the next, Q increases from zero to a maximum and then decreases to zero at the next magic number.

7. The energy of α- or β-particles emitted by magic radioactive nuclei is larger.

All these experimental facts lend a strong support to the shell structure of nucleus.

8.4 Salient features (assumptions) of shell model

This model assumes that each nucleon stays in a well-defined quantum state. But, unlike the atom, the nucleus has *no obvious massive central body acting as force centre of charge*.

In the shell model, therefore, each nucleon is considered as *a single particle that moves independently of others in the time-averaged field of the remaining* $(A-1)$ *nucleons* acting as a *core*, and is confined to its own orbit completing several revolutions before being disturbed by others by way of collisions. This implies that the mean free path before collisions of nucleons is much larger than the nuclear diameter. It amounts to assuming the interaction among the nucleons to be weak. This sounds paradoxical as nuclear matter is super-dense ($\sim 10^{17}$ kg/m^3) and experiments indicate that a nucleus is virtually opaque to any incident nucleon. This '*weak interaction paradox*' was saved by invoking Pauli's principle by Weisskopf. He argued that nucleons are fermions and by exclusion principle, no two neutrons and protons can stay in identical quantum state. Hence the experimentally expected strong interaction among nucleons in a nucleus cannot show itself since all the quantum states (low lying) into which the scattered nucleon after collision may go are already occupied.

In terms of Schrödinger's equation, each nucleon thus moves in the same potential $V(r)$ which may be taken as an *average harmonic oscillator potential* so that $V(r) = \frac{1}{2}kr^2$. Schrödinger equation then becomes

$$\left(-\frac{\hbar^2}{2M}\nabla^2 + \frac{1}{2}kr^2\right)\psi = E\psi \qquad (8.4.1)$$

where M is the mass of the nucleon and E the energy eigenvalues.

Scanned with CamScanner

The solution of equation (8.4.1) is given by :

$$E_n = \left(N + \tfrac{1}{2}\right)\hbar\omega \qquad (8.4.2)$$

where N = oscillator quantum number $= 0, 1, 2, 3, \cdots$ so that in the harmonic oscillator model, all the energy eigen states are *equally spaced*. The wave function ψ has both angular (orbital) and the radial part.

Each nucleon is supposed to have an orbital angular momentum $|\vec{l}| = \sqrt{l(l+1)}\hbar$ where $l = 0, 1, 2, 3, \cdots$, the nuclear orbital quantum number. Another quantum number, very similar to but not the principal quantum number of electronic orbit, characterises the radial part of nuclear wave function and is symbolised by $n = 1, 2, 3, \cdots$. Each nucleon has also spin angular momentum $|\vec{s}| = \sqrt{s(s+1)}\hbar$ where $s = \frac{1}{2}$ and behaves as an independent particle subject to Pauli's principle that *no two identical nucleons can be in the same quantum state*. Again, as suggested by Mayer, Jensen and others, there is a *strong interaction (coupling) between the orbital and the intrinsic spin angular momenta* of each nucleon. The quantum mechanical rules for angular momenta dictate that total angular momentum $j\hbar$ formed by vector addition of orbital angular momentum $l\hbar$ and spin $s\hbar$ must be such that j (total angular momentum quantum number) is restricted to the following two values : $j = l + \frac{1}{2}$ and $j = l - \frac{1}{2}$.

Thus a different energy is associated with each of the two j-levels and each nucleonic energy level with a given l splits into *two sub-levels*, except for $l = 0$, when j has only one value $\frac{1}{2}$. The level $j = l + \frac{1}{2}$ corresponds to $\vec{s}$ and $\vec{l}$ *parallel* ($\uparrow\uparrow$) to each other and $j = l - \frac{1}{2}$ to $\vec{s}$ and $\vec{l}$ *anti-parallel* ($\uparrow\downarrow$) to each other. Empirically, it is found that the nuclear energy level with higher j always lies below that with smaller j. So $j = l + \frac{1}{2}$ sub-level has a *lower energy* than $j = l - \frac{1}{2}$ sub-level, the former giving a more tightly bound nucleonic state. The separation between two sub-levels with a given l is rather large and increases rapidly with l. When $l \geq 4$, the sub-levels lie in different shells. The quantum number j of nucleus is obtained by $\sum j_i$, i.e., adding the j-values of the individual nucleons (similar to *jj-coupling* in atoms), subject however to the usual quantum conditions.

To designate the nucleonic states, spectroscopic notation of atomic physics is followed. Each sub-level can have a maximum of $(2j + 1)$ nucleons of the same kind, for a given j. So it can house $(2j + 1)$ protons and $(2j + 1)$ neutrons. Nucleons are designated with n-values followed by spectroscopic notation of l-values ($s, p, d, f, \cdots$ for $l = 0, 1, 2, 3, \cdots$); the j-values are shown as subscript and the superscript gives the number of nucleons required to complete the sub-shell (Table 8.2).

For instance, for $l = 0$, $j = l + \frac{1}{2} = \frac{1}{2}$ and the number of nucleons in the level $= 2j + 1 = 2 \times \frac{1}{2} + 1 = 2$ and the state is designated along with n-value as $(1s_{\frac{1}{2}})^2$. Similarly, for $l = 1$, $j = l \pm s = l \pm \frac{1}{2} = \frac{3}{2}$ and $\frac{1}{2}$. The number of nucleons in the two sub-levels are thus $2 \times \frac{3}{2} + 1 = 4$ and $\left(2 \times \frac{1}{2} + 1\right) = 2$. The two sub-states are designated as $(1p_{\frac{3}{2}})^4$ and $(1p_{\frac{1}{2}})^2$ respectively. So the total number of nucleons in this

level $= 4 + 2 = 6$, giving the progressive total of 8 nucleons, and so it goes on. Thus we can predict the completed shells and the corresponding total number of nucleons.

The quantum number n, l and j and the designation of energy states in order of the energy and in accordance with the above notational scheme is shown in Table 8.2

Table 8.2 : ***Nucleonic sub-shells and shells***

n	l	j	Designation and no. of p or n to fill sub-levels		Progessive Total
1	0	1/2	$(1s_{1/2})^2$	2	2
1	1	3/2	$(1p_{3/2})^4$		
1	1	1/2	$(1p_{1/2})^2$	6	8
1	2	5/2	$(1d_{5/2})^6$		
2	0	1/2	$(2s_{1/2})^2$		
1	2	3/2	$(1d_{3/2})^4$	12	20
1	3	7/2	$(1f_{7/2})^8$		
2	1	3/2	$(2p_{3/2})^4$		
1	3	5/2	$(1f_{5/2})^6$		
2	1	1/2	$(2p_{1/2})^2$		
1	4	9/2	$(1g_{9/2})^{10}$	30	50
1	4	7/2	$(1g_{7/2})^8$		
2	2	5/2	$(2d_{5/2})^6$		
2	2	3/2	$(2d_{3/2})^4$		
3	0	1/2	$(3s_{1/2})^2$		
1	5	11/2	$(1h_{11/2})^{12}$	32	82
1	5	9/2	$(1h_{9/2})^{10}$		
2	3	7/2	$(2f_{7/2})^8$		
2	3	5/2	$(2f_{5/2})^6$		
3	1	3/2	$(3p_{3/2})^4$		
3	1	1/2	$(3p_{1/2})^2$		
1	6	13/2	$(1i_{13/2})^{14}$	44	126

up to the magic number 126. The thick horizontal lines signal the *closure of a shell* where marked changes occur in the nucleonic binding energy.

The shell model with its spin-orbit coupling thus beautifully accounts for the magic nucleon numbers.

Scanned with CamScanner

Chapter 2

Radioactivity

Nuclear physics may be said to begin with the discovery of radioactivity by Becquerel and the Curies. During his experiments on fluorescence of uranium, the French physicist Henry Becquerel in 1896 was amazed to notice that a photographic plate, wrapped in black paper for protection against radiation, was affected by the salts of uranium kept outside it. In tracing the origin and nature of this invisible radiation, *radioactivity* – the phenomenon of emission of such radiation – was discovered, thanks to the monumental and pioneering work carried out in the field by Mme Curie and Pierre Curie, Ernst Rutherford, Fredric Soddy and others. The Curies were awarded, jointly with Becquerel, the Nobel Prize in physics in 1903 for this discovery. In 1911 Mme Curie was again awarded the Nobel Prize in chemistry for her painstaking efforts in isolating the radioactive element, now called, *radium*.

2.1 Radioactivity

Radioactivity is the phenomenon of *spontaneous disintegration*, attended with emission of corpuscular or electromagnetic radiations, of *heavy* atomic *nuclei* like uranium, radium etc. at a *constant rate*, unaffected by any physical or chemical changes or influences such as temperature, pressure etc. to which the atom (nucleus) may be subjected. It is a *nuclear property* of the active element and in all radioactive processes, a *transmutation* of the element (change from one element to another) occurs and an altogether new nucleus is formed. Radioactivity is in fact the first *nuclear phenomenon* to be discovered.

The radiations from different radioactive substances were classified as α-rays and β-rays by Rutherford from a study on the penetrating power of these radiations. Subsequently, a third type of radiation – γ-rays – which is a very energetic form of electromagnetic waves was added to the list by Paul Villard. In the case of α and β-emission processes, either the atomic number Z or the mass number A or both Z and A of the nucleus change leading to the creation of a new nucleus (transmutation).

Scanned with CamScanner

In γ-emission process, however, no transmutation occurs, the nucleus makes only a transition from a quantum state of higher energy (excited state) to another of lower energy. Any nuclide that undergoes a change in its structure by shedding nuclear particles such as α and β, and gives off γ-rays is called *a radioactive nucleus*. It has been found that there are 272 stable nuclei of naturally occurring elements (they are non-radioactive); the rest are all unstable and hence radioactive, and are known as *radio-isotopes*.

• In spite of the strong nuclear forces holding the constituent nucleons, heavy elements like U, Th, Ra etc. disintegrate *spontaneously* giving off α, β and γ-radiations. What then is the reason behind this spontaneous decay? The cause of this disintegration is that an unstable nucleus decays to attain a new configuration which is either stable or will lead to one which is stable.

2.2 Radioactive decay law

Experimental studies on radioactivity, as conducted by Rutherford and Soddy, show convincingly that

1. On emission of α or β-rays which is usually, but not invariably, accompanied by γ-emission, the emitting parent nuclide transforms into a new daughter element; the daughter element again may be radioactive so that the process of *successive disintegration* continues till the original active parent nuclide gets transformed into a stable one, usually lead (Pb).

2. The *rate of radioactive disintegration*, that is, the number of atoms (nuclides) that disintegrate at any instant t is *directly proportional to the number N_t of the active nuclides present* in the sample under study *at that instant*.

Decay law or decay equation — Let N_t be the number of active nuclides present in the sample at any instant t. Then, we have, experimentally

$$-\frac{dN_t}{dt} \propto N_t \quad \Rightarrow \quad \frac{dN_t}{dt} = -\lambda N_t \qquad (2.2.1)$$

where λ, the constant of proportionality, is known as the *decay constant* – a characteristic constant of the element (nuclide). The negative sign indicates that N_t decreases with t.

Re-arranging equation (2.2.1), we obtain

$$\frac{dN_t}{N_t} = -\lambda dt \qquad (2.2.2)$$

Integrating equation (2.2.2), we have

$$\ln N_t = -\lambda t + A \qquad (2.2.3)$$

where A is the constant of integration.

At $t = 0$, $N_t = N_0$, the initial number of nuclides. So, from (2.2.3),

$$A = \ln N_0$$

∴ From (2.2.3), we obtain finally,

$$\ln (N_t/N_0) = -\lambda t$$

or, $$\boxed{N_t = N_0 e^{-\lambda t}} \qquad (2.2.4)$$

The above relation is the radioactive ***decay law*** or ***decay equation***. It shows that the number of active nuclides decreases exponentially with time (Fig. 2.1).

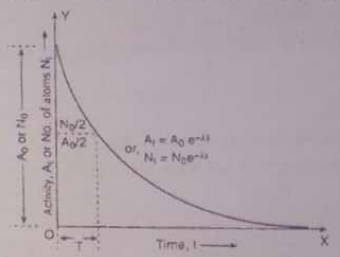

Fig. 2.1 Activity vs. time curve : Radioactive decay law

According to the decay law, therefore, an infinite time is theoretically needed for the *complete* disintegration of a radio-element and in this respect, all radio-elements are the same. So to distinguish one radio-element from another, a quantity called *half-life* T is more often used and we shall soon return to it.

2.3 Statistical nature of radioactivity : Decay law from probability

So long we treated N_t, the number of nuclei present at time t as a continuous variable. As long as N_t is very large compared to dN, the number of nuclei decaying during t and $t + dt$, this is justified and is usually the case. But, in fact, N_t varies discontinuously and the smallest value of $dN_t = 1$, corresponding to the decay of a single nucleus. Thus the decay law is valid only for a sample sufficiently large to treat dN_t as a differential. The concepts of half-life and mean life (see later) are meaningless when the sample consists of just a few nuclei. As the number of nuclei in the sample is increased, we can say that half of them will decay after one half-life, although we cannot say which particular nuclei will decay at a given instant.

The decay law is thus statistical in nature and was deduced by Schweidler assuming that the disintegration of a nuclide of a radio-element is subject to the laws of probability or chance only.

Scanned with CamScanner

The probability p for a nuclide to disintegrate in an interval Δt depends *only* on the length of the interval and for sufficiently short intervals is proportional to Δt.

$$\therefore \quad p = \lambda \Delta t$$

where the constant of proportionality λ is the *disintegration constant*.

Then the probability that the given nuclide will *not disintegrate* during the interval Δt is would be given by

$$1 - p = 1 - \lambda \Delta t$$

The probability that this atom will *not* disintegrate in a second interval Δt is also $1 - \lambda \Delta t$. The probability that this atom will survive both the intervals is therefore $(1 - \lambda \Delta t)^2$. So, for n such intervals, the probability of survival of the atom is

$$(1 - \lambda \Delta t)^n = \left[1 - \lambda \left(\frac{t}{n}\right)\right]^n$$

if the total time $t = \Delta t + \Delta t + \cdots = n \cdot \Delta t$.

The probability that the atom will remain unchanged after a time t is given by

$$\lim_{n \to \infty} \left(1 - \lambda \frac{t}{n}\right)^n = e^{-\lambda t}$$

One may *interpret* this *statistically* as follows :

If N_0 be the initial number of nuclei, the fraction *remaining unchanged* after time t is $N_t/N_0 = e^{-\lambda t}$, where N_t is the number of unchanged nuclei after time t.

$$\therefore \quad \boxed{N_t = N_0 e^{-\lambda t}}$$

which is the relation (2.2.4) obtained earlier.

• The decay constant is also called *disintegration constant, transformation constant* or the *radioactive constant*. It depends on the energy that is available for the nuclear transformation and on the characteristics of the parent and the daughter nuclei. It is *independent* of the *external conditions* and the *age* of the sample.

• **Exponential growth** — From (2.2.4), we find that out of N_0 atoms at $t = 0$, the number left after time t is N_t implying that $N_0 - N_t$ atoms of parent A are converted into daughter (product) B in time t. If the daughter is *non-radioactive*, the rate of growth of the daughter is

$$N_0 - N_t = N_0 - N_0 e^{-\lambda t} = N_0(1 - e^{-\lambda t})$$

The daughter product thus grows on exponentially (Fig. 2.2).

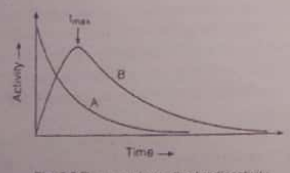

Fig. 2.2 Decay and growth of radioactivity

2.3.1 Statistical fluctuations : Poisson distribution

The time t required for observing a finite number of counts N of radioactive particles (say, in a GM counter) is subject to statistical fluctuations in count rate, $n = N/t$ and leads to an error. We shall now show that the number of counts in a given time t obeys the Poisson's distribution.

Proof. Let P_N = probability of counting N particles in time t. Divide t into n equal intervals, each equal to $\Delta t = t/n$. Now, Δt is so small (i.e., n so very large) that we may neglect the probability of emission of *two* particles within Δt.

∴ Probability of emission of one particle in an interval Δt is $p = \bar{N}/n$, $\bar{N}$ being the average number.

∴ Probability of emission of N particles in first N intervals ($n \gg N$) and none in remaining $(n - N)$ intervals is

$$\left(\frac{\bar{N}}{n}\right)^N \left(1 - \frac{\bar{N}}{n}\right)^{n-N}$$

which is just *one* possible way to having N particles in time t.

The first particle may appear in any of n intervals, the second one in any of remaining $(n - 1)$ intervals and so on, so that finally the Nth particle may appear in any of the remaining $(n - N + 1)$ intervals. So, the number of ways of distributing N particles in n intervals is

$$n(n-1)(n-2)\cdots(n-N+1)$$

But all of these are *not* mutually *independent* and hence, without in any way influencing the results, the positions can be interchanged. The number of possible ways of interchanging the particles $= N!$

$$\therefore \quad P_N = \text{Probability of obtaining } N \text{ counts}$$

$$= \frac{n(n-1)(n-2)\cdots(n-N+1)}{N!} \times \left(\frac{\bar{N}}{n}\right)^N \left(1 - \frac{\bar{N}}{n}\right)^{n-N} \qquad (2.3.1)$$

which is the *binomial distribution law*.

Let now $n \to \infty$. Then (2.3.1) reduces to

$$P_N = \frac{n^N}{N!} \left(\frac{\bar{N}}{n}\right)^N e^{-\bar{N}} = \frac{\bar{N}^N e^{-\bar{N}}}{N!}, \qquad (2.3.2)$$

the well-known **Poisson distribution formula**, illustrated in Fig. 2.3.

• Eq. (2.3.2) is however valid only for integral N. A continuous curve of P_N vs. N plotted through points given by (2.3.2) gives a curve having an asymmetric maximum for small N. As $N \to$ large values, the curve turns symmetric about the maximum and approaches the *Gaussian error curve*.

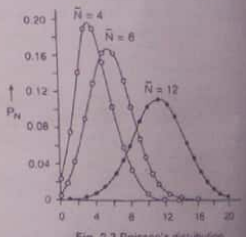

Fig. 2.3 Poisson's distribution

Scanned with CamScanner

2.3.2 Half life and Average life

Half-life — The *half-life* or the *half-value period* of a radioactive nuclide is defined as the *time* T in which the original amount of radioactive nuclide is *reduced* by way of disintegration *to half* its value.

Substituting N_t by $N_0/2$ in (2.2.4), T is given by

$$\frac{N_0}{2} = N_0 e^{-\lambda T}$$

$$\therefore \quad \boxed{T = \frac{\ln 2}{\lambda} = \frac{0.693}{\lambda}} \qquad (2.3.3)$$

$$\text{or,} \quad \lambda T = 0.693 = \text{constant} \qquad (2.3.4)$$

So, T is *independent* of the instant from which it is measured. Depending on the active nuclide, its value may range from 10^{10} years to 10^{-7}s.

Mean or Average life — The fundamental law of radioactive decay, as already indicated, is a **statistical law** implying that the *probability* of decay of a given nuclide in a short time interval dt at time t is $|dN_t/N_t| = \lambda dt$ which is *independent* of the age of the nuclide. It *does not state* anything about the decay of *an individual* atom. Of the N_t nuclides, which one would disintegrate at any instant t is at the mercy of chance. The decay law only states that the decay rate is proportional to N_t. Among the nuclides, some may disintegrate almost immediately, while others may exist for an infinitely long time. We do not know why it is so. The actual life of a nuclide may thus vary from 0 to ∞ and all radio-elements are the same in this respect. We can however speak of an *average* or *mean life* τ of a radio-element.

The *average* or *mean life* τ of a radioelement is the *average life-time* of all the atoms in the given sample and is defined as the ratio of the *total life-time of all the atoms* or *nuclei* to the *total number of atoms* or *nuclei*.

$$\therefore \quad \tau = \frac{\text{Total life time of all nuclei}}{\text{Total number of nuclei}}$$

$$= \frac{t_1 dN_1 + t_2 dN_2 + \cdots}{dN_1 + dN_2 + \cdots} = \frac{\Sigma t dN}{\Sigma dN}$$

$$= \frac{\int t dN}{\int dN} = \frac{\int t dN}{-N_0} \qquad (2.3.5)$$

where dN_1 atoms have a life-time t_1, dN_2 atoms a life-time t_2 and so on.

But, we have, $\quad dN = d(N_0 e^{-\lambda t}) = -\lambda N_0 e^{-\lambda t} dt$

$$\therefore \quad \tau = \lambda \int_0^\infty t e^{-\lambda t} dt, \text{ substituting for } dN \text{ in (2.3.5)}$$

$$= \lambda \left[-\frac{t}{\lambda} e^{-\lambda t} + \frac{1}{\lambda} \int_0^\infty e^{-\lambda t} dt \right]$$

$$= \lambda \left[-\frac{t}{\lambda} e^{-\lambda t} - \frac{1}{\lambda^2} e^{-\lambda t} \right]_0^\infty = \frac{1}{\lambda}$$

$$\therefore \text{ Mean or average life, } \boxed{\tau = \frac{1}{\lambda}} \qquad (2.3.6)$$

The mean or average life of a radioactive element is thus not the same as its half-life. The mean life is the *reciprocal of the decay constant*, that is, the *decay probability per second* and is greater than the half-life.

• To get the equation (2.3.5), the curve of Fig. 2.4 is illuminating. The curve shows that each of dN number of active nuclei has lived a life-time of t seconds, i.e., the total life span of dN nuclei is $dN.t$ seconds.

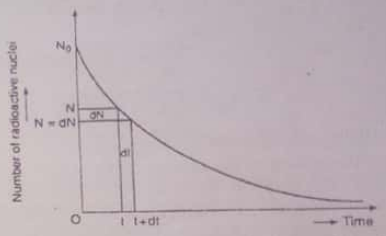

Fig. 2.4 Curve shows how dN number of nuclei decay in time dt

• Since the actual life of an atom extends from 0 to infinity, the mean life τ is not of much physical importance. The decay constant λ and the half-life T are more significant than τ.

• The *decay constant*, the *half-life* and the *mean life* are related to each other as

$$\boxed{T = \frac{0.693}{\lambda} = 0.693\tau} \qquad (2.3.7)$$

Caution ! The decay equation $N_t = N_0 e^{-\lambda t}$ applies to the behaviour of a single, pure radioactive element. Mixtures of radioactive substances and radio-samples having products of initial disintegrations that are themselves radioactive *do not obey* the above decay law.

• As λ increases, T decreases and conversely. Also, from the decay law, as λ increases (i.e., T decreases), the number of active atoms decreases more rapidly. Conversely, if λ is small (T large), the number of active atoms decreases very slowly, e.g., uranium and thorium. The half-lives of U and Th are very long so that their λ-values are very small.

Scanned with CamScanner

• The λ and T are *characteristic constants* of a radioactive substance (Fig. 2.1). The number of radioactive atoms is reduced by a factor $\frac{1}{2}$ after a time T i.e., after one half-life. Plainly, it would be reduced by a factor $(\frac{1}{2})^2$ i.e., $\frac{1}{4}$ after a time $2 \times T$ i.e., after two half-lives. In general the number would be reduced by $(\frac{1}{2})^n$ or $\frac{1}{2^n}$ after a time nT, that is, after n half-lives.

2.4 Activity or strength of a radio-sample

Differentiating the decay equation $N_t = N_0 e^{-\lambda t}$, with respect to t, we obtain

$$\frac{dN_t}{dt} = -\lambda N_0 e^{-\lambda t} \qquad (2.4.1)$$

When $t = 0$, $\left(\frac{dN_t}{dt}\right)_0 = -\lambda N_0$. Hence, from (2.4.1) above, we have

$$\frac{dN_t}{dt} = \left(\frac{dN_t}{dt}\right)_0 e^{-\lambda t} \qquad (2.4.2)$$

or, $$\boxed{A_t = A_0 e^{-\lambda t}} \qquad (2.4.3)$$

where $A_t = dN_t/dt$ and $A_0 = (dN_t/dt)_0$.

A_t is called the *activity* or the *strength* of the sample and is proportional to the rate of disintegration. The graph of the equation (2.4.3) is shown in Fig. 2.1.

Definition : *The* **activity** *or* **strength** A_t *of a radioactive sample at any instant t is defined as the number of disintegrations occurring in the sample in unit time at t,* that is,

$$\text{Activity, } A_t = \left|\frac{dN_t}{dt}\right| = \lambda N_t = \frac{0.693}{T} N_t$$

The activity per unit mass of a sample is called its **specific activity.**

• A_0 $[= (dN_t/dt)_0]$ is the *initial activity* of the sample. The half-life may as well be defined in terms of activity. It is the time in which the activity drops to one-half of the initial activity, (Fig. 2.1).

• Note that a very short-lived substance gives rise to a large activity, even if it is present in minute quantites.

Units of activity — The usual unit of radioactivity is called the **Curie** (Ci) and is defined (since 1950) as the activity of any radioactive substance that disintegrates at the rate of 3.70×10^{10} disintegrations per second.

A thousandth part of a **Curie** is called a **millicurie** (mCi). Still smaller unit is the **micro-curie** (μCi). So, by definition,

$$1 \text{ Ci} = 1 \text{ Curie} = 3.7 \times 10^{10} \text{ disint/sec}$$
$$1 \text{ mCi} = 10^{-3} \text{ Curie}$$
$$1 \ \mu\text{Ci} = 10^{-6} \text{ Curie}$$

Another unit of activity is the **rutherford** (rd), defined as the activity of a radioactive substance disintegrating at the rate of 10^6 disint/s.

• We shall now find the quantity of U-238 having 1 Curie of activity, for U-238

$$\lambda_U N_U = 1 \text{ Ci} = 3.70 \times 10^{10} \text{ distint/s, and}$$

$$\lambda_U = \frac{0.693}{T} = \frac{0.693}{4.5 \times 10^9 \times 365 \times 24 \times 3600} = 4.88 \times 10^{-18}$$

$$\therefore \ N_U = \frac{3.70 \times 10^{10}}{\lambda_U} = \frac{3.70 \times 10^{10}}{4.88 \times 10^{-18}} = 7.58 \times 10^{27}$$

∴ Amount of U-238, having 1 Curie of activity is given by

$$m_U = \frac{7.58 \times 10^{27} \times 238}{6.02 \times 10^{26}} = 2995 \text{ kg}$$

2.5 Radioactive radiations

Soon after the discovery of radioactivity, Curies and others showed that the radioactive radiation was not homogeneous in character but was composed of **three different and distinct types** of radiations.

Experimental set-up — The experimental arrangement (Fig. 2.5) described here is due to Mme Curie. A small quantity of radium preparation is placed in a small hole drilled in a block of lead B. The block is housed in a chamber C evacuated to a high

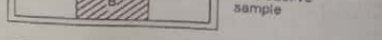

Fig. 2.5 Deflection of α, β, γ rays by a magnetic field

degree to prevent absorption of the radiations by air inside. A strong magnetic field is applied at right angles to the plane of the paper and directed inward (that is, away from the reader). The emerging radiations are received on the photographic plate P.

Observations — The emerging radiations are found to be divided into *three* distinct groups : one bent to the left, the second bent to the right and the third

Scanned with CamScanner

proceeding undeviated. Further, the magnitude of the deflection of the first group is much smaller compared to that of the second.

Conclusion — On applying the *left hand rule*, it is concluded that (i) the first group consists of *positively charged* particles, (ii) the second group is of *negatively charged* particles and (iii) the third group consists of *uncharged* radiations.

Further, the magnitudes of deflection indicate that the particles of the first group are more *massive* compared to those of the second. The three groups are named as α, β and γ-rays respectively.

• A strong electrostatic field will also have a similar effect on the radiations.

2.6 General properties of α, β and γ-rays

We enumerate below some of the important characteristics of α, β and γ-rays.

α-rays — The α-rays consist of *material* particles with a mass four times the protonic mass and a *positive charge* twice that of the proton. These particles are identified as *helium nuclei*. They can ionise gases and penetrate matter. The velocities with which α-particles are ejected from a radioactive substance are very high, ranging from 0.03 c to 0.07 c where $c = 3 \times 10^8$ m/s, the velocity of light in free space.

β-rays — The β-rays also consist of *material* particles but with a *negligible mass* and a *negative charge*. The *specific charge* of β-rays agree with that of the electrons and the β-rays are, in fact, identified as *electrons*. They can ionise gases, affect photographic plate and penetrate matter. The penetrating power is about 100 times greater than that of the α-particles. Because of the low mass, the ionising power is only about 1/100th of that of the α-particles. The velocity of the emitted β-rays from radioactive sources depends on the source and is so high as to sometime approach close to the velocity of light in vacuo.

γ-rays — These are *non-material* and *uncharged* in character, and are unaffected by electric and magnetic fields. In fact, these consist of *electromagnetic radiations* of very small wavelengths, smaller than even the shortest x-rays. Like the α-and β-rays, γ-rays also affect photographic plates, ionise gases through which they pass (photoelectric effect) and penetrate matter. In penetrating power, they are 10–100 times more effective than β-rays, but the ionising power is proportionately much weaker.

2.7 Radioactive series : Displacement law

The α-particles having been identified as helium nuclei ($^4_2$He), an α-emission by a parent nuclide of atomic number Z and mass number A transforms it into a daughter nuclide of atomic number $(Z - 2)$ and mass umber $(A - 4)$. Hence, it becomes a *new element* whose position in the periodic table is two places lower. The α-emission process may be represented as

$$^A_Z X \xrightarrow{\alpha} {}^{A-4}_{Z-2} Y \qquad (2.7.1)$$

Parent element → daughter product + α-particle

Few examples of alpha decay are :

$$^{238}_{92}\text{U} \xrightarrow{\alpha} {}^{234}_{90}\text{Th} + {}^4_2\text{He}$$

$$^{226}_{88}\text{Ra} \xrightarrow{\alpha} {}^{222}_{86}\text{Rn} + {}^4_2\text{He}$$

Similarly, β-particles having been identified as electrons, a β-emission changes the parent nuclide (Z, A) into a daughter $(Z + 1, A)$. The mass number in this case remains unaltered as the mass of an electron is negligible. According to the present day knowledge, electron does *not exist* in the nucleus; the neutron in the nucleus spontaneously transforms into a proton during β-decay, keeping the A-value (= total number of neutrons and protons) of the parent nuclide unchanged. The new element formed in this case thus advances along the periodic table by one place. The β-emission process may be represented as

$$^A_Z X \xrightarrow{\beta} {}^{A}_{Z+1} Y \qquad (2.7.2)$$

Few examples of beta decay are :

$$^{234}_{90}\text{Th} \xrightarrow{\beta} {}^{234}_{91}\text{Pa} + {}^0_{-1}\text{e}$$

$$^{210}_{83}\text{Bi} \xrightarrow{\beta} {}^{210}_{84}\text{Po} + {}^0_{-1}\text{e}$$

The new element formed by β-emission is an *isobar* to the parent nucleus.

• The fact that an element comes down by two places in the periodic table by an α-emission and shoots up by one place by a β-emission constitutes the **displacement** law of Soddy and Fajan, enunciated empirically in 1913, when our present day knowledge regarding neutron-proton structure of nuclei was absent.

• Note that during a radioactive transformation, the mass number and the total charge is conserved. The examples of α-decay (2.7.1) and β-decay (2.7.2) are examples of nuclear reaction. Radioactivity is entirely a nuclear phenomenon; the radioactive radiations come out of the atomic nucleus.

Radioactive series — Now, the daughter of a parent radionuclide may itself be radioactive and decay in its turn into another radionuclide and the process may be repeated till the product is stable, that is, non-radioactive. These *successive transformations* of a radionuclide on being studied are generally found to lie in the range of atomic number $Z = 81$ to $Z = 92$ and form what is called a *radioactive series*. A radioactive series is named after the longest-lived member in it.

There are *three* naturally occurring radioactive series showing successive transformations. These are: (i) *uranium series*, (ii) *thorium series* and (iii) *actinium series*.

Uranium series — The uranium series starts with $^{238}_{92}$U and ends at $^{206}_{82}$Pb, a stable isotope of lead. The series is also called *(4n + 2) series*, for the mass number of any nuclide in the series is given by $A = 4n + 2$, n being an integer. The (N, Z)-chart of the uranium series is given in Fig. 2.6.

Scanned with CamScanner

• The reason of having exactly four radioactive series is due to the fact that the alpha decay reduces the mass number of the nucleus by 4.

2.8 Successive transformation

Consider a radioactive *nuclide* P, symbolised by script 1, to decay into another radioactive nuclide Q (script 2), the latter again decays into a stable end-product R (script 3). For instance,

$$P(1) \xrightarrow{\lambda_1} Q(2) \xrightarrow{\lambda_2} R(3) \text{ [stable]}.$$

Let λ_1, λ_2 be the decay constants of nuclides 1 and 2 respectively, and N_1, N_2, N_3 be the number of atoms of the three kinds at any instant t.

Now the second nuclide would be formed at the rate $\lambda_1 N_1$ by the decay of the parent atom and disappear by its own decay at the rate $\lambda_2 N_2$; the atoms of the end-product i.e. R appear at the rate $\lambda_2 N_2$ by the decay of nuclide 2, but being stable do not disappear. So, we have

$$\frac{dN_1}{dt} = -\lambda_1 N_1 \tag{2.8.1}$$

$$\frac{dN_2}{dt} = \lambda_1 N_1 - \lambda_2 N_2 \tag{2.8.2}$$

$$\frac{dN_3}{dt} = \lambda_2 N_2 \tag{2.8.3}$$

Solving the equation (2.8.1) :

$$(N_1)_t = N_{10} e^{-\lambda_1 t} \tag{2.8.4}$$

where N_{10} is the number of atoms of nuclide 1 at time $t = 0$.

From (2.8.2), using (2.8.4), we obtain

$$\frac{dN_2}{dt} = \lambda_1 N_{10} e^{-\lambda_1 t} - \lambda_2 N_2$$

$$\Rightarrow \quad \frac{dN_2}{dt} + \lambda_2 N_2 = \lambda_1 N_{10} e^{-\lambda_1 t} \tag{2.8.5}$$

Multiplying both sides of (2.8.5) by $e^{\lambda_2 t}$, the integrating factor,

$$e^{\lambda_2 t}\left(\frac{dN_2}{dt} + \lambda_2 N_2\right) = \lambda_1 N_{10} e^{(\lambda_2 - \lambda_1)t}$$

$$\text{or,} \quad \frac{d}{dt}(N_2 e^{\lambda_2 t}) = \lambda_1 N_{10} e^{(\lambda_2 - \lambda_1)t}$$

Integrating, we get

$$N_2 e^{\lambda_2 t} = \frac{\lambda_1}{\lambda_2 - \lambda_1} N_{10} e^{(\lambda_2 - \lambda_1)t} + A \tag{2.8.6}$$

where A is the constant of integration.

Now at $t = 0$, $(N_2)_t = N_{20} = 0$ since only first nuclide is present. So from (2.8.6)

$$A = -\frac{\lambda_1}{\lambda_2 - \lambda_1} N_{10}$$

$$\therefore \quad (N_2)_t = \frac{\lambda_1}{\lambda_2 - \lambda_1} N_{10}\left(e^{-\lambda_1 t} - e^{-\lambda_2 t}\right) \tag{2.8.7}$$

From (2.8.3), using (2.8.7), we obtain on integration

$$(N_3)_t = \left(\frac{\lambda_1}{\lambda_2 - \lambda_1} N_{10}\right) e^{-\lambda_2 t} - \frac{\lambda_2}{\lambda_2 - \lambda_1} N_{10} e^{-\lambda_1 t} + B \tag{2.8.8}$$

At $t = 0$, $(N_3)_t = N_{30} = 0$. So from equation (2.8.8), we get $B = N_{10}$

$$\therefore \quad (N_3)_t = N_{10}\left(1 + \frac{\lambda_1}{\lambda_2 - \lambda_1} e^{-\lambda_2 t} - \frac{\lambda_2}{\lambda_2 - \lambda_1} e^{-\lambda_1 t}\right) \tag{2.8.9}$$

Equations (2.8.4), (2.8.7) and (2.8.9) therefore constitute the solution of the problem.

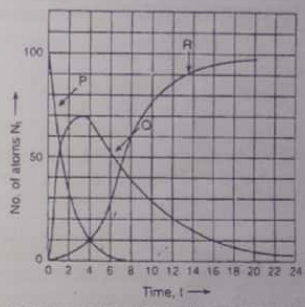

Fig. 2.10 Successive disintegration : Growth of daughter and decay of parent atoms

The decay of the first nuclide P, the growth and decay of the second nuclide Q and the growth of the third nuclide R are shown in Fig. 2.10.

Time for $Q(2)$ to attain a maximum — Eq. (2.8.7) gives how N_2 varies with t. It shows that $N_2 = 0$ at $t = 0$. It increases with increasing t and attains a maximum at $t = t_m$, say. This t_m can be determined by imposing the condition $dN_2/dt = 0$, at $t = t_m$.

$$\text{Now,} \quad \frac{dN_2}{dt} = \frac{\lambda_1}{\lambda_2 - \lambda_1} N_{10}\left(-\lambda_1 e^{-\lambda_1 t} + \lambda_2 e^{-\lambda_2 t}\right)$$

$$\therefore \quad dN_2/dt = 0 \Rightarrow \lambda_2 e^{-\lambda_2 t_m} = \lambda_1 e^{-\lambda_1 t_m}$$

$$\therefore \quad e^{(\lambda_1 - \lambda_2)t_m} = \frac{\lambda_1}{\lambda_2} \Rightarrow (\lambda_1 - \lambda_2)t_m = \ln\frac{\lambda_1}{\lambda_2}$$

Scanned with CamScanner

$$\therefore \quad \boxed{t_m = \frac{1}{\lambda_1 - \lambda_2} \ln \frac{\lambda_1}{\lambda_2}} \tag{2.8.10}$$

That this t_m corresponds to maximum N_2, can be readily verified by obtaining the second time-derivative of N_2 which becomes negative at $t = t_m$.

2.9 Radioactive chain : General case

We can extend the above case of successive transformations to a radioactive chain of any number of members - the so-called *general case*.

$$P(1) \xrightarrow{\lambda_1} Q(2) \xrightarrow{\lambda_2} R(3) \xrightarrow{\lambda_3} S(4) \xrightarrow{\lambda_4} \cdots \text{ etc.}$$

where $P(1)$ is the parent nucleus, and $Q(2)$, $R(3)$, $S(4)$ etc. are the successive products of disintegration.

If $\lambda_1, \lambda_2, \lambda_3, \cdots$ be the decay constants and $N_1, N_2, N_3, \cdots$ be the number of atoms at any instant t of nuclides 1, 2, 3, etc. we have the following set of equations

$$\left.\begin{aligned} \frac{dN_1}{dt} &= -\lambda_1 N_1 \\ \frac{dN_2}{dt} &= \lambda_1 N_1 - \lambda_2 N_2 \\ \frac{dN_3}{dt} &= \lambda_2 N_2 - \lambda_3 N_3 \\ \cdots &= \cdots\cdots\cdots \\ \frac{dN_n}{dt} &= \lambda_{n-1} N_{n-1} - \lambda_n N_n \end{aligned}\right\} \tag{2.9.1}$$

Bateman was the first to solve the above set of equations assuming that only the parent nuclide is present at $t = 0$, that is,

$$N_{20} = N_{30} = \cdots = N_{n0} = 0.$$

Let us first consider the simple case of *three* successive disintegrations, the last (fourth) nuclide being stable.

$$\therefore \quad \frac{dN_3}{dt} = \lambda_2 N_2 - \lambda_3 N_3$$

$$= \frac{\lambda_1 \lambda_2}{\lambda_1 - \lambda_2} N_{10} \left(e^{-\lambda_2 t} - e^{-\lambda_1 t}\right) - \lambda_3 N_3, \quad \text{using (2.8.7)}$$

Multiplying both sides by $e^{\lambda_3 t}$, we obtain

$$\frac{dN_3}{dt} e^{\lambda_3 t} + \lambda_3 N_3 e^{\lambda_3 t} = \frac{\lambda_1 \lambda_2}{\lambda_1 - \lambda_2} N_{10} \left(e^{-\lambda_2 t} - e^{-\lambda_1 t}\right) e^{\lambda_3 t}$$

$$\text{or,} \quad \frac{d}{dt}\left(N_3 e^{\lambda_3 t}\right) = \frac{\lambda_1 \lambda_2}{\lambda_1 - \lambda_2} N_{10} \left(e^{-\lambda_2 t} - e^{-\lambda_1 t}\right) e^{\lambda_3 t}$$

Integrating, $$N_3 e^{\lambda_3 t} = \frac{\lambda_1 \lambda_2}{\lambda_1 - \lambda_2} N_{10} \left\{ \frac{e^{(\lambda_3 - \lambda_2)t}}{\lambda_3 - \lambda_2} - \frac{e^{(\lambda_3 - \lambda_1)t}}{\lambda_3 - \lambda_1} \right\} + A$$

where A is the constant of integration.

Since $N_{30} = 0$, this at once gives

$$\frac{\lambda_1 \lambda_2}{\lambda_1 - \lambda_2} N_{10} \frac{\lambda_2 - \lambda_1}{(\lambda_3 - \lambda_2)(\lambda_3 - \lambda_1)} + A = 0$$

whence $$A = \frac{\lambda_1 \lambda_2}{(\lambda_3 - \lambda_1)(\lambda_3 - \lambda_2)} N_{10}$$

$$\therefore \quad (N_3)_t = \lambda_1 \lambda_2 N_{10} \left\{ A_1 e^{-\lambda_1 t} + A_2 e^{-\lambda_2 t} + A_3 e^{-\lambda_3 t} \right\} \tag{2.9.}$$

where, we have

$$\left.\begin{aligned} A_1 &= \frac{1}{(\lambda_2 - \lambda_1)(\lambda_3 - \lambda_1)} \\ A_2 &= \frac{1}{(\lambda_1 - \lambda_2)(\lambda_3 - \lambda_2)} \\ A_3 &= \frac{1}{(\lambda_1 - \lambda_3)(\lambda_2 - \lambda_3)} \end{aligned}\right\}$$

In the general case of n successive disintegrations, the number of atoms of nth nuclide, i.e., in the nth step, is

$$(N_n)_t = N_{10} \left(A_1 e^{-\lambda_1 t} + A_2 e^{-\lambda_2 t} + A_3 e^{-\lambda_3 t} + \cdots + A_n e^{-\lambda_n t} \right) \tag{2.9.}$$

where

$$\left.\begin{aligned} A_1 &= \frac{\lambda_1 \lambda_2 \lambda_3 \cdots \lambda_{n-1}}{(\lambda_2 - \lambda_1)(\lambda_3 - \lambda_1) \cdots (\lambda_n - \lambda_1)} \\ A_2 &= \frac{\lambda_1 \lambda_2 \lambda_3 \cdots \lambda_{n-1}}{(\lambda_1 - \lambda_2)(\lambda_3 - \lambda_2) \cdots (\lambda_n - \lambda_2)} \\ \cdots &= \cdots\cdots\cdots\cdots\cdots\cdots\cdots \\ A_n &= \frac{\lambda_1 \lambda_2 \lambda_3 \cdots \lambda_{n-1}}{(\lambda_1 - \lambda_n)(\lambda_2 - \lambda_n) \cdots (\lambda_{n-1} - \lambda_n)} \end{aligned}\right\}$$

2.10 Radioactive equilibrium

An *equilibrium*, by definition, refers to the condition in which the *time-derivative* of a function *vanishes*.

Applying the above condition to different radioactive nuclides of a chain, it would mean that the number of atoms of a nuclide in the chain *does not change with time*.

Scanned with CamScanner

Mathematically, from the set of equation (2.9.1), the conditions of equilibrium are:

$$\left.\begin{aligned} \frac{dN_1}{dt} &= -\lambda_1 N_1 = 0 \\ \lambda_1 N_1 &= \lambda_2 N_2 \\ \lambda_2 N_2 &= \lambda_3 N_3 \\ \cdots &= \cdots\cdots\cdots \\ \lambda_{n-1} N_{n-1} &= \lambda_n N_n \end{aligned}\right\} \qquad (2.10.1)$$

Secular equilibrium — Plainly, the first equation of the above set (2.10.1) is a contradiction, for it implies $\lambda_1 = 0$. So the *condition of equilibrium cannot be satisfied rigorously*.

A state *very close to equilibrium* however can be attained if the parent substance is very long-lived, i.e., decays much more slowly compared to the other nuclides in the chain. N_1 then can be taken as nearly constant and $\lambda_1 \ll$ other λ's in the chain. Under this condition, the first equation of set (2.10.1) is a good approximation but the other conditions hold good rigorously. This type of equilibrium is called **secular** or **permanent equilibrium** and is given by the condition

$$\lambda_1 N_1 = \lambda_2 N_2 = \cdots = \lambda_{n-1} N_{n-1} = \lambda_n N_n \qquad (2.10.2)$$

$$\text{or,} \quad \boxed{\frac{N_1}{(T)_1} = \frac{N_2}{(T)_2} = \cdots = \frac{N_n}{(T)_n}} \qquad (2.10.3)$$

where $(T)_i$ is the half-life of the ith member of the given chain.

The relation shows that at *secular equilibrium, the rate of decay of any radioactive product is just equal to its rate of production from the previous member in the chain.*

Approach to secular equilibrium — Consider a case where the *parent is long-lived* and the *daughter is short-lived*. Suppose also that the daughter has been separated from the parent so that the former is initially pure.

In this case, $\lambda_1 \simeq 0$ and also $\lambda_1 \ll \lambda_2$. $\quad \therefore \quad e^{-\lambda_1 t} \simeq 1$

$\therefore$ From the decay equation, $\quad (N_1)_t \simeq N_{10}$

And, from the relation (2.8.7), we obtain

$$(N_2)_t \simeq \frac{\lambda_1}{\lambda_2} N_{10}(1 - e^{-\lambda_2 t})$$

$$\text{or,} \quad \lambda_2 (N_2)_t \simeq \lambda_1 N_{10}(1 - e^{-\lambda_2 t}) \qquad (2.10.4)$$

Equation (2.10.4) expresses the activity $\lambda_2 N_2$ of the daughter as a function of time in terms of the activity ($\sim$ constant) of the parent.

Note that as t increases, the number of daughter atoms, and also its activity, increases exponentially with time. This was actually noted by Crookes during his experiments with UX.

If the *period of observation is long* enough *compared to the half-life* of the daughter, $t \gg (T)_2$, then

$$(N_2)_t = \frac{\lambda_1}{\lambda_2} N_{10} = (N_2)_\infty, \text{ say.}$$

That is, the number of daughter atoms attains a constant value $(N_2)_\infty$ after a time $t \gg (T)_2$. During this period, $(N_1)_t = N_{10}$ is also *practically* constant.

$$\boxed{\frac{(N_2)_\infty}{(N_1)_t} = \frac{(N_2)_\infty}{N_{10}} = \frac{\lambda_1}{\lambda_2} = \frac{(T)_2}{(T)_1}} \qquad (2.10.5)$$

The condition of *secular equilibrium* is thus established.

From the relation (2.10.5),

$$\lambda_1 N_{10} = \lambda_2 (N_2)_\infty \qquad (2.10.6)$$

which shows that although the number of daughter atoms in equilibrium i.e., $(N_2)_\infty$ is small compared to the number of parent atoms $N_1 \simeq N_{10}$, both show equal activities.

For a chain of products in secular equilibrium,

$$\lambda_1 N_{10} = \lambda_2 (N_2)_\infty = \lambda_3 (N_3)_\infty = \cdots \qquad (2.10.7)$$

• Secular equilibrium is maintained so long the parent and the different products remain together. If any of the daughter products is separated from the parent, the product atoms would start growing again and attain a saturation value — a fact utilised in separating a product of comparatively smaller half-life from a very long-lived parent repeatedly.

• From (2.10.3), it is seen that in secular equilibrium, the ratio of the number of parent nuclei and daughter nuclei is constant, being equal to the ratio of their half-lives.

• The above point explains why the percentage of Ra contained in U was always found experimentally to be the same — 1 g of Ra per 3.2 tons of pure U on an average.

Transient equilibrium — Consider the case where the *parent is longer-lived compared to the daughter* ($\lambda_1 < \lambda_2$), but the half-life of the parent is *not very long*. Suppose also that the parent is initially (at $t = 0$) pure.

In this case, obviously the approximation $\lambda_1 \simeq 0$ is not valid.

From (2.8.7),

$$(N_2)_t = \frac{\lambda_1}{\lambda_2 - \lambda_1} N_{10} \left(e^{-\lambda_1 t} - e^{-\lambda_2 t}\right).$$

When t becomes very large, $\quad e^{-\lambda_2 t} \ll e^{-\lambda_1 t}$.

$$\therefore \quad \boxed{(N_2)_t = \frac{\lambda_1}{\lambda_2 - \lambda_1} N_{10} e^{-\lambda_1 t}} \qquad (2.10.8)$$

Scanned with CamScanner

This shows that the number of atoms of the daughter decreases with the half-life of the parent.

Since $(N_1)_t = N_{10}e^{-\lambda_1 t}$, we may re-write (2.10.8) as under.

$$\frac{(N_2)_t}{(N_1)_t} = \frac{\lambda_1}{\lambda_2 - \lambda_1} = \text{constant} \qquad (2.10.9)$$

Although both N_1 and N_2 decrease with time, the ratio however remains constant. This type of equilibrium is called **transient equilibrium** between the parent and the daughter.

∴ The ratio of activities at transient equilibrium is

$$\frac{A_1}{A_2} = \frac{\lambda_1(N_1)_t}{\lambda_2(N_2)_t} = \frac{\lambda_1}{\lambda_2} \cdot \frac{\lambda_2 - \lambda_1}{\lambda_1} = \frac{\lambda_2 - \lambda_1}{\lambda_2} \qquad (2.10.10)$$

Thus, the activity of the daughter is greater than that of the parent by a factor $\lambda_2/(\lambda_2 - \lambda_1)$.

The equations (2.10.8), (2.10.9) and (2.10.10) represent the *characteristics* of transient equilibrium between the parent and the daughter atoms.

Whether an equilibrium is secular or transient depends on the duration of our observation of the sample.

2.11 Branching of radioactivity

While discussing the different radioactive series, we came across of *branching*. The natural radio-elements disintegrate either by an α or a β-emission. In few cases, both α and β transformations occur for the same isotope with a definite *branching ratio* for the α and β-branches. For instance, in U-Ra series, RaC (Bi-214) suffers β-transformation more than 99% of the time and α-transformation only 0.04% of the time. These are the corresponding branching ratios.

When a radio-element shows both α and β-activities, there are definite probabilities of decay in the two branches. Let λ_α and λ_β be the decay constants for the branches. So the probability that in an interval dt, an atom will suffer α-disintegration is $\lambda_\alpha dt$. Similarly, $\lambda_\beta dt$ is the probability of its β-decay in the same interval dt. So the total probability of decay of an atom by both α and β disintegration is $(\lambda_\alpha + \lambda_\beta)dt$. If there are N number of atoms, the total rate of disintegration will be given by decay law as :

$$\frac{dN}{dt} = -(\lambda_\alpha + \lambda_\beta)N = \lambda N,$$

where $\lambda = \lambda_\alpha + \lambda_\beta$ = the total decay constant.

If $(T)_\alpha$, $(T)_\beta$ be the partial half-lives of decay by α and β-emission respectively,

$$\lambda_\alpha = \frac{0.693}{(T)_\alpha}; \quad \lambda_\beta = \frac{0.693}{(T)_\beta}$$

$$\therefore \quad \lambda = \lambda_\alpha + \lambda_\beta = 0.693\left(\frac{1}{(T)_\alpha} + \frac{1}{(T)_\beta}\right) \qquad (2.11.1)$$

But if T be the mean half-life of the substance, then $\lambda = 0.693/T$. So, from (2.11.1), we have

$$\frac{1}{T} = \frac{1}{(T)_\alpha} + \frac{1}{(T)_\beta} \qquad (2.11.2)$$

The ratio λ_α/λ and λ_β/λ are the *branching ratios* for the two branches.

Radon — In all the natural radioactive series, a radio-active isotope of element $Z = 86$ is produced which, at ordinary temperature, is a gas. In fact, it is the heaviest known inert gas similar to Ne, A, Kr etc. and is included in the last column of the periodic table. This isotope of element $Z = 86$ is known as *radon* (Rn).

2.12 Determination of constants of radioactivity

The constants of radioactivity λ, T, τ and A of a single, pure radio-nuclide are interrelated. If one is known, the others could be deduced. Usually, λ is evaluated experimentally. Various methods have been developed for the determination of radioactive constants. We give below, in outlines, a number of such methods.

1. **Direct method** — The activity A of a sample decreases exponentially with time according to the equation

$$A_t = A_0e^{-\lambda t}$$

$$\therefore \quad \ln A_t = \ln A_0 - \lambda t$$

$$\text{or,} \quad y = -\lambda t + c \qquad (2.12.1)$$

where $y = \ln A_t$ and $c = \ln A_0$.

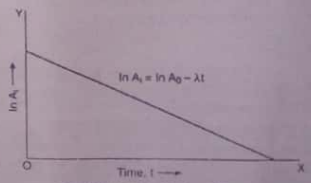

Fig. 2.11 Variation of ln A_t with time t

Scanned with CamScanner

Differentiating (2.12.1), we have

$$\frac{dy}{dt} = -\lambda$$

So when the logarithm of the activity, $\ln A_t$, is plotted against time t, it will give *a straight line with a negative slope* $-\lambda$ (Fig. 2.11). The method would thus give λ, provided we can measure the activity of the sample.

• This method is known as the *direct method*. The number of nuclides disintegrating per unit time at any instant t are obtained by finding the number of particles such as α, emitted by the sample per unit time at t. The counting rate of a Geiger counter, scintillation counter, etc. may be taken as a measure of the activity A_t of the sample at the instant of observation.

• The time-interval used to find the rate of emission of particles, in the experimental determination of activity, should be such that the number of disintegrating nuclides can be assumed to remain constant during the interval. The method is therefore suitable for *short* λ*-values*, e.g., radium. If the activity of the sample be very feeble, the *accuracy* of the method is *not very good*.

• Instead of evaluating λ, the half-life T can be found by plotting the activity against time and reading off from the graph the time corresponding to the drop of the activity to one-half of the original value (Fig. 2.1). Since $T = 0.693/\lambda$, the decay constant λ can be readily found.

2. From secular equilibrium — For *short* λ*-values*, evaluation of λ is also possible from the quantity of the substance in permanent equilibrium. The condition for such an equilibrium is, as we have already seen,

$$N_1\lambda_1 = N_2\lambda_2$$

Hence, if N_1, λ_1 and N_2 are known, λ_2 can be calculated. The decay constant of uranium has thus been determined from the known value of λ for radium.

3. From Geiger Nuttall law — *Another method* of evaluating λ, suitable for radio-nuclides having *extremely high* λ-values, is to use an empirical relation called the **Geiger-Nuttall law.** It connects the *range* R (to be discussed later) of α-particles with the decay constant λ of the corresponding radio-nuclide. Explicitly,

$$\ln\lambda = A + B\ln R$$

where the constants A and B have different values for different radioactive series. So λ can be evaluated from a determination of the range R of the emitted α-particles. This however is an *indirect* method.

4. From nuclear emulsion technique — For *long-lived* α*-emitters*, λ has been determined by the nuclear emulsion photographic technique. The emulsion of the plate is carefully impregnated with a known quantity of the radioactive substance. It is kept for a known interval Δt and developed, the tracks of α-particles are recorded in the plate and their number ΔN is counted under a suitable microscope. The λ-value is determined using the relation $\Delta N = -\lambda N\Delta t$.

5. Calorimetric method — For *long-lived* radioactive α-emitters, the *calorimetric method* is also used to evaluate λ. The method consists in absorbing all the α-particles within a calorimeter and the heat evolved after an interval Δt is measured. From a knowledge about the energy carried by each α-particle, the number ΔN of α-particles emitted in time Δt can be computed. Then λ is evaluated using the relation $\Delta N = -\lambda N\Delta t$.

6. Flow method — The methods described so far are not useful for *very short half-lives* ($\sim$ 1s). The *flow method* is suitable for gaseous substance with half-lives $\sim$ few seconds. It consists in allowing the gas to flow through a tube with a definite velocity v. Appropriate detectors of radiation are placed by the side of the tube, separated by known distances l. The time taken by the gas to flow from one detector to the next is given by $t = l/v$. The ratio by which the activity of the gas decreases (as measured by successive detectors) is equal to $e^{-\lambda t} = e^{-\lambda(l/v)}$ whence λ can be evaluated. This technique was used to determine the half-life of B-12 which is ~ 0.20 s.

7. Recoil distance method — The *recoil distance method* is used in determining *ultra-short half-lives* of radioactive substances. When the parent atom emits α or β-particles, there is a recoil of the daughter atom. If the daughter is radioactive, the recoil atoms disintegrate during their passage from the source at one end in an evacuated tube to the other. If the half-life is very short, the diminution in intensity of radiation (e.g., α or β) emitted by the recoil atoms may be measured by two successive detectors placed along the tube (Fig. 2.12). The half-life of RaC was determined by this method and was found to be 1.64×10^{-4}s.

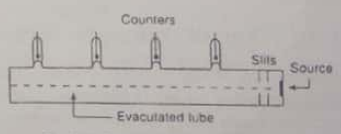

Fig. 2.12 Recoil distance method of measuring half-life

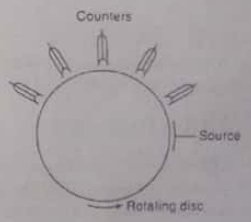

Fig. 2.13 Rotating disc method of measuring half-life

8. Rotating disc method — A similar method is the *rotating disc method* where the short-lived recoiling decay product gets deposited at one point on a rotating disc (Fig. 2.13). A number of detectors are spaced at regular intervals along the circumference of the disc. The disc is rotated uniformly say, anticlockwise and the deposited radioactive substance passes by the window of the detectors one after another in succession. The intensity of the emitted radiation decreases as the deposited source

Scanned with CamScanner

faces one detector and the next. The half-life of Po-216 was determined by this method and was found to be 0.158s.

9. Delayed coincidence method — The most suitable method of measuring *extremely short half-life* (10^{-3} s or less) is the *delayed coincidence method* where two detectors detect two correlated events that occur in a very short time-interval. For instance, when Bi-212 decays into Po-212 by a β-emission, the β-particle is detected by a β-detector. The daughter Po-212 decays with a half-life 3×10^{-7} s by an α-emission and the α-particle is detected by an α-detector. The electrical pulses, resulting from ionisation by β and α-particles, from the two detectors are mixed by delayed coincidence technique. The single pulse thus obtained is recorded electronically. Changing the delay-time between the pulses from the two detectors, the variation in the number of coincidence pulses is measured and a graph is plotted whence λ is determined.

• **Half-lives for complex decays** — We conclude the article by indicating briefly how one can determine *half-lives for complex decays*, e.g. the *two* half-lives when a sample contains a mixture of *two activities* A and B such that $T(A) \gg T(B)$.

A graph of the logarithm of the observed activity of the sample is first plotted against time, the observations however are extended over a time large enough compared to $T(B)$. The tail-end of the curve is due to the activity A, since the contribution from B in this region is negligible. So if the straight part of the graph is extrapolated to $t = 0$, the contribution to the total observed activity of the sample from A at any instant t can be found. Subtracting this activity of A from the observed total activity at t, we get the activity of B at t. Once the contributions from the two activities are known, their half-lives can be evaluated by the usual procedure. Figure 2.14 illustrates the statement.

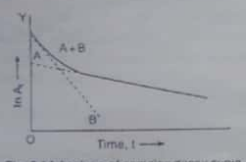

Fig. 2.14 Analysis of complex decay curve

2.13 Radioactive dating : Age of minerals, rocks etc.

The decay of radionuclides is independent of the physical and chemical conditions imposed on them. The decay of an individual nucleus however is a random process, but nevertheless the gross decay of many nuclei in a given sample provides a convenient way of measuring times. This is the basis of *radioactive dating technique*.

We shall describe hereunder some of the important methods that are used in radio-dating of geological, archeological and biological specimens.

A. Geological specimens

1. Lead-Uranium method — In 1913, Joly and Rutherford suggested that the age of geological specimens such as igneous rocks formed as a result of pre-historic volcanic eruption can be determined by making use of the activity of long-lived radionuclides, if any, present in the specimen.

Let a specimen contain a small amount of U-238 to start with. Each U-atom would steadily decay through a series of successive disintegrations with an atom of stable isotope Pb-206 as the end product. A look into the half-life of each of the intermediate products in the series shows that they are negligibly small compared to that of the parent ($= 4.5 \times 10^9$ years) U-atom. We may thus take, practically without error, the half-life of U as the half-life of the chain itself.

Let N_0 be the number of U-atoms present originally in the sample and t the age of the specimen. The specimen would thus presently contain

$$N_U = N_0 e^{-\lambda t} \text{ atoms of U-238} \qquad (2.13.1)$$

$$\text{and} \quad N_{Pb} = (N_0 - N_U) \text{ atoms of Pb-206} \qquad (2.13.2)$$

$$\therefore \quad N_U = (N_{Pb} + N_U)e^{-\lambda t}, \text{ using (2.13.1) and (2.13.2).} \qquad (2.13.3)$$

$$\therefore \quad \boxed{t = \frac{1}{\lambda} \ln \frac{N_{Pb} + N_U}{N_U}} \qquad (2.13.4)$$

The values of N_U, N_{Pb} can be determined experimentally by chemical or spectroscopic analysis of the specimen, and its age t could be estimated using (2.13.4). The value thus obtained is the *minimum* age of the specimen, for it is likely that some of the lead formed in the decay process may have already left the specimen through leaching.

This is an *older method* of radioactive dating and could be extended, with certain assumptions, to estimate the *age of the earth* itself : $(4.55 \pm 0.07) \times 10^9$ years.

2. Helium-Uranium method — This is very similar to the Pb-method. The α-particles emitted during successive disintegrations of U-238 atom get converted into neutral He-atom by acquiring orbital electrons and remain within the specimen. In the long period t, since solidification of the rock (mineral), measurable quantity of He-gas accumulates, and if this is evaluated, the age of the mineral is known.

Assuming the decay constant λ_U of U-238 as that of the chain itself,

$$N_U = N_0 e^{-\lambda_U t}$$

$$N_{He} = 8(N_0 - N_U)$$

(∵ 8 α-particles are emitted in the chain-disintegration)

where N_0 is the initial number of U-atoms in the sample and N_U, N_{He} are the atoms of U-238 and He-4 at the present instant.

$$\therefore \quad N_{He} = 8N_U(e^{\lambda_U t} - 1)$$

$$\therefore \quad e^{\lambda_U t} = \frac{8N_U + N_{He}}{8N_U}$$

$$\therefore \quad \boxed{t = \frac{1}{\lambda_U} \ln \frac{8N_U + N_{He}}{8N_U}} \qquad (2.13.5)$$

Scanned with CamScanner

Thus, by measuring the amount of helium gas in the sample containing a known amount of U-238, the age t of the mineral can be readily obtained from (2.13.5).

• Some of the helium gas may diffuse out of the specimen, and some helium gas from outside is likely to diffuse in, affecting the computation.

B. Archeological and biological specimens

3. Radio-carbon dating — The most *sensitive* method for estimating the ages of archeological and biological specimens is the *radio-carbon dating* due to Libby.

Plants use CO_2 from atmosphere to build up carbohydrates by *photosynthesis*. A small part of atmospheric CO_2 however contains radioactive carbon or radio-carbon, C-14, formed from N-14 of the atmosphere by bombardment of neutrons of cosmic rays. A part of carbon in plants is thus C-14 that makes them slightly radioactive. C-14 however disintegrates into N-14 through β-emission. All living organisms, subsisting directly or indirectly on plants, will also contain a small amount of C-14. Depending on the rate of production of C-14 in the atmosphere and the rate of its decay back into N-14 through plant-animal *carbon cycle*, an equilibrium is established with all living matter having a certain percentage of C-14. An analysis of carbon contents of fresh samples of wood from widely separated regions lend support to this view.

Libby suggested that once a living organism dies, no additional C-14 is taken in and that which is already within begins to decay with half-life 5,568 years, without replacement. Carbonaceous matter, e.g. petroleum that ceased to take part in carbon cycle for millions of years shows no trace of β-activity of C-14 and thus validates Libby's suggestion. The possibility of estimating the age of organic archeological samples thus opens up if it is assumed that relative proportion of C-14 in the sample just at death is the same as that in fresh samples to-day. The latter amount is 16.1 disint/min/g of carbon. If the dead sample gives N_t disint/min per g of carbon, then

$$N_t = N_0 e^{-\lambda t}$$

where N_0 = disint/min/g of carbon in fresh sample, λ = decay constant (obtained from half-life) of C-14 and t = age we wish to estimate.

• Carbon dating can be applied to estimate the ages of only those samples that contain a detectable amount of C-14, i.e. samples which are dead for not more than a few half-lives.

2.14 Radioactivity of light elements

Naturally-occurring radioactive series show that the active lowest Z-value is 81. But the radioactivity of lighter elements (i.e., low Z-values) has also been detected in nature. They have mostly *very high half-lives* and *very low abundances*. Naturally their activity is extremely low. Extensive testing of nuclear weapons has caused *nuclear pollution* of

the atmosphere by new radio-isotopes. The serious hazard from ^{90}Sr wih a half-life of 27.7 years deserves special mention. Some of the important radio-isotopes, mostly of the lighter elements are given below.

Table 2.2 : *Some radioactive lighter elements*

At. No. Z	Element	Mass No. A	Type of activity	Half-life T (Yr.)
1	H	3	β	12.26
6	C	14	β	5730
19	K	40	β	1.3×10^9
38	Sr	90	β	27.70
57	La	138	β	1.1×10^{11}
60	Nd	144	α	2.4×10^{15}
62	Sm	147	α	1.06×10^{11}
72	Hf	176	α	2.0×10^{15}
78	Pt	190	α	6.0×10^{11}

The radio-isotope ^{14}C is constantly being produced in the atmosphere due to the bombardment of ^{14}N by neutrons in the cosmic radiation. It is therefore being continuously replenished.

2.15 Illustrated Examples

► **Example 1.** *A radioactive sample has its half-life equal to* 60 days. *Calculate its* (i) *disintegration constant*, (ii) *average life*, (iii) *the time for* 2/3 *of the original number of atoms to disintegrate and* (iv) *the time for* 1/4 *of the original number of atoms to remain unchanged.*

Solution : (i) Since $T = 60$ days, $\lambda = 0.693/T = 0.693/60 = \mathbf{0.01155\ day^{-1}}$

(ii) Since $\lambda = 0.01155\ \text{day}^{-1}$, $\tau = 1/\lambda = 1/0.01155 = \mathbf{86.58\ days}$

(iii) Number to be disintegrated $= \frac{2}{3}N_0$. So the number to remain unchanged $= \frac{1}{3}N_0$

Thus, $N/N_0 = 1/3$.

∴ From the relation : $N = N_0 e^{-\lambda t}$, we obtain

$$1/3 = e^{-\lambda t} \Rightarrow \lambda t = \ln 3$$

$$\therefore \quad t = \frac{\ln 3}{\lambda} = \frac{2.3026 \times 0.4771}{0.01155} = \mathbf{95.1\ days}$$

Scanned with CamScanner

Chapter 4

Alpha, Beta and Gamma Rays

Alpha rays

4.1 Spectroscopic identification of α-particles

The α-particles were identified as He-nuclei by an elegant spectroscopic experiment conducted by Rutherford and Royds.

Experimental arrangement — A thin-walled glass bulb G contains some pure radon (^{222}Rn). The α-particles emitted from radon escape through the upper stem of G into a relatively thick-walled glass bulb T surrounding G (Fig. 4.1). T is sealed into G and ends at a capillary tube E. Inside the capillary, there are two sealed-in electrodes, P and Q, between which a discharge could be struck. The side tube D attached to T is connected to a mercury reservoir (not shown) that could be raised or lowered to bring the level of mercury in the lower part of T to any desired height.

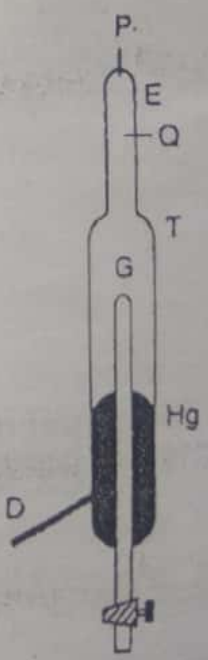

Fig. 4.1 Spectroscopic identification of α-particles

To start with, the region between G and E is evacuated to a high degree. The α-particles emitted from radon escape through G and are collected over mercury in the evacuated region between G and E. After a few days, the collected gas is compressed into the capillary E by adjusting the mercury level. Next a discharge is struck between the gas accumulated in E by applying a potential difference between P and Q. On analysing the light emitted by the discharge with a spectrometer, it is seen that the light exhibits the line spectrum of He-gas.

A blank experiment is performed earlier by filling G with helium gas when it cannot penetrate the wall of G. The possibility of any occluded helium in the source of α-particles is thus completely ruled out.

Scanned with CamScanner

It is thus confirmed that α-particles, because of their high velocity and small size, could penetrate the glass wall of G and are transformed into neutral helium atoms by gaining electrons from the glass walls, residual gas or the mercury vapour and give rise to helium lines.

Rutherford and Royds experiment proved conclusively that α-particles are nothing but doubly-charged helium ions (He^{++}).

4.2 Velocity of α-particles : Determination

The α-particles are emitted with very high velocity from radioactive substances. The velocity of α-particles from RaC′ is as high as 1.9×10^7 m/s which is 1/16 of the light velocity in free space.

The velocity of α-particles can be determined accurately by a magnetic spectrograph, with semi-circular focussing, designed by S. Rosenblum.

Apparatus — The arrangement is sketched in Fig. 4.2. To minimise the energy-loss of the particles, a very thin source — a fine wire S, thinly coated with α-emitter — must be used. A narrow beam of rays is defined by a system of slits A and is subjected to a uniform magnetic field at right angles to the direction of the beam. Under its influence, a slightly divergent beam of α-particles describes semi-circular trajectories

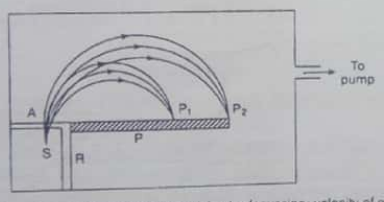

Fig. 4.2 Magnetic spectrograph with semicircular focussing: velocity of α-particles

to be focussed at a point (P_1 or P_2) on the photographic plate P. Trajectories starting at angles differing even by several degrees again come together after having 180° deflection. Since the slit has the appearance of a short line, a reasonably sharp line-image of the point source is formed on P. The whole apparatus is enclosed in an evacuated chamber.

Theory and results — Let v be the velocity of the α-particles, M be its mass, q the charge, r the radius of the track and B the magnetic field used. Then

$$Bqv = Mv^2/r$$

$$\therefore \quad \boxed{v = Bqr/M} \qquad (4.2.1)$$

Since r is known from the geometry of the apparatus, and other quantities are also known, the velocity v can be evaluated using (4.2.1).

The velocity of α-particles from most of the natural radioactive sources is $\sim 10^7$ m/s. With many elements, only *one* line is observed in the magnetic spectrum; with others, *two* or *more* closely spaced lines are obtained. In the former, all the α-particles have the same velocity (**mono-energetic**); the latter indicates the existence of two or more groups of α-particles, each with a given velocity (or energy).

• The kinetic energy, $E = \frac{1}{2}Mv^2$, can be computed from the velocity v and it is found to range from 5 – 10 MeV.

• Rutherford and others used the above method for determining the velocity (or energy) of α-particles, but replaced the photographic plate by an ionization chamber.

4.3 Range of α-particles

The most important property of α-particles is their ability to ionise the material (solid, liquid or gas) through which they pass. Let an α-particle course through a gas. As it moves, it ionises the gas particles by multiple collisions and thereby loses its energy gradually. Finally, when the energy falls below the ionisation potential of the gas, it stops ionising and gets converted, into neutral He-atom by capturing two electrons.

Range — The distance through which an α-particle travels in a specified material before stopping to ionise it, is called its *range* in that material. The *range* is thus a *sharply defined ionisation path-length*.

The range is highest in gases, less in liquids and the least in solids due to more and more dense packing of the particles. Blackett demonstrated such ranges of α-particles beautifully in his cloud chamber photographs (Fig. 4.3).

Fig. 4.3 Cloud chamber photograph of α-particles

Plainly, the *range in a gas, depends on* (i) the *initial energy* of the α-particle, (ii) the *ionisation potential* of the gas and (iii) the *chances of collision* between the α-particles and the gas particles, that is, on the *nature* and the *temperature* and *pressure* of the gas. With increase of pressure, the range decreases; it increases if the temperature of the gas is increased.

Measured in unit of *length*, the range in solids and liquids is very small $\sim 10^{-3}$ mm for α of few MeV. In a gas, it is few cm in length. The *range can also be expressed in unit of the mass* of the material. Let a cylinder of unit cross-section and length equal to the range R be drawn in the substance. The amount of matter in it is $R\rho$, where ρ is the density of the substance. In this case, *the unit of the range is mass per unit area* ($kg.m^{-2}$). Expressed in this unit, the range is of the same order of magnitude in different substances : solid, liquid or gas.

Scanned with CamScanner

4.4.1 Straggling of range : Stopping power

The α-particles of the same initial energy have more or less the same range in a given substance. However, a small spread in the values of ranges about a mean value is observed. This phenomenon is known as the **straggling of the range.**

If we measure the number of ions produced along the path of an α-particle and plot these values against the distance from the source, curve similar to that shown in Fig. 4.8 is obtained. Towards the end of the curve, the number of ions reaches a maximum and then steeply drops down to zero. The curve is called **Bragg curve** and the maximum A of the curve the **Bragg hump.** Thus the maximum number of ions is produced immediately before the particles stop ionising. This is due to the fact that

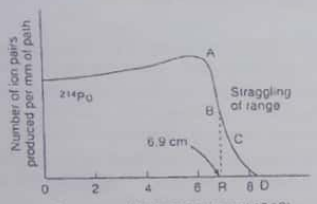

Fig. 4.8 Range of α-particles in air from ^{214}Po and straggling

the α-particles move slowly there and have more time to interact with the surrounding atoms and molecules. The point at which the ion-density sharply drops to zero value gives the range. The Bragg curve shows that the ionisation is fairly constant over the initial part and rises to the hump towards the end when the speed of the α-particles is diminished. Finally, when the energy of the particles falls below the ionisation potential of the gas, the curve steeply falls down. But the x-axis is not met abruptly. Near the end of the path it *tails off* and this is called **straggling.**

The fall in ion-pairs follows the straight line ABC which although steep has a finite slope. If all the α-particles with the same initial energy made equal number of collisions, then ABC would have dropped abruptly vertically downward to zero. The bent part CD is due to *straggling.*

Reasons for straggling — The straggling occurs mainly due to *two reasons* : (i) there is a *statistical fluctuation in the number of collisions* (which is a random process) suffered by the different particles about a mean value in travelling over a given distance, and (ii) there is also a *statistical fluctuation* about a mean value in the *energy loss per collision.*

There are *other factors* as well contributing to straggling such as multiple scattering of the particles during collisions, inhomogeneity in density of the absorber and capture of electrons.

• Straggling of the range may also occur with other charged particles as well.

Stopping power — The energy of α-particles progressively decreases as they pass through increasing thicknesses of matter. The amount of energy-loss of an α-particle per unit path-length in the absorber i.e., $-dE/dx$, is called the *stopping power* of the absorber.

The *air-equivalent* of an absorber is the *thickness*, t_a, of *standard air* that produces the same energy-loss of α-particles as does a given thickness, t of the absorber placed in the path. The ratio t/t_a is called the *equivalent stopping power*, t_e. The **equivalent stopping power** *is thus the thickness of the absorber that produces the same energy loss* in the α-particle *as does unit thickness of standard air,* for since we have, from the definition

$$t_e = t/t_a, \Rightarrow t_e = t, \text{ when } t_a = 1.$$

The **relative stopping power**, S, is the ratio $1/t_e$. It is thus the ratio of the energy loss (of the α-particle) in traversing unit distance in the absorber to that in traversing unit distance in standard air.

The stopping power divided by ρ, the density of absorber, i.e., $-\frac{1}{\rho}\left(\frac{dE}{dx}\right)$ is called the **mass stopping power,** and the mass stopping power divided by the number of atoms per unit volume of the material is known as the **atomic stopping power** of the absorber.

• The contents of this Art. 4.4.1 is valid if the energy-loss of α-particles is small, as is the case with thin radioactive films.

4.5 Geiger-Nuttall law

An important *quantitative relation* between the range R of the α-particles and the decay constant λ of the emitting nuclei was obtained experimentally by Geiger and Nuttall and is called the **Geiger-Nuttall law.** The relation runs as :

$$\boxed{\ln \lambda = A + B \ln R} \qquad (4.5.1)$$

where A and B are constants having values different for different radioactive series. The Geiger-Nuttall law came to prominence as it enabled us to estimate the half-lives of common α-emitters that could not be determined easily experimentally. According to this law, α-particles emitted by substancces having larger λ (or shorter half-lives) have longer ranges and vice versa.

A plot of '$\ln \lambda$' against '$\ln R$' would thus give a *straight line,* the slope of which gives the value of B. For different radioactive series, different straight lines are obtained. They are essentially parallel to one another so that the value of B is the same for all of them, but A is different for different series. These graphs are often utilised to find λ (hence the half-life) of a radio-nuclide by evaluating R experimentally.

Scanned with CamScanner

In Fig. 4.9, the line 1 corresponds to U-series, the line 2 to Th-series and the line 3 to Ac-series.

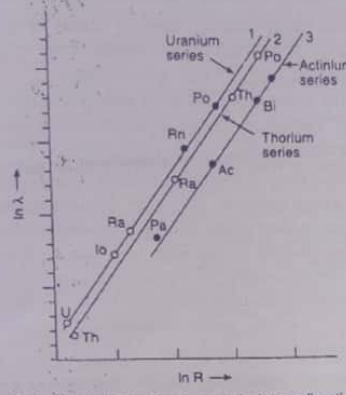

Fig. 4.9 Geiger-Nuttall law for α-emitters in three radioactive series

Since $R \propto E^{3/2}$, the equation (4.5.1) may also be written in the form

$$\boxed{\ln \lambda = C + D \ln E} \tag{4.5.2}$$

where C, D are two constants. This relation may be looked upon as an *alternative form* of Geiger-Nuttall law.

- Since the half life $T = \ln 2/\lambda$, one can express the Geiger-Nuttall law also by relating the variation of $\log T$ with $\log R$ or $\log E$. Then also straight lines will be obtained but with negative slopes.
- The once empirical equation (4.5.1) was put on a sound theoretical basis by Gamow in his quantum mechanical explanation of the **tunnel effect** (see later).
- The Geiger-Nuttall relation however is *not very exact*. More accurate relations have later been obtained. For example, the $\log \lambda$-values of different isotopes of a given element (Z = constant) and the reciprocal of the velocities of the particles emitted from their nuclei are directly related. They represent straight lines for even-even nucleus.

4.6 α-disintegration energy : Fine structure of α-rays

Let us examine a single decay process, represented by the following equation, leading to the emission of an α-particle.

$$^{A}_{Z}\mathrm{X} \rightarrow {}^{A-4}_{Z-2}\mathrm{Y} + {}^{4}_{2}\mathrm{He} \tag{4.6.1}$$

The ejected α-particle can be identified as a He-nucleus by both chemical and physical means and the product nucleus Y chemically. The kinetic energies of the emitted α-particles are of the order of few MeV. This shows that the process is a *nuclear transformation*.

The Q-value (Ch. 6) of the decay process (4.6.1), known as the *α-disintegration energy*, is the total energy released in the disintegration process and is given by

$$Q_\alpha = (M_X - M_\alpha - M_Y)c^2 \tag{4.6.2}$$

where M's are the masses of the particles and c the velocity of light in vacuo.

For heavy nuclei, Q_α is positive; so the decay can occur spontaneously as it does. The kinetic energy T_α of the ejected α-particle can be obtained from the Q-value by the application of the laws of conservation of momentum and energy. Assuming the nucleus to be at rest during decay and that kinetic energies can be treated non-relativistically, we may write

$$0 = M_\alpha v_\alpha - M_Y v_Y \tag{4.6.3}$$

$$\text{and} \quad Q_\alpha = \tfrac{1}{2} M_\alpha v_\alpha^2 + \tfrac{1}{2} M_Y v_Y^2 \tag{4.6.4}$$

From (4.6.3) and (4.6.4), therefore,

$$Q_\alpha = \tfrac{1}{2} M_\alpha v_\alpha^2 \left(1 + \frac{M_\alpha}{M_Y}\right) = T_\alpha \left(1 + \frac{M_\alpha}{M_Y}\right)$$

$$\therefore \quad \boxed{Q_\alpha = T_\alpha (1 + M_\alpha/M_Y)} \tag{4.6.5}$$

Replacing the ratio of masses by the ratio of the mass numbers (i.e., $M_\alpha/M_Y = 4/(A-4)$, the disintegration energy expression becomes

$$\boxed{Q_\alpha = T_\alpha \frac{A}{A-4}} \tag{4.6.6}$$

where A is the mass number of the parent nucleus.

Usually, A is large so that from (4.6.6), $Q_\alpha \simeq T_\alpha$ i.e., the α-particle carries away most of the disintegration energy.

- The experimental values of T_α for the α-particles from a number of nuclei show that the maximum value of the energy always agrees with (4.6.5). But, for a given decay, there exists a *discrete spectrum* of α-particle energies, with groups of particles having slightly different energies, lower than that given by (4.6.5). The α-particles thus exhibit a *fine structure* in their energies. The phenomenon has been confirmed experimentally by Rosenblum using 180° magnetic spectrograph. The observed fine structure is attributed to the existence of *discrete energy levels in nuclei* and can be explained through Fig. 4.10. It represents the α-decay of the ground state (g.s.) of

Scanned with CamScanner

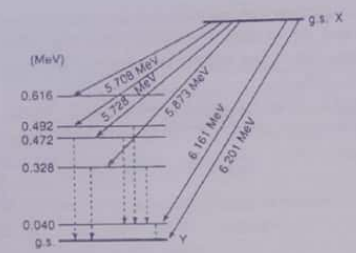

Fig. 4.10 Fine structure of α-particles and discrete energy levels

$X(^{212}Bi)$. The full line arrows indicate transitions leading to ejection of an α-particle with energies shown against each, while dashed arrows show emission of γ-rays. Like electrons, nuclei also have discrete spectra of excited states; so the α-decay would leave the nucleus Y either in the ground state (g.s.) or one of the allowed states of excitation. The kinetic energy T_α must thus have discrete values — the energy difference between the g.s. of X and a particular state in Y. When, however, Y falls from an excited state to its g.s. through electromagnetic transition, the energy difference appears as a γ-ray. The γ-rays are thus found to be associated with α-decay. There is also a correlation between the differences in the energies of the groups of α-particles emitted by the parent nucleus and the energies of the γ-photons the daughter emit.

∴ Energy of the γ-ray, E_γ is given by

$$\begin{aligned} E_\gamma &= Q_\alpha - (T_\alpha + T_Y) \\ &= Q_\alpha - T_\alpha(1 + T_Y/T_\alpha) \\ &= Q_\alpha - T_\alpha(1 + M_\alpha/M_Y) \end{aligned}$$

($\because T_Y/T_\alpha = \frac{1}{2}M_Y v_Y^2/\frac{1}{2}M_\alpha v_\alpha^2 = M_Y M_\alpha^2/M_\alpha M_Y^2 = M_\alpha/M_Y$, for $M_\alpha v_\alpha = M_Y v_Y$, from conservation of momentum).

• The presence of a small number of α-particles with energies much in excess of that of the main group of particles is called the *long range α-particles* discussed in the following article.

4.7 Long range α-particles

The α-particles emitted by radio-nuclides are usually monoenergetic which implies that they are emitted from a definite energy state of the parent to a definite state of the product. However, some radio-nuclides emit groups of α-particles, each of a definite energy. Clearly, this is possible only if transitions from different energy states, excited

or ground, of the parent-nuclide occur to different discrete energy states of the product nuclide.

Consider transitions from different excited states of the parent nuclide ^AX to the ground state (g.s.) of the daughter nuclide ^{A-4}Y (Fig. 4.11). Plainly, these α-particles have energies $E'_\alpha, E''_\alpha, \cdots$ etc. greater than E_α, the energy possessed by the *main group* particles due to transition from the ground state. These high energy α-particles are known as **long range α-particles.**

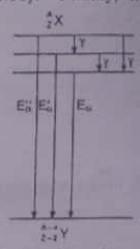

Fig. 4.11 Origin of long range α-particles

The intensities of long range α-particles however is much less compared to the main group particles. But why? Excited parent nuclides usually go down to their respective g.s. by γ-emission of different energies, either directly or stepwise, and then undergo α-disintegration. So the probability of γ-transitions are much higher than that of α-transitions from the excited state directly to the g.s. of the product nucleus. So the intensities of the main group particles are comparatively much higher.

This type of α-emission occurs only if *the half-lives of decay are very short* (e.g. ThC′). So, by Geiger-Nuttall law, α-energies must be fairly high. Hence the name *long range α-particles.*

4.8 An important feature of α-decay : Tunnel effect

There is yet another *important feature* of the α-decay process. The Coulomb force is a long-range force acting down to distances of the order of nuclear radii and is repulsive for like charges. It thus acts as a barrier that prevents a slow projectile from penetrating into the region where the short-range nuclear force, generally attractive, is effective. When an α-particle approaches a nucleus head-on, its kinetic energy gets converted into potential energy and is turned back by the nucleus at such a distance of approach where the conversion of K.E. to P.E. is complete. Calculations on this basis show that to approach the nuclear radius, say of ^{238}U, head-on, the α-particle must have an energy of 35.6 MeV.

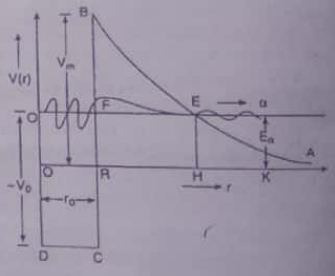

Fig. 4.12 Coulomb potential barrier for α-disintegration

Fig. 4.12 is the diagram of a potential curve obtained by plotting $V(r)$, the potential energy of an α-particle against r, its distance from the centre of ^{238}U-nucleus. Now, $V = V_m = BR$, the highest point on the curve, corresponds to $r = OR = r_0$, the

Scanned with CamScanner

nuclear radius. Inside the nucleus ($r < OR$), the V-value of an α-particle, whether it exists in the nucleus or formed (out of two protons and two neutrons) at the time of emission, is negative as the nucleons are tightly bound by the attractive nuclear force. As the details of nuclear force are lacking, the actual potential curve cannot be plotted for region $r < OR$ where, for simplicity, we assume P.E. to be constant and equal to $-V_0 = OD$. The discontinuity in the curve at $r(= r_0) = OR$ is given by the sudden drop in P.E. at this point. The α-particle has thus to cross a potential barrier of about 35.6 MeV to escape from or enter into the ^{238}U-nucleus. Plainly, the potential curve and its maximum height V_m depend on the nature of the nucleus and the approaching particle. For instance, the barrier presented by the same nucleus to a proton is less than that to an α-particle, and for an approaching neutron, the barrier is vitually non-existent.

Classically, therefore, emission of α-particles is possible only if it can climb the *potential hill* which is of 35.6 MeV for ^{238}U-nucleus. So to escape from the nucleus, the energy of the α-particle must be 35.6 MeV and this should appear as its K.E. when it is at distances $r \gg OR$. Experimentally, however, the kinetic energy T_α of α-particle emitted from ^{238}U-nucleus is about 4 MeV. This means that even when the total energy of the α-particle, $E_\alpha < V_m$, then also it can escape from the nucleus. In doing this, it crosses the region $OR < r < RH$ where P.E. exceeds the total energy, i.e. the K.E. is negative. Classically, this is an *utter impossibility*.

The problem was next attacked *quantum mechanically* by Gamow, Condon and Gurney. Using Schrodinger's equation, they showed that there is *a finite probability for an α-particle with energy less than the potential barrier to leak through* the barrier of thickness $OH - OR$ and appear on the outside (or conversely, for an external particle to enter the nucleus). This is known as the **tunnel effect**. The analysis shows that the *probability of penetration decreases with increasing width of the barrier and decreasing T_α*. Read also Gamow's theory from '*Quantum Mechanics*'.

4.8.1 Tunnel effect : An optical analogy

George Gamow gave a very interesting but simple optical analogy to explain the *tunnel effect*.

In refraction of light from a denser to a rarer medium, say from glass into air, if the angle of incidence exceeds the critical angle, *total internal reflection* occurs and no light penetrates into the second medium. But it can be shown, from wave optics, that the incident light waves are not totally reflected from denser-rarer interface but penetrates into the rarer medium to a depth of several wave-length (Fig. 4.13(a)). The original light breaks into many components, penetrate to different depths and then come back as reflected light. However, if another glass-piece be placed under the first (Fig. 4.13(b)) so that the thickness of air layer is only a few wave-lengths, some light enters the air layer and reach the surface of the second glass-piece and form in it a light beam parallel to the incident one as shown. The intensity, of course, decreases with increasing thickness of air-layer and becomes insignificant when the air-layer is several wave-lengths thick.

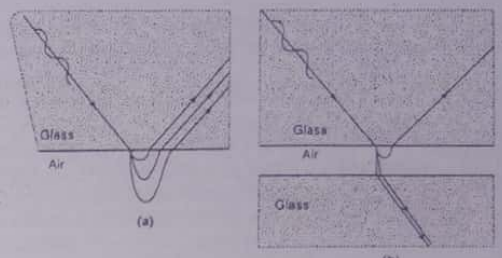

Fig. 4.13 (a) Total reflection of light from glass-air interface, (b) Partial penetration into another glass-piece

Similarly, for a particle with energy E falling on a potential barrier of height U where $U > E$, classical mechanics dictates that the particle cannot enter the region occupied by the potential barrier. But if the motion of the particle is guided by de Broglie waves, the situation is analogous to that of the total internal reflection, the potential barrier plays the same role as the air layer between the glass-pieces. One can think that de Broglie waves incident on a potential barrier will in part be reflected from the boundary and penetrate in part into the barrier and reach the other side to come out of the boundary (Fig. 4.14). As in optical case, the intensity of de Broglie waves

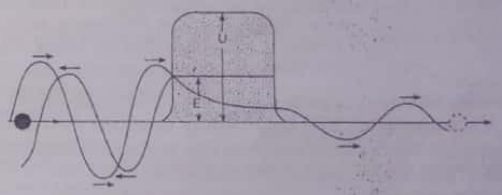

Fig. 4.14 Partial reflection and partial transmission of de Broglie waves falling on a potential barrier of U > E

passing out of the barrier is negligible if the barrier layer exceeds several wave-lengths in width. So the number of particles leaking through the barrier will also be very small, since the number of particles guided by de Broglie waves is proportional to the intensity.

• **Tunnel effect explains differences of half-life:** The leakage of de Broglie waves through the potential barrier thus opens up the possibility for escape of α-particles. For example, in U-nucleus, calculations show that α-particle has only *one chance* in 10^{38} to come out of the barrier. Now the velocity of α-particles inside the nuclear prison is $\sim 10^9$ cm/s while the nuclear size is $\sim 10^{-12}$ cm. So the number

Scanned with CamScanner

of collisions per sec with the surrounding walls is $\sim 10^{21}$. Hence the time required to come out is $10^{38}/10^{21} = 10^{17}\text{s} \simeq 3 \times 10^9$ years. Indeed, the life time of U is billion of years.

For RaC', the half-life however, is ~ 0.0001s. This is because α-particle in RaC' nucleus has (it can be shown), *one* chance out of 10^{17} to come out. This *increase in probability* is due to *two* reasons : (i) less height of potential barrier due to less electric charge of RaC' nucleus, and (ii) energy of α-particle of RaC' is almost twice that of α-particle of U. So, the time required for α-particles to come out is $10^{17}/10^{21} = 0.0001$s.

Tunnel effect can thus account for the great differences in half-lives among the radio-elements.

4.9 Gamow's theory of α-decay

Any successful theory of α-decay must (i) *derive an expression for* λ, the decay constant, (ii) *explain* the phenomenon of *α-emission* and (iii) *obtain a relation showing a dependence of λ on the energy E* of α-particles similar to that of Geiger and Nuttall. Gamow's theory in this context is worth discussion as it explains α-emission on the basis of *tunnelling*, derives quantum mechanically an expression for λ and also shows a dependence of λ on E in a manner very similar to Geiger and Nuttall.

The α-particle inside the nucleus moves back and forth with velocity v along the radius and will arrive at the barrier ($r = R$), $v/2R$ times per second.

$\therefore$ The *frequency* of its hitting the barrier, $\omega = \dfrac{v}{2R}$

The rate of emission of α-particles, i.e. the decay constant, λ, would then be

$$\lambda = \omega P$$

where P is the *probability of penetration* of the potential barrier.

The α-particle moving with large velocity inside the nucleus behaves wave mechanically as a wave with large amplitude that gets attenuated exponentially between $R \le r \le b$. If $\psi(r)$ be the wave function representing such a wave at r, the *transmission* or *penetration probability*

$$P = \left\{|\psi(r)|^2\right\}_{r=R}^{r=b}$$

The Schrödinger equation for s wave of the α-particle of mass m and charge ze moving with potential energy $V(r)$ at r to a point at $r = b$ with energy eigenvalue E may be written as

$$\frac{d^2\psi}{dr^2} + \frac{2m}{\hbar^2}(E - V)\psi = 0 \qquad (4.9.1)$$

Its solution gives the probability of barrier penetration of the form $P = e^{-\gamma}$.

Let $\psi(r) = e^{-y(r)/\hbar}$ so that we obtain

$$\frac{d\psi}{dr} = -\frac{1}{\hbar}(e^{-y/\hbar})\frac{dy}{dr}; \quad \frac{d^2\psi}{dr^2} = \frac{1}{\hbar^2}e^{-y/\hbar}\left(\frac{dy}{dr}\right)^2 - \frac{1}{\hbar}e^{-y/\hbar}\left(\frac{d^2y}{dr^2}\right)$$

Substituting $d^2\psi/dr^2$ in Schrodinger equation (4.9.1), we obtain

$$\left[\frac{1}{\hbar^2}e^{-y/\hbar}\left(\frac{dy}{dr}\right)^2 - \frac{1}{\hbar}e^{-y/\hbar}\left(\frac{d^2y}{dr^2}\right)\right] + \frac{2m}{\hbar^2}(E - V)e^{-y/\hbar} = 0$$

$$\Rightarrow \quad \left(\frac{dy}{dr}\right)^2 - \hbar\left(\frac{d^2y}{dr^2}\right) + 2m(E - V) = 0$$

$$\Rightarrow \quad \left(\frac{dy}{dr}\right)^2 = 2m(V - E) \qquad (4.9.2)$$

since $\hbar(d^2y/dr^2)$ is negligible compared to $(dy/dr)^2$.

$$\therefore \quad \frac{dy}{dr} = \pm\sqrt{2m(V - E)}$$

$$\Rightarrow \quad y = \int \sqrt{2m(V - E)}\, dr$$

taking the positive sign only as the α-particle is supposed to be in the nucleus and th chance of finding it at $r = b$ *is much less than at* $r = R$.

Substituting $\psi = e^{-y/\hbar} = e^{-\frac{1}{\hbar}\int\sqrt{2m(V-E)}dr}$, we obtain the *penetration probabilit*

$$P = \left\{\left|\psi(r)^2\right|\right\}_{r=R}^{r=b} = e^{-\frac{2}{\hbar}\int_R^b\sqrt{2m(V-E)}dr} = e^{-\gamma}$$

where $$\gamma = \frac{2}{\hbar}\int_R^b \sqrt{2m(V - E)}dr = \frac{2}{\hbar}\sqrt{2mE}\int_R^b \left(\frac{V}{E} - 1\right)^{\frac{1}{2}} dr$$

$$= \frac{2}{\hbar}\sqrt{2mE}\int_R^b \left(\frac{b}{r} - 1\right)^{\frac{1}{2}} dr \qquad \left[\because \frac{V}{E} = \frac{Zze^2}{r}\cdot\frac{b}{Zze^2} = \frac{b}{r}\right]$$

$$= K\int_R^b \left(\frac{b}{r} - 1\right)^{\frac{1}{2}} dr, \text{ where } K = \frac{2}{\hbar}\sqrt{2mE}$$

Substituting $r = b\cos^2\theta$ and $R = b\cos^2\theta_0$, we have $dr = -2b\cos\theta\sin\theta d\theta$,

$$\therefore \quad \gamma = K\int_{\theta_0}^0 \left(\frac{b}{b\cos^2\theta} - 1\right)^{\frac{1}{2}} (-2b\cos\theta\sin\theta)d\theta$$

$$= -2bK\int_{\theta_0}^0 (1 - \cos^2\theta)^{\frac{1}{2}}\sin\theta d\theta$$

$$= -2bK\int_{\theta_0}^0 \sin^2\theta d\theta$$

$$= -2bK\int_{\theta_0}^0 \tfrac{1}{2}(1 - \cos 2\theta)d\theta$$

$$= -2bK\left|\frac{1}{2}\theta - \frac{1}{2}\frac{\sin 2\theta}{2}\right|_{\theta_0}^0 = bK(\theta_0 - \sin\theta_0\cos\theta_0) \qquad (4.9.3$$

Scanned with CamScanner

Now, since $R = b\cos^2\theta_0$, $\cos\theta_0 = \sqrt{R/b} \Rightarrow \sin\theta_0 = \sqrt{1 - R/b}$

$$\therefore \quad \gamma = \frac{2b}{\hbar}\sqrt{2mE}\left\{\cos^{-1}\sqrt{\frac{R}{b}} - \sqrt{\frac{R}{b}\left(1 - \frac{R}{b}\right)}\right\} \qquad \left(\because K = \frac{2}{\hbar}\sqrt{2mE}\right)$$

$$= \frac{2b}{\hbar}\sqrt{2mE}\left[\frac{\pi}{2} - \sqrt{\frac{R}{b}} - \sqrt{\frac{R}{b}} + \text{higher powers of } \sqrt{\frac{R}{b}}\right]$$

($\because \sin^{-1}\theta = \theta - \theta^3/3! + \theta^5/5! + \cdots$; and $\sqrt{R/b} < 1 \Rightarrow$ higher powers of $\sqrt{R/b}$ negligible)

$$= \frac{2b}{\hbar}\sqrt{2mE}\left(\frac{\pi}{2} - 2\sqrt{\frac{R}{b}}\right)$$

$$= \frac{2Zze^2}{\hbar E}\sqrt{2mE}\left(\frac{\pi}{2} - 2\sqrt{\frac{E}{B}}\right) \qquad \left[\because b = \frac{Zze^2}{E}\right]$$

where B = Coulomb's potential barrier $= Zze^2/R$,

$$\therefore \quad \gamma = \frac{2Zze^2}{\hbar}\sqrt{\frac{2m \times 2}{mv^2}}\left(\frac{\pi}{2} - 2\sqrt{\frac{E}{B}}\right)$$

$$= \frac{4Zze^2}{\hbar v}\left(\frac{\pi}{2} - 2\sqrt{\frac{E}{B}}\right)$$

$$= \frac{8\pi Zze^2}{hv}\left(\frac{\pi}{2} - 2\sqrt{\frac{E}{B}}\right) \qquad [\because \hbar = h/2\pi]$$

$$= \frac{4\pi^2 Zze^2}{hv} - \frac{16\pi Zze^2}{hv}\sqrt{\frac{E}{B}} \qquad (4.9.4)$$

$$\therefore \quad \lambda = \omega P = \frac{v}{2R}e^{-\gamma} = \frac{v}{2R}\exp\left[\frac{16\pi Zze^2}{hv}\sqrt{\frac{E}{B}} - \frac{4\pi^2 Zze^2}{hv}\right]$$

$$\therefore \quad \ln\lambda = \ln\left(\frac{v}{2R}\right) - \frac{4\pi^2 Zze^2}{hv} + \frac{16\pi Zze^2}{hv}\sqrt{\frac{E}{B}} \qquad (4.9.5)$$

which shows the dependence of λ on E similar to that given by **Geiger-Nuttall law.**

The relation (4.9.5) can be used to find the half-life T.

$$T = \frac{\ln 2}{\lambda} = \frac{\ln 2}{(v/2R)e^{-\gamma}} = \frac{2R(\ln 2)}{v}\exp\left[\frac{4\pi^2 Zze^2}{hv} - \frac{16\pi Zze^2}{hv}\sqrt{\frac{E}{B}}\right], \quad \text{using (4.9.4).}$$

This shows that for higher energy of α-particles, the half-life T decreases.

Beta rays

4.10 Beta decay : Determination of β-energy

Both positive and negative electrons (positrons and negatrons) are emitted spontaneously from radioactive nuclei. The reverse process is the *electron capture* where the nucleus absorbs one of its own orbital electrons, mostly from the shell closest to it, the K-shell. This also comes under *β-decay* and is known as *K-capture*. In fact, all the above three processes are closely related, and are known as *β-decay*. In β-decay, there is no change in mass number, i.e., $\Delta A = 0$.

Now, the β-particles ejected from a radioactive source are *not monoenergetic*, but possess a range of velocities and hence a range of energies. The distribution or spread of these energies of β-particles is called the **β-ray spectrum** of the given nuclide. This distribution can be studied experimentally by deflecting them in a magnetic field. Such an arrangement is known as a *β-ray spectrometer*.

β-ray spectrometer — This apparatus, used by Rutherford and Robinson, is shown schematically in Fig. 4.15. The source of β-rays — a thin wire coated with radioactive material — is placed at A under a slit S, in the same horizontal plane as that of the supported photographic plate P on a lead block. The chamber housing these parts is highly evacuated. A uniform magnetic field is maintained over the region and is at right angles to the plane of the paper. Under its influence, the β-particles emitted from A would pass through the slit systems S and D and describe circular tracks, to be received finally on the plate P.

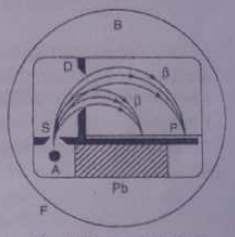

Fig. 4.15 β-ray spectrometer

Velocity determination — Let v be the velocity of a given β-particle, B the magnetic flux density, m the relativistic mass of the β-particle and r the radius of the track. Then, we have

$$\frac{mv^2}{r} = Bev \qquad (4.10.1)$$

$$\therefore \quad r = \frac{mv}{Be} = \frac{m_0}{\sqrt{1 - v^2/c^2}}\,\frac{v}{Be} \qquad (4.10.2)$$

where m_0 is the rest mass of the β-particle, c the velocity of light in vacuo and e the electronic charge.

Eq. (4.10.2) shows that the β-particles having the same velocity will move in circles intersecting at the plate P. For a wide slit, a given velocity of particles corresponds to a line formed at P; particles with higher energy (velocity) will have arcs of higher radii of curvature.

Scanned with CamScanner

If x be the distance between slit and the point of intersection P, and if $AS = h$,

$$(2r)^2 = h^2 + x^2$$

$$\text{or,} \quad \boxed{r^2 = \frac{h^2 + x^2}{4}} \tag{4.10.3}$$

Thus r can be easily measured and v could then be calculated from (4.10.2), using the known values of e, m_0, B and c.

Discussion — The photographic plate, when developed, shows that a region from the plate-end nearest the source up to a certain maximum distance is blackened *continuously*. The density of blackening however is not the same at all parts. This proves that the β-particles from various emitters have velocities (hence energies) varying *continuously* between *zero and a certain maximum* value.

Instead of photographic plates, a GM-counter could as well be used to count the emitted β-particles. From (4.10.2), we have, therefore

$$\text{momentum, } p = mv = Ber$$

Since $p \propto r$, the particles with higher velocities have larger radii, that is, they are focussed at a greater distance from the source. The number of β-particles of a given velocity can thus be counted by shifting the positions of the GM-counter. The counting confirms that the blackening of plate is from zero up to a certain maximum distance.

If E be the total energy of the β-particles, we have

$$E^2 = p^2c^2 + m_0^2c^4$$

$$\therefore \text{ Kinetic energy, } W_k = E - m_0c^2$$

$$= \sqrt{p^2c^2 + m_0^2c^4} - m_0c^2 \tag{4.10.4}$$

So the momentum, p and the kinetic energy, W_k become known from a determination of the velocity of the particles.

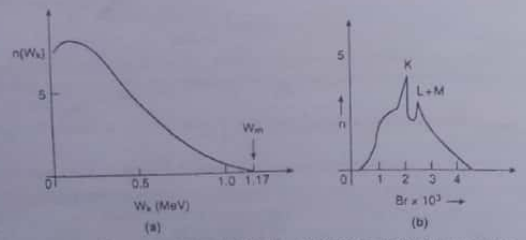

Fig. 4.16 (a) Energy distribution of β-particles, (b) Momentum distribution of β-particles

The distribution of the kinetic energy, W_k of the β-particles with the number of particles, $n(W_k)$, is shown in Fig. 4.16a. This is called the *continuous* β-*spectrum*. In Fig. 4.16b, instead of W_k, a plot of Br (which depends on W_k) has been made along the abscissa. It shows a number of sharp peaks K, L, etc. superimposed on the continuous background — the so-called *line spectrum* of the β-rays. The existence of *discrete well-defined lines* is also found in the photographic plate.

Nature of β-spectrum — The process of β-decay differs from α-decay in *two* important respects. *First*, the α-particle is composed of nucleons already present in the initial nucleus; in contrast, the electron *cannot be present within the nucleus* and must be created in the decay process itself. *Secondly*, unlike α-decay, the energy spectrum of the emitted electrons is *not only discrete* but is *also* found to be *continuous*. The magnetic deflection experiments with various β-emitters show that a single source produces β-particles with all energies (velocities) from zero up to a definite maximum W_m, characteristic of the nuclide, the so-called **end-point energy**. It is the *maximum energy with which a β-particle is emitted* from a radioactive nuclide. This is the *continuous β-spectrum*, the shape of which is generally the same for all nucleus.

Superposed on the continuous background, however, there is a number of discrete sharp lines (peaks) which are found to be very prominent on the photographic plate. This is the so-called *line spectrum* of the β-rays representing characteristic X-rays emitted following a K-capture or L, K etc.-capture, being obviously due to atomic re-adjustment caused by the vacancy in K or any other shell.

4.10.1 Energetics of β-decay

In all the *three* processes of β-*decay*, namely β^- decay, β^+ decay and orbital electron capture, the mass number A of the parent nucleus does not change, only the atomic number Z changes by one unit. ***In β^- decay***, Z increases to $Z+1$ and consequently the neutron number N decreases to $N-1$ since a neutron transforms into a proton. ***In β^+ decay***, on the other hand, Z decreases to $Z-1$ and N increases to $N+1$ due to the transformation of a proton into a neutron. In ***orbital electron capture*** however, like β^+ decay, Z reduces to $Z-1$ and N increases to $N+1$ as the process involves the transformation of a proton into a neutron.

So, for β^- **decay** : $\boxed{{}^{A}_{Z}X \rightarrow {}^{A}_{Z+1}Y + {}^{0}_{-1}e}$

The disintegration energy in β^- decay is therefore

$$\begin{aligned} Q_{\beta^-} &= [M_n(A,Z) - M_n(A,Z+1) - m_e]c^2 \\ &= [M(A,Z) - Zm_e - M(A,Z+1) + (Z+1)m_e - m_e]c^2, \\ &= [M(A,Z) - M(A,Z+1)]c^2 \\ &= M(A,Z) - M(A,Z+1), \text{ in energy unit} \end{aligned} \tag{4.10.5}$$

where M_n is the nuclear mass, M the atomic mass and m_e the mass of electron.

Scanned with CamScanner

$$\therefore \quad Q_{\beta^-} > 0, \text{ if } M(A,Z) > M(A,Z+1)$$

This implies that β^- decay occurs only if the mass of the parent atom is greater than that of the daughter atom.

Similarly, for β^+ decay : $\boxed{{}^{A}_{Z}X \rightarrow {}^{A}_{Z-1}Y + {}^{0}_{+1}e.}$

So, the disintegration energy in β^+ decay is

$$\begin{aligned} \therefore \quad Q_{\beta^+} &= [M_n(A,Z) - M_n(A,Z-1) - m_e]c^2 \\ &= [M(A,Z) - Zm_e - M(A,Z-1) + (Z-1)m_e - m_e]c^2 \\ &= [M(A,Z) - M(A,Z-1) - 2m_e]c^2 \\ &= M(A,Z) - M(A,Z-1) - 2m_e, \text{ in energy unit} \end{aligned} \qquad (4.10.6)$$

$$\therefore \quad Q_{\beta^+} > 0, \text{ if } M(A,Z) > M(A,Z-1) + 2m_e$$

which implies that β^+ decay is possible if the mass of the parent atom is greater than that of the daughter atom by *at least* twice the electronic mass, i.e. 2×0.51 or 1.02 MeV.

Finally, the **orbital electron capture** may be represented as

$$\boxed{{}^{A}_{Z}X + {}^{0}_{-1}e \rightarrow {}^{A}_{Z-1}Y}$$

$\therefore$ Disintegration energy, $Q_e = [M_n(A,Z) + m_e - M_n(A,Z-1)]c^2 - B_e$

where B_e is the binding energy of the electron to the orbit. Substituting for the nuclear masses, we therefore get

$$\begin{aligned} \therefore \quad Q_e &= [M(A,Z) - Zm_e + m_e - M(A,Z-1) + (Z-1)m_e]c^2 - B_e \\ &= [M(A,Z) - M(A,Z-1)]c^2 - B_e \\ &= M(A,Z) - M(A,Z-1) - B_e \end{aligned}$$

if the masses are expressed in energy unit.

$\therefore$ In electron capture, we have

$$Q_e > 0, \text{ if } M(A,Z) > M(A,Z-1) + B_e$$

This implies that the electron capture is possible if, and only if, the mass of the parent atom is greater than that of the daughter atom by *at least* the binding energy of the electron.

4.10.2 Difficulties in interpreting continuous β-spectrum

The β-ray spectrum appeared enigmatic and serious difficulties arose in interpreting the continuous nature of the β-spectrum. The main problem is that, like the α-decay, β-decay is also due to transition between two definite energy states (Fig. 4.17). The

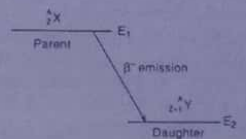

Fig. 4.17 β-decay is due to transition between two definite energy states

parent nucleus ${}^{A}_{Z}X$ emits a β-particle forming the daughter nucleus ${}^{A}_{Z+1}Y$. So, our expectation is that we shall have *monoenergetic* β-rays, but the observed spectrum is *continuous*, implying that all the electrons in β-decay do not possess the same kinetic energy. If we look into β-ray spectrum closely, the following points would show that the situation is indeed serious.

1. The nuclear energy states are discrete. So the continuous β-spectrum appears to be a violation of the *conservation of energy principle*.

2. When a β-particle is emitted with an energy W_k, the difference $W_m - W_k$ cannot be accounted for.

3. By placing the decaying nuclei in a delicate calorimeter with thick wall that stops the β-particles, the heat produced is related to the *average energy* and *not* to the *maximum energy*. The missing energy is thus *not* absorbed in matter immediately surrounding the emitter.

4. Attempts to explain the observed *continuous distribution* by way of loss of different amounts of energy due to scattering of β-particles in the source also failed.

5. The emitted β-particle also does *not* travel in the direction opposite to the recoil velocity of the daughter product. It thus appears to violate the *principle of conservation of linear momentum* also.

6. The β-emission from a radioactive nuclide is supposed to be the result of the transformation of either (a) or (b) below :

(a) $p \rightarrow n + \beta^+$

(b) $n \rightarrow p + \beta^-$

Since all the particles in the above two transformations are known to have half-integral spin, the law of *conservation of angular momentum* is also violated.

• It is important to note that the *end point energy* W_m is found to be the total energy available for disintegration by β-decay. For, the mass-energy of nuclear reaction is *exactly balanced* if the Q-value is made *equal* to W_m, the upper limit of W_k of the β-particles. Take the nuclear reaction

$${}^{210}_{83}\text{Bi} = {}^{210}_{84}\text{Po} + {}^{0}_{-1}e + Q$$

If $Q = W_m$ (= 1.17 MeV), the mass-energy of the reaction is balanced.

Scanned with CamScanner

For low values of Z, the Fermi function $F(Z,p)$ is *almost a constant* and in these cases, the number of β-particles with zero kinetic energy ($W_k = 0, p = 0$) becomes zero. For higher Z-values, however, $F(Z,p)$ is *not a constant* and this results in a relatively higher number of low-energy β^--particles; also, the number of β^--particles with zero kinetic energy is not zero. Due to the effect of $F(Z,p)$, the number of low-energy β^+-particles becomes relatively very small.

Interestingly, if instead of kinetic energy, we draw the graph by plotting the momentum, the number of β^+-particles with $p = 0$ becomes zero, even taking into consideration the effect of $F(Z,p)$.

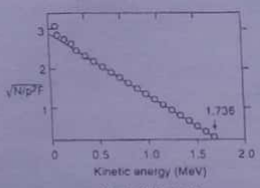

Fig. 4.19 Kurie plot

From equation (4.11.15), we obtain

$$\sqrt{N(p)/p^2F(Z,p)} = K(W_m - W_k) \quad (4.11.20)$$

where K is a constant.

So the graph of $\sqrt{N/p^2F}$ against W_k, the kinetic energy of the particle would be a *straight line*. Such plots, as shown in Fig. 4.19, are called ***Kurie plots*** and the function $\sqrt{N/p^2F}$, the ***Kurie function***.

The β^+-particles emitted from ^{15}O-nucleus give such a straight line experimentally. The abscissa of the point at which the graph cuts the energy axis gives the value of W_m, the maximum β-energy.

• The Fermi-and *GT-selection rules* can be understood from what follows. Electrons and anti-neutrinos are emitted without orbital angular momentum. They will carry no angular momentum if emitted with anti-parallel spins. If however they are emitted with parallel spins, they will carry a total angular momentum 1. In the first case, the spin of the nucleus *does not change* in β-decay $\Rightarrow \Delta I = 0$. In the second case, the vector difference between the initial and final angular momenta of nucleus must be 1 corresponding to $\Delta I = \pm 1$.

4.12 Electron capture or K-capture : Inverse β-decay

In some cases, as already indicated, the nucleus can absorb one of the orbital electrons of the atom, the process being opposite to that of β-decay. Since the electrons most likely to be captured are those closest to the nucleus, it is the K-shell electrons that are most often absorbed. Such *electron capture* is commonly known as K-*capture*. The captures of L- and M-electrons, though possible, are much less probable.

When K-capture occurs, the daughter obviously has a proton number one less than in the parent and the remaining electrons re-arrange themselves in the shells to correspond to the structure of the new atom. In the process, characteristic X-rays of the new atom, are emitted.

K-capture can be interpreted as :

$$p + e^- \rightarrow n + \nu$$

Since only two particles, neutron and neutrino, are produced, they should move off in opposite directions with equal and oppositely directed momenta to conserve the momentum. This assures that the neutrinos and the daughter nuclides move with definite energies. The energy spectra of the daughter nuclide as well as the neutrino are *monoenergetic* in character.

The β-decay of a proton in a nucleus, is given by

$$p \rightarrow n + e^+ + \nu \quad (4.12.1)$$

The electron capture (K-capture), on the other hand, is represented as

$$p + e^- \rightarrow n + \nu \quad (4.12.2)$$

Essentially, the reaction (4.12.2) is the same as (4.12.1), for the emission of a particle is equivalent to the absorption of its antiparticle.

Since, the absorption of an antineutrino is equivalent to an emission of a neutrino, the reaction

$$p + \bar{\nu} \rightarrow n + e^+ \quad (4.12.3)$$

involves the same physical process as that of (4.12.1).

The reaction (4.12.3) is known as the **inverse β-decay** and provides opportunities for establishing the actual existence of neutrinos. The probability of such reactions, however, is vanishingly small since the cross-section for the interaction of neutrino or antineutrino with nuclei is about 10^{-46} to 10^{-45} m^2. That is why neutrino freely traverses through space and matter indefinitely eluding detection.

• While a neutron can undergo negative β-decay *outside a nucleus* into a proton because its mass is greater than that of the proton, the relatively lighter proton however cannot be converted into a neutron *except within a nucleus*.

4.13 Parity is not conserved in β-decay

The concept of parity was introduced in Chapter 1 and a parity operator P was defined.

An even parity wave function on reflection about the origin gives

$$\psi(x,y,z) = \psi(-x,-y,-z)$$

$$\therefore \quad P = +1$$

Similarly, an odd parity wave function on such reflection gives

$$\psi(x,y,z) = -\psi(-x,-y,-z)$$

i.e., a change in sign occurs so that $P = -1$

Scanned with CamScanner

For a system of particles, the parity is the product of the parities of individual particles. Prior to 1957, parity was assumed to remain conserved in all nuclear interactions, implying that the mirror image of an object or process is not distinguishable from the object or the process itself. In 1957, Lee and Yang hinted at the non-conservation of parity in β-decay.

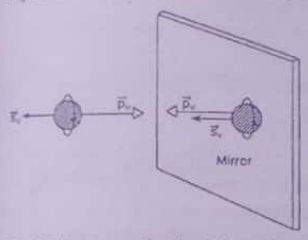

Fig. 4.20 Non-conservation of parity by neutrino

Let a neutrino travel towards a mirror with momentum $\vec{p}_\nu$; its spin $\vec{s}_\nu$ is directed opposite to $\vec{p}_\nu$ (Fig. 4.20). Plainly, the mirror image of the neutrino is a new particle—the antineutrino, for $\vec{s}_\nu$ and $\vec{p}_\nu$ are now in the same direction. Thus, the motion of the neutrino as given by the mirror image is not a possible motion for it; it refers to a different particle. This is known as *non-conservation of parity* by neutrino.

• We may as well discuss the matter from another point of view. The coordinates (x, y, z) of a physical quantity *change in sign* to become $(-x, -y, -z)$ on reflection at origin, e.g., components (p_x, p_y, p_z) of $\vec{p}$ on reflection become $(-p_x, -p_y, -p_z)$, so that $\vec{p}$ is a polar vector.

Now, we consider the angular momentum vector, $\vec{L} = \vec{r} \times \vec{p}$.

∴ Its component, $L_z = xp_y - yp_x$, and similarly we have for L_x and L_y.

Since on reflection both $\vec{r}$ and $\vec{p}$ change sign, $\vec{L}$ will suffer *no change in sign*. $\vec{L}$ is thus an *axial or pseudovector*. Vector and pseudovectors behave similarly for translation and rotation of a coordinate system, but on reflection they behave differently.

The scalar product of two polar or two axial vectors gives a scalar which remain invariant under reflection. But the scalar product of a polar vector and an axial vector gives a number that changes sign on reflection. These numbers are called *pseudoscalars*. If a pseudoscalar is obtained in an experiment, it follows that the mirror reflection of the experimental process is distinguishable from the process itself. So, *observation of pseudoscalar* quantity implies *non-conservation of parity*.

Wu and co-workers in 1957 conducted an experiment using the nuclei of β-emitter Co-60, designed specifically to detect a pseudoscalar in β-decay and they got it proving conclusively the non-conservation of parity.

4.14 Detection of neutrino

The inverse β-decay process

$$p + \bar{\nu} \rightarrow n + \beta^+$$

provides an opportunity of detecting the existence of neutrino (or antineutrino). The problem however is that the probability of such reactions is extremely small.

Fortunately, the availability of intense antineutrino flux in nuclear reactors made possible to carry out experiments to show antineutrino-nucleus interaction and thereby establish the existence of neutrino.

Reines and Cowan's experiment — Reines and Cowan first detected the existence of neutrino with experimental set up shown schematically in Fig. 4.21.

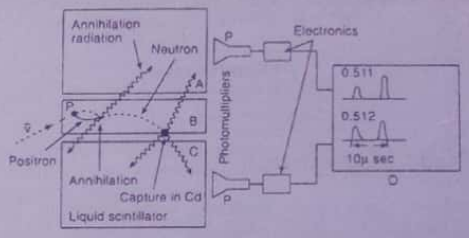

Fig. 4.21 Detection of neutrino : Reines and Cowan's experiment

B is a large liquid tank, called *target tank*, containing an aqueous solution of $CdCl_2$ acting as a source of hydrogen (proton) target nuclei and also as neutron-absorbing Cd-nuclei. A and C are two large *scintillation detector tanks* between which B is sandwiched. Although only one target tank and two scintillation detectors are shown, there are, in fact, two target tanks and three scintillation detectors so arranged that each target tank is surrounded by two scintillation tanks on either side.

Signals from scintillation tanks are observed by photomultipliers P, P and fed through a network of electronic circuits (coincidence circuit) to a double beam oscilloscope O.

The entire set up was shielded against neutrons and γ-radiations by surrounding it with lead-paraffin cover and placing it deep underground.

Action — The intense antineutrino beam from the reactor enters into the target tank B where the *antineutrino and proton interact*, resulting in inverse β-decay and thereby producing a positron and a neutron.

Soon after, the *positron* is annihilated with an electron and simultaneously two γ-photons are emitted. These photons produce scintillations in the scintillating counters and generate in the photomultipliers P, P two electrical pulses which are fed into the coincidence circuit.

The *neutron* undergoes repeated elastic collisions with *proton* in the target tank and loses energy. Thus slowed down, it is eventually *captured* by a Cd-nucleus (which has a high thermal neutron cross-section) in a (n, γ) reaction, resulting in the emission of few γ-photons which are also registered in the detectors.

The electronic device analyses the amplitude of the γ-pulses and records the coincidence displacement time. Reines and Cowan obtained two γ-pulses — a *prompt*

Scanned with CamScanner

pulse corresponding to the annihilation of the positron and a *delayed* pulse after few microseconds ($1 - 25\mu s$) due to the capture of neutron by Cd-nucleus.

Conclusion — This detection of simultaneous emission of a neutron and a positron by bombardment of hydrogeneous material (proton) with antineutrino proves that the inverse β-decay really occurred, demonstrating thereby the *existence of antineutrino*.

Gamma rays

4.15 Origin of the γ-rays

It is observed that γ-rays usually accompany α-and β-emission. Their origin can be explained on the basis of *quantized energy states of the nucleus*. Usually, when a nucleus decays by emission of α or β, it is left in an excited state. If it is not energetically possible for this nucleus to emit another particle then it decays by electromagnetic interaction. Thus, one way an excited nucleus can shed its energy of excitation is by emission of γ-rays and the excited nucleus returns to the ground state. The γ-decay is thus represented as

$$^{A}_{Z}X^{*} \rightarrow {}^{A}_{Z}X + \gamma$$

where the star ($*$) indicates an excited nucleus, and both the daughter and the parent have the same nuclear structure.

The other two eletromagnetic interactions are (i) internal conversion and (ii) internal pair production.

The γ-decay is governed by the principles of conservations of *linear momentum* and the *mass-energy*. For instance, if E^* be the energy associated with the excited state and E the energy of the ground state, then, neglecting the small recoil energy of γ-emitter,

$$E^* - E = h\nu$$

where ν is the frequency of the emitted γ-photon.

The energy of photons emitted by nuclei range in energy up to several MeV and are traditionally called *γ-rays*.

If the decaying nucleus is initially at rest, the conservation of linear momentum demands that it must recoil with a momentum p_N, equal and opposite to that of the emitted photon.

$$\therefore \quad p_N = \frac{h}{\lambda} = \frac{h\nu}{c}$$

where λ and ν denote respectively the wavelength and the frequency of the emitted γ-photon.

Most of the excited nuclei have very short half-lives against γ-decay, although few do have longer half-lives of several hours. *A long-lived excited nucleus is known as an isomer of the same nucleus in the ground state*, e.g. $^{87}_{38}Sr^{*}$ is an isomer of $^{87}_{38}Sr$.

- We have the following **selection rules** for γ-decay.

1. The γ-photon must carry away at least one unit of angular momentum.
2. Parity is always conserved in γ-decay.

Obviously, $\Delta\vec{I}$ for a γ-tansition cannot be zero since the intrinsic spin of the photon is one.

4.16 γ-ray spectrum

If the daughter nucleus finds itself in an excited state after the decay of the parent nucleus, and this is usually the case, then the resulting γ-rays emitted have well-defined energies corresponding to the two nuclear states involved in the transition. Such γ-rays are called **characteristic γ-radiation.**

Apart from the sharp characteristic *line spectrum* of γ-rays, there is also the *continuous γ-spectrum*. Its origin is very similar to that of the continuous X-ray spectrum. It is due to the radiation emitted when the β-particle gets accelerated in moving close to any nuclei during its passage through the emitter or any neighbouring material. The continuous γ-spectrum was discovered by Gray while bombarding different substances with β-particles from RaE.

The continuous spectrum may also originate from a re-adjustment of charges inside the nucleus due to β-emission. This was demonstrated by Wu who used ^{32}P, a β-emitter, with an end-point energy 1.71 MeV, without any accompanying characteristic γ-emission.

Internal conversion — Sometimes it happens that the excited nucleus returns to the ground state by giving up its excitation energy to the orbital electrons around it resulting in an electron emission. The phenomenon in which nuclear transition gets transferred *directly* to a bound electron of the atom is known as *internal conversion*. It is a process alternative to γ-decay. The electron that gets knocked out of the atom is called a *conversion electron*. If W be the excitation energy of the nuclei and W' the binding energy of the electron in the shell from which it is released, the kinetic energy W_k of the emitted electron would be

$$W_k = W - W'$$

Obviously, the difference in energies of the electrons released by a transition in the daughter nuclei should be equal to the difference between *X-ray energy levels* of the daughter nuclide. The vacancies in the shells will be filled up by outer electrons, giving rise to the characteristic X-rays. From the energy difference between groups of internal conversion electrons and the nature of the subsequently emitted X-photons, one can identify the daughter nuclide.

Scanned with CamScanner

• We have already studied the continuous β-spectrum. It is usually observed that continuous β-spectra are superimposed by discrete lines due to conversion electrons. Fig. 4.22 shows two internal conversion lines from Cs-137 along with the continuous β-spectrum.

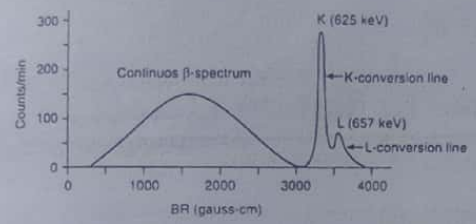

Fig. 4.22 Continuous β-spectrum of ^{137}Cs, showing K and L internal conversion lines

• While internal conversion was once wrongly looked upon as an *internal photoelectric effect* in which a nuclear photon is absorbed by an atomic electron, it is in better agreement with experiments to regard internal conversion as a *direct transfer of excitation energy* from a *nucleus* to a *bound electron*.

• If a given source emits N_γ gamma-rays and N_e conversion electrons during identical time-interval, then the *conversion coefficient*, α is defined as

$$\alpha = \frac{N_e}{N_\gamma}$$

$\alpha \equiv \alpha_K$ for K-conversion electrons, $\alpha \equiv \alpha_L$ for L-conversion electrons etc.

• A γ-photon may also be produced by the annihilation of an electron-positron pair, a phenomenon called *annihilation radiation* which would be discussed later.

4.17 γ-ray absorption in matter

The nature of absorption of γ-rays in matter is different from that of charged particles such as α- and β-rays. Whereas α- and β-particles lose their energy by inelastic collisions and slow down to rest, the γ-rays do not *slow down*; as they penetrate matter, there occur mainly *three processes* by which they get attenuated (absorbed). These processes are :

1. **Compton scattering** — where the loss of energy of γ-photons occur by way of collisions (scattering) with electrons;

2. **Photoelectric effect** — where the γ-rays act on the orbital electrons of the atom which absorbs the γ-photon and an electron from one of the shells is ejected.

3. **Pair production** — in which there occurs simultaneous creation of an electron-positron pair from a γ-photon, only in the presence of nuclear Coulomb field which helps

to balance energy and momentum, when the γ-photon has energy more than twice the rest mass energy, $2m_0c^2$, of the electron (1.02 MeV) :

$$\gamma \rightarrow e^- + e^+$$

The *three* factors should therefore be combined into *one* single (total) *absorption coefficient*, μ in the absorption law. The absorption coefficient μ is equal to the ratio between the fractional decrease in the radiation intensity, $-dI/I$ and the absorber thickness, dx.

$$\frac{dI}{I} = -\mu dx \qquad (4.17.1)$$

or, $$\boxed{I = I_0 e^{-\mu x} = I_0 e^{-x/l}} \qquad (4.17.2)$$

where I_0 is the initial intensity of the γ-beam, I the intensity of the beam after traversing a distance x in the absorbing medium. The quantity $l = \mu^{-1}$ is known as the *mean free path* or *relaxation length*.

• Of the *three processes* of attenuation of γ-rays, *all are not of equal importance* in all situations. The likelihood of the processes is energy-dependent. **At low photon energies**, below a few keV, the photoelectric effect dominates, the Compton effect is negligible and pair production is energetically impossible. There are definite thresholds for both photoelectric effect (several eV) and the electron-positron pair production (1.02 MeV). The probability of both Compton scattering and the photoelectric effect decreases with increasing energy of γ-photons; that of pair production however goes on increasing. **At high photon energies, the mechanism of energy loss of γ-rays is mainly the pair production.** The situation has been illustrated in Fig. 4.23.

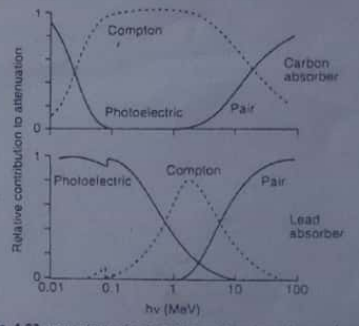

Fig. 4.23 γ-ray absorption in matter; relative importance of pair production, Compton effect and photoelectric effect

• The above equation (4.17.2) holds good only when (a) the γ-rays are monoenergetic, (b) the beam is collimated and of small solid angle, and (c) the absorber is thin.

Scanned with CamScanner

Chapter 3

Nuclear Radiation Detectors

3.1 Introduction

The understanding of the interaction of ionising particles and radiation in their passage through matter is the key to the design of a nuclear radiation detector that plays a vital role in studying the invisible micro-world of atomic nucleus. We shall restrict ourselves however only to a discussion of the main features of this interaction.

When a collimated beam of energetic particles passes through a material medium, the following *two extreme cases* deserve our attention : (i) where the particle suffers *many interactions*, losing each time a small amount of its energy and a small-angle scattering results, and (ii) where the particle either passes unaffected through the material or is simply removed from the beam in *one single encounter* — the 'catastrophic' encounter. These two cases are shown in Fig. 3.1a and b.

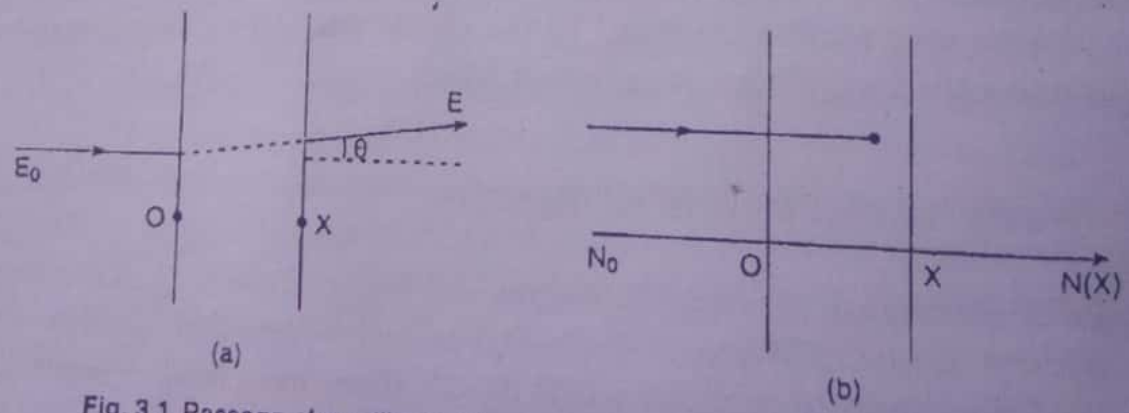

Fig. 3.1 Passage of a collimated beam of energetic particles through matter
(a) Each particle suffers many interactions
(b) The particle is either removed from the beam or passes unaffected

Case 1. When a particle suffers a large number of interactions, it progressively loses energy and a monoenergetic beam of such particles will show a *spread in energy* as illustrated in Fig. 3.2a.

The behaviour of a number of particles transmitted through the absorbing material as a function of the thickness of the absorber is shown in Fig. 3.2b. All particles are

Scanned with CamScanner

transmitted up to a certain thickness and at a thickness R_0, half of the particles are stopped. R_0 is called the *mean range* of the particle. At extreme thickness, all the particles are absorbed. The so-called fluctuations of the range is called *straggling* (see later for details).

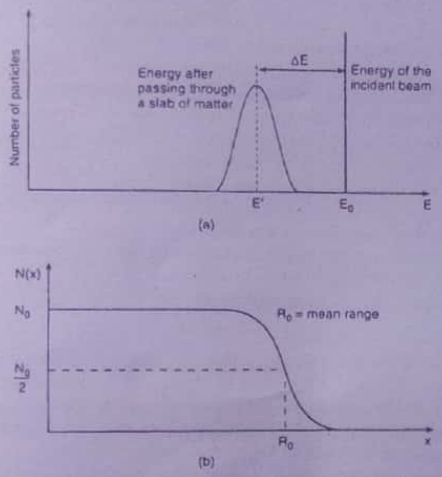

Fig. 3.2 (a) Energy spread of a beam of monoenergetic, heavy and charged particles after passing through matter
(b) Existence of range for a beam of heavy charged particles

Protons, α-particles, fission-products and such other heavy charged particles belong to this type, all having a fairly definite range in a gas, liquid or solid. While the energy-loss is by way of a large number of small interactions, the momentum of the particle is high enough for any significant change in direction. The energy-loss is mainly through excitation and ionisation of atoms in its path. The range is related to energy through *Geiger's law* (see later) and the *measurement of range* of heavy charged particles is a common technique to *evaluate their energy*. Fig. 3.3 shows that for the same energy, the range (in air) of α-particle is much shorter than that of proton since an α-particle is slower and carries more charge than a proton and hence more ionising.

The energy-loss per unit length $-dK/dx$ is known as the *stopping power* that varies with substances since their atomic levels are different. It is also affected by the density with substances since their atomic levels are different. It is also affected by the density ρ of the absorber as number-density of electrons is roughly proportional to density. For comparison of stopping power, therefore, we should use $-(dK/dx)/\rho$ instead of $-dK/dx$.

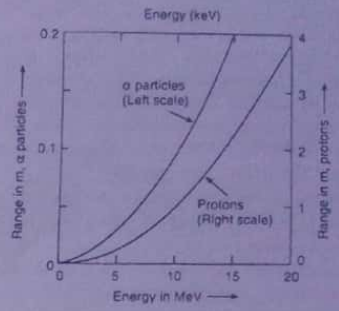

Fig. 3.3 Ranges of α-particles and protons in air at 15°C and 76 cm Hg pressure

Case 2. When the interaction removes the particle from the beam, the features of the transmittted beam are quite different from those described under Case 1. The transmitted beam has the same particle energy since the transmitted particles underwent no interaction. For each thickness dx of the material, the number of particles having interaction is proportional to the number of incident particles.

$$\text{i.e.,} \quad -\frac{dN}{dx} = \mu N(x) \tag{3.1.1}$$

where μ is called the *absorption coefficient*.

Integrating (3.1.1), $\boxed{N(x) = N_0 e^{-\mu x}}$

that is, the number of transmitted particles decreases exponentially (Fig. 3.4).

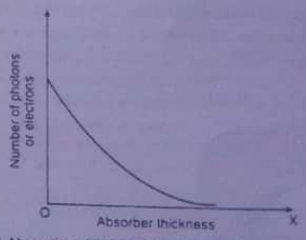

Fig. 3.4 Absorption of light particles like photons or electrons by matter

Unlike Case 1, no range is definable here; instead, we may define the so-called *mean free path* as the average distance covered by a particle before making a collision. The mean free path is thus $1/\mu$. *Electrons* and *photons* approximate to this behaviour.

Scanned with CamScanner

The slowing down of *electrons* with kinetic energies < 1 MeV is like the slowing down of heavy charged particles. This is mainly due to ionisation and excitation-collision processes. Electrons show no well-defined range since it is much lighter than proton and can be easily deflected from the direction of the original beam; also, a few collisions is enough to stop an electron. At K.E. > 1 MeV, the energy-loss of electrons is mainly due to production of *continuous X-rays*. With increase in energy, the probability of the process only increases.

Photons however interact with matter through the following *three main processes* : (i) *photoelectric effect*, (ii) **Compton effect**, and (iii) **pair production**.

In photoelectric effect, the photon is absorbed by the atom and an electron from one of its shells is ejected. In Compton effect, an atomic electron scatters the photon. And in pair production, the photon is converted into an electron-positron pair and the process occurs only in presence of nuclear Coulomb field that helps to balance the energy and the momentum.

The probability of the three processes is a function of the energy. At low energies (< 1 keV), the photoelectric effect is dominant, Compton effect is *negligible* and pair production is energetically *not possible*. For more details, read Chapter 4, Art 4.17.

• Quantitative measurements of ionising radiations are based on counting the individual particles and the determination of total radiation received in a given interval of time. The *principle of detection* of nuclear radiation may broadly be classified as : (i) method based on *the detection of free charge carriers* by the ionisation produced by them e.g. **ionisation chambers, proportional counters, Geiger-Muller counters** and **semiconductor detectors,** (ii) method based on *visualisation of the tracks* of radiation e.g. **Wilson's cloud chambers, bubble chambers, nuclear emulsion plates, spark chambers** etc. and (iii) method based on *light sensing* e.g. **scintillation counters, Cerenkov counters** etc.

There are, of course, hybridized detectors in which both the ionization and the light sensing method have been combined to satisfy special requirements.

3.2 Ionisation chamber

An extensive class of *particle detectors* exists that depends for their performance on the electric *pulse of current* produced when ions are formed by the passage of a *charged particle* between two electrodes maintained at a sufficient potential difference. These detectors are usually called *gas-filled detectors*, the simplest of which is the *ionisation chamber* described below.

Construction and action — An *ionisation* chamber essentially consists of a *closed vessel* having a *suitable gas* e.g. argon in which ions have rather long life-time and *two electrodes* maintained at a moderate (~ few hundred to few thousands) voltage. Commonly used chambers possess either *parallel-plate* geometry or *cylindrical* geometry. While in the former class, two parallel plates are separated by a distance, in the latter

a cylindrical conducting shell with a coaxial insulated metallic wire (dia ~ 1 cm) acts as electrodes.

In Fig. 3.5 where a typical ionisation chamber is shown schematically, one of the electrodes is the *outer metal cylinder* connected to the *negative terminal* of a dc-power supply and the other electrode is the *central straight wire* connected in series to a resistor R, to the *positive* of the power supply (220 V). The gas inside is maintained under some pressure to enhance the sensitivity of the instrument by providing more targets for the incoming colliding particles. A thin mica *window* W, provided in the chamber, allows photons or charged particles to enter the chamber and ionise the gas inside. The ions produced are attracted towards the respective electrodes due to the electric field maintained between them. A *voltage pulse* is thereby developed between A and B and is then amplified and registered.

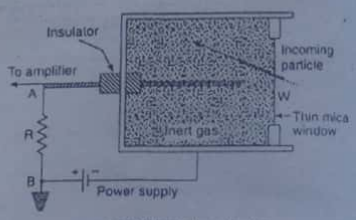

Fig. 3.5 Ionisation chamber

Fig. 3.6 gives the **voltage pulse vs. applied voltage** between the electrodes. The region AB, from a few volts to about 200 V, typically corresponds to ionisation chamber. In this region, all the ions produced by the incident particles or incoming photons are collected by the electrodes. Note that the *pulse height* between A and B is practically *independent* of the applied *voltage*. So the chamber *does not measure* the *energy* of the incoming particles. The *energy* deposition however is *proportional* to the *number of ions* produced and is a measure of the *charge* and the *velocity* of the particle. These then are the quantities an ionisation chamber measures.

The energy required to make an ion-pair is about 35 eV for air; but the ionisation produced by a single charged particle is very small. The chamber therefore detects *bursts of particles* rather than individual particles. It is however capable of distinguishing between bursts of α-particles and bursts of β-particles. Since x-rays and γ-rays readily ionise gases, they are also easily detected by an ionisation chamber.

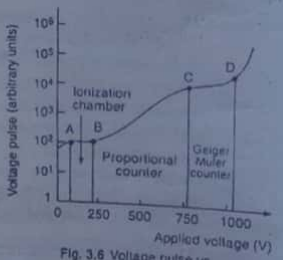

Fig. 3.6 Voltage pulse vs. Applied voltage

• An ionisation chamber is said to be, for a particular ionising radiation, *deep* or *shallow* according as it can completely absorb or not, the ionising radiation.

Scanned with CamScanner

3.3 Proportional counter

A second type of *gas-filled* detector, derived in a sense from ionisation chamber, is the *proportional counter*. Low energy ionising particles cannot be detected by an ionisation chamber since the voltage pulses they produce have very small amplitude. If the field between the electrodes be increased, it is possible to produce pulses of higher amplitude with such particles, utilising *gas multiplication*. This is done in a proportional counter.

Construction and action — It consists (Fig. 3.7) essentially of a metal chamber filled with a gas and having a thin wire of dia ~ 0.1 mm running *axially* along the centre. The *wire* acts as the *anode* and the *metal case* as the *cathode*, being connected to a power supply as shown. A voltage of 250–800 V which causes no discharge is applied

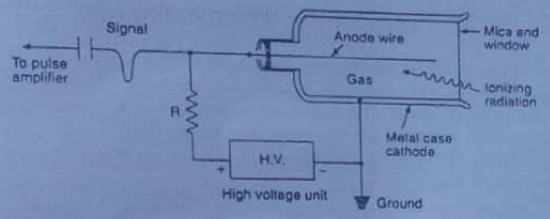

Fig. 3.7 "End window" type proportional counter

between the electrodes. Let now an ionising particle enter into the counter through the thin mica 'end window'. The electrons produced are attracted toward the central wire. In its vicinity, the electric field is very high compared to other regions. So, an electron near the anode-wire acquires sufficient kinetic energy between two successive collisions with gas atoms to ionise them to produce additional ion-pairs (*secondary ions*). The process is known as *gas multiplication* and the number of ions may increase by a factor of about 10^4.

The total amount of charge collected is thus greater than the original charge produced. The output pulse of the current is *proportional* to the number of ion-pairs formed by the ionising particle. The counter thus used is therefore termed *proportional counter*. By the IR-drop across the resistance R, the current pulse forms a *voltage pulse* which is amplified and recorded.

In Fig. 3.6, BC corresponds to the proportional counter region. In this region, the pulse height is practically proportional to the energy of the incident particle.

If the pulses are fed into an oscilloscope, the *pulse heights* could measure the *energies* of the ionising radiation. *Such information is of great importance* in the study of nuclear disintegration. The proportional counters may be accurately calibrated to give *distinctive voltage pulses characteristic of different particles* or they may be set to completely ignore some types of particles. With the help of such a counter, therefore,

it is easy to distinguish α-particles from β and the protons by the larger voltage pulses they produce due to greater electric charge.

• If the radius of the wire (anode) be a and that of the counter (cathode) be b, then the radial field E at any point distant r from the centre will be given by

$$E = \frac{V}{r \ln(b/a)} = \frac{k}{r} \qquad (3.3.1)$$

where V is the p.d. between the anode and the cathode, $k = V/\ln(b/a) =$ constant.

The field is thus very strong near the anode wire and the *avalanche production* (a very rapid increase in the number of ions) thus takes place near the central wire.

The potential difference V across the tube is given by

$$V = k \ln(b/a) = 2.3\, k \log_{10}(b/a) \qquad (3.3.2)$$

The potential gradient, dV/dr, can thus be calculated using (3.3.1), for different values of r.

• This counter not only counts the incoming particles, but is also capable of measuring the energy of the particles.

3.4 Geiger-Muller counter (GM-counter)

The chief among the gas-filled counters is the *Geiger-Muller counter* which is one of the *most versatile* instruments for *detecting* the ionising radiations *and measuring* their *energies*.

If the electrodes of a gas-filled counter are so shaped that there exists a high field near one of them even when a moderately high dc-voltage is applied to it, then the amplification of an ionic charge reaches, in the region of high voltage, an *avalanche condition*. Practically, all of the gas present in the local volume of the electrode gets ionised. This results in a *much larger voltage pulse* on the electrode. The pulse height is independent of the amount of ionisation originally produced by the particle. It depends only on the counter potential and increases with it. Only a single ion reaching the vicinity of high voltage electrode may trigger the process. This counter is very *simple to construct* and is *extremely sensitive* to the passage of charged particles.

Apparatus — It is similar in construction to proportional counters and consists of a *cylindrical metallic tube* TT inside which is fitted a *fine tungsten wire* CW, stretched *along its axis* and is mounted inside a *glass tube* GC.

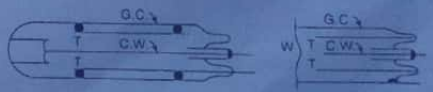

Fig. 3.8 Two common types of GM-counters

Scanned with CamScanner

Two common types of GM-counters are shown in Fig. 3.8. In the first, the particle enters the counter through the glass envelope, while in the second type, called *end-window GM-counter*, the tube has a thin mica sheet W at one end to serve as a *window*. The former is used for counting penetrating particles, the latter for less penetrating ones. In the window-type, the central wire CW does *not* extend throughout the length of the tube, but terminates at a point.

The counter is filled with an *inert gas* (e.g. monatomic argon which is transparent to UV-light), at a pressure of *few cm* (2-10) of mercury, together with a *trace of polyatomic organic vapour* (e.g. alcohol) acting as a *quenching agent* that quenches the initial discharge soon after it is initiated. The diameter of the tube varies, depending on the purpose of its use, from 1-5 cm and its length from 2-100 cm.

Action — The central wire CW acts as the anode and is mounted at so high a positive potential ($H.T.$), about 1000 V, with respect to the metallic cylinder TT (Fig. 3.9a) that acts as the cathode, that a discharge *just not* sets in. Then even a single ion-pair formed by a single incident particle can produce an electric discharge. The important fact is that the electric pulse produced in this discharge is the *same*, no mater what is the energy of the incident particle. The central wire is *very thin*, the electrical field in its vicinity is *very high*.

Let an ionising particle enter the GM-tube and produce one single ion-pair in the volume enclosed by the outer cylinder. The resulting electron would be rapidly accelerated towards the central wire and reach a relatively high velocity producing rapidly a large number of additional ion-pairs by *repeated collisions*. The new electrons are also accelerated and may in turn produce more ion-pairs. The process is cumulative and an *avalanche* occurs. A very large number of electrons reaches the anode which gets surrounded by the massive slow-moving positive ion sheath. The initial formation of a single ion-pair thus results in a *very large pulse of current* to the anode.

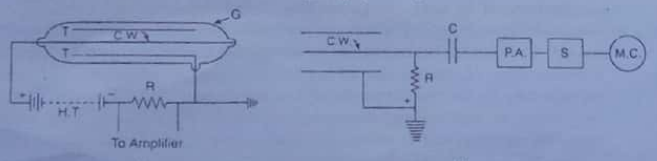

Fig. 3.9 (a) GM counter : conversion of current pulse into voltage pulse
(b) GM counter with an amplifying circuit and counting arrangement

Some free electrons on collision with argon atoms merely *excite* them which, on return to the normal state, emit photons. If a photon is absorbed by another excited atom, it may get ionised releasing electrons which produce further avalanches. The avalanche thus spreads rapidly in the *entire volume* of the counter and an amplification as high as 10^8 is attained. *The total number of ions is now 'independent' of the initial number of ions formed by the incoming particle.*

In a short time $\sim 1\,\mu s$, the space charge (i.e., positive ion-sheath) becomes enough dense to cancel the field round the anode, discharged and ionisation stops; positive ions are drawn to the cathode and the ionisation restarts. The time interval during which the ionisation remains suspended is known as the '*dead time*' of the counter as it is not then ready to receive another incident particle. Therefore, *some mechanism must be devised for quenching* (i.e., terminating) the *discharge after each event*.

Counting and quenching : The entry of a single particle in the counter triggers a pulse of current, independent of the energy and nature of the ionising particle. If a resistance R is connected in series in the circuit as shown in Fig. 3.9, the current pulse I produces a corresponding voltage pulse IR which is fed to a pulse amplifier $P.A$ through a capacitor C (Fig. 3.9b). The amplified pulse is finally passed on to a scalar S and a mechanical counter MC. The scaler records the arrival of each individual pulse separately, giving the exact number of particles entering the tube in a given interval.

The resistance R in the counter circuit not only provides a p.d. that can be amplified but also has another function. When a large current pulse occurs, the momentary voltage drop IR across the resistance *lowers* the tube voltage to $(V - IR)$ which is insufficient to maintain the discharge and the counter is said to be *quenched* or *dead*. This prolongs the time-interval before the counter may become ready to accept another fresh particle and pulse.

This time interval is called the '*dead time*' because the counter is unable to detect any ionising particle during this interval. The *sensitivity* of the counter depends largely on its dead time : ***the lesser the dead time, the greater is the sensitivity***. The traces of organic vapour like ethyl alcohol present in the tube, along with inert gas such as argon, *increase the sensitivity* of the counter considerably.

3.4.1 Some terms relating to GM-counter

Operating voltage — The operation of a GM-counter should be in the proper voltage region, the region CD in Fig. 3.6, between 800-1000 V. At such voltages, the tube operates in a plateau such that even with changes in applied voltage, the pulse height is practically constant, being independent of the number of ions formed in the tube. This is called the *Geiger region* which starts at *Geiger threshold voltage C*. The Geiger region is the normal operating region of a GM-counter and if it is exceeded, the tube may go to a *continuous discharge* with breakdown of the gas within it and may be ruined.

Self-quenching of GM-counter — A typical GM-counter contains 90% Ar and 10% alcohol. The ultra-violet photons from Ar on getting absorbed by alcohol cannot reach the cathode. As positive ions move towards the cathode they collide with alcohol molecules resulting in electron-transfer from alcohol to Ar to neutralise the latter. The alcohol molecules on arrival at the cathode dissociate rather than eject electrons. The discharge thus gets quenched. Such self-quenching by dissociation of organic molecules uses up the molecules after about 10^9 discharges, when a refilling of the counter is needed.

Scanned with CamScanner

It is also possible to use *halogen molecules* for quenching. The *advantage* is that they recombine after dissociation. If a diatomic (or polyatomic) gas such as Br is introduced in the tube, the positive Ar-ions in their *slow* motion to the cathode would have multiple collisions with Br-molecules and transfer their charge to them. Only neutral Ar-atoms would thus reach the cathode. Br-ions (*molecular*) in their turn reach the cathode, gain electrons, and move into excited states. The excited Br-molecules lose their excitation energy *not by photon emission* but *by dissociation* into Br-atoms. No spurious pulses are thus produced. In course of time, Br-atoms recombine into Br-molecules. Bromine thus quenches the discharge and the tube becomes ready to receive the next particle within 10^{-4} s.

Dead time, recovery time, resolving time — The *dead time* of a GM-counter is the time interval between the production of the initial pulse and initiation of second Geiger discharge. It is called *dead time* because during this period the counter is insensitive (dead) to further pulses. It is usually $\sim$ 50-100 μs and arises due to slow mobility of heavier positive ions from anode region to cathode. The presence of positive ion-sheath around the inner electrode lowers the electric field below the Geiger threshold, $V_{th}(= V_s)$.

As the ion-sheath moves towards the cathode, the field at the central electrode recovers quickly as the external resistance is usually small. *The time for recovery to threshold is the dead time.* The counter can record another ionising particle only after the field has been restored to a value above $V_{th}(= V_s)$. Since a finite pulse must be developed for the counter circuit to count it, the actual *resolving time* of the counter is slightly longer than the dead time.

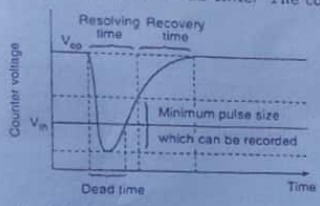

Fig. 3.10 Three time intervals associated with the operation of a GM-counter

The *recovery time* of the counter is defined as *the time interval for the counter to return to its original state to produce full sized pulses again*. Fig. 3.10 gives the three time-intervals – *dead time, resolving time* and *recovery time* – of operation of a GM-counter.

• The resolving time of a counter is often taken to be synonymous with dead time. During the resolving time, pulses are recorded but they are of smaller size. During dead time, a high flux through the counter should be avoided.

• **Expression for resolving time** — To determine the true counting rate of a GM-counter, its resolving time τ should be known. Plainly, the counter does not respond to ionising events that occur during τ. If n be the counting rate of a counter and N the actual rate of arrival of the particles in the counter,

$$N - n = Nn\tau$$

since the counter was insensitive for an interval $n\tau$ second, missing thereby $Nn\tau$ particles per second.

We, therefore, get

$$\boxed{N = \frac{n}{1 - n\tau}} \qquad (3.4.1)$$

From (3.4.1), we can find the *true* counting rate N from the *observed* counting rate n, if τ is known.

Determination of τ — By measuring separately the counting rates n_1' and n_2' with two radioactive sources 1 and 2 of nearly equal strength, τ can be determined. Let n_t' denote the total counting rate when both sources are placed in the same position as before and n_b be the background rate (i.e., with no source).

$$\therefore \quad n_1 = n_1' - n_b; \quad n_2 = n_2' - n_b; \quad n_t = n_t' - n_b \qquad (3.4.2)$$

where n_1, n_2, n_t are the above counting rates corrected for background.

If N_1, N_2 and N_t be the true rates of arrival of particles in the counter in the above three situations, we have, using (3.4.1)

$$N_1 = \frac{n_1}{1 - n_1\tau}; \quad N_2 = \frac{n_2}{1 - n_2\tau}; \quad N_t = \frac{n_t}{1 - n_t\tau} \qquad (3.4.3)$$

$$\text{Also,} \quad N_t = N_1 + N_2 \qquad (3.4.4)$$

Assuming the values of terms involving τ^2 to be negligible, we have, solving for τ

$$\boxed{\tau = \frac{n_1 + n_2 - n_t}{2n_1 n_2}} \qquad (3.4.5)$$

• **Usefulness and limitations** — This counter is *very simple* to construct and is *very sensitive* to the passage of charged particles. In fact, with a suitable counting circuit, it is one of the most *versatile detecting instruments*.

Two GM-counters are said to be *in coincidence* if they are so arranged that there is no response unless the radiation passes through both. Such an arrangement of GM-counters has been widely used in cosmic ray researches to scan the sky for studying the directional variation in the cosmic ray intensity at a given place. It is called a *cosmic ray telescope*.

Another method of connecting GM-counters is known as *anti-coincidence*. In this case, two counters are connected in such a way that the counts would be registered only when a ray goes through one counter or another but not through both. This arrangement has also been widely used in cosmic ray studies.

The counter however *does not distinguish between the types of particles, nor does it measure their energies*, because the magnitude of the pulse is independent of the nature or energy of the incoming particle. A proportional counter however does it. It is usually designed to count α-particles, β-particles, x-rays and γ-rays. The particles, however, could be distinguished by finding what absorber placed in their path can stop them to enter the tube.

Scanned with CamScanner

3.5 Neutron detection

Neutrons are *uncharged particles* and cannot therefore be deflected by electric or magnetic fields. Nor can they be produced by ionisation process. They do not cause fluorescence, nor produce cloud chamber tracks or emulsion tracks, nor trigger Geiger counters. For these reasons, special techniques are needed to detect neutrons.

Methods for detecting neutrons are based on some *intermediate nuclear reactions* involving neutrons in which charged particles capable of producing ionisation are released. The usual reaction is

$$^{10}_{5}B + ^{1}_{0}n \rightarrow ^{4}_{2}He + ^{7}_{3}Li$$

Each neutron interacting with a boron nucleus produces one α-particle and a lithium nucleus. The α-particle in its turn produces an ionisation track which can be used to detect *indirectly* the presence of neutron.

Thus a **neutron counter** must contain some gas that ionises after neutron-collision with its molecules. This is possible with *boron-trifluoride gas*, BF_3, in which the boron atoms produce α-particles which are detected in the usual manner. Neutron counters are thus either *ionisation chambers with electrodes coated with boron* or *proportional counters with BF_3 gas in it*.

A typical BF_3-counter consists of a cylindrical cathode, usually made of stainless steel, with an axial anode wire of tungsten of dia ~ 0.5 mm. The operating voltage ranges between 2000-2500 V at a gas pressure ~ 100-600 torr (1 torr = 1 mm of Hg). For greater efficiency of detection, the gas is prepared using boron, highly enriched in ^{10}B isotope.

The efficiency of a BF_3-counter depends on the energy of the neutron.

• He-3 *proportional counters* are also used as a *neutron detector*. The pulse-producing charged particles (protons) are produced in nuclear reactions induced by thermal neutrons in the nuclei of He-3 gas filling the counter. They *can be operated at higher pressures*. The *reaction cross-section* is also *larger*. These *two factors* make the He-3 proportional counters *more efficient* than BF_3-counters.

3.6 Spark chamber

A method of detecting high energy particle events is to use the *spark chamber*, developed by Fukui and Miyamoto. It is based on the simple fact that if the voltage across two metal plates few cm apart is increased beyond a limit, a breakdown in the form of sparking occurs. It combines some of the advantages of triggered track detectors and counters e.g., high resolution in space (cycling time 50/s) and also in time ($< 1\,\mu s$). Its operation depends on the *stability of an ionised gas against spark breakdown*.

Apparatus : It consists of a set of *equally spaced identical plane conducting plates*, usually of aluminium, *mounted* few mm apart, as shown in Fig. 3.11, in an *air-tight* chamber containing a mixture (90 : 10) of *neon-helium gas* at a pressure of 1 atmos. It is also provided with *counters* and a *logic circuit* for determining the arrival of a particular particle. The alternate plates are connected to a source of high d.c. voltage (10-20 kV) which is almost but *not just* sufficient to produce a discharge.

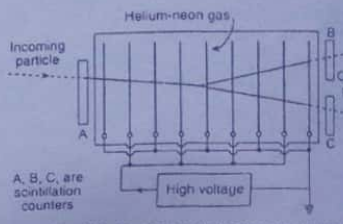

Fig. 3.11 A typical spark chamber arrangement

In a typical chamber, the number of plates varies from 25–100, the area of each plate is about 1 m square and thickness 1 mm accurately. The spacing between any two successive plates is about 3-5 mm. The sudden application of high voltages to alternate plates, say the odd-numbered ones, when the others i.e., even-numbered ones are left at ground potential, results in *very high electrical fields across the gaps*. A spark breakdown of the gas then occurs, being initiated by the trails of ions produced by the ionising particle traversing the chamber. The *trajectory of the particle is marked by a series of sparks* that jumps from one plate to the next, close to the path of the particle. The light from the spark is intense and the spark trails are *photographed stereoscopically* so that the three-dimensional path of the particle inside the chamber may be re-projected for measurements.

A clearing field (~ 10 kV/m) is applied between the plates to sweep away unwanted electrons and ions to make the chamber ready for the next firing.

Usefulness and limitations — The *chief advantage* of a spark chamber over a bubble chamber is that it can be made sensitive for a very short time. The *sensitive time* of a spark chamber is ~ 0.5μs. Because of this very short sensitive time, the chamber *can be operated in an intense beam* (10^6 particles/s) and can *still record single particles*.

The *photographs* of the sparks can be *analysed* and the track coordinates can be digitized with the help of an image tube. It is also possible to register *multiple tracks* (Fig. 3.12) in a spark chamber since the spark discharges follow the actual particle trajectories.

In a multiplate spark chamber, the *tracks* show *broken appearances*. But if the interplate gaps are made relatively wider (up to about 0.4 m), the tracks appear somewhat continuous, when it may be possible even to identify the vertices of different nuclear events.


Fig. 3.12 Multiple tracks in a spark chamber

The spark chamber may be *magnetically controlled* to yield information about the momentum and the sign of the charge of the ionising particle from the curvature of the

Scanned with CamScanner

track. But the information as given by spark chamber is *not as accurate* as the bubble chamber. Nevertheless, spark chambers are *simpler in construction* and relatively *cheaper* to build. Further, it is capable of rapid operation to provide excellent definition of direction. As it is sensitive for a very short time, it is used to detect and also to record rare nuclear events.

3.7 Cloud chamber

The *cloud chamber* is an ingenious apparatus devised by C.T.R. Wilson for studying individual nuclear reactions. It makes the paths of particles taking part in nuclear reactions visible so as to photograph the individual tracks and study them at leisure.

Principle — When a volume of a *saturated gas-vapour mixture* is suddenly *expanded adiabatically* in a chamber, the temperature of the mixture falls considerably (*supercooling*) and it becomes *supersaturated*. This vapour condenses on the dust particles present in the chamber. A *cloud* is thus formed. But if the chamber is dust-free, the cloud does not and cannot form. Wilson found that if *ions* are present in the chamber, they act as *nuclei* for condensation and the cloud is formed. So if an ionising particle passes through the chamber during an expansion, ions are produced along its path, droplets condense on them and the *track* of the particle is made visible to the eyes.

If expansion is just greater than 25% of the original volume, condensation occurs on the *negative ions* only. If greater than 31%, condensation is caused on the *positive ions* as well. If it is greater than 38%, there is *no preferential condensation* and the cloud appears. The gases that are commonly used in cloud chambers are argon, air and CO_2, and the vapours used are water vapour and alcohol.

3.7.1 Modern cloud chamber

Wilson's cloud chamber in its original form is now obsolete. We shall therefore describe here a modern form of cloud chamber.

A *modern cloud chamber* essentially consists of a large chamber A (Fig. 3.13) with an optically flat glass front G. A piston P, supported by the rubber diaphragm RR, is provided for smooth and fast expansion. S_1 and S_2 are two adjustable screws which limit the expansion and thus control the *expansion ratio*.

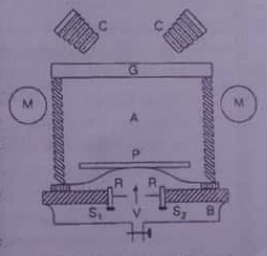

Fig. 3.13 Modern cloud chamber: PMS Blackett's modification

The space behind P is closed by a smooth valve V and is filled with compressed air. As V is released, air rushes into the chamber B and the piston quickly completes the stroke. If then a charged particle passes through the chamber A, *during* or *immediately after* the expansion, its track is made visible by the condensing vapour.

On being illuminated by high pressure Xenon lamps, the tracks are photographed by stereo-cameras, CC, to enable three-dimensional events to be reconstructed.

A small potential difference applied between the top and the floor of the chamber, immediately on completion of photographing the tracks, sweeps away any residual ions left and makes the chamber ready for the next event.

Counter-controlled cloud chamber : Blackett's modification — There is no guarantee however that just when an expansion is made, an ionising particle would pass through the chamber. In fact, in earlier days, the matter was left to the mercy of chance with wasteful photographic exposures. This situation was saved by P.M.S. Blackett who made an ingenious modification of the cloud chamber.

Two GM counters, MM, are mounted on either side of the chamber (Fig. 3.13) connected *in coincidence* to control the expansion of the chamber. When a charged particle passes through both the counters, it has to pass through A and the output coincidence pulse from the counters, suitably amplified, is made to operate the valve V to expand the chamber A, switch on illumination, click the camera and wind the film ready for the next arrival. After the photograph of the track is taken, the ions are swept away from the chamber by an automatic 'switching on' of a clearing field.

Such an arrangement, first introduced by Blackett and Occhialini, is called a **counter-controlled cloud chamber**.

Magnetically-controlled cloud chamber — The cloud chambers are often used in conjunction with magnetic fields. Such an arrangement is known as **magnetically controlled cloud chamber** and is extremely useful in determining the momenta of the particles and in their identification.

The cloud chamber is placed in the magnetic field at right angles to the plane of the figure. The tracks would then get *bent*. The *direction of bending* and a measurement of the *curvature* of the track would give the *sign of the charge* and the *momentum* p of the particle respectively : the relation is

$$mv^2/r = qvB \quad \Rightarrow \quad mv(= p) = qBr$$

where B is the applied magnetic field, r the radius of curvature of the track, q the charge of the particle and $p(= mv)$ its momentum.

• Often, regularly spaced metal plates are introduced inside the cloud chamber for determining the range and energy-loss of particles and also for observing such nuclear events as *cosmic ray showers* etc. The discovery of *positron* was confirmed by such an arrangement with cloud chamber.

3.7.2 Usefulness and drawbacks of cloud chamber

The following particles can be detected by their tracks produced in a cloud chamber :

(i) **α-particles** - produce very large number of ions along its path, the droplets

Scanned with CamScanner

Fig. 3.14 Tracks of α-particles in a cloud chamber

coalesce and produce a *thick* and *continuous track* as shown in Fig. 3.14; (ii) **protons** – do not ionise so heavily and the track appears *thinner* though *continuous*; (iii) **electrons** – produce very few ions so that the track is very *thin* and is *discontinuous*; (iv) **γ-rays** – being uncharged do not produce a track of their own, but the Compton electron or the photoelectron they knock out, now and then, produces *short, thin tracks*; the γ-ray may at times materialise into an electron-positron pair forming a *forked track*.

With magnetically-controlled cloud chambers, the tracks could be *bent* and from the *direction of bending* and the *curvature*, the particle can be *identified* and their *ranges* and *momenta* evaluated.

Wilson's cloud chamber has a *glorious history* in the field of high energy physics. The following phenomena observed with this instrument illustrate its versatility. They are : (a) particle *ranges*, (b) *absorption* of rays by different substances, (c) *ionisation densities* of tracks, (d) discovery of *unknown sub-atomic particles*, (e) *collision* phenomenon, (f) nuclear *transmutation*, (g) *pair production*, (h) *fission products*, (i) *decay processes*, (j) *cosmic ray showers* etc. etc.

The discovery of *positron* and *lambda particle*, and also the first accurate determination of the *rest mass of muons* (μ) have been made with cloud chamber. However, bubble chambers and spark chambers are now being more extensively used.

The cloud chamber suffers from the following **drawbacks**.

1. The device is *slow* and *sluggish* and the ionisation *tracks persist* for quite sometime so that a number of tracks are photographed.

2. The chamber remains *ineffective* for a considerable time.

3. Interaction of particles with different materials can be studied only with much difficulty as it is a hard task to introduce the material in it. If introduced as plates, they must be few and wide apart for the chamber to work.

4. The most serious drawback is that tracks of ionising particles are formed in a gas and so the *stopping power* of a cloud chamber is *much lower*. This makes the *probability* of occurrence of *interesting nuclear events* with high energy particles *very low*.

3.7.3 Diffusion cloud chamber

Diffusion cloud chamber is a variant of the usual cloud chamber where the gas requires no preliminary expansion and therefore remains *continuously sensitive* to the passage of swift particles.

Construction — This is much *simpler* in construction as it has *no moving part, valve* and *re-setting mechanism* etc. The diffusion cloud chamber is shown schematically in a simplified manner in Fig. 3.15.

The chamber contains a suitable *gas-vapour mixture* (alcohol) and a *large vertical temperature gradient* is set up in it by using a hot top plate and a cold bottom plate or vice versa, depending on whether it is of *downward diffusion type* or *upward diffusion type* respectively. A *vapour density gradient* is maintained by keeping a vapour source (alcohol-filled trough) T, T near the hot plate. In the warm region, the vapour is unsaturated and as the vapour diffuses downward to regions of lower and lower temperature, it becomes *supersaturated*. Thus in a given region the gas is supersaturated at all times and is continuously renewed by diffusion of fresh vapour from other parts of the chamber. The location and the extent of the region of supersaturation depend on the geometric design of and the temperature gradient in the chamber. The system is illuminated by a strong light source and the track is photographed by a camera at the top.

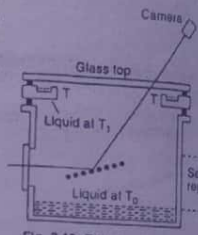

Fig. 3.15 Diffusion cloud chamber

Advantages and demerits — The diffusion cloud chamber is *simple* and *continuously sensitive*. The drawbacks due to *convection and turbulence* are far *less* compared to those in cloud chambers of Wilson type. The fraction of the *total useful time* for observing tracks is *much longer* than in an expansion chamber. The *recovery time* being *very small* (further reducible by the application of an electrostatic field), it is very suitable for use with *pulsed* accelerators.

But since it is continuously sensitive, it *cannot be operated* at a background level higher than the cosmic ray level. The sensitive region does not extend to the surfaces placed inside it and is thus not possible to introduce absorbers to record nuclear reactions, unlike in a chamber of Wilson type. The sensitive layer of the diffusion chamber is less than 7.5 cm thick and *cannot* be made vertical to detect cosmic rays.

3.8 Bubble chamber

One of the serious drawbacks the cloud chamber suffers from is the *low stopping power* of the gas which has a very low density. The probability of occurrence of interesting nuclear events with *high energy* particles is thus *quite low*.

In this context, Glasser developed the *bubble chamber* where tracks are formed in liquids with a density about 1000 times higher than that of a gas and hence possess a much higher stopping power. Bubble chamber is now considered as one of the most modern methods of recording tracks of *high energy* charged particles.

Principle — The principle of operation of a bubble chamber is the *instability of superheated liquids against bubble formation*. Any liquid normally starts boiling with evolution of bubbles when its temperature reaches the boiling point. It is possible however to heat a liquid under high pressure beyond its normal boiling point –

Scanned with CamScanner

Operating cycle — The operating cycle of the chamber consists of the following sequential steps :

1. The liquid is heated to a temperature *above* its boiling point and kept at a *high pressure* to prevent boiling.

2. The pressure is suddenly released by a small *adiabatic expansion* causing the liquid superheated and the chamber becomes sensitive to *bubble-formation* on ions until normal boiling occurs.

3. The sensitive time is reduced to a few ms by *recompression* of the liquid and the cycle is then *repeated*.

The operating cycle of the bubble chamber is not fast enough and hence it is not possible to have counter-control in its operation, unlike in the cloud chamber. It can however be operated fast enough to synchronise with the arrival time of the beam pulse of high energy particles from an accelerator.

Applications — Several types of measurements can be made by bubble chambers. *Energies* of particles can be deduced from the *depth of penetration* required to stop them in the dense liquid. If immersed in a magnetic field, the *curvature* of the particle track can be used to compute the *momentum* of the particles. From the *density of bubbles* along a track, the *charge* and the *speed* of the particle can be found. The *scattering* of a particle track is a measure of its *momentum times the speed*. When these measurements are combined with simple geometric measurements of track lengths and angles between tracks, one can calculate the *masses, charges* and the *life times* of particles observed. It is also possible to calculate the *energy* released, the *relative frequencies* of different kinds of processes, and the *angular distribution* of outgoing particles. Such information is basic to a proper understanding of the nuclear structure and processes'.

Advantages — There are several advantages of bubble chambers over the cloud chambers. In a cloud chamber, the highest energy particles are likely to escape through the contained gas without hitting anything. But because of *high stopping power* of bubble chambers, interesting nuclear events too often occur before the particles escape from the chamber. The first ever *neutrino-interaction* in pure hydrogen was recorded in hydrogen bubble chamber in 1970. The remarkable event is schematically shown in Fig. 3.18 where it is seen that a neutrino enters from the right and interacts with pure H-atom to give rise to a π^+ meson, a proton and a muon μ^-.

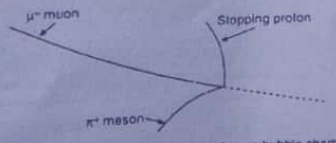

Fig. 3.18 Neutrino interaction in the hydorgen bubble chamber

The *high cycling rate* of bubble chambers is another distinct advantage. The *sensitive time* of bubble chambers is also very *small*. This reduces, to a great extent,

the background of unwanted tracks. Further, the *life time* of bubbles produced by the ionising particle is less than 1 ms, much shorter than the time it takes to release the pressure on the liquid. So there is *no need of any clearing field* to remove the old tracks. Another merit is that the liquid can be *selected* to suit the nuclear reaction to be studied. For instance, for studying the interaction of high energy particles with protons, the liquid of choice is liquid H_2. For all these advantages, bubble chambers have become indispensable in particle physics research. For effective use, millions of pictures are to be scanned rapidly by semi-automatic methods and the output fed into computers and analysed.

Demerits — The bubble chamber however is not without its demerits. Since the cycling time is very long compared to the life time of the bubble nuclei, it is impossible to trigger a bubble chamber by any *random ionising particle*. Another demerit is the *distortion of the tracks* due to optical inhomogeneity of the liquid due to temperature gradient and the *curvature of tracks* due to multiple scattering of a charged particle by liquids of high atomic number.

Table 3.1 : *Cloud chamber vs. Bubble chamber*

Cloud chamber	Bubble chamber
1. It uses supercooled vapour.	1. It uses superheated liquid.
2. Tracks consist of tiny droplets of vapour and hence the name.	2. Tracks consist of a series of closely spaced bubbles and so the name.
3. Density of vapour being low, most of the particles go right through the chamber before any significant event occurs.	3. Density of liquid is high, even 1000 times greater than gas. So interesting nuclear events often occur before particles escape.
4. Rate of cycling is low.	4. Rate of cycling is high.
5. Clearing field is necessary to remove the background tracks.	5. No clearing field is needed to remove the background tracks.
6. Suitable for low energy particles and for random events.	6. Suitable for very high energy particles but not for random events.
7. Cloud chamber tracks are completely free from distortion.	7. Optical inhomogeneity of liquid due to temperature gradient distorts the track.

3.5 Scintillation counter

Principle : When a screen of zinc sulphide (ZnS) is hit by an ionising particle, *luminiscence* or *scintillation*, that is, emission of a small flash of light is produced. This is one of the earliest methods for detection and counting α-particles and was utilised by Rutherford and others. This forms the basis of the **scintillation counter.** But since the method involves visual observation through a low power microscope, it

Scanned with CamScanner

is *extremely tedious* and as the counting rate could hardly exceed 100 per minute, it is also *insensitive*.

But (i) the invention of the *photomultiplier tube* that emits photoelectrons when appropriate radiation falls upon it and multiplies them stagewise to produce a measurable current pulse and (ii) a better understanding of the luminiscent properties of many organic and inorganic substances, called *phosphors*, *led a modern scintillation counter, a combination of a phosphor and a photomultiplier tube*, to become one of the most widely used instruments for studying nuclear radiations.

Two types of scintillator are widely used — sodium iodide and plastic. Single crystals of *sodium iodide* are usually doped with thallium and is denoted by NaI (Tl). Thallium atoms act as luminiscence centres. While NaI (Tl) are enough dense to have a good efficiency for γ-ray detection, the decay time of each pulse is rather slow ($\sim 0.25\mu$ sec). Plastic, on the other hand, has low γ-ray collection efficiency but has much shorter decay time ($\sim 10^{-9}$ sec). The latter is mainly used for detecting charged particles.

Apparatus — A scintillation counter is a combination of a scintillator and a photomultiplier tube. The cathode C of the multiplier tube T is *semi-transparent* and *light-sensitive* so that a certain percentage of the luminiscent photons may reach it and generate photoelectrons. Depending on the conditions of the experiment, the photomultiplier tube may be kept either in contact with the scintillator S (Fig. 3.19) or at a distance from it. In the latter case, the luminiscent radiation is guided to the cathode C by way of *total internal reflections* in a suitable perspex (lucite) pipe.

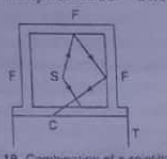

Fig. 3.19 Combination of a scintillator and a photomultiplier tube

The tube and the phosphor are enclosed in a light-tight case and made air-tight, for otherwise the phosphor crystals may deliquesce.

A wide variety of phosphor is used for different ionising particles. This is deposited on a perspex plate mounted on the end of the photomultiplier. Since the radiation is emitted in all directions, it is covered with a thin aluminium foil F as *reflector*. The reflection prevents the escape of radiation in the unwanted directions, but high energy charged particles reach the phosphor penetrating the reflector. The phosphor must be transparent to the luminiscent radiation so that the latter may reach the photocathode of the tube.

Fig. 3.20 shows a scintillation counter. The incoming charged particles or γ-rays produce a flash at A. A photoelectron is thereby released at the point B in the photocathode. Due to secondary emission from cathode to cathode (dynode) - 12 to 14 stages - more and more electrons are released until the effect of the single electron has been multiplied many times (10^9 or more). The accelerating potential between any two consecutive electrodes is about 100 V. The amplified signal is finally collected at the plate P of the photomultiplier tube and detected by a sensitive micro-ammeter (μA) in series with a resistor R. The voltage pulse is then monitored by a recorder,

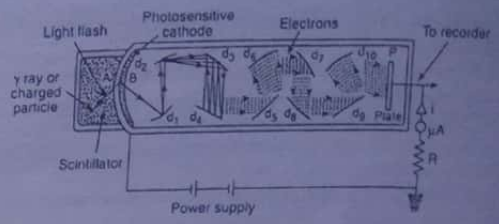

Fig. 3.20 A scintillation counter

measured and made proportional to the amount of light collected and to the energy deposited by the charged particle in the scintillator, by suitable electronic circuit. The block diagram illustrates the arrangement in Fig. 3.21a.

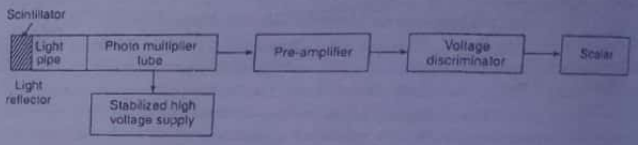

Fig. 3.21a Block diagram of electronic circuit used in a scintillation counter

Calculations — We shall now calculate the height of the output voltage pulse. Let E_i = energy of incident ionising particle, E_ν = mean energy of emitted photons and η = the efficiency of conversion. So the number of photons produced in phosphor by an ionising particle is given by

$$N_1 = \eta \frac{E_i}{E_\nu} \tag{3.9.1}$$

The number of photons incident on photocathode of the photomultiplier is

$$N_2 = \alpha T N_1 \tag{3.9.2}$$

where α is the fraction of total photons falling on photocathode and T the optical transparency.

These photons get converted into photoelectrons with an efficiency η_e.

∴ Number of photoelectrons produced by the cathode is

$$N = \eta_e N_2 \tag{3.9.3}$$

∴ No. of photoelectrons reaching the first dynode = DN, where D is the fraction of photoelectrons reaching the first dynode.

If m be the multiplication factor of each dynode, numbering n in total, then the number of electrons collected is DNm^n.

Scanned with CamScanner

$\therefore$ Charge carried to anode $Q = DNm^n e$, where e = electronic charge.

$$\therefore \quad Q = D\eta_e N_2 m^n e, \qquad \text{using (3.9.3)}$$
$$= D\eta_c(\alpha T N_1)m^n e, \qquad \text{using (3.9.2)}$$
$$= D\eta_e\alpha T(nE_i/E_v)m^n e, \qquad \text{using (3.9.1)}$$

$\therefore$ Pulse height, $$\boxed{V = \frac{Q}{C} = \frac{E_i}{E_v C}\eta\alpha T\eta_e D m^n e} \qquad (3.9.4)$$

The above factors are subject however to *statistical fluctuations*. So if V be the amplitude of the output voltage pulse appearing on a capacitor of capacitance C, connected to the plate P and the earth through a high resistance, $V(= Q/C)$ will also fluctuate about a mean value for a given E_i. From (3.9.4), the amplitude of output pulse is proportional to the particle energy dissipated in the phosphor. The linear relation does not hold good for low energy particles with organic scintillators. For a given phosphor, the duration of output pulse which is used to detect and count the charged particle is $\sim 10^9$s, the mean decay time of luminiscent radiation.

Usefulness and advantages — The method is capable of *rapid counting* since the pulses given by scintillation counters are of extremely short duration.

It has the special merit that the *strength of the flash depends on the type and energy of the particle* that causes it. Using suitably biassed electronic circuits, particles in a given range can be sorted out and the distribution of energy in the incident radiation can be analysed. The arrangement would then behave as a *scintillation spectrometer*.

Further, the stopping power of solid and liquid phosphors is much greater than that of the gas used in gas-filled counters. This instrument is therefore *preferred where high stopping power is demanded*, as in experiments with γ-rays. In fact, one of the most important applications of the scintillation detector is in the field of γ-ray detection and spectrometry.

Scintillation tanks — To detect very weak signals, detectors of very large volume have to be built with liquid. It is interesting to note that the extremely weak signals produced by *neutrinos* coming from a nuclear reactor were first detected in a large liquid scintillation system—*Scintillation tank*—to demonstrate the existence of this elusive particle. The detection of anti-proton was also made by employing scintillation counters.

• The pulses due to the passage of the charged particles through the scintillator are also accompanied by smaller *unwanted pulses* due to small thermionic emission of the photomultiplier; when the desired pulses are quite large, the unwanted ones can be *biassed out* easily. If however they are small, as with β-and γ-rays, the unwanted pulses can be eliminated by operating the photomultiplier at a *very low temperature*.

3.9.1 Detection of γ-rays : γ-ray spectrum

It is possible not only to detect but also to measure the energies of γ-ray by a scintillator mounted on a photomultiplier.

γ-rays are *uncharged* and are therefore to be detected *indirectly*. They interact with matter through (i) *photoelectric effect*, (ii) *Compton effect* and (iii) *electron-positron pair production*. For γ-rays having energy up to 2 MeV, the process (i) and (ii) are important. But actually it is the photoelectric effect which is utilised. The reason is that when a γ-ray produces a photoelectron, its energy is essentially the same as that of the absorbed γ-photon. In photoelectric effect, the γ-ray loses all its energy so that all the γ-rays of one energy will produce in a scintillator photoelectrons of the same energy. The amount of light produced in the crystal being proportional to this energy, the electric pulse obtained by photomultiplier will also be *proportional to this energy*. A computer-like device, called *multichannel analyser*, can select and sort out the output electronic pulses according to magnitudes and the number of pulses of each magnitude are recorded in the instrument. The data constitute an *energy spectrum* of γ-rays penetrating the crystal.

γ-ray spectrometer—A scintillating counter fortified with a mechanical analyser constitutes a γ-ray spectrometer. It must be calibrated with γ-rays of known energy. A typical γ-ray spectrum is shown in Fig. 3.21b. The width of the full energy peak at

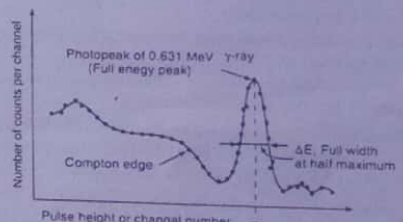

Fig. 3.21b A typical γ-ray spectrum of ^{137}Cs. The single photoelectric peak of 0.631 MeV γ-ray follows the Compton edge

half-height, ΔE, is called the *full width at half maximum* (FWHM), the value of which depends on the number of light photons produced by the incident γ-ray.

The ratio $\Delta E/E_\gamma$ is called the *energy resolution*, that is,

$$\boxed{\text{Energy resolution} = \frac{\Delta E}{E_\gamma}}$$

which is $\sim 20\%$ at $E_\gamma = 100$ keV, 6–8% at 1 MeV etc.

Scanned with CamScanner

by scanning microscopic observations are made of the range, track densities (variation of grain density), direction of travel of the particles and the small angle of scattering of particles due to collision with atomic nuclei in the emulsion. High quality microscope with small depth of view, accurate depth gauges etc. are used to scan the developed plates. The small depth of focus of high magnification scanning microscopes makes it imperative to focus on short sections of the track. By taking microphotographs of such short sections, the mosaic picture of the whole track through the emulsion is constructed by putting together the enlargements of these sections.

Information : From the above measurements, information about the *charge, mass* and the *energy* of the particle can be obtained. For instance, the variation of grain-density along the track, dn/dx, is related to the specific energy-loss of the particle, dE/dx, by an *empirical* equation

$$\frac{dn}{dx} = A\left(1 - e^{\alpha Ze\sqrt{dE/dx}-\beta}\right)$$

where A, α, β are constants and Ze is the charge of the particle.

The mass m (in protonic mass unit) of the particle and its kinetic energy E are related through the range R by

$$E = BZ^{2\mu}m^{1-\mu}R^{\mu}$$

where B and μ are constants.

The total number of grains, n, on the track is obtained from the relation

$$n = CZ^{2\nu}m^{1-\nu}R^{\nu}$$

where C and ν are two empirical constants.

Identification of the particle is possible from the range R and the variation of grain-density along the track, dn/dx, when the grains are resolved. The energy of the particle is usually evaluated from its range in the emulsion.

Advantages — The nuclear emulsion detector has a number of *special* advantages.

1. The method is *simple* and *cheap*, requiring no elaborate arrangement, either electronic or mechanical.
2. It is *continuously sensitive*, unlike the cloud chambers or the bubble chambers.
3. It is *light weight* and *portable* and suited for studying high altitude cosmic rays.
4. Being a solid medium, the emulsion detectors give the *complete tracks* of high energy particles.
5. Emulsions in '*stripped*' form may be stacked, one on to the top of the other, and the track of the particle recorded for *considerable lengths*.
6. The tracks of different types of particles show different appearances, characteristic of the particle and can thus be *distinguished* from one another.
7. Since the density of emulsion is high, its *stopping power* is also *high* (about 1000 times that of standard air) and *significant nuclear events* take place too *frequently*.
8. *Emulsion detector can also be adapted to the study of* **neutrons.** High energy neutrons can knock off protons in the emulsion, which in turn develop tracks in it. By studying the direction of emission of protons with respect to that of neutrons, the incident neutron energy can be estimated by measuring the range of proton. For detection of slow neutron, the emulsion is of a special type containing *lithium* or *boron* having high thermal neutron cross-section.
9. It gives the highest spatial resolution and 4π acceptance.

The plates are now-a-days exposed under strong magnetic field and computerised scanning and measurement systems have been developed and are extensively used.

Disadvantages — Some of the *drawbacks* of the technique are as under :

1. The sensitivity and the thickness are affected by factors such as *temperature, humidity, age of the emulsion*, the conditions under which they are developed etc.
2. The nuclear plate tracks, unlike the cloud chamber tracks, *cannot be bent* satisfactorily in a magnetic field since the scattering obscures the curvature which is small.
3. The tracks are *relatively short* (because of the density of emulsion), at best few mm in length, and must be studied only after proper enlargement or under a high power microscope.
4. They *remain always sensitive* to ionising particles and there is no method to trigger them by particles one wishes to study, unlike in cloud chambers.

Applications — Nevertheless, many outstanding discoveries were made with nuclear emulsion technique. These include (i) discovery of pions of rest mass 273 m_e, (ii) the discovery of K-mesons and (iii) the anti-lambda hyperon $\bar{\Lambda}^0$. In fact, extensive applications of nuclear emulsions have been made in cosmic ray research. Nuclear 'stars' produced by cosmic rays and high energy particles from accelerators are also studied by this technique. In neutron physics, measurements of neutron energy spectra and neutron flux have been made using emulsion technique; α and β-activities of very long-lived radioactive substances have also been recorded by nuclear emulsion and that led to the discovery of α-emission by nuclei known earlier to be stable.

3.12 Solid state track detector

Principle : The *principle* of a solid state track detectors is rather simple. If a high energy charged particle passes through a solid, it causes a continuous damage to the material due to excitation and ionisation of its atoms along the path of the particle. In some materials, this path can be etched by strong acid or alkali solutions that preferentially attack the damaged region to make the path visible. The usual solids are mica, glass, etc. or commercially available plastics such as cellulose nitrate, polycarbonates etc. The commonly used reagents for etching are hydrofluoric acid for mica and glass, and caustic soda for plastics.

Scanned with CamScanner

The *specific energy loss* (SEL) of the particles is the key factor that determines the track recording property of different materials possessing different etching thresholds for SEL. The etched tracks are observed under optical microscopes.

Plastic detectors — Recently, some special plastics have been developed for being used as solid state track detectors, e.g. CR-39 that can record particles having Z^2/β varying from 6-100, where Ze is the charge on the ion and $\beta = v/c$. For CR-39, the etching is done with 6N NaOH solution for 8-32 hours at 79°C. The etching time is *critical* in that any over-etching or under-etching may spoil the purpose. Electrochemical method of etching makes the tracks in plastics large enough to be visible even to the naked eye. For rapid scanning of etched tracks, spark counting technique may be used where a spark is passed through the etched region and the resulting electric pulses counted electronically.

Usefulness : These detectors can *identify nuclear particles* and *measure their energy* with fairly high resolution. Further, they are *cheap, easy to use* and provide *permanent records* of events. The additional advantage is that they can be used in *different environmental conditions*.

3.13 Semiconductor detector

Principle — A semiconductor detector, schematically illustrated in Fig. 3.25 is essentially a *reversed biassed p-n junction*. So, the electrons and holes are drawn away from the junction region to form a *depletion layer* there, with no charge-carriers. Due to reverse bias, no current flows through the junction and the diode is cut off. The thickness of the depletion layer depends on (i) the nature of impurities and (ii) the applied voltage. It ranges from several hundred μm to few mm. As the conductivity of

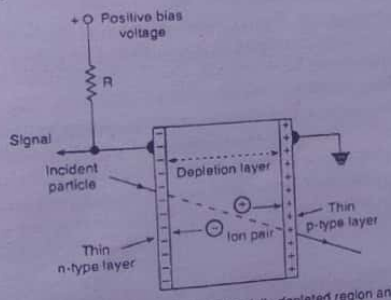

Fig. 3.25 An ideal semiconductor detector, fully depleted region and thin heavily doped surface layers of opposite types are seen

the depletion layer is low, a large potential difference can be maintained across it and it acts like a *solid ionisation chamber*.

Action — When a high energy charged particle passes through the depletion layer, which is free from any charge, it produces the electron-hole pairs. The electrons are raised to the conduction band and are free to move through the crystal under the applied electric field. The holes, left out in the valence band, also move freely through the crystal. Due to both of these, a momentary current pulse, proportional to the number of electrons and holes, is generated. The amplitude of the corresponding voltage pulse across R as the output depends on the energy deposited by the incoming particle. It is the voltage pulse which is used to detect and count the ionising particles.

Counter — Most of the modern semiconductor counters are of surface barrier type. A typical semiconductor counter is schematically shown in Fig. 3.26. The diode is formed by diffusing a n-type impurity to a depth of about 10^{-4} mm from the surface into say silicon, having a small concentration of a p-type impurity. In the process, junction is established just below the surface where the n-type impurity cancels the p-type one. Thin films of gold, of about 0.3 micron thickness, are evaporated on to the diode so that the electrical contact could be made without hindrance to the entry of incoming ionising particles into the junction. Considerable reduction in noise pulses occurs if the counter is operated at liquid nitrogen temperature.

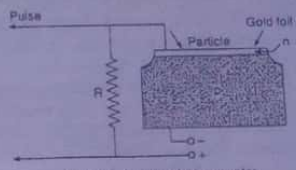

Fig. 3.26 Semiconductor counter

Semiconductor detector vs. ionisation chamber — A semiconductor detector, like an ionisation chamber, collects and also measures the charge given out by the incident radiation. But it possesses *two important advantages* over an ionisation chamber that uses a gas.

First, since the density of a solid is much greater than that of the gases, a semiconductor detector has a much *higher stopping power* for the incident radiation, so that even for highly penetrating γ-rays, a semiconductor can be used.

Secondly, the *energy required* for producing an ion-pair in solids is *much lower* compared to that in gases, e.g., 35 eV for air, 42 eV for helium; but only 2.9 eV for germanium and 3.5 eV for silicon. This is because in a semiconductor, ionisation occurs from the valence band to the conduction band and not from an atomic level to the continuum.

Usefulness and limitations — The semiconductor counters are useful in detecting all types of heavily ionising particles e.g. α-particles, protons, heavy ions, fission fragments etc. Unfortunately, however, they are not suitable (excepting GeLi counter and similar ones) for detecting γ-radiations since their specific ionisation is extremely small.

The voltage pulse produced in such a counter is about 10 times the size of the pulse from an ionisation chamber for the passage of the same particle. This is because only 1/10th of the energy required to produce a charge-carrier pair in an ionisation chamber

Scanned with CamScanner

and 1/100th of that in a scintillation counter are enough to produce a similar pair in a semiconductor. In a semiconductor detector, therefore, the *statistical fluctuation is lower* by a factor of $\sqrt{10}$. This makes the counter *extremely sensitive* by improving the inherent *resolving power* and achieving *high counting rates* – 10^4 to 10^5 particles per sec. In fact, semiconductor detectors have the *best energy resolution* (1%) among all types of radiation detectors for most purposes. The very narrow width of depletion region makes the *pulse rise time also very small* ($\sim 10^{-8}$ s).

These detectors are *linear* over a wide range of energies. The size being very *small*, the detector can be placed in convenient positions (close or remote) for studying nuclear reactions. The sensitivity can be changed by changing depletion thickness and can as well be designed to study low energy particles. These detectors can also selectively detect only charged particles in a heavy background of γ-rays or neutrons.

The leakage current due to intrinsic conductivity can be reduced by operating the counter at liquid nitrogen temperature. For particles having ranges less than the junction thickness, the counter can also act as a **spectrometer** since the pulse is then proportional to the kinetic energy of the particles. This explains why the counter is unsuitable for γ-rays. The absence of the so-called *windows* and the relatively *low values of the externally applied potential* are distinct advantages of the semiconductor detectors over the complicated gas-filled ones.

3.13.1 GeLi detector : γ-ray detection

With very pure semiconductor, the depletion layer is only about 1 mm thick. While this is enough to stop a proton or an α-particle, it cannot stop a γ-ray photon. An ingeneous technique, called *lithium drifting*, was thus developed for the purpose and lithium drifted germanium (GeLi) detector almost completely replaced since 1960 the scintillation counters.

Usually, lithium ions are diffused into the surface of a p-type germanium and the device heated to about 200°C to increase the mobility of lithium ions, and a reverse bias is applied. The positive Li-ions then *drift* into the depletion layer where they are *neutralised by the negative impurities* in the p-type region. Thus, the drift of Li-ions produces a very pure semiconductor region (n-i-p junction device) between the n and p type regions, i being the intrinsic semiconductor. The region has no charge carrier and forms the effective area of the detector. In this way, a depletion layer of several centimeter ($\sim$ 7 cm) has been produced, making the detector extremely useful for γ-rays as well.

This type of detector *must* be maintained at liquid nitrogen temperature at all stages--from operaion to preservation, for some hole-electron pairs can be formed by as small as 0.66 eV and the thermal energies at room temperature are enough to form such pairs. GeLi-detector are thus thermally connected with a copper finger, the tip of which is always kept dipped into liquid nitrogen.

The energy resolution of a GeLi detector is about 0.4% and is thus particularly useful in γ-ray detection. Fig. 3.27 shows the γ-ray spectrum of Co-60 as observed by GeLi detector and a NaI (Tl) scintillation detector.

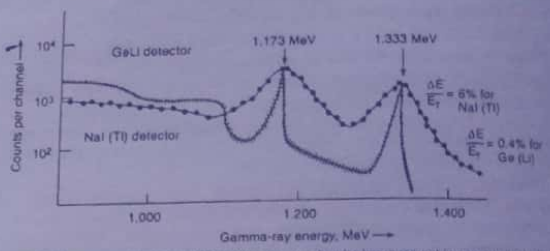

Fig. 3.27 Gamma ray spectrum of ^{60}Co. Note the spectacular improvement in energy resolution provided by Ge(Li) detector compared to NaI(Tl) scintillation detector

• GeLi detectors of volumes up to 100 cm^3 have been routinely built and are used in high energy physics. SiLi-detectors are also used and have the same principle of operation and action. But Ge has a density higher than Si and is thus more suitable for being used in the detection process.

3.14 Nuclear electronics

In conjunction with nuclear detectors, various types of electronic circuits are employed — some for shapping the input pulses, some for amplifying them, some other for analysing the pulse height, others to know when two pulses occur simultaneously and so forth. We cannot enter here into any detailed description of those electronic circuits. Earlier, they were based on vacuum tubes, but have now been almost completely superseded by transistors and semiconductors. Introduction of microprocessor chips has made possible to carry out the functions of complete solid state electronic circuits. In fact, nuclear electronics is now a specialised branch of electronics and the interested readers should consult any specialised text book on the subject. We shall rest satisfied in this section by discussing, in bare outlines, some relevant electronic circuits used in nuclear radiation detection.

3.14.1 Differentiating circuit or a Differentiator

A *differentiator* is one that changes the shape of the pulse (wave) — *pulse shaping* – and is often used to obtain sharp-peaked pulses. A pulse is said to be differentiated when it is used to develop another pulse with a shape proportional to the time derivative de_i/dt of the original pulse (input voltage).

Scanned with CamScanner

Chapter 5

Particle Accelerators

5.1 Introduction

With the possibility of transmutation of elements by bombarding atomic nuclei with sub-atomic particles, the search for particles with higher and higher energies began. This culminated in the development of a number of powerful particle-accelerators. An **accelerator** is a device used to accelerate and thus impart high kinetic energy to charged particles and produce thereby a beam of high energy particles. Apart from transmutation, such high energy particle beams are needed for an understanding of the nuclear structure and are used in the study of nuclear scattering and other nuclear properties, including the nature of nuclear forces. In fact, to a nuclear physicist, the accelerators are what a microscope is to a biologist and a telescope to an astronomer.

The *essential parts* of an accelerator are the following : (a) an *ion source* whence the particles are injected into the accelerator, (b) a *collimator* which collimates the particles into a parallel beam, (c) an *arrangement for acceleration* of particles by electric and magnetic fields along specific trajectories and (d) *deflectors* that would deflect the beam of particles towards the targets.

A number of accelerating machines has been devised since 1930's and continuously been improved to impart energies varying from few MeV to several TeV. As the maximum energy to be imparted increases, the cost of construction and maintenance also rises several folds so as to become astronomical in figures. Different types of accelerators have been constructed to accelerate protons, deuterons, α-particles, electrons etc. for bombarding various targets and resulting in the discovery of a number of elementary particles.

The machines that can produce a high dc voltage fall under the general denomination of accelerators. In fact, earlier accelerators were only high voltage generators in which a charged particle was accelerated through high p.d.

Scanned with CamScanner

The contents of this chapter would essentially be the description of the construction, the principle of action and applications of a number of present-day accelerators.

• *But why are high energies needed to study the nuclear structure?* The de Broglie wavelength λ of a particle of momentum p is $\lambda = h/p$ where h is Planck's constant. It is known from optics that to see the structure in detail of an object of linear dimensions d, the wavelength λ must satisfy $\lambda \leq d$. So, for this λ, the momentum, $p \geq h/d$. Thus, to 'see' the nuclear particles, high momenta and hence high energies are required. For instance, for $d = 10^{-15}$ m and with protons as probes, calculations show that the kinetic energy should be about 20 MeV which no naturally produced beam can provide. They must be produced artificially.

5.2 Cockroft-Walton voltage multiplier

Cockroft and Walton constructed a dc particle accelerator in which a stream of electrons was used to ionise hydrogen gas and produce protons. The protons were next accelerated through a p.d. 0.15 MeV and allowed to fall upon a target of thin lithium foil. The protons ejected two α-particles, each with an energy of 8.5 MeV, according to the reaction

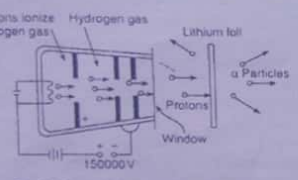

Fig. 5.1 Cockroft-Walton voltage multiplier

$$ {}_1^1\mathrm{H} + {}_3^7\mathrm{Li} \rightarrow 2\,{}_2^4\mathrm{He}. $$

This original version of Cockroft-Walton accelerator (Fig. 5.1) is now obsolete and is only of historical interest.

Improved Cockroft-Walton accelerator — It is essentially a combination of capacitors and rectifiers. The *basic principle* consists in *charging* a set of capacitors *in parallel* and *discharging* them *in series* to add up their potentials (Fig. 5.2).

$C_1, C_2, C_3, \cdots$ etc. are a set of capacitors having equal capacitance and are arranged as shown in the diagram. $S_1, S_2, S_3, \cdots$ are associated switching mechanisms which are, in fact, thermionic valves. T is a transformer, the source of high voltage alternating potential. The valves $S_1, S_2, S_3, \cdots$ operate in such a fashion that during one half of the cycle of ac-potential, the odd-numbered ones – $S_1, S_3, S_5, \cdots$ etc. are closed, and the even ones – $S_2, S_4, S_6, \cdots$ etc. are open (Fig. 5.2a). In the subsequent half cycle, the condition is just reversed (Fig. 5.2b).

During the first half-cycle, the capacitor C_1 gets charged; during the next half cycle S_1 is open, S_2 closed and so C_1 shares its charge with C_2. During the following half cycle, C_1 is again charged to full voltage and C_2 shares its charge with C_3 (S_2 being open, S_3 closed). During the next half-cycle, C_1 again charges up C_2, and C_2 shares it charge with C_4. So, as the alternations go on, the charge is *pumped up*, as it were, to all the capacitors and finally they are all charged to the same potential. As shown in

the diagram, the p.d. between A and B would be five-fold greater than that between A and D (Fig. 5.2). The multiplied output voltage can be used to accelerate ions. While the ion source is placed at one end of an evacuated accelerating tube, the target for the beam is at its other end (Fig. 5.3).

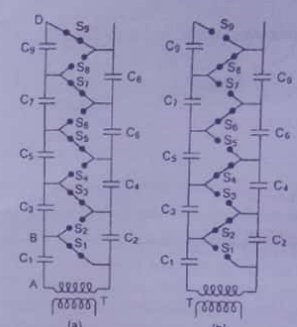

Fig. 5.2 Improved Cockroft-Walton accelerator

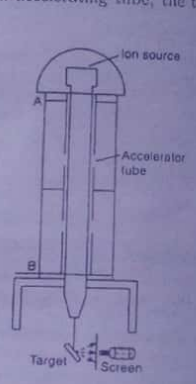

Fig. 5.3 Accelerating tube and target of C–W accelerator

Cockroft and Walton used 0.1 MeV across the secondary of the transformer and obtained an output of 0.8 MeV which they used for the purpose of accelerating protons. Now-a-days, however, energies up to 3 MeV could be obtained with this improved version of the machine.

5.3 van de Graaff electrostatic generator

The *principle* on which this *electrostatic* machine, developed in 1931 by van de Graaff, works is that the potential of a hollow conductor can be increased to a very high value by repeated transfer of charge from one hollow conductor to another by internal contact.

Construction : It consists of a giant hollow metallic *sphere* or shell S (Fig. 5.4) and an *endless belt* B of *insulating material* such as paper, silk, rayon etc. The belt runs vertically between two pulleys P_1 and P_2, P_1 being driven by a motor. It thus continuously transfers charge to the sphere. From a d.c. power supply, the belt picks up a positive charge at a high voltage of about 10 kV, the charge being spread on to the belt by comblike pointed conducting *spray points* P. The charge is removed at the top by similar sharp points O – the *discharge points* – and is passed on to the sphere S by a corona discharge. The belt returns to the bottom after delivering the charge and is recharged at P to repeat the process. The charge thus rapidly accumulates on the

Scanned with CamScanner

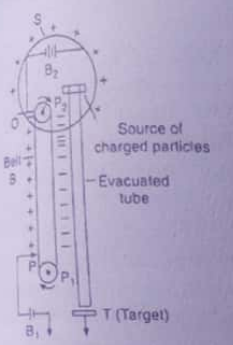

Fig. 5.4 van de Graaff generator

sphere where the potential rises ($V = Q/C$), the ceiling of accumulation being set by the rate of leakage through the supporting columns of the sphere or the surrounding air.

To build up the potential by increasing the insulation of the surrounding air, the sphere is usually enclosed in a *steel pressure tank* containing N_2-gas at a high pressure ~ 10 atmos.

The *ion source* consists of an evacuated discharge tube that can be raised to potentials ~ 10 MeV. It is placed inside the shell at the high voltage end so that ions are accelerated from the high voltage to the low voltage end of the tube, where accumulated particles strike the target T which is earthed.

Uses : van de Graaff generator can be used to accelerate protons, deuterons etc. up to an energy of about 12 MeV beyond which the air-insulation breaks down. It is also used to accelerate electrons by a reversal of the potential of spray-voltage and using a hot filament as the source of electrons. An *important feature* of van de Graaff generator is the *constancy of voltage* to within 1%. Another *distinctive feature* is the *sensitivity* and *control of voltage*. The terminal potential is controlled in most generators by regulating the corona discharge current.

• A *Tandem electrostatic accelerator* (Fig. 5.5) is an improvement over the usual single stage van de Graaff generator. It accelerates particle in *two* stages and is more economical: (i) negative ions (H^-) are produced at ground potential at one end and are accelerated by the positive potential of the terminal which is in the middle of a long

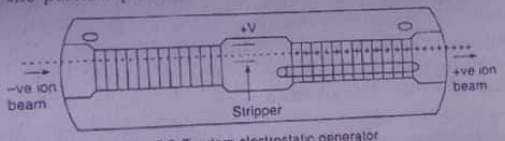

Fig. 5.5 Tandem electrostatic generator

pressure tank, constituting the *first stage*, and (ii) when the ions are still inside the positive terminal, they enter a gas-containing canal, called *stripper*, and are stripped of their electrons to become positive ions and are accelerated (being repelled) from positive terminal to ground potential to hit the target – the *second stage*. It can produce heavy ion beam of energies up to 30 MeV.

5.4 Linear (resonance) accelerator

The idea of *linear resonance accelerator*, shortly called *linear accelerator* or *linac*, was suggested around 1930 and various heavy-ion linacs were built. Unfortunately, however,

they were hardly of any significance in accelerating charged particles to produce nuclear disintegrations. After the World War II, Louis Alvarez and his co-workers were able to produce a successful linear accelerator that energised protons up to 32 MeV.

The *basic principle* of a *linear accelerator* is to increase the velocity of charged particles in *successive steps* along a *straight line* (hence the name) when they are subjected repeatedly to an accelerating electric field. The particles in a linear accelerator are energised by a series of linear pulses at radio-frequencies, that is, by extra pushes at the right moments of time (*correct phase*).

Apparatus — Fig. 5.6 shows a schematic diagram of a linear accelerator. It consists essentially of a long tube LT evacuated to a high degree inside which a series of *coaxial hollow* metal cylinders $C_1, C_2, C_3, \cdots$ etc., called *drift tubes*, is arranged

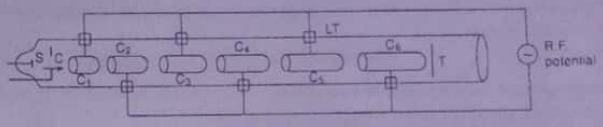

Fig. 5.6 Linear accelerator

Each succeeding drift tube is *greater in length* than its preceding one by a *calculated amount*. At one end of the main tube is placed the ion source S where positive ions are produced. The ions are collimated by a collimator C along the axis of the accelerator so that they pass through the drift tubes. The alternate drift tubes are in electric contact and the two sets of tubes so formed — odd and even — are connected to a high frequency (~10 megcycle) oscillator. The peak ac voltage is about 40 kV. The reversal of potential takes place periodically according to the frequency of alternation of the oscillator. The ions in their passage through the drift tubes are accelerated in steps to leave finally the last drift tube to impinge on the target T placed at the other end of the main tube.

Principle of action — The charged ions get accelerated *only in the gaps* between two adjacent cylinders where they are acted upon by the electric field present. But they travel with uniform velocities inside the drift tubes, as there is no field inside.

If a positive ion leaves the collimator C at a time when the first cylinder C_1 has a negative potential, the ion will be accelerated across the gap but travel with constant velocity in C_1. When the ion comes out of C_1 and if it is positive w.r.t. C_2, it will again be accelerated across the gap between C_1 and C_2, and its velocity will further increase. If q be the charge on the ion, the increment in energy due to acceleration would be qV where V is the potential. In this way, in every gap between two cylinders there will be successive accelerations, provided the ion always enters the field leaving a cylinder, exactly when the potential is changing favourably. This *matching* is *critical* and is achieved only if the *time taken by the ion to traverse a cylinder is exactly equal to half the time period of rf-oscillator*.

Scanned with CamScanner

If l_n be the length of the nth cylinder, the time t_n taken by an ion to travel through it is given by

$$t_n = l_n / v_n \tag{5.4.1}$$

where v_n is the velocity of the ion inside the nth cylinder. So, the **condition for synchronisation** is

$$t_n = \frac{l_n}{v_n} = \frac{T}{2} = \frac{1}{2f} = \frac{1}{2}\frac{\lambda}{c} \tag{5.4.2}$$

where T and f are respectively the time period and the frequency of the rf-oscillator, λ the wavelength of rf-waves and c the velocity of light in vacuo.

Drift tube length and energy of an ion — Let an ion of charge q be accelerated through the nth drift tube at a time when the rf-oscillator provides maximum potential V_m across the gap.

$\therefore$ Energy imparted to the ion $= nqV_m$

since the ion has undergone n-accelerations in the preceding n gaps and each acceleration gives rise to an energy increment qV_m.

$$\therefore \quad nqV_m = \tfrac{1}{2}mv_n^2 \quad \text{(non-relativistic)} \tag{5.4.3}$$

where m is the mass of the ion and v_n the velocity inside the nth drift tube.

$$\therefore \quad \boxed{v_n = \sqrt{\frac{2nqV_m}{m}}} \tag{5.4.4}$$

Substituting this value of v_n in (5.4.2),

$$l_n = \frac{v_n}{2f} = \frac{1}{2f}\sqrt{\frac{2nqV_m}{m}} = \frac{1}{f}\sqrt{\frac{nqV_m}{2m}} \tag{5.4.5}$$

The lengths of the drift tube should therefore be proportional to the square root of natural numbers, i.e. in the ratio $1 : \sqrt{2} : \sqrt{3} \cdots$ etc.

Treating **relativistically**, if E be the total energy of the ion, then $nqV_m = E - m_0c^2$.

$$\text{But,} \quad E = mc^2 = \frac{m_0}{\sqrt{1 - v_n^2/c^2}}c^2$$

$$\text{or,} \quad \frac{nqV_m}{m_0c^2} = \frac{1}{\sqrt{1 - v_n^2/c^2}} - 1$$

$$\text{or,} \quad nr = \frac{1}{\sqrt{1 - v_n^2/c^2}} - 1 \tag{5.4.6}$$

where $r = qV_m/m_0c^2$, and m and m_0 are respectively the moving and the rest mass of each ion.

Combining (5.4.2) and (5.4.6), and on simplification,

$$\boxed{l_n = \frac{\lambda}{2(nr+1)}\sqrt{(nr+1)^2 - 1}} \tag{5.4.7}$$

If the accumulated kinetic energy nqV_m is quite small, compared to the rest mass energy m_0c^2, then $nr \ll 1$. So, from (5.4.7)

$$l_n = \frac{\lambda}{2}\sqrt{2nr} \tag{5.4.8}$$

This shows that the *first few drift tubes may be mere rings*. But towards the high energy limit, $nr \gg 1$ and the length of the drift tubes, as seen from (5.4.7), approaches the constant value $\lambda/2$. This is because, in this limit, the speed of the ions approaches c, the velocity of light.

The *total length* L of a linear accelerator with n gaps is obtained by adding the lengths l_n. So, from (5.4.8),

$$\therefore \quad L = \sum l_n = \frac{\lambda}{2}\int_0^n \sqrt{2nr}\,dn = \frac{\lambda}{3}\sqrt{2r}\,n^{\frac{3}{2}} \tag{5.4.9}$$

The *final energy* acquired by the ions in such accelerators is given by

$$W = nqV = \left(\frac{3L}{\lambda}\right)^{\frac{2}{3}}\left(\frac{1}{2}m_0c^2\right)^{\frac{1}{3}}(qV)^{\frac{2}{3}} \tag{5.4.10}$$

using (5.4.9) and the value of $r\,(= qV/m_0c^2)$.

Equation (5.4.10) shows that to obtain high energies, we require (i) *heavy ions* carrying *large charges*, (ii) a *long* accelerator and (iii) an *oscillator* having a very *high frequency* and *large voltage* amplitude.

Usefulness — The linear accelerators are useful for accelerating protons and other heavier ions to energies of about 32 MeV.

The main *advantage* of a linear accelerator is that here *no magnet* is necessary to guide the particles. They emerge from the machine automatically as an excellent well-collimated beam and hit the target directly, unlike the circular type of machines like cyclotron (see later) where the emergent beam spreads out. Moreover, in linear accelerators, the emergent beam is *highly intense* and *homogeneous*. Since again the acceleration takes place in a straight line, the *radiation loss is much less* unlike circular machines.

It is however *not possible* to accelerate electrons to very high energies in such machines as the electrons become relativistic even at few MeV and start moving out of phase. Also, these machines require ultra-high-frequency oscillator for synchronisation.

• The linear accelerator meant for the electrons however is different, consisting essentially of a *continuous tube* down which an electromagnetic wave propagates. The tube is rather a *wave guide*, as it contains apertures deployed at intervals determined by the frequency of the travelling wave and also the size of the tube.

Scanned with CamScanner

5.5 Cyclotron

The cyclotron, first devised in 1931 by Lawrence and Livingstone, is a device to speed up charged particles in successive steps under the combined influences of electric and magnetic fields along circular or spiral trajectories.

Construction — It consists essentially of *two flat semi-circular hollow metal boxes* D_1, D_2, called the *dees* (D) because of their shape (Fig. 5.7). These hollow chambers have their diametric edges *parallel* and *slightly separated* from each other so as to produce a narrow gap between them. The dees are placed in an evacuated chamber or

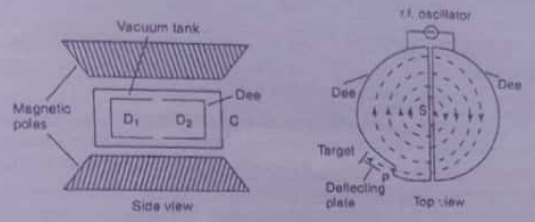

Fig. 5.7

vacuum tank C and are connected to an rf-oscillator so that a *high frequency* (10 MHz) alternating potential is applied between the dees acting as electrodes. The potential between the dees thus alternates rapidly and the electric field in the gap is first directed to one dee and then to the other. The space within each dee is however *field-free* (zero field). The chamber C is mounted *horizontally* between the pole pieces of a *huge electromagnet* that provides an intense and *uniform vertical* magnetic field of several Tesla. Since the field must be uniform over the whole of the dees, the diameter of the poles should be slightly greater than that of the dees.

The ion-source S is located near the mid-point of the gap between the dees. The ions, after being accelerated, are brought out of the chamber through a *window* P by a *charged* deflecting *plate* to eventually bombard the target.

Principle of action — Let a positive ion of charge q leave the ion-source between the dees and enter the negative dee at the instant with velocity $\vec{v}_0$, normal to the magnetic lines of force. Due to the magnetic field $\vec{B}$, the force $\vec{F}$ acting on the particle is given by

$$\vec{F} = q\vec{v}_0 \times \vec{B} \tag{5.5.1}$$

But $\vec{B}$ is perpendicular to the direction of the force so that we obtain

$$F = qv_0B \tag{5.5.2}$$

Under the action of the field, the path of the particle is bent into a circle of radius r_0, given by

$$qv_0B = \frac{mv_0^2}{r_0} \quad \Rightarrow \quad r_0 = \frac{mv_0}{qB} \tag{5.5.3}$$

where m is the mass of the ion (particle).

When the particle is inside the dee, its speed stays constant, but as it leaves the dee to reach the gap, after describing the semicircular path inside the dee, the electric field of the rf-source changes direction *synchronously*. The particle thus gets a 'kick' and is accelerated into the other dee where, because of its increased speed v, it moves in a semi-circular path of comparatively larger radius r, given by

$$r = \frac{mv}{qB} \tag{5.5.4}$$

to emerge out again into the gap between the two dees.

The *frequency of revolution* of the particle in the circular orbit is given by

$$f = \frac{v}{2\pi r} = \frac{vqB}{2\pi mv} = \left(\frac{q}{m}\right)\frac{B}{2\pi}, \text{ using (5.5.4).} \tag{5.5.5}$$

The *important fact* that emerges from (5.5.5) is that *the frequency of revolution is independent of the speed of the ion and the radius of the path* in the dees. So if the electric field reverses regularly at a frequency f', exactly equal to f, the field in the gap is always in the right direction to accelerate a charged particle by an impulse, each time the gap is crossed.

$$\therefore \quad \boxed{\left(\frac{q}{m}\right)\frac{B}{2\pi} = f = f'} \tag{5.5.6}$$

This is called the **basic resonance equation** *for a fixed frequency cyclotron*.

Thus the revolving charged particle is steadily speeded up describing a *flat spiral* of increasing radius. Finally, it reaches the periphery of the dees and is brought out of the chamber through the window by a negatively charged deflector to impinge on the properly mounted target.

Energy of the particle — The kinetic energy W_k of the charged particle is

$$W_k = \tfrac{1}{2}mv^2$$

∴ The maximum kinetic energy of the particles when they leave the cyclotron is

$$W_m = \tfrac{1}{2}mv_m^2 = \tfrac{1}{2}m\left(\frac{r_m qB}{m}\right)^2, \text{ using (5.5.4).}$$

$$\therefore \quad \boxed{W_m = \frac{q^2B^2}{2m}r_m^2} \tag{5.5.7}$$

where r_m = the maximum radius of the trajectory.

Scanned with CamScanner

Thus the *maximum energy* that can be imparted to a particle in a cyclotron is directly proportional to (i) the *square* of *radius* of the dees and (ii) the *square* of the *magnetic field* strength of the magnet.

• The maximum energy of the particles expressed in equivalent voltage V is given by

$$qV = W_m$$
$$\Rightarrow V = qB^2r_m^2/2m \tag{5.5.8}$$

• An alternative expression for W_m can be obtained on an elimination of B from (5.5.7), using (5.5.6).

$$W_m = 2m(\pi f r_m)^2 \tag{5.5.9}$$

Usefulness and limitations — The cyclotron can energise protons, deuterons, α-particles to 10-50 MeV. Its main *advantage* is that it does *not* demand any excessively high voltage source for producing high energy particles. Further, *no accelerating tube* capable of withstanding high potential gradients is necessary.

The *most serious limitation* imposed on the action of a cyclotron is however due to the *relativistic increase in mass* of the accelerated particle, given by

$$m = \frac{m_0}{\sqrt{1 - v^2/c^2}} \tag{5.5.10}$$

where m_0 is the rest mass of the particle and m its moving mass at v.

∴ The frequency of revolution of the particle

$$f = \left(\frac{q}{m}\right)\frac{B}{2\pi} \tag{5.5.11}$$
$$= \left(\frac{q}{m}\right)\frac{Bc^2}{2\pi c^2} = \frac{Bqc^2}{2\pi(m_0c^2 + W_k)} \tag{5.5.12}$$

where W_k is the kinetic energy of the particle corresponding to the speed v.

So, as the mass or speed of the particle increases for a fixed B and q, f decreases. Thus in a fixed frequency cyclotron the particle, as it spirals out from the source, will lag in phase behind the accelerating dee voltage. It would thus cease to get accelerated. The frequency of oscillation must be suitably modified to ensure *resonance acceleration* in the gaps. This cannot be done without upsetting the condition for low energy particles. ***With electrons, the relativistic change in mass is more pronounced than with positive ions, even for low energies. This makes the cyclotron rather impractical for accelerating electrons to high energies.***

The *other limitation* is that the limit to the maximum energy in a cyclotron is set by the engineering difficulties and expense. Also, from (5.5.7) the energy $W_k \propto r^2$, for a given particle so that the size of a cyclotron increases more rapidly than the corresponding increase in energy.

5.6 Compensation for relativistic mass gain

There are however ways to overcome the limitation imposed on the action of a cyclotron due to relativistic mass-variation by proper compensation for relativistic mass gain. This could be done by either of the following *two* methods.

1. The orbital frequency f of the ions can be kept unchanged in spite of the relativistic effect if $B\sqrt{1 - v^2/c^2}$ is kept constant for, from (5.5.10),

$$f = \frac{qB}{2\pi m} = \frac{qB\sqrt{1 - v^2/c^2}}{2\pi m_0}$$

This is achieved by using a type of electromagnet for which the *magnetic field increases* slowly as ions move over the orbits of increasing radius. An accelerator using this method of synchronisation is called a **synchrotron**.

2. The other method of compensation for the decrease in ion-frequency f due to relativistic effect is to keep the magnetic field constant and slowly *reduce the frequency of the applied alternating electric field* with increase in speed of the ion such that it is always equal to the rotation-frequency f of the ions. Accelerators employing this principle are known as **synchro-cyclotrons** or *frequency-modulated cyclotrons*.

5.6.1 Phase stability and phase oscillations

The synchrocyclotron is based on the possibility of the so-called *phase stable orbits* by varying the voltage at the dee-gap as a function of phase angle. This important idea was first conceived by Veksler and independently by McMillan in 1945.

Consider an ion in a uniform magnetic field moving in a circular path with constant speed in synchronisation with the applied a.c potential. The orbit under this condition would be a *stable orbit*. The energy, frequency and radius of this orbit are referred to as *synchronous* and the particle as synchronous particle.

Consider next an ion that crosses the gap between the dees at a phase such as ϕ_0 on the waning portion of the accelerating voltage (Fig. 5.8). As the ion gains energy in this crossing, its frequency of circulation f decreases and as a result it moves in

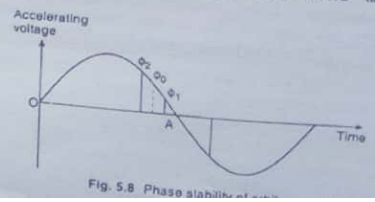

Fig. 5.8 Phase stability of

Scanned with CamScanner

This relation (5.6.3) gives the *fractional frequency shift* required to impart a final energy W_k to the charged particle.

If V_0 be the peak accelerating voltage, then at the dee-crossing the particle has its energy increased by an amount ΔW given by

$$\Delta W = qV_0 \sin \phi_0$$

where ϕ_0 is called the *synchronous phase angle* and is measured from the cross-over point A (Fig. 5.8).

5.7 Betatron

The maximum energy that could be imparted to a particle in a cyclotron is limited by the relativistic increase in mass that disturbs synchronisation. In particular, the cyclotron cannot be used to accelerate electrons as their relativistic mass-increase even at low energies is quite high. The above difficulty is overcome in a *betatron* (also called *induction accelerator*) designed and developed by Kerst in 1940 for accelerating specifically the electrons.

Basic principle — The *basic principle* of a betatron is to accelerate electrons in a stable orbit of essentially constant radius by the application of an alternating magnetic field, called the *induction field*. The induction field mainly produces *two* effects : *First*, the increasing magnetic flux produces an electromagnetic force that accelerates the electrons along their orbits and thus increases their energy in each successive orbital revolution. *Secondly*, the varying magnetic field, acting perpendicular to the electron-orbit, simultaneously constrains the electrons move in a circular trajectory of constant radius.

• In the betatron, the rate of increase of the flux linking the electron-orbit is very slow compared to the circulation frequency. The electrons are continuously accelerated during the beginning of the rising magnetic field.

Betatron condition — We first derive the *condition for a stable orbit* of constant radius in a betatron.

As the magnetic field varies with time, the induced emf ε is given by

$$\varepsilon = \frac{d\phi}{dt} \quad \text{(save the sign)} \tag{5.7.1}$$

where ϕ is the magnetic flux enclosed by the orbiting electrons.

If r be the radius of the electron orbit, the induced emf is also given by

$$\varepsilon = 2\pi r X \tag{5.7.2}$$

where X is the induced electric field.

∴ The force acting on the electron of charge e is

$$F = eX = e\frac{\varepsilon}{2\pi r} = \frac{e}{2\pi r}\frac{d\phi}{dt}, \quad \text{using (5.7.2) and (5.7.1).} \tag{5.7.3}$$

As the electron of mass m and velocity v is deflected by magnetic induction B along an orbit of radius r, we have

$$\frac{mv^2}{r} = Bev$$

∴ Momentum, $p = mv = Ber$ (5.7.4)

$$\therefore \quad F = \frac{dp}{dt} = \frac{d}{dt}(Ber) = er\frac{dB}{dt}, \quad \text{using (5.7.4).} \tag{5.7.5}$$

Comparing (5.7.3) and (5.7.5), we obtain

$$\boxed{\frac{d\phi}{dt} = 2\pi r^2 \frac{dB}{dt}} \tag{5.7.6}$$

This *important* equation is known as the **betatron condition** which must be satisfied during the entire period of acceleration if the electrons are to be kept on a track of constant radius r.

Integrating (5.7.6) with respect to t, we obtain

$$\phi = 2\pi r^2 B \tag{5.7.7}$$

For a *uniform magnetic induction*, however, the flux should be $\pi r^2 B$.

Thus for a *stable orbit of constant radius*, the *pole pieces* of the magnet are to be *so designed* that the *flux must change at twice the rate at which it would have changed if the magnetic induction were uniform* throughout the area enclosed by the orbit.

• The above condition is achieved by designing pole pieces from *laminated* iron core in which the varying magnetic field is produced by an a.c. supply of about 60 Hz. Then the flux density at the centre of the orbit is larger than that at the edges. This condition is valid for relativistic and non-relativistic energies of the electron.

Construction — The betatron (Fig. 5.10) consists essentially of : (i) a *highly evacuated doughnut-shaped* glass *chamber* containing the source of electrons; the chamber is coated inside with a thin layer of silver to prevent accumulation of surface charges. The silver film has low conductivity so that the induced eddy currents that are set up and disturb the magnetic fields are at low values; (ii) a *specially shaped powerful*

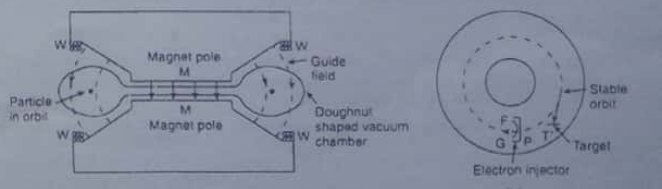

Fig. 5.10 Betatron : cross-sectional view

Scanned with CamScanner

electromagnet MM between the pole pieces of which the doughnut is mounted — the pole pieces being so designed that they have a *strong field at the centre* with *gradient towards the edges*, (iii) the *windings* WW through which passes an alternating current to energise the electromagnet; (iv) the *filament* F which is the source of electrons produced thermoionically. The thermoelectrons are given an initial energy of 50 kV by applying a high potential between F and the plate P, G being the grid to focus the electrons. The electrons are injected into the doughnut (equilibrium orbit) at a time when the magnetic flux of the electromagnet rises from zero in the first quarter cycle so as to be guided on to the orbit of radius r. T' is the *target* to be hit by the accelerated stream of electrons.

When the magnetic field increases from zero to the final positive maximum, the electrons complete enough number of revolutions (thousands) in the fixed stable orbit gaining higher and higher energies. When the desired energy is attained, the radius of the orbit is suddenly increased by increasing the flux ϕ, without changing the field, using the relation (5.7.7) : $r = (\phi/2\pi B)^{\frac{1}{2}}$, and the electrons are deflected onto the target T'. This is ensured by the discharge of a capacitor through the primary of the electromagnet that increases the flux without changing the flux density.

Energy computation — The momentum p imparted to an electron of charge e by a field B is given by (5.7.4) :

$$p = mv = Ber$$

$\therefore$ The energy (relativistic) is $E = pc = Berc$

where B is the magnetic field at the end of the acceleration time.

In a betatron, the acceleration time is $\frac{1}{4}T$ where T is the period $(= 2\pi/\omega)$, ω being the angular velocity.

$$\therefore \quad \frac{T}{4} = \frac{1}{4} \times \frac{2\pi}{\omega} = \frac{\pi}{2\omega} \tag{5.7.8}$$

$\therefore$ Distance travelled by the electron in time $T/4$ is $d = \pi c/2\omega$, since the velocity of electron approaches that of light c, on being accelerated.

$\therefore$ **Number of revolutions** executed per sec by the electron is

$$n = \frac{d}{2\pi r} = \frac{\pi c}{2\omega} \times \frac{1}{2\pi r} = \frac{c}{4\omega r} \tag{5.7.9}$$

where r is the radius of the stable orbit.

When the flux changes with time, the energy gained per second by the electron is

$$e\frac{d\phi}{dt} = e\frac{d}{dt}(\phi_0 \sin\omega t) \quad [\because \ \phi = \phi_0 \sin\omega t]$$
$$= e\omega\phi_0 \cos\omega t.$$

Since the acceleration occurs in time $T/4$, the *average energy* gained in revolution is

$$\frac{\int_0^{T/4} e\omega\phi_0 \cos\omega t \, dt}{\int_0^{T/4} dt} = e\omega\phi_0 \int_0^{T/4} \cos\omega t \, dt \Big/ \int_0^{T/4} dt$$
$$= \frac{2e\omega\phi_0}{\pi}, \text{ using (5.7.8).}$$

$\therefore$ **Total energy** imparted to the electron in n revolutions is given by

E_T = mean energy per revolution × no. of revolutions

$$\Rightarrow \quad \boxed{E_T = \frac{2e\omega\phi_0}{\pi} \times \frac{c}{4\omega r} = \frac{ec\phi_0}{2\pi r}} \tag{5.7.1}$$

using the equation (5.7.9) for the number of revolutions.

The upper limit of performance of a betatron is limited by *two* factors : (i) th *relativistic variation in mass* and (ii) the *radiation loss*, as discussed under '*Use and limitations*' that follows. Once the relativistic effect becomes important, furthe acceleration of the particles becomes slight.

• As a typical example of betatron parameters, take the case of the GEC 100 MeV betatron. It has pole face diameter about 2 m, the weight of the magnet is 130 tons. To achieve an energy of 100 MeV, the electrons pick up 420 eV in each turn, for a total number of 2.4×10^5 turns. Interestingly, the equivalent linear distance is about 130 km.

Uses and limitations — Betatrons can energise electrons to about 100 MeV. As the machine is relatively small, it is quite suitable for laboratory work. It is also a powerful x-ray generator and is used in hospitals for therapeutic x-rays. Betatron can produce x-rays so short in wavelength as to surpass the γ-rays from radioactive sources.

But the machine suffers from the *problem of orbital stability*. The stability must be assured by proper design. The other drawbacks are (i) a *huge magnet* (dia exceeding 2 m) is needed for supplying the variable flux to accelerate the electrons, (ii) an accelerated electron loses energy by radiation and the rate of radiation increases, according to classical electrodynamics, with the fourth power of the energy so that a limit is set for the high energy electrons by *radiation loss* and (iii) in the practical condition, the maximum energy that can be imparted to an electron is about 1000 MeV or 1 BeV.

• Note that the final energy E_T given by (5.7.10) is *independent of* ω, the angular frequency of the changing flux. However, ω should not be too small, for otherwise the time of acceleration is increased and the radiation loss (ignored to derive (5.7.10)) of energy also increases.

Scanned with CamScanner

5.7.1 Cyclotron vs. Betatron

Cyclotron	Betatron
1. Fixed-frequency cyclotron employs no alternating magnetic field; field is *constant*.	1. Betatron, however, employs an oscillating field which is called the *induction field*.
2. Particles are accelerated in *helical orbits* and orbital radius goes on increasing and equals the radius of the dees in the limit.	2. The acceleration of the particles in a betatron takes place in *a circular orbit* which is essentially of constant radius.
3. A fixed-frequency cyclotron is unsuitable for accelerating electrons.	3. A betatron is specifically meant for accelerating the electrons.
4. Cyclotron suffers from the problem of orbital stability.	4. It also suffers from the problem of orbital stability.
5. This cannot be used as an X-ray generator.	5. This is a very highly efficient X-ray generator.

5.8 Electron synchrotron

The disadvantages of a betatron in accelerating electrons are greatly eliminated in electron synchrotron which, in fact, combines the *accelerating system* of the cyclotron with the *ring-shaped pulsating guide field* of a betatron.

Construction — The essential parts of an electron synchrotron (Fig. 5.11) are (i) a *doughnut shaped toroidal vacuum chamber* or *tube* into which are injected electrons, initially accelerated by a linear accelerator to an energy of about 50-100 keV when their speed is about 0.5c, (ii) the *magnetic pole pieces*, which are *annular* and closely follow the outline of the doughnut to guide the electrons into an equilibrium orbit inside the

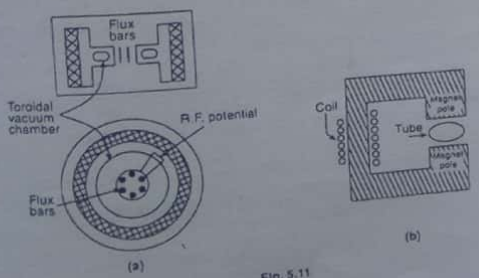

Fig. 5.11

doughnut, (iii) *soft-iron flux bars*, located in the central gap and serving as the central magnetic core to start the machine as a betatron, and (iv) copper or silver coating in a part of the interior of the doughnut to give a *D*(dee)-shaped *resonance cavity* and is connected to a *rf-oscillator*.

Action — The machine acts in *two phases*. The electrons are *first* accelerated to energies of about 1–2 MeV by the varying magnetic flux as in a betatron. As the flux varies, the electrons move in circular orbits and get accelerated. At energies of about 2 MeV, the flux bars become *magnetically saturated* and cannot accelerate the electrons further. The *betatron action* thus *ceases* and the first phase of the machine is over.

In the *second phase*, the H.F. oscillator becomes active. If the potential applied to the resonance cavity is at the proper frequency, the electrons resonate and are accelerated periodically, as in a cyclotron, at the beginning and end of the *D*. When the electrons are accelerated to the maximum energy, the oscillator is suddenly switched off to deflect the electrons outward towards the target. The energy acquired is as high as 1000 MeV or 1 BeV. Using tungsten target, very hard X-rays of energy about 300 MeV have been produced.

The machine however suffers from a *limitation* imposed on the energies of the electrons due to *radiation loss*.

Energy attained — The energy attained by the electrons may be calculated from the relation

$$E = \sqrt{p^2c^2 + m_0^2c^4} = W_k + m_0c^2 \qquad (5.8.1)$$

where p is the momentum and W_k the kinetic energy of the electron.

If p and W_k are very large compared to the rest mass energy m_0c^2, we obtain from the above relation (5.8.1)

$$W_k \simeq pc \simeq Berc \qquad (5.8.2)$$

where r is the equilibrium orbit radius and B the magnetic flux density.

If B is expressed in Wb/m^2, r in metre and the energy in MeV, then we have from equation (5.8.2)

$$W_k = 300Br \text{ MeV}$$

The condition for a stable orbit, as in betatron : $\phi = 2\pi r^2 B$, must still be fulfilled. The use of a very heavy magnet over the entire volume of the vacuum chamber is *no longer needed*.

• The accelerating system is usually a metallic quarter-wave resonant cavity, resonant at electron-orbital frequency. The resonant cavity is formed by coating the inside and outside of an angular sector of the doughnut-shaped vacuum chamber with silver or copper.

Scanned with CamScanner

5.14 Accelerators in India

Attempts for an installation of an accelerator in India began during the World War II at the Palit Laboratory of Physics, University of Calcutta. This culminated in commissioning in 1960 a 37″ fixed frequency cyclotron (Berkeley model) that produced proton beams of 3.7 MeV used for studies in γ-ray spectroscopy and biomedical investigations. It has since been de-commissioned.

In 1971, a 66 cm fixed frequency cyclotron with variable energy, received as a gift from the University of Rochester, started operation at the Punjab University, Chandigarh. Earlier, during 1953–64, it was in operation at Rochester. This produced a proton beam of 5 MeV.

The biggest accelerator of India, in operation, is the sector-focussed 224 cm AVF type cyclotron at the Variable Energy Cyclotron Centre (VECC) in Kolkata. Designed to deliver proton beams of 6–60 MeV, deuteron beams of 12–65 MeV and α-particle beams of 24–130 MeV, it gives at present α-beam of 80 MeV energy and the beam current is a few mA.

Among the other accelerators, mention may be made of (a) K-14 tandem type pelletron of TIFR, Bombay (1986) that gives 28 MeV protons, 42 MeV α-particles and heavier ions of still higher energies, and (b) a K-15 tandem type pelletron at Nuclear Science Centre, Delhi, under UGC to cater the need of the University community. Both these machines were purchased (1990) from High Voltage Corporation, USA and are used for heavy ion reaction studies. K-15 is capable of giving energy 8-30 MeV.

Apart from these, a number of low energy electrostatic accelerators are in operation in different Indian labs e.g. a 5.5 MeV van de Graaff accelerator at TIFR, 2 MeV Tandem van de Graaff accelerators at BARC, at the Institute of Physics, Bhubaneswar, at IGCAR, Kalapakkam and at IIT, Kanpur. Also a number of Cockroft-Walton generators are in operation: a 1 MeV machine at the University of Calicut, a 400 kV machine at TIFR and a 250 kV machine at Bose Institute, Calcutta.

Exclusively for biomedical purposes, a number of electron accelerators are also in operation. For instance, a 42 MeV betatron at CMC, Vellore; a 20 MeV linear accelerator at AIIMS, New Delhi; a 12 MeV linac at the Dept. of Radiotherapy, Srinagar; a 10 MeV linac at Tata Memorial Hospital, Bombay and a 8 MeV microtron in the Physics Dept., University of Pune, etc.

In addition to these, (i) a synchrotron radiation facility is being built at the Centre of Adv. Technology (CAT), Indore, using storage rings, for a maximum energy of 2 GeV and (ii) it has been proposed to build a K-50 cyclotron with superconducting magnets, completely indigenously, at VECC, Kolkata. Design studies have since been in progress.

5.15 Illustrated Examples

► **Example 1.** *If the maximum electric field that can be tolerated perpendicular to the surface of its belt is 2 MV/m, find the maximum charging current in a van de Graaff generator. The width of the belt is 0.5 m and its speed is*

Scanned with CamScanner

Nuclear Reactions : The Q Equation

6.4 Nuclear reactions

Our knowledge of nuclear structure is mostly the outcome of experiments of bombarding a nucleus with various projectiles such as protons, neutrons, deuterons, α-particles etc. After the bombardment, it may so happen that the mass number and/or atomic number of the target nuclei changes, that is, nuclear transmutation takes place. We then say a *nuclear reaction* has occurred.

A **nuclear reaction** is thus a process that takes place when a nuclear particle, such as proton, neutron, deuteron, α-particle, a nucleus etc., comes in close contact (within 10^{-15} m) with another, and energy and momentum exchanges occur. The final products of the reaction are also some nuclear particle or particles that leave the point of contact in different directions. The process results in the *transmutation* of the target nucleus.

The changes that occur in a nuclear reaction usually involve *strong nuclear force*. Processes that involve weak interactions (e.g. β-decay) or are purely electromagnetic (e.g. Coulomb scattering) are *not usually included* under nuclear reactions. Changes of nuclear states due to electromagnetic interactions however are included.

A *general equation* representing a *nuclear reaction* is of the form :

$$X + x \rightarrow Y + y$$

$$\text{or,} \qquad X(x, y)Y$$

where X is the target nucleus, x the bombarding particle, Y the residual product nucleus and y the ejected particle.

In a nuclear reaction, charge number, mass number, total energy etc. are conserved. (See Art. 6.4).

Scanned with CamScanner

6.2 Artificial transmutation : Early experiments

Since the days of radioactivity, physicists knew of nuclear transmutations occurring in nature. But the first ever nuclear transmutation by artificial means (man-made) was achieved by Rutherford in 1919 by bombarding nitrogen (N-14) with high energy (7.68 MeV) α-particles emitted from Po-214.

Rutherford's apparatus — Rutherford's apparatus is shown in Fig. 6.1. C is a glass chamber that could be filled with any desired gas. Inside is kept a source S of α-particles. F is a silver foil that closes the side-opening of the chamber; the thickness of the foil is sufficient to absorb α-particles. Close to F is a zinc sulphide screen Z.

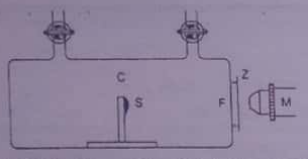

Fig. 6.1 Artificial transmutation : Rutherford's experiment

The microscope M is meant for observing scintillations, if any, on the screen Z. The distance between F and S can be readily varied and Rutherford kept it at a value more than the range of α-particles in the gas inside. So, the α-particles emitted from S cannot reach F.

Observations and inference — With N-14 in the chamber, in a condition as described, Rutherford observed scintillations on the screen Z, even when the distance between Z and S was 40 cm. Under no circumstances, the α-particles could create them. What then were the scintillations due to? Rutherford concluded that they were due to high speed particles ejected from nitrogen nuclei when bombarded by α-particles, a *rare nuclear event*.

Magnetic deflection experiments and determination of the specific charge confirmed that the suspected particles were protons (hydrogen nuclei). Rutherford also eliminated the possibility that these protons were *not* the ones ejected from the hydrogen present as impurity, if any, in the nitrogen gas taken. He explained : when the high speed α-particles collided head-on with nitrogen nuclei, some of them were absorbed by the latter forming a composite system that disintegrated immediately (within $\sim 10^{-15}$ s) emitting a high speed proton and leaving a new residual nucleus. Such a *nuclear transformation* (transmutation) is called a **nuclear reaction**. The reaction under reference is an *alpha-proton* (α, p) *reaction* represented by

$$^{14}_{7}\mathrm{N} + {}^{4}_{2}\mathrm{He} \rightarrow {}^{17}_{8}\mathrm{O} + {}^{1}_{1}\mathrm{H}$$

or, $^{14}_{7}\mathrm{N}(\alpha, p)^{17}_{8}\mathrm{O}$

Rutherford thus transmuted ordinary nitrogen into a rare isotope of oxygen. Feverish attempts soon started the world over to transmute one element into another by accelerating projectiles like α-particles, protons, deuterons etc. to higher and higher energies. And this attempt of transmuting one element to another led to the production of giant accelerators in different laboratories.

For instance, in 1930, Cockroft and Walton used artificially accelerated protons to produce the nuclear reaction

$$^{7}_{3}\mathrm{Li} + {}^{1}_{1}\mathrm{H} \rightarrow {}^{4}_{2}\mathrm{He} + {}^{4}_{2}\mathrm{He}$$

or, $^{7}_{3}\mathrm{Li}\,(p, \alpha)\,{}^{4}_{2}\mathrm{He}$

6.3 Types of nuclear reactions

On the basis of the projectile used, the particle ejected and the residual nucleus formed, there are different types of nuclear reactions and they may be classified as follows.

1. **Elastic scattering** — In *elastic scattering* reaction, *the projectile and the outgoing particle are the same*, i.e., the projectile is scattered in different directions and there is no loss of energy. The *residual nucleus is the same as the target nucleus* and is left in the ground state as the latter. So, it can be represented as $X(x, x)X$. An example of elastic scattering is the scattering of neutrons by graphite : $^{12}\mathrm{C}\,(n, n)\,{}^{12}\mathrm{C}$.

2. **Inelastic scattering** — In *inelastic scattering*, the *projectile and the outgoing particle are also the same*. They are scattered in different directions with different energy, as there is loss of energy due to collision. The residual nucleus, which is the same as target nucleus, is left in an *excited state* so that the process can be represented as $X(x, x)X^*$. An example is the collision of fast neutrons and U-238.

3. **Pickup reactions** — When the projectile gains nucleons from the target, the nuclear reaction is called *pickup reaction*. For example,

$$^{16}_{8}\mathrm{O}\left({}^{2}_{1}\mathrm{H}, {}^{3}_{1}\mathrm{H}\right){}^{15}_{8}\mathrm{O}$$

4. **Stripping reactions** — In *stripping reactions*, one or more nucleons from the projectile are captured by the target nucleus i.e., the projectile loses nucleons to the target; the remaining stripped nucleus is emitted in a different direction.

• In pickup or stripping reactions, the involved nucleon is assumed to enter or leave (the shell of) the target nucleus without disturbing the other nucleons. So, these reactions are also called **direct reactions**.

5. **Compound nuclear reactions** — Here the incident projectile A is captured by the target nucleus B to form a compound nucleus C^* in an *excited* state. The de-excitation of the compound nucleus C^* occurs into a product nucleus D and an emission of a particle E or a γ-photon.

So, this type of nuclear reaction may be represented by

$$A + B \rightarrow C^* \rightarrow D + E$$

Scanned with CamScanner

The same compound nucleus may be formed in a number of different ways and may also decay in a number of ways independent of the mode of its formation. For instance, the compound nucleus $^{64}_{30}Zn$ may be formed in an excited state $(^{64}_{30}Zn)^*$ by two different ways and then decays variously as shown :

1. $^{63}_{29}Cu + {}^{1}_{1}H \rightarrow \left(^{64}_{30}Zn\right)^* \rightarrow {}^{63}_{30}Zn + {}^{1}_{0}n$
$\rightarrow {}^{62}_{30}Zn + {}^{1}_{0}n + {}^{1}_{0}n$
$\rightarrow {}^{62}_{29}Cu + {}^{1}_{0}n + {}^{1}_{1}H$

2. $^{60}_{28}Ni + {}^{4}_{2}He \rightarrow \left(^{64}_{30}Zn\right)^* \rightarrow {}^{63}_{30}Zn + {}^{1}_{0}n$
$\rightarrow {}^{62}_{30}Zn + {}^{1}_{0}n + {}^{1}_{0}n$
$\rightarrow {}^{62}_{29}Cu + {}^{1}_{0}n + {}^{1}_{1}H$

• We shall study Bohr's idea of compound nucleus and the experimental investigations of the above reactions by Ghoshal later in appropriate time and place.

6. **Radiative capture** — Here, the incident particle is absorbed by the target nucleus to form the excited compound nucleus which disintegrates to produce one or more γ-*photons* and goes down to the ground state. So the process is $X(x,\gamma)Y$.

7. **Photodisintegration** — Here, a very *energetic photon is absorbed* by the target nucleus so that it is raised to an excited state and subsequently disintegrates. It can be represented as $X(\gamma,y)Y$.

There are many other types of nuclear reactions such as *elementary particle reaction* involving production of elementary particles, *many body reaction* in which two or more particles are emitted by the compound nucleus, **nuclear fission** in which heavy nuclei disintegrate into two nuclei of comparable size, **nuclear fusion** in which light nuclei combine to form a heavier nucleus etc. etc.

• So, nuclear reactions can be broadly divided into two distinct classes known as *compound nuclear reactions* and *direct reactions*.

In the former, the incident particle is captured to form a nucleus in highly excited state, called **compound nucleus** which then decays.

In direct reactions, the incident nucleon interacts with the nucleus as it passes, without forming an intermediate state. A quantitative difference between the two types of reactions is the time of interaction. In direct reaction, it is of the order of time of transit of the incident particle over a nuclear diameter, which is $\sim 3 \times 10^{-22}$s. The fastest decay time known is longer than this by several orders of magnitude.

6.4 Conservation laws in nuclear reactions

The principal properties of nuclei are mass, charge, spin, linear and angular momenta, statistics, parity etc. Some of these properties are conserved in nuclear reactions and it is possible, using these conservation laws, to make an analysis of the reactions. The principal conservation laws are:

1. **Conservation of mass number** — *The total number of neutrons and protons in the nuclei in a nuclear reaction remains unaltered after the reaction.* That is, in the reaction $X(x,y)Y$, the sum of the mass numbers of X and x must equal the sum of the mass numbers of Y and y.

2. **Conservation of atomic number** — The *total number of protons in a nuclear reaction remains unaltered after the reaction.* That is, in the reaction $X(x,y)Y$, the sum of the atomic numbers of X and x equals the sum of the atomic numbers of Y and y.

• Obviously, because of the laws 1 and 2 above, the neutron number N also remains conserved in nuclear reactions.

3. **Conservation of energy (including mass-energy)** — The total energy, that is, the sum of rest-mass energies and the kinetic energies of all the nuclei taking part in the reaction must equal the sum of the rest-mass energies and kinetic energies of the products.

4. **Conservation of linear momentum** — The sum of the linear momentum vectors p's of nuclei taking part in a nuclear reaction must equal the sum of the linear momentum vectors of the products.

$$p_X + p_x = p_Y + p_y$$

5. **Conservation of angular momentum** — In any nuclear reaction, the total angular momentum of the nuclei before and after the reaction remains the same. In a nuclear reaction $X(x,y)Y$,

$$I_X + I_x + l_x = I_Y + I_y + l_y$$

where I_X, I_x, I_Y and I_y are the spins (i.e., total angular momentum) of X, x, Y, y respectively, and l_x and l_y are the relative orbital angular momentum of X and x (initially) and of Y and y (finally).

• The conservation of angular momentum, along with its quantum-mechanical properties, gives rise to certain *selection rules*.

6. **Conservation of parity** — The nuclear reactions considered in this chapter are due to strong interaction; and hence the parity remains the same before and after the reaction.

7. **Conservation of isotopic spin or isospin** — In a nuclear reaction, involving strong interaction, the isotopic spin vectors for the initial and the final states remain the same

$$T_X + T_x = T_Y + T_y$$

where the initial isotopic spin vector $T_i = T_X + T_x$ and the final isotopic spin vector $T_f = T_Y + T_y$.

For more details see Chapter '*Elementary particles*' and Appendix 1.

Isotopic spin is a characteristic of nuclear level so that its conservation in nuclear reactions may be used to identify the levels of the nuclei. For instance, for deuteron or α-particle since $T_x = T_y = 0$, $T_X = T_Y$.

Scanned with CamScanner

6.5 Energetics of nuclear reactions : Q-values

Consider the nuclear reaction, $X(x, y)Y$, represented by the equation

$$X + x = Y + y$$

where X is the target nucleus of mass M_X, Y the product or recoil nucleus of mass M_Y, x the incident particle of mass m_x and y the product particle of mass m_y.

Also let K_X, K_Y, K_x and K_y be the kinetic energies of X, Y, x and y respectively. We assume that X is initially at rest so that $K_X = 0$. The total energy of a particle is the sum of its kinetic and rest energy. For the conservation of energy in a nuclear reaction, therefore,

$$\begin{aligned} & M_X c^2 + (K_x + m_x c^2) = (K_Y + M_Y c^2) + (K_y + m_y c^2) \\ \text{or,} \quad & K_Y + K_y - K_x = (M_X + m_x - M_Y - m_y)c^2 \end{aligned} \tag{6.5.1}$$

where c is the velocity of light in free space.

Now the quantity on the left hand side of (6.5.1) is the difference between the kinetic energies of the products of the reaction and that of the interacting particles. This is usually denoted by Q which is equal, from (6.5.1), to the difference of the rest mass energies of the interacting particles and that of the product particles.

$$\left.\begin{aligned} \therefore \quad Q &= K_Y + K_y - K_x \\ &= (M_X + m_x - M_Y - m_y)c^2 \\ &= M_X + m_x - M_Y - m_y, \quad \text{in energy units} \end{aligned}\right\} \tag{6.5.2}$$

The quantity Q is known as the *energy balance* of the nuclear reaction, or more often the **Q-value**. The Q-*value* is thus the *net surplus or the deficit of energies of the reaction products* $K_Y + K_y$ *over the energy supplied* K_x.

There are now *three possibilities* which are discussed below :

1. **Exoergic reaction** — From (6.5.2), if $(M_X + m_x) > (M_Y + m_y)$, then $(K_Y + K_y) > K_x$ and $Q > 0$. Such a nuclear reaction is said to be *exoergic* or *exothermic* **reaction** because it releases energy.

In exoergic reaction, there is thus a net decrease in the mass after the nuclear reaction and the lost mass gets converted into surplus energy according to the relation $E = mc^2$. This energy is imparted as kinetic energy to the product particles.

2. **Endoergic reaction** — If, however, it happens that $(M_X + m_x) < (M_Y + m_y)$, then $(K_Y + K_y) < K_x$ and $Q < 0$. Such a nuclear reaction is said to be *endoergic* or *endothermic* **reaction** because some energy is to be supplied from outside in order that the reaction may occur.

In endoergic reaction, there is a net increase in the mass after the nuclear reaction and the increase in mass is provided by supplying energy to the incident particle so that the reaction proceeds in the forward direction. In endoergic reaction, a minimum

amount of energy equal to the negative Q-value of the reaction must thus be given to the incident particle so that the reaction occurs. Such an energy is called the *threshold energy* of the endoergic reaction.

3. The *third possibility* is that $Q = 0$ which occurs if $(M_X + m_x) = (M_Y + m_y)$, that is, the sum of the masses of the interacting particles is equal to the sum of the rest masses of the product particles. It gives rise to an *elastic collision* where there is no loss of energy but only a change in the direction of the particles.

• The nuclear reactions involve information about the nuclear masses and the particle energies and can be employed to derive information about the mass of nuclei, particle energies or Q-values. The quantity K_Y, the *recoil energy* of the product nucleus is usually small and is difficult to measure. It can however be *eliminated* by applying the principle of conservation of momentum to the reaction.

6.5.1 Kinematics of nuclear reactions : The Q-equation

Let a particle of mass m_x, moving along x-axis with a velocity v_x, collide elastically with a target nucleus, of mass M_X, at rest. Due to the nuclear reaction, the product nucleus of mass M_Y is scattered at an angle ϕ with velocity v_Y and the product particle of mass m_y is emitted with velocity v_y at an angle θ (Fig. 6.2). Angles θ and ϕ are *coplanar* since the linear momentum normal to θ-plane is zero.

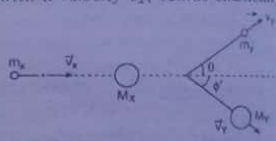

Fig. 6.2 Kinematics of a nuclear reaction

From the law of conservation of linear momentum along x and y-directions,

$$\left.\begin{aligned} M_Y v_Y \cos\phi + m_y v_y \cos\theta &= m_x v_x \\ -M_Y v_Y \sin\phi + m_y v_y \sin\theta &= 0 \end{aligned}\right\}$$

$$\text{or,} \quad \left.\begin{aligned} M_Y v_Y \cos\phi &= m_x v_x - m_y v_y \cos\theta \\ M_Y v_Y \sin\phi &= m_y v_y \sin\theta \end{aligned}\right\} \tag{6.5.3}$$

To eliminate ϕ, we square each of the relations in (6.5.3) and add to get

$$M_Y^2 v_Y^2 = m_x^2 v_x^2 + m_y^2 v_y^2 - 2m_x m_y v_x v_y \cos\theta \tag{6.5.4}$$

$$\text{or,} \quad 2M_Y K_Y = 2m_x K_x + 2m_y K_y - 4\sqrt{m_x m_y K_x K_y}\cos\theta$$

since, non-relativistically, K = kinetic energy $= \frac{1}{2}mv^2$.

$$\therefore \quad K_Y = \frac{m_x}{M_Y}K_x + \frac{m_y}{M_Y}K_y - \frac{2}{M_Y}\sqrt{m_x m_y K_x K_y}\cos\theta \tag{6.5.5}$$

To eliminate K_Y, we shall use : $\quad Q = K_Y + K_y - K_x$

$$\therefore \quad Q = K_y\left(1 + \frac{m_y}{M_Y}\right) - K_x\left(1 - \frac{m_x}{M_Y}\right) - \frac{2}{M_Y}\sqrt{m_x m_y K_x K_y}\cos\theta \tag{6.5.6}$$

Scanned with CamScanner

This gives the Q-value of the reaction in terms of K_y, K_x and θ without involving the kinetic energy of the recoil nucleus, K_Y and the mass M_X of target nucleus.

The analytical relationship (6.5.6) between the *kinetic energies of the projectile and the outgoing particle, and the nuclear disintegration energy* Q is known as the Q-equation in its standard form.

• The kinetic energies K_x, K_y and angle θ are all measured in the *laboratory-frame*. The Q-equation is based on the conservation of mass-energy in a nuclear reaction and would thus hold for all types of nuclear reactions. Without any significant error, one may use mass numbers in place of exact masses, in many applications. For accurate calculations, however, the neutral atomic masses are to be used.

If the angle $\theta = 90°$, we get

$$Q = K_y\left(1 + \frac{m_y}{M_Y}\right) - K_x\left(1 - \frac{m_x}{M_Y}\right) \tag{6.5.7}$$

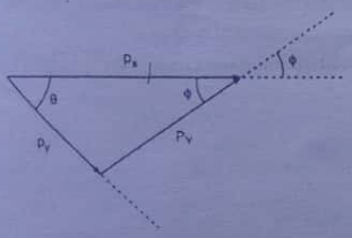

Fig. 6.3 The momentum triangle

If Q is negative, it gives the minimum value of threshold kinetic energy to be given to the incident particle for an endoergic reaction to proceed in the forward direction.

• **An alternative method of deriving the Q-equation** — Interestingly, the Q-*equation* may be derived by solving the so-called ***momentum triangle*** (Fig. 6.3)

In reference to Fig. 6.3 which is rather self-explanatory, we may write

$$P_Y^2 = p_x^2 + p_y^2 - 2p_x p_y \cos\theta \tag{6.5.8}$$

$$\Rightarrow \quad 2M_Y K_Y = 2m_x K_x + 2m_y K_y - 2.2\sqrt{m_x K_x m_y K_y}\cos\theta$$

$$\Rightarrow \quad K_Y = \frac{m_x}{M_Y}K_x + \frac{m_y}{M_Y}K_y - \frac{2\sqrt{m_x m_y K_x K_y}}{M_Y}\cos\theta \tag{6.5.9}$$

But, we have, $K_Y = Q - K_y + K_x$

Substituting this value of K_Y in (6.5.9), we obtain

$$Q = \left(1 + \frac{m_y}{M_Y}\right)K_y - \left(1 - \frac{m_x}{M_Y}\right)K_x - \frac{2}{M_Y}\sqrt{m_x m_y K_x K_y}\cos\theta$$

which is the *standard form* of the Q-**equation.**

6.5.2 Threshold energy of endoergic reactions

In an endoergic reaction, the energy $-Q$ is necessary to excite the compound nucleus sufficiently for its breakage. This energy is to be supplied in the form of kinetic energy

of the incident particle. *At first sight*, the minimum energy required to initiate an endoergic reaction appears

$$(K_x)_{min} = -Q$$

where it is assumed that $K_y = K_Y = 0$. This however *cannot be true*. Before the reaction occurred, the incident particle must have had a linear momentum at least

$$p_x = \sqrt{2(K_x)_{min}m_x} = \sqrt{2Qm_x} \neq 0$$

and if K_y and K_Y are also zero, p_y and p_Y are zero, and this would *violate the principle of conservation of linear momentum*.

In fact, not all of the kinetic energy supplied by the incident projectile is available for the reaction since some of it is used to impart momentum to the compound nucleus which is finally distributed among the products of reaction. So, in addition to $-Q$, the projectile must provide some energy so that $-Q$ is available for the reaction.

The smallest value of projectile energy needed for an endoergic reaction to occur is called the **threshold energy** of that reaction.

Computation of threshold energy — We shall now compute the minimum amount of energy necessary for an endoergic reaction to occur, the *threshold energy*, E_{th} of the reaction.

For the conservation of linear momentum,

$$m_x v_x = M_c v_c \tag{6.5.10}$$

where M_c and v_c are the mass and velocity respectively of the compound nucleus and v_x, the velocity of the incident particle. It is *assumed* that v_c and v_x agree in direction, i.e., $\theta = 0$.

$$\therefore \quad v_c = m_x v_x / M_c \tag{6.5.11}$$

The part of the kinetic energy of the incident particle that excites the compound nucleus is given by

$$-Q = \tfrac{1}{2}m_x v_x^2 - \tfrac{1}{2}M_c v_c^2$$

$$= \tfrac{1}{2}m_x v_x^2\left(1 - \frac{m_x}{M_c}\right), \quad \text{using (6.5.11)}$$

$$= \tfrac{1}{2}m_x v_x^2 \frac{M_X}{M_X + m_x} \quad (\because\ M_c = M_X + m_x) \tag{6.5.12}$$

$$\therefore \quad \boxed{E_{th} = \tfrac{1}{2}m_x v_x^2 = (-Q)\frac{M_X + m_x}{M_X}} \tag{6.5.13}$$

using (6.5.12).

Equation (6.5.13) evidently shows that $E_{th} > (-Q)$. Their difference

$$E_{th} - (-Q) = E_{th} + Q$$

will appear as the *energy carried away by the compound nucleus*, while $-Q$ will be the *minimum energy available for the reaction*.

Scanned with CamScanner

So the minimum input energy for an endoergic reaction is

$$(K_x)_{min} = E_{th} = -Q\frac{M_X + m_x}{M_X} = -Q\left(1 + \frac{m_x}{M_X}\right) \tag{6.5.14}$$

and the minimum energy available for an endoergic reaction is, from (6.5.12),

$$(K_A)_{min} = (K_x)_{min}\frac{M_X}{M_X + m_x} = -Q \tag{6.5.15}$$

E_{th} can be determined experimentally and (6.5.13) could then be used to evaluate the Q-value. $E_{th} = -Q$ when $m_x = 0$, as is the case in γ-induced reactions — the **photo-disintegrations**.

The equation representing a nuclear reaction often includes Q, as shown below.

$$x + X \rightarrow C^* \rightarrow Y + y + Q$$

This is a convenient way of showing the energy balance.

Equation (6.5.2) gives the least value of Q corresponding to the reaction that leaves the product nucleus Y in the *ground state*. If however the nucleus Y is in an *excited energy state* represented by K_e, the energy balance gives

$$Q = K_Y + K_y - K_x + K_e \tag{6.5.16}$$

• These considerations however are *not* limited to *two* products only. For instance, consider the following reaction :

$$x + X \rightarrow Y + z + y$$

The Q-value of the above reaction is given by

$$\begin{aligned} Q &= (M_X + m_x - m_z - m_y - M_Y)c^2 \\ &= (M_X - m_y - M_Y)c^2 \\ &= M_X - m_y - M_Y, \text{ in energy units.} \end{aligned}$$

If this Q-value is *positive*, the nucleus is *unstable* for the decay process $X \rightarrow y + Y$. If *negative*, the nucleus is *stable* against this decay and $|Q|$ gives the energy required to remove the sub-group y from the nucleus X, leaving the product nucleus Y in the ground state. This is called the **separation energy**, S which is the *minimum energy that must be supplied to remove the least tightly bound nucleon from the nucleus* (i.e. the binding energy of the least tightly bound nucleon). So,

$$S = (M_Y + m_y - M_X)c^2. \tag{6.5.17}$$

6.6 Solution of the Q-equation

We may study the variation of the energy K_y of the outgoing particle with the energy K_x of the incident projectile, for a fixed value of Q. For this, we need a recasting of the Q-equation (6.5.6) as follows.

$$M_Y Q = K_y(m_y + M_Y) - K_x(M_Y - m_x) - 2\sqrt{m_x m_y K_x K_y}\cos\theta$$

$$\text{or,} \quad K_y - 2\frac{\sqrt{m_x m_y K_x K_y}}{m_y + M_Y}\cos\theta - \frac{M_Y Q + K_x(M_Y - m_x)}{m_y + M_Y} = 0$$

$$\text{or,} \quad K_y - 2p\sqrt{K_y} - n = 0 \tag{6.6.1}$$

$$\text{where} \quad p = \frac{\sqrt{m_x m_y K_x}}{m_y + M_Y}\cos\theta; \quad n = \frac{M_Y Q + K_x(M_Y - m_x)}{m_y + M_Y} \tag{6.6.2}$$

Eq. (6.6.1) is a *quadratic equation* in $\sqrt{K_y}$, having the general solution

$$\boxed{\sqrt{K_y} = p \pm \sqrt{p^2 + n}} \tag{6.6.3}$$

which is a rather important relation as it provides valuable information regarding the nuclear reactions.

Obviously, when $\sqrt{K_y}$ is *real* and *positive*, the reaction is energetically possible.

I. Let us consider *first* the **exoergic reactions**, for which $Q > 0$.

1. For *projectiles of very low energy* (e.g., thermal neutrons) : In this case, we have

$$K_x \simeq 0, \text{ so, from (6.6.2), } p = 0, \; n = M_Y Q/(m_y + M_Y)$$

$$\therefore \quad \boxed{K_y = \frac{M_Y}{m_y + M_Y}Q} \quad \text{using (6.6.3).} \tag{6.6.4}$$

Thus, K_y *is the same for all values of the angle* θ.

2. For *projectiles of finite energy* : In most cases, $m_x \ll M_Y \Rightarrow n > 0$ for all K_x. So, from (6.6.1), K_y is *single-valued* for all K_x and is given by

$$\sqrt{K_y} = p + \sqrt{p^2 + n} \tag{6.6.5}$$

• Cases, however, are there when K_y is double-valued. Let ^{15}N be bombarded by deuterium with ^{16}O as residual nucleus and neutron as an outgoing particle.

$$^{15}_{7}\text{N} + ^{2}_{1}\text{H} \rightarrow ^{16}_{8}\text{O} + ^{1}_{0}\text{n} + Q \; (= 10\,\text{MeV})$$

If the outgoing particle m_y be taken for residual nucleus ^{16}O, then $m_y \simeq$ mass number $A_y = 16$ and $M_Y - A_Y = 1$ (for neutron).

$\therefore$ From (6.6.2), we obtain

$$n = \frac{Q - K_x}{16 + 1} = \frac{Q - K_x}{17}$$

which is *negative* for all deuteron bombarding energies greater than

$$K_x = Q = 10\,\text{MeV}.$$

$\therefore$ For $K_x > 10$ MeV, $\sqrt{K_y}$ have *two real, positive* values at $\theta = 0$.

Scanned with CamScanner

What does it imply? It implies that in the forward direction there are *two monoenergetic groups* of ^{16}O and physically it means that in the *centre of mass system, the above two groups are projected forward and backward.*

II. We *next* consider the **endoergic reactions** where $Q < 0$.

1. For *very low energy projectiles* : Here $K_x \simeq 0$ and $Q < 0$.

$$\therefore \quad p^2 + n < 0 \quad \Rightarrow \quad \sqrt{K_y} \text{ is } \textit{imaginary}.$$

It implies that *no nuclear reaction* occurs or, in other words, K_x is not sufficient enough to initiate the reaction.

2. Threshold energy of reaction : From (6.6.3), the nuclear reaction is just possible if K_x is large enough to make

$$p^2 + n = 0 \tag{6.6.6}$$

The minimum possible value of K_x is at $\theta = 0$ and is the *threshold energy*, E_{th}.

∴ The required condition gives

$$\frac{m_x m_y K_x}{(m_y + M_Y)^2} + \frac{M_Y Q + K_x(M_Y - m_x)}{m_y + M_Y} = 0 \tag{6.6.7}$$

Writing, $m_y = m_x + M_X - M_Y$, we have from (6.6.7), on simplification,

$$\boxed{E_{th} = -Q\frac{m_x + M_X}{M_X}}$$

which is the same as equation (6.5.13).

6.7 Experimental determination of Q-value

The Q-value of a nuclear reaction may be determined using the relation

$$\boxed{Q = K_Y + K_y - K_x}$$

by measuring the energies K_Y, K_y and K_x precisely.

The Q-value can also be evaluated from an accurate determination of the atomic masses of the nuclei involved in the reaction, using the relation

$$\boxed{Q = (M_X + m_x - M_Y - m_y)c^2}$$

It is difficult, as said already, to measure K_Y accurately, particularly if the product nucleus Y is a heavy particle. But K_Y can be determined using the equation (6.5.5) :

$$K_Y = \frac{m_x}{M_Y}K_x + \frac{m_y}{M_Y}K_y - \frac{2}{M_Y}\sqrt{m_x m_y K_x K_y}\cos\theta$$

from a knowledge of the masses m_x, m_y and M_Y and by measuring the energies K_x, K_y accurately. Instead of the accurate masses, the use of mass numbers will suffice.

In determining the energy K_y, we may use a scintillation counter, a proportional counter, a solid state counter or a magnetic spectrograph provided the particle y is a *charged* particle.

Both the energy and the angular distributions of the particles are recorded simultaneously in a multigap magnetic spectrograph with nuclear emulsion plates as detectors, as was used by Enge and Buechner at MIT. The angular distributions of energy at an interval of 7.5° can be obtained. The plates are developed after the exposure and scanned under microscopes to get the number of tracks of particles having correct length and direction.

6.8 Centre of mass frame in nuclear physics

Apart from the usual laboratory coordinate system, nuclear physicists often use a coordinate system that moves with the centre of mass (c.m.) of the colliding particles to simplify analysis of collision problems. Such a frame is termed the *centre of mass frame*. To elucidate, we shall make a study of two cases of perfectly elastic nuclear collisions from the centre of mass frame.

Case 1. Proton-proton collision (p–p scattering) — Consider a typical p–p collision as shown in Fig. 6.4, a typical photoemulsion record, where the proton to be collided is at rest before collision. The paths of the two protons after collision are at right angles to each other. This *orthogonality of tracks is a common characteristic of all p–p collisions*, if the energy of the incident colliding proton is in the *non-relativistic range*.

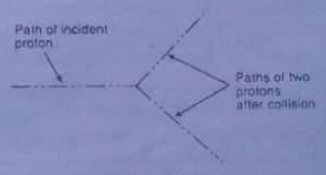

Fig. 6.4 p-p collision. Sketch of a typical photoemulsion record

But why? For this, we shall conveniently view the above collision process *from c.m. frame*. Let $\vec{v}$ be the velocity of the incident proton as observed in the lab. frame. Then, the c.m. frame has the velocity $\vec{v}/2$ and in this frame the protons approach and recede each other with equal and opposite velocities. The situation is represented in Fig. 6.5a. Let one proton move, after collision, in the direction θ'. Then, the other one would move oppositely at an angle $(\pi - \theta')$.

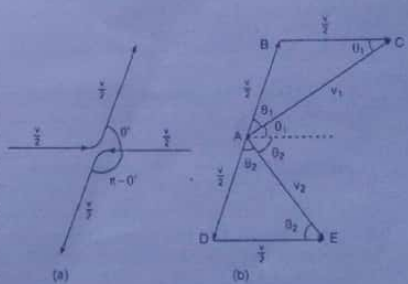

Fig. 6.5 (a) View of p–p collision in the centre of mass frame, (b) Shows how to revert back to the lab frame

Scanned with CamScanner

window W and are detected by observing scintillations produced on a zinc sulphide screen S with the microscope M. The absorber foils A could evaluate the range of the α-particles. Ranges showed that energy was 8.6 MeV each.

The two α-particles are emitted in *opposite* directions for conservation of momentum. For instance, an α-particle of energy 8.6 MeV possesses a momentum

$$p_\alpha = \sqrt{2m_\alpha K_\alpha}$$
$$= [2 \times 4 \times 1.66 \times 10^{-27} \times 8.6 \times 1.6 \times 10^{-13}]^{\frac{1}{2}}$$
$$= 13.5 \times 10^{-20} \text{ kg.ms}^{-1}$$

Momentum of a proton of energy 0.25 MeV is

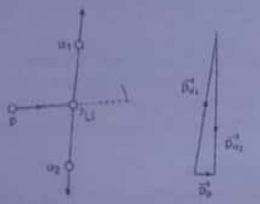

Fig. 6.8 Momentum conservation in Cockroft-Walton's experiment

$$p_p = \sqrt{2m_p K_p}$$
$$= [2 \times 1.66 \times 10^{-27} \times 0.25 \times 1.6 \times 10^{-13}]^{\frac{1}{2}}$$
$$= 1.15 \times 10^{-20} \text{ kg.ms}^{-1}$$

The α-particles thus have much higher momentum each, compared to that of the incident proton. The conservation of momentum is thus possible if the two α-particles are emitted in almost opposite directions as is evident from Fig. 6.8.

• The *importance* of the experiment is that it provides the *first direct experimental verification* of Einstein's mass-energy relation.

• Subsequently, Dee and Walton repeated the experiment in a cloud chamber with 0.25 MeV proton beam. They obtained photographs of the two α-particles ejected in opposite directions of the target and from a measurement of their ranges, they were found to have energy of 8.6 MeV each.

6.10 Cross-section of nuclear reactions

An important parameter in nuclear reactions is the **reaction cross-section**, σ. It is a *quantitative measure* of the *probability of occurrence of a nuclear reaction*.

Let a parallel beam of N *monoenergetic* particles be incident per unit time normally on a target foil of surface area A and thickness Δx, having n nuclei per unit volume. Now, the number ΔN of nuclei in the foil undergoing nuclear reaction will be proportional to (i) the *intensity of the beam* and (ii) the *number of target nuclei* contained in the foil (Fig. 6.9).

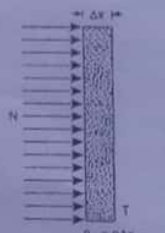

Fig. 6.9 Nuclear reaction cross-section: bombardment of target foil

The intensity I of the beam $= N/A$ and the number of nuclei in the foil $= nA \cdot \Delta x$. So, the number of nuclei transmuted is

$$\Delta N \propto \frac{N}{A} nA \cdot \Delta x$$
$$= \sigma N n \cdot \Delta x$$
$$= \sigma N n_A$$

where σ = a constant, $n_A = n \cdot \Delta x$, the number of nuclei per unit area of target foil.

The constant σ is called the *nuclear reaction cross-section* and is given by

$$\therefore \quad \boxed{\sigma = \frac{\Delta N}{N n_A}} \qquad (6.10.1)$$

Since ΔN and N are pure numbers, σ has the dimensions of area and is therefore termed the *cross-section*.

From (6.10.1) it is apparent that σ is the *probability of occurrence of the reaction when a single particle* $(N = 1)$ *falls on a single target nucleus* $(n_A = 1)$ *present per unit area*.

Since the nuclear radius is $\sim 10^{-14}$ to 10^{-15} m, the cross-section is $\sim 10^{-28}$ m^2. The common unit of reaction cross-section is a *barn* being defined as :

$$\boxed{\textbf{1 barn} = 10^{-28} \text{ m}^2}$$

Geometrical significance of σ — The geometrical significance of σ can be understood in reference to Fig. 6.10. If R be the effective radius of the target nucleus for a given reaction, then the projection of its surface on a plane normal to the direction of incidence of the incoming particles (assumed to be mass-points) is πR^2.

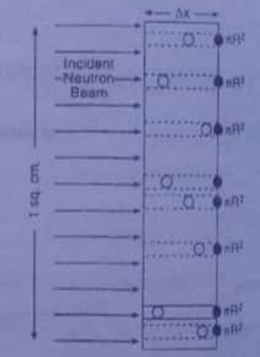

Fig. 6.10 Geometrical significance of nuclear reaction cross-section

∴ Number of particles encountering each target nucleus $= \pi R^2 N_A$, where $N_A = N/A$ is the number of particles incident per unit area of the target.

But the number of nuclei per unit area of the target is n_A. So the number of incident particles intercepted by the target nuclei in the foil is

$$n_A A \times \pi R^2 N_A = \pi R^2 N n_A \quad (\because N_A = N/A)$$

∴ The probability of encounter of a single particle $(N = 1)$ with a single target nucleus per unit area $(n_A = 1)$, that is, σ is given by

$$\sigma = \frac{\pi R^2 N n_A}{n_A} = \pi R^2$$

which is the *geometrical significance* of the reaction cross-section, σ.

Scanned with CamScanner

Geometrically, therefore, the *reaction cross-section* is the *area of cross-section of an imaginary disc associated with each target nucleus such that if the incident projectile passes through it, the reaction occurs.*

Differential cross-section — In many nuclear reactions, the product particles are *not* emitted *isotropically* in all directions. The angular distribution is measured in terms of *differential cross-section*, $d\sigma/d\Omega$, the number of product particles emitted per sec in a solid angle $d\Omega$ at some angle θ with respect to the direction of the incident beam.

$$\text{But,} \quad \frac{d\sigma}{d\Omega} = \frac{dN}{Nn_A}\Big/ d\Omega = \frac{dN/d\Omega}{Nn \cdot \Delta x} \tag{6.10.2}$$

where dN number of product nuclei are emitted per sec. in a *small* solid angle $d\Omega$ at θ with the incident beam, n being the number of nuclei per unit volume of target of thickness Δx.

The differential cross-section, $d\sigma/d\Omega$, however varies with the solid angle

Total cross-section — The *total* or *integral cross-section*, σ, over solid angle Ω is given by

$$\sigma = \int_{\Omega} \frac{d\sigma}{d\Omega} d\Omega \tag{6.10.3}$$

The reaction cross-section, σ depends on (i) the *nature of the projectile*, (ii) the *nature of the absorber* and (iii) the *energy of the projectile*. It may vary from a value as small as 10^{-20} barn, as in neutrino interactions, to as high as 10^5 barn in nuclear reactions of large cross-section.

6.11 Theory of compound nucleus

Background—The primary evidence of the idea of the compound nucleus came when neutrons were introduced as projectiles. It was observed that for *high energy*, the total cross-section for neutron absorption and scattering was $\sim \pi R^2$, R being the nuclear radius. For *very low energies* however it is higher and tends to the limit $\pi\lambda^2$, where λ is the reduced de Broglie wavelength of neutron.

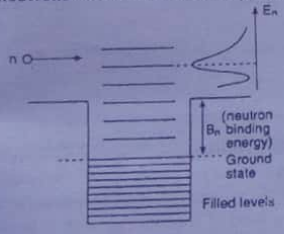

Fig. 6.11 Motion of incident neutron in an average single particle potential well

To explain the results, it was presumed that the incident neutron moves in an average potential well due to all the nucleons in the nucleus (Fig. 6.11) for a time

$$\tau \sim \frac{\text{Nuclear dia}}{\text{Neutron velocity}} \sim \frac{10^{-14}}{10^7} \sim 10^{-21}\text{s}$$

The incident neutron has thus a large probability of escape without an absorption. So, the elastic cross-section, σ_e would be *large* or reaction cross section, σ_r *quite low*. At very low energies, σ_r would be relatively large and depend on $1/v$. So, at thermal energies σ_e and σ_r should be comparable and both would approach the value $\pi\lambda^2$.

The energy levels in this single particle potential well should be *wide apart* (~5-10 MeV) and the *width of the level* that measures the probability of its decay would be $\Gamma = \hbar/\tau = \hbar/10^{-21} = 1$ MeV. The levels would thus be *quite broad*.

When the neutron energy corresponds to the excitation energy of the nuclear level, resonances are expected in cross-section vs. energy gaps (Fig. 6.11). The resonances should be *widely spaced* (~ several MeV) and having *large widths* (~ MeV). At very low energies (near thermal), *no resonance is expected*.

The *observed results however do not fit with this picture*. In many cases, the cross-section σ_r is quite large and σ_e quite small *at thermal energies*. At these very low energies, the absorption cross-section is due to *radiative capture* i.e., (n,γ)-reactions. Resonances are seen in most nuclei for both σ_e and $\sigma(n,\gamma)$ and they occur at neutron energies between 0.1 to 10 eV, i.e., they are *closely spaced*.

In the background of these observations, Bohr (1936) proposed the **compound nucleus hypothesis** as a possible mechanism of nuclear reactions.

Bohr's compound nucleus hypothesis — When an incident projectile x enters into a target nucleus X to produce a nuclear reaction, a highly excited intermediate state C^* is formed which finally decays into the product nucleus Y and another particle y.

$$X + x \rightarrow C^* \rightarrow Y + y$$

Inside the nucleus X, the projectile x rapidly dissipates its energy and merges with the closely packed nucleons. In the process, the general random motion of the nucleons gets disturbed, each gaining some extra energy. The gain however is not enough for an exit from the nucleus. But after a relatively long time, the large number (~ millions) of inter-nucleonic collisions may result into concentration of enough energy on a nucleon for an escape from the nucleus which de-excites into the ground state. The de-excitation may as well occur by γ-emission. The emission of a nucleon (or a group) from the excited nucleus is analogous to the phenomenon of evaporation of a liquid drop. Indeed, this idea worked behind formulating the ***liquid drop model*** of nucleus.

The composite system C^* formed by absorption of x and X is called the **compound nucleus**. Prior to its eventual decay, it lives long enough compared to the time a nucleon of few MeV takes to run through the mean free path of inter-nucleonic collisions. The mean time between collisions is about 10^{-22}s so that the life time of the compound nucleus, $t \sim 10^7 \times 10^{-22} = 10^{-15}$s.

As the compound nucleus is relatively long-lived, the reaction proceeds in two steps : (i) ***formation of the compound nucleus*** by absorption of the projectile by the target nucleus and (ii) the ***decay of the compound nucleus***, in a way independent of the method of its formation, into reaction products y and Y in definite quantum

Scanned with CamScanner

5. Californium has been produced by Thompson and others by bombarding curium with 35 MeV α-particles.

$$^{242}_{96}\text{Cm} + ^{4}_{2}\text{He} \rightarrow ^{245}_{98}\text{Cf} + ^{1}_{0}\text{n} \qquad \text{(Half-life = 44 min)}$$

$$^{242}_{96}\text{Cm} + ^{4}_{2}\text{He} \rightarrow ^{244}_{98}\text{Cf} + 2\,^{1}_{0}\text{n}$$

Californium may as well be produced by bombarding ^{238}U by cyclotron-accelerated ^{12}C and ^{14}N ions.

$$^{238}_{92}\text{U} + ^{12}_{6}\text{C} \rightarrow ^{244}_{98}\text{Cf} + 6\,^{1}_{0}\text{n}$$

$$^{238}_{92}\text{U} + ^{14}_{7}\text{N} \rightarrow ^{248}_{98}\text{Cf} + ^{1}_{1}\text{H} + 3\,^{1}_{0}\text{n}$$

6. Einsteinium is produced by bombarding ^{238}U with ^{14}N ions accelerated by synchrocyclotron :

$$^{238}_{92}\text{U} + ^{14}_{7}\text{N} \rightarrow (^{252}_{99}\text{Es})^{*} \rightarrow ^{247}_{99}\text{Es} + 5\,^{1}_{0}\text{n}$$

Its longest-lived isotope is $^{254}_{99}$Es with $T = 500$ days. Interestingly, it was first found in the debris of thermonuclear explosion in the Pacific in 1953 and later created in the laboratory.

7. Fermium is produced by bombarding ^{238}U with ^{16}O ions accelerated to 120 MeV by synchrocyclotron

$$^{238}_{92}\text{U} + ^{16}_{8}\text{O} \rightarrow (^{254}_{100}\text{Fm})^{*} \rightarrow ^{250}_{100}\text{Fm} + 4\,^{1}_{0}\text{n}$$

Fermium may as well be produced by bombarding ^{240}Pu by ^{12}C ions :

$$^{240}_{94}\text{Pu} + ^{12}_{6}\text{C} \rightarrow (^{252}_{100}\text{Fm})^{*} \rightarrow ^{248}_{100}\text{Fm} + 4\,^{1}_{0}\text{n}$$

8. Mendelevium resulted from α-bombardment of ^{253}Es in a cyclotron in 1956.

$$^{253}_{99}\text{Es} + ^{4}_{2}\text{He} \rightarrow (^{257}_{101}\text{Md})^{*} \rightarrow ^{256}_{101}\text{Md} + ^{1}_{0}\text{n}$$

It decays into fermium by orbital electron capture and has a half-life of 30 min.

9. Nobelium was discovered in 1958 by Ghiorso, Sikkleano, Watton and Seaborg by bombarding $^{246}_{96}$Cm with ^{12}C ions accelerated by synchrocyclotron.

$$^{246}_{96}\text{Cm} + ^{12}_{6}\text{C} \rightarrow (^{258}_{102}\text{No})^{*} \rightarrow ^{254}_{102}\text{No} + 4\,^{1}_{0}\text{n}$$

followed by $\quad ^{254}_{102}\text{No} \rightarrow ^{250}_{100}\text{Fm} + ^{4}_{2}\text{He}$

and $\quad ^{250}_{100}\text{Fm} \rightarrow ^{246}_{98}\text{Cf} + ^{4}_{2}\text{He}$

10. Lawrencium was discovered in 1961 in Lawrence Radiation Lab at California by the bombardment of ^{249}Cf with accelerated ^{11}B ions.

$$^{249}_{98}\text{Cf} + ^{11}_{5}\text{B} \rightarrow (^{260}_{103}\text{Lw})^{*} \rightarrow ^{257}_{103}\text{Lw} + 3\,^{1}_{0}\text{n}$$

The isotope of Lawrencium, $^{256}_{103}$Lw, was produced in the then USSR by the bombardment of ^{243}Am with $^{18}_{8}$O ions.

$$^{243}_{95}\text{Am} + ^{18}_{8}\text{O} \rightarrow (^{261}_{103}\text{Lw})^{*} \rightarrow ^{256}_{103}\text{Lw} + 5\,^{1}_{0}\text{n}$$

The isotope of Lawrencium, $^{257}_{103}$Lw, is an α-emitter that decays into ^{253}Md.

$$^{246}_{98}\text{Cf} + ^{11}_{5}\text{B} \rightarrow ^{257}_{103}\text{Lw}$$

$$^{257}_{103}\text{Lw} \rightarrow ^{253}_{101}\text{Md} + ^{4}_{2}\text{He} \qquad \text{(Half-life = 8.6 s)}$$

11. Kurchatovium was produced by the Soviet scientists in 1967 by the bombardment of ^{242}Pu with accelerated ^{22}Ne ions :

$$^{242}_{94}\text{Pu} + ^{22}_{10}\text{Ne} \rightarrow ^{260}_{104}\text{Km} + 4\,^{1}_{0}\text{n}$$

Its half-life is only 0.3 s.

12. Hahnium was produced by bombarding a mixture californium isotopes : $^{249}_{98}$Cf, $^{250}_{98}$Cf and $^{252}_{98}$Cf with ^{15}N ions.

$$^{249}_{98}\text{Cf} + ^{15}_{7}\text{N} \rightarrow ^{260}_{105}\text{Hm} + 4\,^{1}_{0}\text{n}$$

$$^{250}_{98}\text{Cf} + ^{15}_{7}\text{N} \rightarrow ^{261}_{105}\text{Hm} + 4\,^{1}_{0}\text{n}$$

An element has been reported to be discovered with $Z = 106$ by bombardment of $^{249}_{98}$Cf with high energy ^{18}O ions :

$$^{249}_{98}\text{Cf} + ^{18}_{8}\text{O} \rightarrow ^{264}_{106}? + 3\,^{1}_{0}\text{n}$$

• Of the above transuranics, two elements – *neptunium* and *plutonium* – are of *special importance*, for they have a major role in the production of *nuclear energy* by the fission process, Pu being the fuel for nuclear reactors. The absence of transuranic *elements in nature*, with the possible exception of Np and Pu, is attributed to their extremely short half-lives compared to the age of the earth. An interesting feature is that they form a series beginning with actinium (*actinide series*), analogous to the rare-earth series.

7.13 Nuclear fission

Fermi's experiments on neutron-bombardment of uranium to produce transuranic elements were repeated by other workers and the results, as already mentioned, were somewhat puzzling. There appeared too many kind of β-emissions with different half lives and too many kinds of product atoms. Working with meticulous care, Otto Hahn and Fritz Strassmann finally succeeded in 1938 to give a correct interpretation of the phenomenon.

Scanned with CamScanner

Hahn and his collaborators performed a series of painstaking chemical separations of the uranium sample to pinpoint the element to which the new radioactivity belonged. They found, much to their amazement, that all new radioactive atoms were members belonging nearly to the centre of the periodic table. In 1939, Otto Frisch and Lisa Meitner suggested that the uranium atom was being fragmented into two parts of more or less comparable size, $^{141}_{56}Ba$ and $^{92}_{36}Kr$. This phenomenon of the *division or disintegration of a heavy nucleus into two nuclei of comparable masses* is termed **nuclear fission** or simply **fission**, in analogy with 'cell division' in biology. Hahn and Strassmann are credited with the observation of the first neutron-induced fission.

The schematic equation for the fission process may be written as

$$^{235}_{92}U + ^{1}_{0}n \rightarrow (^{236}_{92}U)^{*} \rightarrow X + Y + \text{neutrons}$$

where $^{1}_{0}n$ is a *slow neutron* (having therefore a high value for capture cross-section), $^{236}_{92}U$ a highly unstable isotope of uranium and X, Y are the fission fragments.

It is to be noted that the fragments are *not uniquely* determined and there could be various possible combinations and that a number of *neutrons* are also *given off*. It is found that more than 30 modes of fission of ^{235}U exist in each of which a different pair of fission fragments is formed.

The fission results in two massive fragments, having equal and opposite momenta as are seen beautifully in cloud chamber photographs (Fig. 7.5a) where two tracks travel almost in opposite directions. The fragments are neutron-rich having too many neutrons to be stable. (Fig. 7.5b). Each fragment emits one or two neutrons—about 3 on an average — per fission of ^{235}U.

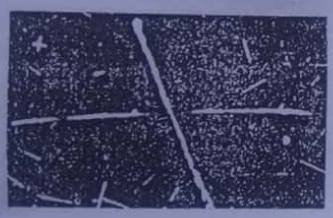

Fig. 7.5a Cloud chamber tracks of fission fragments

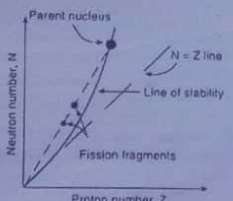

Fig. 7.5b Diagram showing that fission fragments are neutron-rich

Typical fission reactions are

(i) $^{235}_{92}U + ^{1}_{0}n \rightarrow (^{236}_{92}U)^{*} \rightarrow ^{140}_{54}Xe + ^{94}_{38}Sr + 2\,^{1}_{0}n + Q$

(ii) $^{235}_{92}U + ^{1}_{0}n \rightarrow (^{236}_{92}U)^{*} \rightarrow ^{144}_{56}Ba + ^{89}_{36}Kr + 3\,^{1}_{0}n + Q$

where Q represents the energy released in the reaction.

The β-activity observed by Fermi was due to the radioactive decay of fission fragments. These are known as *fission chains*.

$$^{140}_{54}Xe \xrightarrow{\beta^-} ^{140}_{55}Cs \xrightarrow{\beta^-} ^{140}_{56}Ba \xrightarrow{\beta^-} ^{140}_{57}La \xrightarrow{\beta^-} ^{140}_{58}Ce \text{ (stable)}$$

and $$^{94}_{38}Sr \xrightarrow{\beta^-} ^{94}_{39}Y \xrightarrow{\beta^-} ^{94}_{40}Zr \text{ (stable)}$$

from the fission reaction (i) above. In each β-emission, there was an emission of an anti-neutrino, $\bar{\nu}$.

So the end product in the fission reaction (i) are $^{140}_{58}Ce$, $^{94}_{40}Zr$, 6β-particles, 6 anti-neutrinos and 2 neutrons.

Similarly, for the fission reaction (ii), the following β-decays of fission fragments (*fission chains*) have been observed.

$$^{144}_{56}Ba \xrightarrow{\beta^-} ^{140}_{57}La \xrightarrow{\beta^-} ^{144}_{58}Ce \xrightarrow{\beta^-} ^{144}_{59}Pr \xrightarrow{\beta^-} ^{144}_{60}Nd \text{ (stable)}$$

and $$^{89}_{36}Kr \xrightarrow{\beta^-} ^{89}_{37}Rb \xrightarrow{\beta^-} ^{89}_{38}Sr \xrightarrow{\beta^-} ^{89}_{39}Y \xrightarrow{\beta^-} ^{89}_{40}Zr \text{ (stable)}$$

- Nuclear fission is a *special type of nuclear reaction* where a nucleus splits into two (or more) lighter nuclides of intermediate mass numbers.

- **Why do the fragments exhibit β-activity?** Taking the reaction (ii), the stable isotope of barium with maximum A-value is ^{138}Ba and the stable isotope of Krypton with maximum A-value is ^{86}Kr. So, these fission fragments must show much β-activity to get rid of the excess neutrons.

- For fission, the projectile *need not* necessarily be neutron. Protons, deuterons, α-particles and even electrons or γ-rays may also induce fission. But the only type of nuclear fission that has assumed *practical significance* is the neutron-fission of uranium and plutonium. There could be nuclear fission even without the projectile – the so-called **spontaneous** or **auto-fission**.

- All the isotopes of uranium are *not fissionable* by slow neutrons. While U-235 is, U-238 is not.

7.14 Energy released in fission of U-235

The energy released in fission of ^{235}U-nucleus is so high that the two main fission fragments fly apart in opposite directions with great speeds as confirmed by cloud chamber photographs. Measured by *delicate calorimetric method*, the actual kinetic energy of the separate particles is about 180 MeV and the energy of the γ-radiation emitted in the process is about 20 MeV. So the total energy per fission of ^{235}U-nucleus is *about* **200 MeV**, and this is also seen from the following calculation.

Scanned with CamScanner

7.16 Prompt and delayed neutrons

A look at the stability curve for nuclides (Fig. 1.1 or Fig. 7.5b) show that all the fission fragments are found to fall to the left of the curve. Since these fragments have an excess number of neutrons, they are unstable. Each excited fragment therefore gives off one or two neutrons almost immediately, within about 10^{-15} s. These neutrons, are called *prompt neutrons* and constitute 99% of the total neutrons ejected in uranium fission.

In addition to *prompt neutrons*, a small number (0.75%) of neutrons are ejected in the fission process rather late, after few seconds. These are called *delayed neutrons*. Fission fragments undergo beta decay since they are rich in neutrons. Neutron emission occurs if in the β-decay, the product nucleus is left in an excited state with an energy greater than the binding energy of a neutron in that nucleus. But this neutron emission follows the β-decay of the preceding nucleus and thus the neutron activity of a sample and the β-activity of the parent nuclide will have the same apparent half-life. Such neutron emission is known as *delayed neutron emission*.

The best known example is

$$^{87}_{35}\mathrm{Br} \xrightarrow{\beta^-} {}^{87}_{36}\mathrm{Kr} \xrightarrow{n} {}^{86}_{36}\mathrm{Kr},$$

the half-life of which is 55.6 s. The decay scheme for fission fragment ^{87}Br for delayed neutrons as given by Snell and co-workers is shown in Fig. 7.10.

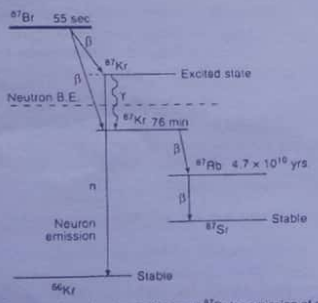

Fig. 7.10 Decay scheme for fission fragment ^{87}Br for emission of delayed neutrons

Importance of delayed neutrons — The number of delayed neutrons in fission is quite small, but their delays, as reflected in 'apparent' half-lives of several seconds, are taken advantage of in maintaining a chain reaction. In a reactor, the delayed neutrons prevent rapid changes in neutron density when it is operating in a near critical condition. This increases effectively the *time constant* of the reactor and controls the rate of reaction.

7.17 Fission of light nuclei

Batzel and Seaborg (1951) bombarded ^{63}Cu by high energy protons, obtained from cyclotron, with the idea of producing ^{38}Cl that shows β-activity with a half-life of about 37 min. They succeeded to detect ^{38}Cl when the energy of the protons crossed 60 MeV and with further increase of bombarding energy, the probability of production of ^{38}Cl increased. The following fission reaction was initiated

$$^{63}_{29}\mathrm{Cu} + {}^{1}_{1}\mathrm{H} \rightarrow {}^{38}_{17}\mathrm{Cl} + {}^{25}_{13}\mathrm{Al} + {}^{1}_{0}\mathrm{n}$$

They also obtained the following fission reaction with ^{63}Cu for which the proton energy threshold was about 50 MeV.

$$^{63}_{29}\mathrm{Cu} + {}^{1}_{1}\mathrm{H} \rightarrow {}^{24}_{11}\mathrm{Na} + {}^{39}_{19}\mathrm{K} + {}^{1}_{0}\mathrm{n}$$

7.18 Neutron speeds, classification : Moderation

Neutrons are classified according to their kinetic energy for a discussion of the interactions of neutrons with particles, nuclei and matter in bulk.

Neutrons with energies 0.1 MeV or more are called ***fast neutrons***. If however they are slowed down to such speeds as those of gas molecules at NTP, they are known as *thermal neutrons*. Between these two extreme cases, there are neutrons of *intermediate* speeds. Neutrons slower than the thermal neutrons are termed *cold neutrons*. Thermal neutrons have energies of approximately 0.03 eV ($\sim kT$). Neutrons of energies from 0.03 up to 10 eV are sometimes spoken of as *slow neutrons*. To sum up :

Fast neutrons	... ...	0.1 MeV and up
Intermediate neutrons	... ...	10 eV to 0.1 MeV
Slow neutrons	... ...	0.03 eV to 10 eV
Thermal neutrons	... ...	0.03 eV (approx.)
Cold neutrons	... ...	less than thermal.

The ranges however are not uniquely fixed as the boundaries of classification are not well-defined.

The *interaction of fast and slow neutrons* with matter is of great importance in nuclear technology. Fast neutrons may pass directly through the nucleus of an atom without being captured, while slow neutrons get captured more readily. The probability of neutron capture is dependent on the speed and at certain speeds the probability increases greatly (*resonance*). But the fast neutrons may produce some such effects that slow neutrons cannot.

• Fast neutrons may again include sub-classes such as *very fast* (10-50 MeV), *ultra fast* (>50 MeV) etc.

Scanned with CamScanner

Moderation — The neutrons that are not captured by nuclei may be scattered *elastically* by the colliding nuclei. These collisions are *random*, and on an average, 63% of the energy of a colliding particle is *lost per collision* with particles of *equal masses*. Calculations thus show that a 2 MeV neutron would be reduced to thermal energy of a gas molecule in about 18 collisions in hydrogen, and these might occur in 1 ms. With carbon nuclei, 114 collisions would be necessary on the average. This *process of slowing down neutron speed by elastic collision is called* **moderation.**

To slow down neutrons, therefore, they are just passed through **moderators** which are *materials rich in protons* or in *nuclei of small mass* and would *not capture* them. Most common moderators are *water* and *paraffin*. Heavy water (D_2O) is effective for its very low capture-probability. *Graphite* is also often used.

7.19 Nuclear chain reaction : Critical mass

The energy released per fission of ^{235}U-nucleus is about 200 MeV or 16×10^9 K cal/kg. Could this energy be tapped? The answer is 'yes', only if we can initiate a *fission chain reaction*; otherwise 'not'.

But what is a *chain reaction*,? In each event of a fission reaction with heavy nuclei, the highly excited nuclei emit two or three prompt (but fast, ~ 2 MeV) neutrons. Fermi correctly suggested that these fission-producing neutrons may, if slowed down, interact with neighbouring nuclei and produce in turn fissions in them so that more neutrons are emitted. The result is an avalanche-like build-up of fission events. Such a fission reaction is called a **chain reaction** (Fig. 7.11).

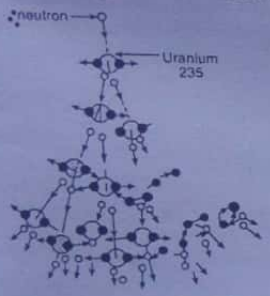

Fig. 7.11 Nuclear chain reaction

The *continuous regeneration* of active centres is the *distinctive feature* of such reactions, since the formation of each new centre is accompanied by a greater number of repeating links of chains of the reaction. A chain reaction which would just sustain itself occurs if for each neutron one successor (on an average) is generated. The average number of neutrons emitted per fission of U-235 is 2.46 and of Pu-239 is 2.88 as indicated by experiments.

To sustain a chain reaction with uranium however is *not an easy task* for there exists the following competing processes.

1. Fission emits more neutrons than are captured.
2. There is non-fission capture of neutrons by uranium nuclei.
3. Neutrons escape without being captured at all, and
4. Materials other than U-nuclei (e.g., moderator nuclei, structural material etc.) make non-fission capture of the neutrons.

Obviously, therefore, a favourable balance is to be struck among the proceeses to achieve the chain reaction. If the total loss of neutrons incurred by processes 2, 3 and 4 above is less than what is produced by process 1, then and *then only*, the chain reaction can be *sustained*.

The important point in the possibility of achieving a chain reaction is the *size* of the *core*; the core is the space in which the chain reaction takes place. A reduction in the size of the core would increase the number of neutrons that escape beyond the core and would thus reduce the possibility of further development of the chain reaction. The *minimum size* of the *core* at which a chain reaction can still be obtained is called the **critical size.** The mass of the fissionable material contained in a system of critical size is called the **critical mass.**

7.20 Neutron cycle : Reproduction factor

Based on what has been described in Art 7.19, we shall now discuss the **neutron cycle** in a reactor. ***A reactor is an assembly of nuclear fuel and moderator capable of sustaining a chain reaction.*** An essential constituent of a reactor is an arrangement for controlling the chain reaction to arrest it from 'running away'. We shall restrict ourselves to *homogencous reactor* only where the *fuel* is *homogeneously mixed with a moderator* to slow down neutrons to thermal energies. The fuel may be a mixture of ^{238}U and ^{235}U and the moderator may be heavy water or graphite.

Neutron cycle : Let N_0 fast neutrons be produced due to thermal neutron fission of a ^{235}U-nucleus. A small fraction ε of these may induce fission resulting in some additional neutrons. The total number of fast neutrons thus becomes $N_0\varepsilon$, where ε is called the *fast fission factor*. Usually, $\varepsilon \simeq 1.03$ and this 3% effect is rather important for neutron balance in a chain reaction.

These $N_0\varepsilon$ fast neutrons diffuse into the assmebly and most of them are thermalised by collision with moderator nuclei. If p be the fraction of neutrons that escape before thermalisation, the remaining $N_0\varepsilon(1-p)$ neutrons are slowed down by moderator. Again, during slowing down, some may be captured by ^{238}U to form $(^{239}U)^*$ which is β-active,

$$\left(^{239}_{92}U\right)^* \xrightarrow{\beta^-} {}^{239}_{93}Np \xrightarrow{\beta^-} {}^{239}_{94}Pu$$

and the capture reaction : $^{238}_{92}U + {}^{1}_{0}n \rightarrow (^{239}_{93}U)^*$ is a *resonance reaction*. Whenever the neutron energy corresponds to any energy state of $(^{239}_{92}U)^*$-nucleus, it is readily absorbed. If a fraction ν escapes resonance capture, $(1-\nu)$ fraction gets captured to form $^{239}_{94}Pu$, ν being known as *resonance escape probability*.

∴ Number of neutrons reduced to thermal energies $= N_0\varepsilon(1-p)\nu$. Of these, again a fraction f may escape the system.

∴ Number of thermal neutrons left $= N_0\varepsilon(1-p)\nu(1-f)$.

Not all of these however are available for the chain reaction, since a fraction a is absorbed by uranium and $(1-a)$ by the moderator and other materials.

Scanned with CamScanner

∴ Number of thermal neutrons available for chain reaction is given by

$$N = N_0\varepsilon(1-p)\nu(1-f)a$$

a being known as *thermal utilization factor*.

But, not all the neutrons absorbed in uranium initiate fission of ^{235}U as some may get absorbed only to convert ^{235}U into ^{236}U. If σ_f be the *fission cross-section* of ^{235}U and σ_a the *absorption cross-section* of ^{235}U to form ^{236}U, the fraction of thermal neutrons absorbed to cause fission of ^{235}U is σ_f/σ_a which is ~ 0.84 ($\because \sigma_f \simeq 576$ barn; $\sigma_a \simeq 680$ barn).

Reproduction factor — Whether or not, any size or mass of an assembly would sustain a chain reaction at all is determined by what is called the *reproduction factor* or *multiplication factor*, k. The quantity k is defined as the ratio of the number of second generation fission in ^{235}U per fission of ^{235}U by a first generation neutron.

$$\therefore\ k = \frac{\text{No. of neutrons in } (n+1)\text{th generation}}{\text{No. of neutrons in } n\text{th generation}} \qquad (7.20.1)$$

$$= N_0\varepsilon(1-p)\nu(1-f)a\cdot\frac{\sigma_f}{\sigma_a}$$

$$= \eta\varepsilon\nu a(1-p)(1-f) \qquad (7.20.2)$$

where $\eta = N_0\sigma_f/\sigma_a$ = number of fast fission neutrons emitted per thermal neutron absorbed in uranium to cause fission.

The k-value as given by (7.20.2) corresponds to an assemby of finite size.

Now, (i) when $k = 1$, the chain reaction operates in *steady state* and the size or the mass of the assembly (or reactor) is said to be **critical**.

(ii) When $k > 1$, the number of neutrons in the chain reaction in a given generation is more than that in the previous one implying that the rate of fission increases from cycle to cycle—a *divergent chain reaction*. The mass or size of the assembly is said to be **supercritical**.

(iii) When $k < 1$, then no sustainable chain reaction is possible and the rate of fission decreases. The mass or size of the assembly is called **subcritical**.

In a reactor with **control rods in**, $k < 1$ and with **control rods out**, $k > 1$. The control rods are set, by adjustments, for $k = 1$ for steady operation. The curve in Fig. 7.12 shows the control of power in a nuclear reactor. In pure U-235 or Pu-239 for the size of a marble, $k = 0.1$ nearly; for a sphere of the size of a basket ball, however, $k = 2.4$.

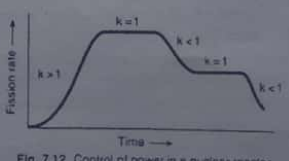

Fig. 7.12 Control of power in a nuclear reactor

7.20.1 Some important observations

• The first step in the design of a nuclear reactor is to calculate the value of the reproduction factor k for an assembly of infinite size. Since, no leakage of neutrons is now there, we have from (7.20.2)

$$\boxed{k_\infty = \eta\varepsilon\nu a} \qquad (7.20.3)$$

which is known as the **four factor formula**.

Obviously, we have $k = (1-p)(1-f)k_\infty$

• Of the four factours, (i) η depends on nuclear properties of the fuel, (ii) ε depends not only on the nuclear properties of the fuel, but also on its size and shape and (iii) ν and a depend on the nuclear properties of the fuel, the moderator and also on how these materials are arranged.

The basic problem in the design of a reactor is to optimise all the materials so as to obtain the largest value of ν and a. For a given fuel, such an arrangement makes k_∞ maximum.

• For natural uranium, $\eta \sim 1.3$, but for pure ^{235}U, $\eta > 1.3$ *for all neutron energies* so as to make a **nuclear bomb** possible.

• The thermal utilization factor a strongly depends on the ratio of the number of atoms of the fuel and the moderator. In a homogeneous reactor with natural uranium as fuel and graphite as moderator,

$$a = \frac{N_U\sigma_a(U)}{N_U\sigma_a(U) + N_C\sigma_a(C)}$$

where N_U and N_C are the number of U-atoms and C-atoms.

• The resonance escape probability $\nu \sim 0$ for natural uranium (^{238}U), since for the compound nucleus $^{239}_{92}U$, between 6–70 eV, the capture probability for neutron is high. So, moderation of neutrons increases ν and also k_∞ reaches the maximum value of 0.82 for N_C/N_U ratio $\simeq 400$. But even this value of k_∞ *cannot sustain* a chain reaction.

If however heavy water is used as a moderator $k_\infty \simeq 1.15$ for a homogeneous reactor using natural uranium with a moderator-fuel ratio 167 and a chain reaction is sustained. With H_2O as moderator, $k_\infty = 0.838$ and with C, $k_\infty = 0.849$ for moderator-fuel ratio 243 and 452 respectively. So, a homogeneous reactor with ^{238}U can operate *only with heavy water as moderator*. With other moderators, the fuel must be *enriched* in ^{235}U.

7.21 Moderator and moderating ratio

The key to the function of a reactor is the *control of neutrons*. The substance used to control the neutron flux is called the *moderator*, as already stated.

Scanned with CamScanner

The mass of a neutron is almost equal to that of a proton (^1_1H). It was therefore supposed that hydrogen would slow down neutrons by exchange of energy through elastic collisions and thereby act as an effective moderator. But it has a high cross-section for $^1_1H(n,\gamma)^2_1H$ reaction and the neutrons, instead of being slowed down, are removed from the circulation. ***A good moderator should*** thus not only ***contain a light element that can slow down the neutrons by energy exchange*** but must also ***have a small cross-section for other reactions*** that involve neutron absorption and use up the available neutrons.

• For a given material as moderator, there is a cross-section σ_s for neutron scattering by collision, and also a cross-section, σ_a for neutron absorption. Another relevant parameter is ξ which is the *average value of the logarithm of the ratio of energy lost per collision*. So, by definition,

$$\xi = \left(-\ln \frac{E_0}{E}\right)_{av} = \left(\ln \frac{E}{E_0}\right)_{av} \qquad (7.21.1)$$

where E is the energy before collision and E_0 the energy after collision.

It can however be approximated as

$$\xi = \frac{2}{A + \frac{2}{3}} \text{ for } A > 10 \qquad (7.21.2)$$

where A is the atomic mass of the moderator.

Moderating ratio — The *moderating ratio* ($M.R.$) is a parameter that measures the effectiveness of a moderator and is the capacity for the nuclei in 1 cm^3 of the material to slow down neutrons. It is given by :

$$\boxed{M.R = \xi \frac{\sigma_s}{\sigma_a}} \qquad (7.21.3)$$

where the relevant quantities have already been defined earlier.

7.22 Nuclear reactor

A *nuclear reactor* is a device wherein a neutron-induced self-sustained chain reaction involving fission of heavy elements takes place. The purpose of the reactor is to (i) *initiate nuclear fission reaction*, (ii) *control these reactions*, and (iii) *extract the energy produced* by fission. The **control of neutrons** is the key to the functioning of a reactor.

The first nuclear reactor came into operation in 1941 at the Columbia University under the leadership of Fermi and it was then called a *uranium-carbon pile*. The design, construction and operation of a nuclear reactor however are now parts of a huge and expanding field of nuclear engineering. Naturally, we cannot delve deep into the various features of a reactor. For instance, the detailed calculation of the critical size or mass of a nuclear reactor is beyond our scope. We shall study here only its basic elements, its different types etc. A schematic diagram of a reactor is shown in Fig. 7.13a.

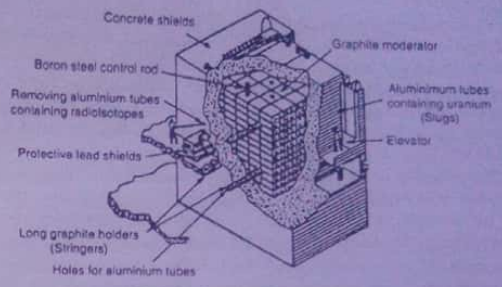

Fig. 7.13a Schematic diagram of a reactor

Basic elements of a reactor — All types of nuclear reactors contain the following essential *basic* elements :

(a) the *fuel*, a material that undergoes fissions and thereby supplies neutrons for inducing further fissions;

(b) the *moderator* for slowing down the speed of the fast neutrons (this however is not needed in case of fast nuclear reactors);

(c) the *neutron reflector* to prevent neutrons from escaping from the core;

(d) the *cooling system* to control the temperature of fuel elements and transport the generated heat to heat engine, and

(e) the *control and safety arrangements* to control the chain reaction against, 'running away' and protect the surroundings.

We shall now spend hereunder few lines on each of the above aspects.

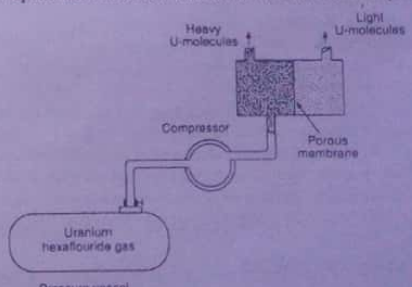

Fig. 7.13b Schematic arrangement of separating ^{235}U from ^{238}U by gas diffusion

Scanned with CamScanner

The commonly used *fissionable materials* are the uranium isotopes : U-233, U-235, U-238; the thorium isotope Th-232 and the plutonium isotopes: Pu-239, Pu-240 and Pu-241. In natural uranium, the two isotopes ^{238}U and ^{235}U are in the ratio 140 : 1. One of the common methods to *enrich* natural uranium with isotope ^{235}U is the *gaseous diffusion through a porous barrier* and is schematically illustrated (only one stage, out of many) in Fig. 7.13b. In many reactors, natural uranium enriched with isotope ^{235}U, is also used.

The materials to be used as ***moderators*** should have a large inelastic scattering cross-section and small neutron capture (absorption) cross-section. The usual moderators are : graphite, heavy water (D_2O), beryllium oxide, hydrides of metals and organic liquids. The nuclei of these materials hardly absorb neutrons.

A ***reflector*** is a material placed around the reactor core (that contains the fuel and the moderator) to *prevent neutrons from escaping from the core*. *Good moderators* are usually *good reflectors* and the efficiency of a reflector increases rapidly with its thickness.

The ***cooling system*** in a reactor *helps to control the temperature of the fuel element and transports the heat generated by fission to the heat engine*. There are four types of possible coollants. These are (i) *gases* : air, CO_2, He or steam, (ii) *water type liquids* : water or heavy water, (iii) *molten metals* : Hg, Na, K, Na-K eutectic, Pb, Bi or Pb-Bi eutectic and (iv) *fused salts*. Each type has its own merits and demerits.

The ***control and safety system*** is intended to *control the chain reaction against its 'running away' spontaneously* and also for *protecting the surroundings against the intense neutron flux and dangerous γ-radiation inside* the core. While the first is achieved by pushing *control rods* of a material having *large neutron absorption cross-section* (e.g. boron, cadmium) into the core, the second one is accomplished by surrounding the reactor with massive layers of concrete and lead and by providing completely *closed* coolant circuits.

• The power level at which a reactor operates depends on the rate of fission and hence on the number of neutrons in it. By controlling the number of neutrons, therefore, the power level can be controlled. For this cadmium rods or steel rods with boron are used. Both cadmium and boron have high absorption cross-section for thermal neutrons and can change the reproduction factor k. To control the *criticality* of a reactor, control rods are *inserted into* the reactor. In the process, so many neutrons are absorbed that the reactor *shuts down*. Rods are then *moved out* until enough neutrons are present for the reactor to start toward *supercriticality* and then they are re-inserted until it is *critical* and the reactor operates at a constant power level. Needless to mention, *the process of reactor control is made automatic to eliminate any possible human error*.

7.23 Types of reactor

Reactors are broadly classified according to the type of fuel, moderator and the heat-transfer agents used.

With respect to the arrangements of the fuel and the moderator, the reactors are classed as (i) **homogeneous** and (ii) **heterogeneous**. In homogeneous reactors, the fuel and the moderator are finely divided and uniformly mixed together, while in heterogeneous reactors these two substances are in separate elements as blocks.

Depending on the energy of neutrons, the reactors may be **thermal, intermediate** and **fast**. In fast reactors, the fission-neutrons are directly used and as such the *moderator* is completely *dispensed with*.

Purpose-based division of the reactors is : **power reactor, test and research reactor, breeder reactor, isotope producing reactor** etc. In a *power reactor*, the energy available from the chain reaction is transformed into useful power form such as electricity. The *test and research reactors* are designed for a number of different testing purposes such as dimensional stability or instability of materials under irradiation and other radiation damage phenomena. In a *breeder reactor*, the fissionable materials are bred and in an *isotope producing reactors*, radioactive isotopes are produced for use in various sectors e.g. industry, agriculture, medicine etc.

Taking into account all the above features, the nuclear reactors can be classed as : *uranium-graphite, water-cooled, water-moderated, boiling* etc.

7.24 Homogeneous reactor

A *homogeneous reactor*, as already stated, is the one where the fuel and the moderator are uniformly mixed so that each U-nucleus has the same chance of capturing a neutron. We have already mentioned that with natural uranium, a homogeneous reactor can attain criticality only with heavy water (D_2O) as moderator. Ordinary water (H_2O) may instead be used provided the fuel is enriched with ^{235}U.

A common type of such reactors uses a solution of uranyl nitrate in water with highly enriched fuel (^{235}U : $^{238}U \simeq 1 : 6$). The critical mass of ^{235}U in this case is nearly 0.8 kg, when the container is *spherical* with walls surrounded by graphite — a *neutron-reflector*. With no reflector, however, the critical mass is about 2 kg.

If the nuclear fuel is ^{235}U, the critical mass is about 0.6 kg and if the fuel is ^{239}Pu, it is 0.5 kg nearly.

7.25 Heterogeneous reactor

A *heterogeneous reactor* is one in which lumps of nuclear fuel are embedded in the moderator. It was suggested by Fermi and Szilard in the context of the fact that both enriched uranium and heavy water are highly expensive, and that in natural uranium the resonance escape probability is low for a sustained chain reaction. When uranium is used in lumps, the chance of capturing a neutron, unlike in a homogeneous reactor, is not the same for each U-nucleus. The neutrons with energies corresponding to resonant states of $(^{239}_{92}U)^*$ are mostly absorbed *on the surface only*, and once they are inside, the energies do not change much and thus escape the resonant absorption. The probability

Scanned with CamScanner

of neutron absorption inside uranium being much less than on the surface, it acts itself as *self-shielding* of uranium against neutron absorption.

Once the neutron is out of the lump, it enters a *uranium-free zone* of moderator only, where it colides with moderator nuclei losing much of its energy. Neutron can thus skip over several resonance, absorption levels before being with the next uranium lump where the same story is repeated.

What then are the effects of lumping fuel in a moderator? These are :

1. *Increase in fast fission factor* by about 10% ($\varepsilon \sim 1.1$), since the probability of fast neutron fission increases.

2. *Better moderation in uranium-free region*, for resonance absorption of neutrons by ^{238}U is very strong.

3. Resonance absorption in uranium is a *surface phenomenon* and the *resonance escape probability ν is not lowered inside a lump*. It implies that compared to the total volume, the surface layer volume in large lumps is small.

4. Large lumps however *lower the thermal utilisation factor* a, since the neutron-density in or near the lumps tends to be less than in the moderator—a condition favouring *unwanted neutron absorption in moderator*.

Factors (3) and (4) are mutually antagonistic and obviously therefore a compromise between them is to be struck.

7.26 Breeder reactor

U-235 is the only naturally occurring isotope that undergoes fission by thermal neutrons. As this fuel in a uranium reactor gets used up by fission and the neutrons themselves are lost in the fission products by absorption, the reproduction factor k becomes less than 1. The reactor thus ceases to function as a chain-reacting source within a few decades of operation, and the nuclear fuel has to be replenished to restart the reactor. If nuclear energy is to be used for the generation of power, such a continuous depletion of world's uranium resource should be halted. The other fissionable materials are ^{239}Pu and ^{233}U, none of which is available naurally in plenty. ^{239}Pu is obtained from fission of ^{235}U in a reactor with ^{238}U—a process both expensive and tedious; ^{233}U is not available in nature but is generated in a reactor containing ^{232}Th. The *breeder reactor* is the way out of this difficulty and is based on the fact of emission of *more than two neutrons per fission*.

Breeder reactors, also called *breeders*, *transform nuclei of one fissionable material into another* fissionable one *through reaction with the reactor neutrons themselves, such that they make more fuel available than what they consume*. Hence the name. For instance, breeders use fast neutrons which are captured by fertile materials like U-238; by consecutive β^- decays U-238 gets converted into fissile Pu-239 which is fissionable by thermal as well as high energy neutrons.

$$^{238}_{92}\mathrm{U} + {}^{1}_{0}\mathrm{n} \rightarrow {}^{239}_{92}\mathrm{U} \xrightarrow{\beta^-} {}^{239}_{93}\mathrm{Np} \xrightarrow{\beta^-} {}^{239}_{94}\mathrm{Pu}.$$

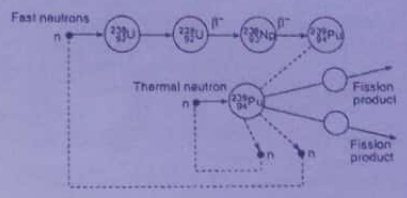

Fig. 7.14 Scheme for the Breeder reactor

The scheme for the breeder reactor is shown in Fig. 7.14. Note that *two neutrons in excess of those captured and lost by other processes must be produced to maintain the reaction* and it is so designed that more fissile materials are produced than consumed for fission. But how? A note of explanation that follows may be useful in this regard.

• **Note.** Suppose three neutrons are emitted per fission of which one keeps the reaction going to initiate fission in another fuel atom, say ^{235}U and one converts a U-atom to a Pu-atom. If the last neutron left could produce, another Pu-atom, then in the whole process one ^{235}U atom would give rise to two atoms of ^{239}Pu, i.e., more fissionable material would be produced than consumed. And this indeed is the *process of breeding*. What is stated here is an oversimplication, for some neutrons would be lost by leakage or by non-fission absorption. Nonetheless, it enlightens the process of breeding.

Breeding rests on *two* materials—one *fissionable* and the other *fertile*. Two such pairs are : (^{235}U and ^{239}Pu) and (^{232}Th and ^{233}Th). Let in the first, enough ^{239}Pu be available for chain reaction in a system which can be used to obtain power. Thermal fission of ^{239}Pu emits three neutrons per fission so that if some are absorbed in ^{238}U to produce more ^{239}Pu, a breeding cycle may be initiated.

Breeding enables a reactor to not only make new fuel for itself but also, in addition, to build up a stockpile of fissionable materials for use in new reactors.

• Another fertile material that can be used in breeders to produce fissile fuel is Th-232, available in plenty, particularly in India in the monazite sand of the South. It captures low energy neutrons to finally result in U-233, a stable α-emitter and can be fissioned with thermal neutrons.

• Within a few years, a breeder can make available double the original quantity of the fuel taken up by it.

7.27 Power reactor : Nuclear power plant

The basic principle of one type of *power reactor* is illustrated in Fig. 7.15.

A quantity of enriched U-235 in the form of a pure metal or in the form of a solution of soluble salt in water forms the *core* of the power plant. The energy released by fission

Scanned with CamScanner

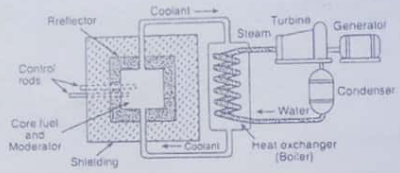

Fig. 7.15 Basic principle of a power reactor

produces large quantities of heat and the rising temperature is regulated to a certain pre-determined value by cadmium *control rods*. To reduce the fission rate, and thereby the temperature, the control rods are *pushed* in a little further to absorb more neutrons, while to raise the temperature they are *pulled out* a little further.

Because of the harmful effects of the intense radiation to both men and equipments, it is not resonable to vaporise a liquid directly as in a steam boiler. Instead, a fluid (*coolant*) is circulated through the *shielded* reactor and the *heat exchanger* (boiler).

The hot liquid flowing through the heat exchanger vaporises a more volatile liquid, say water; the issuing steam under pressure drives a *special type* of *turbine* which in turn drives an *electric generator*. The power that is developed is supplied to light our cities and factories or drive ships and submarines and for being used in other relevant fields purposefully.

Problems — There are *two important problems* associated with power reactors.

1. The intense neutron radiation weakens the crucial mechanical parts by transmuting some atoms and permanently dislodging others from their positions in the crystal lattice of the solids.

2. The coolant used must be able to withstand high temperatures, not absorb neutrons and become appreciably radioactive, and yet transfer heat efficiently in both the reactor and the heat-exchanger. Certain *metals* with *low melting points* appear highly promising.

7.28 Fission bomb : A-bomb

In a uranium or plutonium bomb (also called *fission bomb*), an uncontrolled nuclear chain reaction occurs. The device is designed to be *as supercritical as possible*, the chain reaction grows as high a rate as practicable and maximum energy is released in minimum time – within a fraction of a second. The explosive nature is due to the release of huge energy all on a sudden. A *fission bomb* (and a reactor) has a *critical size*. If the dimensions are too small, too many neutrons escape from the surface without fission. The secret of detonating a fission bomb lies in keeping it divided into subcritical sections until the moment of explosion, (for otherwise, a passing cosmic radiation may

trigger the bomb) when they are to be brought together rapidly to form a size exceeding the critical size (Fig. 7.16).

The **chief effects** of the explosion of a fission bomb are the following :

(a) the *intense heat* forming thermal waves that propagate with the speed of light. The temperature rises to as high as 5×10^7 K ;

(b) the mechanical *shock wave* consisting of a blast of air pressure, and

(c) the *radioactivity* of the fission products.

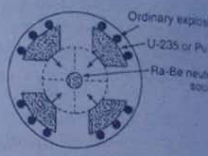

Fig. 7.16 Sub-critical sections of a fission bomb

The intense heat generated causes fatal burns and serious damage to lives and properties due to fires. The shock wave is equally dangerous and causes death and devastation (Recall the devastation of the two Japanese cities, Nagasaki and Hiroshima in August, 1945). The radiation pollutes the entire environment by emitting deadly gamma-radiation and other rays.

7.29 Nuclear power in India

India has rich deposits of uranium and thorium in Bihar, Tamil Nadu and Kerala. In fact, the world's largest deposit of thorium ore is in South India—the monazite sands—a phosphate compound of rare earth elements and thorium silicates.

The development of nuclear power in India, under the aegis of Atomic Energy Commission (AEC) of India, dates back to 1956 when the first Indian, nay the first Asian outside the then Soviet Union, reactor *Apsara* was commissioned. The second Indian reactor is *Cirus* and was commissioned in 1960. It was built with the assistance of Canada and has an energy of about 40 MW. The third reactor in the series, commissioned in 1964, is *Zerlina*, a zero energy experimental reactor. All these reactors are used for experimental researches and for the production of radio-isotopes to be provided to industry, agriculture and medicine. The research reactors that followed are *Purnima* (1972), *Dhurva* (1984) and *Kamini*. In 1964, India commissioned its first *plutonium plant* in Trombay. Plutonium helps to breed a fissionable material U-233 from thorium. Recently, India had her first *breeder reactor* set up.

India built her first *atomic power station* at Tarapur in Maharashtra with the assistance of the United States. It has an estimated capacity of 342 MW. Similar power stations have also been set up at Rana Pratap Sagar near Kota in Rajasthan and at Kalapakkam in Tamil Nadu.

India became a member of the so-called World Nuclear Club by initiating in 1974 the first *nuclear explosion* (underground) at Pokhran in Rajasthan. India undertook a series of nuclear explosions recently in May 1998, also at Pokhran.

Scanned with CamScanner

7.30 Fusion : Thermonuclear reaction

The release of energy in fission is essentially due to the binding energy per nucleon being less in heavier nuclei than in those of intermediate mass numbers formed as fission fragments. The binding energy curve (Fig. 1.2) shows that precisely an equivalent situation exists at the low mass number end. The binding energy per nucleon in light nuclei on the steep portion of the curve is less than for nuclei of intermediate mass numbers. So, *if two light nuclei combine or fuse together to produce a relatively heavier nucleus, there would be a greater binding energy and a consequent decrease in nuclear mass. This would therefore result in a positive Q-value and a release of energy.* This type of nuclear reactions is known as **nuclear fusion**, a process opposite to that of nuclear fission. Eddington had shown, in as early as 1920, that the fusion of four hydrogen atoms into a helium atom would release energy ~ 7 MeV/nucleon or about 28 MeV in all.

Fusion reactions are now readily observed in experiments with high energy beam of protons and deuterons, energised by accelerators.

$$^1_1\mathrm{H} + ^1_1\mathrm{H} \rightarrow ^2_1\mathrm{H} + ^0_1\mathrm{e} + \nu; \qquad Q = 0.42 \text{ MeV}$$

$$^2_1\mathrm{H} + ^2_1\mathrm{H} \rightarrow ^3_2\mathrm{He} + ^1_0\mathrm{n}; \qquad Q = 3.3 \text{ MeV}$$

with accompanying release of energy as shown.

Fusion depends for its action on the collisions of two very energetic nuclei, a subsequent re-arrangement of nucleons and the release of energy as kinetic energy of the product particles and their excitation energy. The primary nuclei are positively charged and repel each other electrostatically. For fusion, therefore, *the kinetic energy of the colliding particles must be high enough to overcome the electrostatic coulomb repulsion.* And in order that fusion could be of any practical value as an alternative source of energy production, the reaction must be *self-sustaining*, i.e. more energy must be released than what is consumed in initiating the reaction. A large kinetic energy implies a high temperature such that fusion energy should be sufficient to provide enough energy to secondary particles to make the process self-sustaining. For this reason, fusion reactions are also known as **thermonuclear reactions.** Unfortunately, the so-called high temperature is as high as $\sim 10^9$ °C and it increases rapidly with atomic number. That is why promising experiments in the field have been carried out with the *three isotopes of hydrogen, particularly deuterium.*

Since there is practically an inexhaustible store of deuterium fuel (in water ^{2}H : ^{1}H = 1 : 5000), thermonuclear reactions hold a great promise for a permanent solution of the problem of *depletion of chemical, mineral and fossil fuels.* We have yet to be fully successful to control thermonuclear reactions so as to produce thermonuclear reactors; physicists the world over are quite optimistic.

Advantages of fusion reactor — But once made, the fusion reactor would have a number of *advantages* over the fission reactors.

First, the process of extraction of fission fuel from the limited amount of ores is quite complicated and costly, but the fusion fuel like ^{2}D is rather easily obtainable from natural water which is almost an inexhaustible source.

Secondly, unlike fission, fusion is *clean* for it does not leave behind any harmful radioactive waste for disposal.

Thirdly, the fusion reactor will have an inherent safety unlike the fission reactor that may 'run away'.

Also, the nuclei taking part in fusion are light and so the energy released per unit mass of the reaction material is comparatively much greater.

7.31 Source of stellar energy : Natural fusion

The sun discharges energy at the rate of 10^{26} joules a second. This is also more or less true with any star with the interior temperature of about 20 million degrees. The estimated age of the sun is at least 5×10^9 years. So the loss of energy by the sun during this time is tremendously high. What then is the source of this exceedingly high stellar energy? Helmholtz and Kelvin suggested that a slow gravitational attraction might be the source. Jeans proposed annihilation of high energy protons and electrons in the stars as the source. It was indeed a puzzle until the discovery of nuclear reactions.

Atkinson and Houtermans were the first to suggest in 1928 that successive capture of four protons by some light nuclei to produce an α-particle could release energy at such rates as to account for the loss of energy by the sun for so long a time. They proposed the idea of *cyclic nuclear reactions.*

Proton-proton cycle — In 1938, Hans Bethe suggested that the stellar energy is produced by *thermonuclear reactions* in which protons are combined and transformed into helium nuclei. This is known as **proton-proton cycle** applicable for relatively low stellar temperature. The cycle is :

$$\text{(a)} \quad ^1_1\mathrm{H} + ^1_1\mathrm{H} \rightarrow ^2_1\mathrm{H} + ^0_1\mathrm{e} + \nu + 0.42 \text{ MeV}$$

$$\text{(b)} \quad ^2_1\mathrm{H} + ^1_1\mathrm{H} \rightarrow ^3_2\mathrm{He} + \gamma + 5.5 \text{ MeV}$$

$$\text{(c)} \quad ^3_2\mathrm{He} + ^3_2\mathrm{He} \rightarrow ^4_2\mathrm{He} + 2\,^1_1\mathrm{H} + 12.8 \text{ MeV}$$

In this cycle of reactions, fusion reaction (a) and (b) must occur twice to yield two $^3_2$He nuclei in (c). The net result of these reactions is that four protons are fused to produce an α-particle, two positrons, two neutrinos and two γ-photons.

$$4\,^1_1\mathrm{H} \rightarrow ^4_2\mathrm{He} + 2\,^0_1\mathrm{e} + 2\nu + 2\gamma$$

The energy released in the cycle is 24.6 MeV, for the mass difference is $(4 \times 1.0078 - 4.0026)$ or 0.0286 u. Since the neutrinos escape, the energy left is about 24.3 MeV after the fusion of 4 protons into 1 helium nucleus. The protons thus get gradually depleted and the concentration of helium builds up.

Scanned with CamScanner

The *proton-proton* cycle is an important source of energy in the sun and in stars of comparatively low temperatures (*red dwarfs*). A conclusion that follows from the above cycle is that the older stars are expectedly richer in helium compared to the younger ones.

Carbon-nitrogen cycle — For the *main sequence stars* having higher temperatures, Bethe suggested an alternative to the proton-proton cycle – the **carbon-nitrogen cycle.** The cycle is (* means radioactive)

$$\text{(a)} \quad {}^{1}_{1}\text{H} + {}^{12}_{6}\text{C} \rightarrow {}^{13}_{7}\text{N}^{*} + \gamma + 1.95 \text{ MeV}$$

$$\text{(b)} \quad {}^{13}_{7}\text{N}^{*} \xrightarrow{10.1 \text{ min}} {}^{13}_{6}\text{C} + {}^{0}_{1}\text{e} + \nu + 2.22 \text{ MeV}$$

$$\text{(c)} \quad {}^{1}_{1}\text{H} + {}^{13}_{6}\text{C} \rightarrow {}^{14}_{7}\text{N} + \gamma + 7.54 \text{ MeV}$$

$$\text{(d)} \quad {}^{14}_{7}\text{N} + {}^{1}_{1}\text{H} \rightarrow {}^{15}_{8}\text{O}^{*} + \gamma + 7.35 \text{ MeV}$$

$$\text{(e)} \quad {}^{15}_{8}\text{O}^{*} \xrightarrow{2.05 \text{ min}} {}^{15}_{7}\text{N} + {}^{0}_{1}\text{e} + \nu + 2.7 \text{ MeV}$$

$$\text{(f)} \quad {}^{1}_{1}\text{H} + {}^{15}_{7}\text{N} \rightarrow {}^{12}_{6}\text{C} + {}^{4}_{2}\text{He} + 4.96 \text{ MeV}$$

Adding up the above reactions, we get the overall reaction as

$$4\,{}^{1}_{1}\text{H} \rightarrow {}^{4}_{2}\text{He} + 2\,{}^{0}_{1}\text{e} + 2\nu + 3\gamma + 26.72 \text{ MeV}$$

the energy release being almost the same as in proton-proton cycle. Of this energy, an amount ~ 25 MeV heats up the star, the rest being carried off by neutrinos.

The conversion of hydrogen into helium is a mass-exchange reaction and would continue till the whole of hydrogen in the star is completely used up. For the sun, both the cycles occur with equal probability. The estimated time for the complete conversion of all the hydrogen of the sun into helium is about 3×10^{10} years, the calculation being based essentially on the mean reaction times for the reactions (a) and (d) only which are 2.5×10^{6} yr and 3×10^{8} yr respectively. Our sun is therefore still in its prime of life.

7.31.1 Some important observations

The following observations in this regard are worth mentioning.

- C-12 acts as a catalyst only in that it was a part of the initial reaction and a product of the final reaction. Instead of taking (a) as the starting point and (f) the end point of the cycle, one could as well take (f) and (e) as the beginning and end of the cycle respectively in which case N-15 would act as the catalyst.
- Fusion of 4 protons into helium, overcoming the Coulomb repulsion, is possible only because of the extremely high initial temperature. But *why do 4 protons not directly combine but only via the cycle.* The reason is that even at that high temperatures, protons do not have enough kinetic energy to overcome the mutual repulsion.
- There are evidences to believe that the *carbon-nitrogen cycle* starts at a rather late stage in the life of a star. According to the modern view of stellar evolution, a star is formed by way of condensation of an enormous amount of matter at a certain point in space. As the mass contracts, its temperature increases and when it reaches the value of about 2,00,000°C, the *proton-proton cycle* starts operating.
- When the deuterons, formed as a product in the proton-proton cycle, are completely exhausted, the star shrinks and the temperature again increases. At a temperature of about million degrees, protons interact with heavier elements such as beryllium, lithium and boron forming helium nucleus. At this stage, the star looks very bright and is called a *red giant*. When the above type of nuclei is also exhausted, further contraction takes place and the temperature rises to about 20×10^{6} °C. The carbon-nitrogen cycle operates at this stage and supplies the energy for the major portion of the radiating life of a star. When the protons are all exhausted, further contraction takes place at a rapid rate; the star releases a large amount of energy and quickly attains the last phase of its life which may be one of the *three* end states – the **white dwarf**, the **neutron star** or the **black hole.** The *white dwarf* is usually the common end state of stellar evolution. The *neutron star* is comparatively a recent discovery through radio-astronomy. *Pulsars*, identified since 1967, are regarded as pulsating, that is, rotating neutron stars. The *black hole* is believed to be formed by the gravitational collapse of a neutron star. It is too dense for even photons (light) to escape from its pull.
- Stars with masses between 0.4-2.5 solar mass produce energy mainly by carbon-nitrogen cycle rather than the proton-proton cycle. Stars having masses of 0.4 solar mass or lower, which constitute the bulk of stellar population in our galaxy, mainly derive energy from proton-proton cycle.
- The temperature of the sun is practically constant for at least 10^{9} years. But why? The sun is in a state of *equilibrium* due to two opposite effects. If the sun's temperature were to rise, the fraction of protons taking part in carbon cycle would increase, heating up the sun further. Again, if the temperature rises, the sun tends to expand and the concentration of nuclei in the cycle tends to diminish, reducing the fusion rate. The two effects balance each other. Fusion process in the sun is *contained* by the massive gravitational field of the sun.

7.32 Uncontrolled fusion : H-bomb

When the trial atomic bomb (A-bomb) exploded at Alamogordo on July 16, 1945, it was realised that it would be possible now to make fusion-energy the way the sun does. When an A-bomb containing U-235 or Pu-239 explodes, the temperature at the central core becomes, for a fraction of a second, comparable to that at the heart of the sun. And the pressure is millions of atmosphere.

The exact materials used, their proportion, the physical size, the shape of the device and the mechanical and electrical systems used in hydrogen bomb (H-bomb) are all hidden in military secrecy. Nevertheless, an H-bomb, *in principle*, consists of a device in which *fission-fusion* process is applied. The central part of the device is

Scanned with CamScanner

a fission bomb (A-bomb) containing U-235 or Pu-239 and this is surrounded by an atmosphere of deuterium and tritium. The A-bomb acts as the igniting 'fuse' of the H-bomb, providing an extremely high temperature (10^7-10^8 °C) necessary for the fusion process to start. Once the fusion starts, it maintains the temperature to keep the process going. The reactions are :

$$^2_1H + ^2_1H \rightarrow ^3_1H + ^1_1H + 4.04 \text{ MeV}$$

followed by

$$^2_1H + ^3_1H \rightarrow ^4_2He + ^1_0n + 17.6 \text{ MeV}$$

and

$$^2_1H + ^2_1H \rightarrow ^3_2He + ^1_0n + 3.26 \text{ MeV}$$

followed by

$$^2_1H + ^3_2He \rightarrow ^4_2He + ^1_1H + 18.3 \text{ MeV}$$

Fusion reactions based on deuteron-deuteron and deuteron-triton are known as *wet hydrogen bomb* reactions.

The first successful H-bomb was exploded on Eniwetok Atoll in the Pacific on November 1, 1952. The explosion not only melted the whole island but boiled it away. India exploded its first successful H-bomb in Pokhran (underground) during May, 1998.

• A *hydrogen bomb* being a fusion bomb cannot explode until 'ignited', that is, fusion reaction is to be started by tremendously high temperature. But once ignited, any amount of fusible material can be used for there is no limit to the size of an H-bomb, as there is no necessity for any critical mass in the process.

7.33 Controlled fusion : Possibility of fusion reactor

Ever since the realisation of the fusion process in a hydrogen bomb, the physicists had been after a controlled fusion reaction for making fusion reactor a possibility. For it has a great advantage over fission reaction. The fuel is both cheap and available in plenty. While there are still much to be discovered before any successful power source based on fusion is achieved, much however has already been learnt from the various study projects in the field.

One of the main difficulties involved in reproducing the conditions favourable to thermonuclear reactions in the laboratory is that the temperature requirement is extremely high – millions of degrees – and fusion ***cannot be effected in a container with material walls***, for that would at once vaporise at such high temperatures.

One approach would be to use particles with *high kinetic energy* produced in accelerators, rather than ultra-high temperature. From kinetic viewpoint, temperature is associated with random motion of atoms and molecules in an assembly. When the energy of an individual particle is considered, one may refer to its kinetic temperature. For instance, an energy as small as 1 keV imparted to a particle corresponds to a kinetic temperature of more than 1 million Kelvin. It may be possible, as warranted by calculations, to maintain fusion at a kinetic temperature of ~ 45 million degrees that can be easily provided to a particle by accelerating it through 4 kilo volt.

The *other approach* to solve the problem, in fact solved to a great extent, is to first convert the fusion fuel into the *plasma state*. A *plasma* is a neutral assembly of ionised atoms, molecules and electrons and could be produced in a *number of ways*. A high current arc constitutes a good source of plasma. Plasma is usually held in suspension in space by the lines of force of an electromagnet, the so-called *magnetic bottle*. The basic principle of this *magnetic confinement of plasma* is this : Moving charged particles get deflected from their straight paths by magnetic field. A high pressure hot plasma, under appropriate conditions, develops a magnetic field *of its own*. This field may be strong enough to exclude the external applied field. Particles would move in such a plasma in straight lines except at the boundary whence they would be deflected back. So the strong magnetic field will confine the plasma like a gas in a bottle – the magnetic bottle.

First, a 'cool' dilute plasma is formed by an electric discharge. The plasma is next imparted sufficient kinetic energy by passing a heavy induced current through it so that the nuclei in it overcome the Coulomb repulsion. In terms of kinetic energies of the nuclei, the temperature is then in the range of 100 million Kelvin. The chances of fusion in such a hot plasma at a given temperature are functions of the density of the particles and their confinement time. In this context, a criterion known as 'Lawson criterion' is important. According to *Lawson criterion*,

$$\text{Density} \times \text{confinement time} \sim 2 \times 10^{16} \text{cm}^{-3}\text{s} \quad \ldots\ldots \text{(DD-fusion)}$$

$$\sim 10^{14} \text{ cm}^{-3}\text{s} \quad \ldots\ldots \text{(DT-fusion)}$$

An *interesting feature* of a magnetic bottle is that a fusion reaction sustained in it can never 'run away', unlike the chain reaction of fission process. Whenever the plasma pressure exceeds the magnetic field, the plasma moves towards the chamber wall causing rupture of the magnetic walls and this immediately quenches the fusion reaction. A fusion reaction, by its very character, can never explode.

A schematic diagram of a plasma held in a magnetic bottle is shown in Fig. 7.17. *AC* is a hollow solenoid into the central region of which is injected a stream of ionised atoms. The ions spiral around in the field with the lines of force as guides. The field at the ends is stronger than that at the centre and as ions spiral into the stronger field, the force components drive them back into the centre. The plasma stream could be widened or narrowed, as desired, modifying the shape of the field, by increasing or decreasing the current strength in the windings in the coil. By such modification, the plasma could be transported lengthwise from one bottle to another.

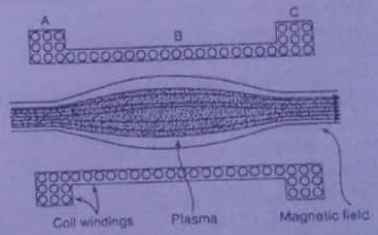

Fig. 7.17 Schematic diagram of a plasma held in a magnetic bottle

Scanned with CamScanner

Pinch effect — An example of containment of plasma by a magnetic field is the so-called **pinch effect**. It is the self-construction of a group of ions moving such that a unidirectional current is produced. Let a low pressure discharge be generated in a straight tube. If the current density within the discharge is very high, the magnetic field due to the current and surrounding it will be intense enough to compress the discharge into a narrow filament. This is what is known as the *pinch effect*.

The pinch however is very unstable lasting only for about 0.1μs and tighter the pinch, faster it gets destroyed. The reason is not far to seek. First, any small kink in the pinched column grows rapidly as the magnetic pressure is stronger on the concave side of the kink (region where magnetic lines of force are more crowded). This is illustrated in Fig. 7.18a. Secondly, there is the *sausage effect* due to which the plasma necks itself at one or more points along the column cutting it into points resulting in *pinch instability* (Fig. 7.18b). The problem was solved by applying a strong longitudinal

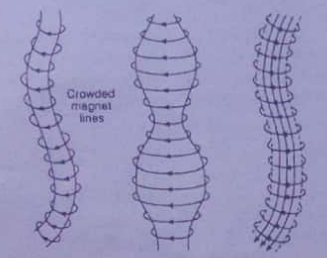

Fig. 7.18 Pinch effect, its instability and pinch stabilisation

magnetic field within the plasma column, over and above the pinching magnetic field around the plasma (Fig. 7.18c).

But the straight line pinch columns are not desirable, as electrodes at the end would have a quenching (cooling) effect. Pinch experiments are thus conducted in doughnut-shaped tube. A very high voltage is applied to a large iron core transformer primary, an electric discharge in the doughnut is produced, the doughnut acting as a single turn secondary. Thus heavy currents can be induced in the plasma.

If all the fields are increased, the plasma volume would be compressed resulting in an increase of the temperature. This causes an increase in the kinetic energy of the ions and also in the probability that collision would produce fusion. If however the field is decreased at one end and increased at the other, the plasma may quickly move

along the axis forming a *jet*. If such a jet of fusible material (e.g. deuterium) be fed from a nozzle into a cavity, fusion might be consummated and tremendous quantity of energy in heat-form could be generated continuously and be tapped off.

• There is another device developed for plasma containment – the *magnetic mirror machine* or *pyrotron*. It consists of an axial magnetic field (non-uniform) having a high concentration of field lines towards the ends. The ions describe spiralling paths with radii of curvature proportional inversely to the field strength. So when they reach near the ends, their paths are more sharply curved causing them to reflect back. So, under proper conditions, the ions will be reflected back and forth between the two ends.

• One of the serious problems in controlled fusion research is the so-called *magneto-hydrodynamic instability*. It arises from the generation of electrostatic and electromagnetic waves in the plasma at the expense of energy from the free energy sources in it, e.g. inhomogeneities in density. The instability expels plasma as a whole very rapidly from the confining magnetic bottle. This is prevented and stabilisation is achieved by making the lines of force of the magnetic field helical instead of closed circles.

7.33.1 Stellarator, Levitron and Tokamak

• **Stellarator** of the United States, **Levitron** of United Kingdom and **Tokamak** of previous USSR obtain the helical configuration differently. For instance, in *stellarator* currents in helical conductors wrapped round the torus produce the helical field by interaction with the torroidal field. In *levitron*, a leviated superconducting ring inside the plasma produces the field and the latter generates the helical field in combination with the torroidal field. In *tokamak*, the helical field is produced by combining the torroidal field with the azimuthal field generated by plasma heating current. Tokamak is technically simple and its behaviour can be subjected to theoretical analysis. It is thus most popular among the three.

A *fusion reactor* is a device in which the nuclear fusion could occur in a controlled way and useful energy, in excess of what is required to operate it, could be extracted from it. The problems of realising such a device are many; the task is one of the most difficult and challenging one. The physicists are however conscious of the formidable nature of the task but they are also quite optimistic.

7.34 Radiation hazards[1]

Living matter is surprisingly sensitive to ionising radiation. For instance, human beings are killed by a whole body irradiation with so small a dose of γ-rays or x-rays that the energy absorbed increases the body-temperature by as little as one thousandth of a degree Celsius. More primitive animals and plants are somewhat less sensitive, and bacteria and viruses even less so.

[1] From 'Chemistry To-day' published by OECD.

Scanned with CamScanner

Chapter 11

Elementary Particles

11.1 Introduction

It is indeed a difficult task to define the term '*elementary particles*'. The purport of the word 'elementary' is 'ultimate' and hence the meaning of the term continuously gets shifted as research progresses with time. The search for the ultimate particles of which all matter is composed has, in fact, been a strenuous exercise for the physicists since long. Beginning with atoms and its electronic structure, the search was eventually extended to the nucleus. And now it has been into the very structure of nucleons themselves. With the development of more and more gigantic accelerators, physicists could produce higher and higher energy atomic and sub-atomic projectiles to bombard the nuclei and shatter them into a host of new and interesting particles. Many, too many (> 200) have been already discovered and it is believed that many of them will be explainable in terms of only few of them.

The first elementary particle discovered was the negatively charged **electron** by Sir J.J. Thomson in 1898. The scattering experiments of Rutherford (1914) indicate the presence of positively charged **protons** inside the nucleus. With the discovery of **neutron** by Chadwick (1932), the number of elementary particles became *three* : *electron* (e^-), *proton* (p) and *neutron* (n). The proton-neutron hypothesis of the composition of nuclei could successfully explain most of the observed properties of the nuclei. Soon after, with the progress of cosmic ray research, a dramatic change occurred in the number of elementary particles. The discovery of **positron** or positive electron (e^+) was made by Anderson (1933) from the track of the particle in a magnetically controlled cloud chamber to vindicate Dirac's prediction. The particle concept of radiation — light quantum hypothesis — of Einstein introduced **photon** (γ) as a quantum of radiation and was also considered as an elementary particle. Pauli (1931) postulated the existence of a neutral particle of negligible mass called **neutrino** (ν) to account for the missing energy of β-particles in β-decay. Fermi (1934) used Pauli's hypothesis of emission of *neutrino* (ν) and **antineutrino** ($\bar{\nu}$) to get the correct shape

Scanned with CamScanner

of β-spectrum of radioactive β-emitters. The discovery of these *seven* elementary particles, viz., $p, n, e^-, e^+, \gamma, \nu$ and $\bar{\nu}$ could very well explain most of the atomic and nuclear phenomena.

However, to account for the stability of the nucleus against Coulomb repulsive forces, Yukawa (1935) predicted the existence of a particle of mass between 200–300 electronic mass and showed that such an intermediate particle would provide a strong nucleon-nucleon (N–N) interaction between protons and neutrons. In 1935, Anderson and Neddermeyer observed the track of a positively charged cosmic ray particle of mass in the above range—the *positive* **muon** (μ^+). This was immediately followed by the discovery of *negative* **muon** (μ^-) by Street and Stevenson. Both μ^+ and μ^- have a mass of about $207m_e$, but they were *not* Yukawa particle as they interacted *weakly* with nucleons. Powell and Occhialini discovered another cosmic ray particle in their emulsion detector of mass $273m_e$ that interacts *strongly* with nucleons and was identified with Yukawa particle. It was called *pi-meson* or **pion** (π). Between 1937–50, three π-mesons : π^+, π^- and π^0 (neutral) were discovered. The charged pions (π^+, π^-) had a mass $273m_e$, but the neutral pion (π^0) has a mass of $264m_e$. Both muons and pions are *short lived*.

Up to this stage, all the observed particles fitted rather well into the prevailing theoretical ideas regarding the atomic and nuclear structure. But soon other short-lived **heavy mesons** like $K^+, K^-, K^0, \bar{K}^0$ and η^0 were also discovered of which $K^{+,0}$ behaved somewhat *strangely* (strange particles). Subsequently, a number of short-lived particles of mass greater than nucleon (between neutron and deuteron) was discovered : **lambda** (Λ^0), **sigma** ($\Sigma^{\pm,0}$), **Xi** (Ξ^{-0}) and **omega** (Ω^-) **particles**. These have been produced with the help of high energy accelerators in the laboratory and are also observed in the interaction of high energy cosmic radiation. The situation at this stage demanded the introduction of revolutionary concepts regarding elementary particles and the basic interactions governing their behaviour.

11.2 Kinematics of high energy (relativistic) collisions

Many elementary particles are the product of high energy (relativistic) collisions. We shall now study the kinematics of such collisions, restricting to those that results in the production of *two* product particles only, but it can be easily generalised. For the sake of compactness, we shall use a system of unit where the light velocity c would be taken as unity, i.e., $c = 1$. So that mc^2 would be denoted by the mass m, the energy pc by momentum p, etc.

Let us take the reaction : $A_1 + A_2 \rightarrow A_3 + A_4$ (11.2.1)

The conservation principles of energy and momentum dictate that

$$W_1 + W_2 = W_3 + W_4 \tag{11.2.2}$$

and $$p_1 + p_2 = p_3 + p_4 \tag{11.2.3}$$

where W's represent total energies and p's the momenta of the particles.

Using relativistic relations for different particles, we get

$$W_n^2 = p_n^2 + m_n^2, \quad n = 1, 2, 3, \cdots, \tag{11.2.4}$$

From relativity, again, the total energy W and the components of momentum vector $\vec{p}$ constitute a *four vector* $p_\mu = (W, \vec{p})$, and the scalar product $p_\mu p_\mu$ in 4-space is an invariant at a particular time.

$$\therefore \quad p_\mu p_\mu = W^2 - p^2 = \text{invariant} \tag{11.2.5}$$

p^2 being the square of 3d-momentum vector.

∴ For a *system of particles*, in initial or final state,

$$p_\mu p_\mu = \left(\sum W_n\right)^2 - \left(\sum p_n\right)^2 = \text{invariant} \tag{11.2.6}$$

In reference to the reaction (11.2.1), therefore, we have

$$\begin{aligned}(p_\mu p_\mu)_{\text{initial}} &= (W_1 + W_2)^2 - (p_1 + p_2)^2 \\ &= \left(\sqrt{p_1^2 + m_1^2} + \sqrt{p_2^2 + m_2^2}\right)^2 - (p_1 + p_2)^2\end{aligned} \tag{11.2.7}$$

In Lab-frame (L-frame), assuming the target A_2 to be at rest, $p_2 = 0$. The kinetic energy T_1 of the incident particle A_1 is then

$$T_1 = W_1 - m_1 = \sqrt{p_1^2 + m_1^2} - m_1$$

From (11.2.7), we therefore obtain directly

$$\begin{aligned}(p_\mu p_\mu)_{\text{initial}} &= \left(\sqrt{p_1^2 + m_1^2} + m_2\right)^2 - p_1^2 \\ &= m_1^2 + m_2^2 + 2m_2\sqrt{p_1^2 + m_1^2} \\ &\simeq m_1^2 + m_2^2 + 2m_2(m_1 + T_1) \\ &= (m_1 + m_2)^2 + 2m_2 T_1\end{aligned} \tag{11.2.8}$$

Threshold energy : At the threshold, A_3 and A_4 are produced with *zero* momentum, i.e., $p_3 = p_4 = 0$. So, using (11.2.8)

$$(p_\mu p_\mu)_{\text{final}} = (m_3 + m_4)^2, \tag{11.2.9}$$

Substituting $m_i = m_1 + m_2$ and $m_f = m_3 + m_4$ and exploiting the *invariance*, we get from (11.2.8) and (11.2.9),

$$m_i^2 + 2m_2 T_1 = m_f^2$$

$$\Rightarrow \quad \boxed{T_1 = (m_f^2 - m_i^2)/2m_2} \tag{11.2.10}$$

Scanned with CamScanner

Again, the Q-value of the reaction is

$$Q = m_1 + m_2 - m_3 - m_4 = m_i - m_f \qquad (11.2.11)$$

$\therefore$ Threhold energy, $E_{th} = T_1 = \dfrac{(m_f + m_i)(m_f - m_i)}{2m_2}$, using (11.2.10)

$$= -(Q/2m_2)(m_i + m_f)$$

$$= (Q/2m_2)(Q - 2m_i), \quad \text{using (11.2.11)}$$

$$\therefore \quad \boxed{E_{th} = Q\,[Q/2m_2 - (m_1 + m_2)/m_2]} \qquad (11.2.12)$$

1. **Non-relativistic collision** : Here $Q \ll m_1$ (or m_2). So from (11.2.12), we obtain

$$\boxed{E_{th} = -Q\frac{m_1 + m_2}{m_2}}, \qquad (11.2.13)$$

the same as obtained in Chapter : *Nuclear reactions*.

2. **Extreme relativistic case** : Here $Q \gg m_1$ and also m_2 so that

$$\boxed{E_{th} = Q^2/2m_2} \quad \Rightarrow \quad E_{th} \propto Q^2 \qquad (11.2.14)$$

$$\therefore \quad \frac{Q}{E_{th}} = \frac{2m_2}{Q} \ll 1$$

This implies that only a small fraction of E_{th} goes to provide the reaction energy.

11.3. Pions and Muons

Pi-mesons ($\pi^{\pm,0}$) are particles with mass intermediate between that of an electron and a proton. To explain the short range internucleon force, the pion was considered as a quantum of this force and was predicted by Yukawa. Subsequently, it was discovered in the cosmic radiation by Powell and co-workers.

As regards their production in the laboratory and their properties, we made a detailed discussion in Chapter : *Cosmic rays*, and would not be repeated here.

Muons ($\mu^{\pm}$), like the charged pions, are also elementary particles with mass intermediate between that of an electron and a proton.

The muons are electrically charged—either positively or neatively — and carry one unit of electronic charge. They are unstable particles.

The muons were also discovered in cosmic radiation, earlier than the discovery of pions, by Anderson and Neddermeyer. Their mass, mean life etc. were first determined during the cosmic ray studies and later more accurately in the laboratory.

As regards the production and properties of muons, we made a detailed discussion in the Chapter : *Cosmic rays* which may now be consulted again.

11.4. K-mesons or Kaons

While working with a counter-controlled cloud chamber in a strong magnetic field, with a lead sheet (3 cm thick) interposed along the diameter of the chamber, Rochester and Butler observed a *paired track of oppositely charged pions* originating apparently at a *common point*. It was not a case of collision process producing the pair, for then a host of other particles would have originated in the lead-plate. The event was attributed to spontaneous disintegration of a neutral particle that left no track in the chamber and the particle was termed K^0-*meson*. The disintegration was represented as

$$K^0 \rightarrow \pi^+ + \pi^-$$

The rest mass of this new particle was estimated from the measurement of energy released in the above decay to be about $966\,m_e$.

Another type of rare events was soon recorded in photographic emulsion that showed the existence of both *negatively and positively charged* K-*mesons* ($K^{\pm}$) that decay into *three* charged pions in accordance with the following scheme.

$$K^+ \rightarrow \pi^+ + \pi^+ + \pi^-$$
$$K^- \rightarrow \pi^- + \pi^+ + \pi^-$$

All K-decays are now assigned to a single group of mesons, the K-*mesons or kaons* both charged and neutral, the masses being $975m_e$ for K^0 and $966m_e$ for $K^{\pm}$. They are similar to pions but have many more possible decay schemes. The common decay modes are :

$$K^{\pm} \rightarrow \pi^{\pm} + \pi^0$$
$$K^{\pm} \rightarrow \mu^{\pm} + \nu_{\mu}$$
$$K^+ \rightarrow \pi^+ + \pi^+ + \pi^0 \quad (\tau = 12.4\,\text{ns})$$
$$K^0 \rightarrow \pi^0 + \pi^0$$

Since the mean life of kaons is 10^{-10} to 10^{-8}s, it is characteristic of *weak interaction* decays. But the kaons could be *artificially produced* in many high-energy reactions involving pions and nucleons—either N-N (nucleon–nucleon) or π–N collisions—and there are indications of *strong interactions between kaons and nucleons*. Kaons are thus known as **strange particles** in that a *new type of selection rules* determines their decay.

All kaons have *zero spin* and they are therefore *bosons*.

• Kaons are now readily available from the giant accelerators.

The *other neutral mesons* include η (549)-particles with *zero spin* and mean life 2.51×10^{-19}s. The decay modes are :

$$\eta^0 \rightarrow \gamma + \gamma$$
$$\eta^0 \rightarrow \pi^0 + \pi^0 + \pi^0$$
$$\eta^0 \rightarrow \pi^+ + \pi^0 + \pi^-$$

Other neutral mesons of established existence are $\rho^0(765)$, $\omega^0(784)$, $\phi^0(1019)$ and $\eta^0(1060)$.

Scanned with CamScanner

11.5 Hyperons

Hyperons are *unstable particles* having *masses greater than that of the nucleons* and were first discovered in cosmic rays by Rochester and Butler who obtained from an analysis of the cloud chamber photographs an evidence for the existence of a particle called the *lambda particle* (Λ^0) that decays by the following scheme.

$$\Lambda^0 \rightarrow \pi^- + p^+ \quad (66\%)$$
$$\text{and} \quad \Lambda^0 \rightarrow \pi^0 + n^0 \quad (34\%)$$

The rest mass of the lambda particle is estimated to be $2182m_e$ with a mean life of 0.27×10^{-9}s. The Λ^0 particles were so named from the *fork-like tracks* produced by the secondary charged particles. For reasons mentioned in the case of K-mesons, the *lambda particles are also* **strange particles**. The lambda particle with zero charge only can be absorbed by a nucleus to form a relatively long-lived *hyperfragment*.

The other hyperons are the sigma particles, both *charged and neutral* ($\Sigma^{\pm}$, Σ^0), and the Xi-particles, *neutral and negatively charged* (Ξ^0, Ξ^-) only. Some of the probable decay schemes for these particles are as under :

$$\Sigma^+ \rightarrow p^+ + \pi^0; \qquad \Sigma^- \rightarrow n^0 + \pi^-$$
$$\Sigma^+ \rightarrow n^0 + \pi^+; \qquad \Xi^0 \rightarrow \Lambda^0 + \pi^0$$
$$\Sigma^0 \rightarrow \Lambda^0 + \gamma; \qquad \Xi^- \rightarrow \Lambda^0 + \pi^-$$

The anti-Xi-particles also decay by the corresponding modes :

$$\bar{\Xi}^0 \rightarrow \bar{\Lambda}^0 + \bar{\pi}^0$$
$$\bar{\Xi}^+ \rightarrow \bar{\Lambda}^0 + \bar{\pi}^+$$

The Xi-particles are also called *cascade hyperons* for they do not decay directly into nucleons but *via* the lambda particles.

The hyperons can be *artificially produced* in the laboratory by high energy (>1 GeV) pion or kaon interactions with protons :

$$\pi^+ + p^+ \rightarrow K^0 + \Lambda^0; \qquad K^- + p^+ \rightarrow K^+ + \Xi^-$$
$$K^- + p^+ \rightarrow \pi^- + \Sigma^+; \qquad K^- + p^+ \rightarrow K^0 + \Xi^0$$
$$\pi^- + p^+ \rightarrow K^+ + \Sigma^-;$$

These hyperons are *spin* $\frac{1}{2}$ particles and are therefore *fermions*.

The other hyperons are delta and omega particles. The Δ-particles form a number of known quartets Δ^{++}, Δ^+, Δ^0, Δ^-, each with a *spin* $\frac{3}{2}$ and mean life 5.5×10^{-24}s. The decay modes are :

$$\Delta^{++} \rightarrow p^+ + \pi^+; \qquad \Delta^+ \rightarrow p^+ + \pi^0$$
$$\Delta^0 \rightarrow n^0 + \pi^0; \qquad \Delta^- \rightarrow n^0 + \pi^-$$

The omega particles (Ω) form a pair of *singlets* with a *spin* $\frac{3}{2}$. Although a very heavy particle (1762 MeV), its mean life is rather long : 1.30×10^{-10}s.

11.6 Fundamental interactions

Elementary particles are rather large in number. But only few of them—proton, electron, positron, neutrino and photon—are stable. The rest are all unstable. Some of them have mean lives much larger than the *characteristic nuclear time*, being defined as the *time taken by a pion to travel past a proton* ($\sim 4 \times 10^{-24}$ s) and decay by weak interaction; few like π^0 and Σ^0 decay by electromagnetic interaction. A large number again decays by strong interaction, with mean lives $\sim$ characteristic nuclear time. They are called *resonance particles*.

To understand the significance of the existence of these large number of particles, a study of the fundamental interactions that act between them is worth-making. In nature, there are *four* different types of fundamental *interactions*. These are *gravitational, electromagnetic, weak* and *stong interactions*. According to the quantum field theory, all the interactions rely on the mechanism of exchange of quanta. The mediators of different interactions along with their strength and ranges are given in Table 11.1. All the interactions are transmitted from one particle to the other by successive processes of emission, propagation and absorption of such mediators.

1. Gravitational interaction — It is the *weakest* of all the fundamental *interactions* and acts between all bodies having mass and is described by the long range inverse square type Newtonian law of gravitation : $F = Gm_1m_2/R^2$ where m_1, m_2 are the two masses separated by R and $G(= 6.7 \times 10^{-11}$ SI units) is the gravitational constant. Subsequently, Einstein extended it to describe gravitational interaction in terms of *curvature of space*. This interaction is believed to be mediated through the quantum of interaction — *graviton* — which is yet to be discovered and provides a large attractive force between the planets producing the acceleration due to gravity in their vicinity. It is of extreme importance for astral bodies in galaxies and on cosmological scale since large masses and distances are involved.

The gravitational interaction however becomes inappreciable when the interaction of elementary particles, nuclei and atoms are considered and is totally left out.

2. Electromagnetic interactions — This interaction is much stronger than gravitational one and is described by long range inverse square type law : Coulomb's law. It is due to the charges of particles and their motion. In quantum field theory, it is visualised as an *exchange of virtual photons* which are the quanta of the field. This type of interactions occur in the chemical behaviour of atoms and molecules, Rutherford's scattering etc.

3. Weak interactions — The third fundamental interaction, weak nuclear interaction, takes place in the nuclear characteristic time $\sim 10^{-6}$ to 10^{-10}s. The

Scanned with CamScanner

β-decay of radioactive nuclei and weak decays of strange particles are typical of weak interactions. Unlike the previous two interactions, weak interaction is a very *short range force* and is *mediated through bosons named* $W^{\pm}$ *and* Z^0 discovered rather recently by Arnison et al. The intrinsic strength of weak interaction is 10^{-10} times that of electromagnetic interaction.

In weak interactions, the *parity is not conserved* and this violation of parity *distinguishes* weak interaction from other fundamental interactions. The important development in the study of this interaction is the *unification* of weak and electromagnetic interaction into the *electro-weak interaction*.

4. Strong interaction — This is the *strongest force* in nature and occurs between a neutron and a proton, or a neutron and a neutron, or a proton and a proton. This is a *short range* ($\sim 10^{-14} - 10^{-15}$ m) *attractive force, charge-independent* and is mediated through the *exchange of* π*-mesons* (π^+, π^-, π^0) which are the quantum of internucleon field. It has got a relative magnitude of strength of about 10^{13} times that of weak interactions involving time of interaction $\sim 10^{-23}$s. It explains *strong nuclear interactions between hadrons*.

Since protons, neutrons, π-mesons are thought to be built up of more fundamental, entities—*quarks*—the strong interaction is believed to be mediated through the exchange of another particle called *gluons* (massless quanta of spin $\hbar$) between the quarks. Neither gluons nor quarks have been observed in free state.

In Table 11.1 are given the relative strengths and other properties of different fundamental interactions.

Table 11.1 : *Different fundamental interactions*

Interaction	Relative strength	Range	Characteristic time	Mediators
Strong	1	10^{-15} m	10^{-23}s	Pions (or gluons)
Electromagnetic	$\sim 10^{-3}$	long range	10^{-20}s	Photons
Weak nuclear	$\sim 10^{-13}$	10^{-18} m	10^{-10}s	$W^{\pm}, Z^0$ bosons
Gravitational	$\sim 10^{-40}$	long range	10^{16}s	Gravitons

The four known fundamental interactions are illustrated in Fig. 11.1.

• The fundamental interactions are characterised by the value of a *characteristic dimensionless constant* related through a coupling constant to the interaction cross-section and interaction time. Stronger the interaction, larger is the cross-section and shorter the interaction time. For gravitation, the dimensionless constant is $Gm_p m_p/\hbar c \simeq 6 \times 10^{-39}$; for electromagnetic interaction, it is $\alpha = e^2/4\pi\varepsilon_0 \hbar c \simeq 1/137$, the *fine structure constant*; for weak interaction, it is $g_w^2/\hbar c = G_F m_p^2 c/\hbar^3 \simeq 10^{-5}$ where G_F is *Fermi coupling constant* of β-decay, etc.

• The properties of strong nuclear force manifest in building up complex nuclei, but a quantitative connection between nuclear structure and nuclear force is yet to be fully

understood. An important method of studying the characteristics of strong nuclear force is to study the properties of *hypernuclei*, where a nucleon in a nucleus is replaced by a hyperon.

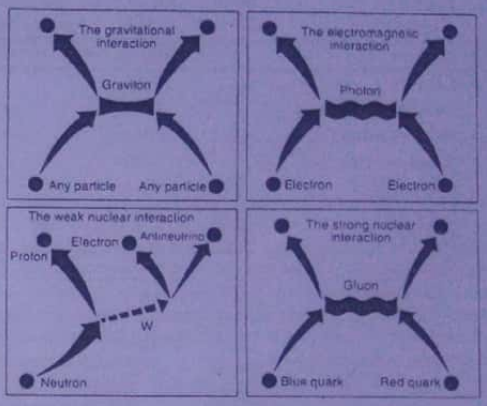

Fig. 11.1 Four fundamental interactions

11.7 Classification of elementary particles

The discovery of various *elementary particles* was followed by an extensive study of their characteristic properties. This led to the determination of their mass, charge, life-time, quantum numbers, decay schemes, interactions etc.

The elementary particles may be *classified* in a number of different ways depending on their masses, interactions, statistics etc. Commonly however they are mainly classified into *three* broad classes, namely

(i) the **photons**,

(ii) the **leptons** and

(iii) the **hadrons**.

Hadrons, again, are further classified into two groups, namely (a) mesons and (b) baryons. Baryons, again, are further subdivided into (i) nucleons and (ii) hyperons. The following table, Table 11.2, shows the basic properties of most of the common elementary particles.

Scanned with CamScanner

Table 11.2 : *Some elementary particles and their properties*

Particle (Symbol)	Mass (MeV/c^2)	Mean life (sec)	Charge (in units of proton charge)	Spin ($\hbar$)
1. Photon (γ)	0	Stable	0	1
2. Leptons				
Electron-neutrino (ν_e)	0	Stable	0	$\frac{1}{2}$
Muon-neutrino (ν_μ)	0	Stable	0	$\frac{1}{2}$
Tauon-neutrino (ν_τ)	0	Stable	0	$\frac{1}{2}$
Electron (e^-)	0.51	Stable	−1	$\frac{1}{2}$
Muon (μ^-)	105.66	2.2×10^{-6}	−1	$\frac{1}{2}$
Tauon (τ^-)	1784.2	—	−1	$\frac{1}{2}$
3. Hadrons				
3.1 Mesons				
π^+	139.57	2.60×10^{-8}	+1	0
π^-	139.57	2.60×10^{-8}	−1	0
π^0	134.96	0.83×10^{-16}	0	0
K^+	493.67	1.24×10^{-8}	+1	0
K^-	493.67	1.24×10^{-8}	−1	0
K^0	497.67	—	0	0
η^0	548.8	$< 10^{-18}$	0	0
3.2 Baryons				
3.2.1 Nucleons				
Proton (p)	938.28	Stable	1	$\frac{1}{2}$
Neutron (n)	939.57	640	0	$\frac{1}{2}$
3.2.2 Hyperons				
Lambda (Λ^0)	1115.60	2.63×10^{-10}	0	$\frac{1}{2}$
Sigma (Σ^+)	1189.36	0.80×10^{-10}	+1	$\frac{1}{2}$
Sigma (Σ^0)	1192.46	5.8×10^{-20}	0	$\frac{1}{2}$
Sigma (Σ^-)	1197.34	1.48×10^{-10}	−1	$\frac{1}{2}$
Xi (Ξ^0)	1314.9	2.90×10^{-10}	0	$\frac{1}{2}$
Xi (Ξ^-)	1321.32	1.64×10^{-10}	−1	$\frac{1}{2}$

1. **Photons** — It represents a *quantum of radiation* that travels with the velocity of light and possesses an energy $h\nu$, where h is Planck's constant and ν the frequency of radiation. Photon is *stable* and *neutral* having *no rest mass* and *no rest energy*, but possesses, by virtue of its motion, a *mass* $h\nu/c^2$. Its spin is 1 and is thus a *boson*.

2. **Leptons** — Leptons are *weakly interacting* particles. Charged leptons also show *electromagnetic interaction*. There are up to now *twelve* leptons : *electron* (e^-), *positron* (e^+), pair of *muons* (μ^+, μ^-), pair of *tauons* (τ^+, τ^-) and *three neutrinos* : electron-neutrino (ν_e), muon-neutrino (ν_μ) and tauon neutrino (ν_τ) and their antiparticles (antineutrinos : $\bar{\nu}_e, \bar{\nu}_\mu$ and $\bar{\nu}_\tau$).

Leptons appear to have *no internal structure* and are *point particles*.

Electrons, the first of the elementary particles discovered, are *negatively charged*, *stable*, having a *rest mass* 9.11×10^{-31} kg and a *rest energy* 0.511 MeV/c^2. It is a *spin* $\frac{1}{2}$ particle. *Positron* is an antiparticle of electron and hence is also called *positive electron*.

Muons were first observed in cosmic radiation and have a *mass* of about 200m$_e$. Muons are also *spin* $\frac{1}{2}$ particles.

Tauons have comparatively recently been discovered, having a *large mass* (1784.2 MeV/c^2)—*heavier than nucleons*. They are *unstable* and decay into muons and two *neutrinos*.

$$\tau^- \rightarrow \mu^- + \bar{\nu}_\mu + \nu_\tau$$

Neutrinos were first discovered in β-emission, and thereafter other neutrinos were obtained in other nuclear reactions.

All *neutrinos are stable*, having *zero charge*, *spin* $\frac{1}{2}$ and *negligible* (or zero) mass.

All the *leptons interact weakly with other particles* and they are all *fermions* as they obey Fermi-Dirac statistics.

3. **Hadrons** — Particles which are subject to strong nuclear interaction are called *hadrons*. They are sub-divided into (a) **mesons** and (b) **baryons**.

(a) **Mesons** – These particles are *strongly interacting* and include *pions* ($\pi^{\pm,0}$), *Kaons* ($K^{\pm,0}$) and *η-meson* (η^0), all having *having masses between that of a pion and a nucleon*. Subsequently, two more were added to the list—*charmed mesons* ($D^{\pm,0}$) and *beautiful mesons* ($B^{\pm,0}$), which are *heavier than nucleons*.

Pions that can exist as positively and negatively charged or neutral particles have *zero spin* and are responsible for *short-range nuclear forces*.

K-mesons or *Kaons* are produced due to interactions of high energy particles and very short range due to strong nuclear forces. The η^0 exists as a *neutral particle* which has a *very short life time*.

• Of the mesons, Kaons are *strange particles*, but the rest are non-strange. The neutral pion and η^0 decay by *electromagnetic interactions*, while the rest undergo weak *decay*. All mesons have *zero spin* and *odd parity* and are *bosons*.

(b) **Baryons** — Hadrons of half-integer spins are called *baryons*. Baryons have *rest mass* intermediate *between that of a nucleon and a deuteron*. These include the *nucleons*—*protons* and *neutrons*—and the *hyperons* that include *lambda* (Λ^0), *sigmas* ($\Sigma^{\pm,0}$), *Xi's* ($\Xi^{-,0}$) and *omega* (Ω^-) particles, and their antiparticles.

Scanned with CamScanner

Proton is *stable* (?), a free neutron is *unstable* with a mean life of 640s and *decays* into a *proton*, an *electron* and an *electron-antineutrino*.

Hyperons are *strange particles*, *unstable* and were first discovered in cosmic rays.

Baryons have *even parity* and they are *fermions* obeying the FD-statistics. It is believed that the total number of baryons in the universe is a conserved quantity.

11.8 Conservation laws

We are already familiar with a number of conservation laws such as conservation of energy, momentum, charge etc. that control the occurrence of all physical processes. In addition, certain other conservation laws are believed to hold in the realm of elementary-particle reactions to explain the non-occurrence of some processes even when they satisfy the usual well-known conservation laws. This would constitute our discussion that follows.

11.8.1 Exact laws

1. Energy conservation — The total energy, including the rest mass energy, is conserved in *any interaction*. This is related to the invariance of physical laws under translation along the time axis (homogeneity of time) implying that the laws of interaction are independent of the time of measurement.

To illustrate, consider the reaction : $\pi^- \rightarrow \mu^- + \bar{\nu}_\mu$.

If pion be initially at rest, its total energy $E_\pi = m_\pi c^2$ where m_π is its rest mass. Applying the law of conservation of energy,

$$m_\pi c^2 = E_\mu + E_\nu \tag{11.8.1}$$

where $E_\mu = \left(p_\mu^2 c^2 + m_\mu^2 c^4\right)^{1/2}$; $E_\nu = p_\nu c$, taking $m_\nu = 0$. (11.8.2)

• The energy-conservation is however limited by the *uncertainty principle*. There is an uncertainty of energy, $\Delta E = \hbar/\Delta t$, where Δt is the uncertainty of time.

2. Conservation of linear momentum — The total linear momentum is conserved for *all types of interactions*. This is related to the invariance of physical laws under translation in space (homogeneity of space) implying that the laws of interaction are independent of the place of measurement.

In the previous reaction, applying the law of conservation of linear momentum, we obtain

$$0 = p_\mu + p_\nu \tag{11.8.3}$$

where p_μ and p_ν are the momenta of μ^- and $\bar{\nu}_\mu$. Since the pion is assumed to be at rest, its initial momentum is zero.

$$\therefore \quad p_\mu = -p_\nu \tag{11.8.4}$$

• From the above two conservation laws, namely

$$\left.\begin{aligned} m_\pi c^2 &= \left(p_\mu^2 c^2 + m_\mu^2 c^4\right)^{1/2} + p_\nu c \\ \text{and} \quad p_\mu &= -p_\nu \end{aligned}\right\}$$

one can easily show, on simplification, that

$$E_\nu = \frac{(m_\pi^2 - m_\mu^2)c^2}{2m_\pi} \tag{11.8.5}$$

$$\text{and} \quad E_\mu = \frac{(m_\pi^2 + m_\mu^2)c^2}{2m_\pi}. \tag{11.8.6}$$

3. Conservation of angular momentum — This is also valid for *all types of interaction* and, according to it, if an isolated system is in a definite state of angular momentum, its initial angular momentum is the same as the final angular momentum. This is related to the invariance of physical laws under rotation (*isotropy* of space).

The angular momentum of a particle is the sum of its orbital angular momentum and spin angular momentum. One should note that the total angular momentum is conserved, but the orbital and spin angular momentum *may not be separately conserved*.

4. Conservation of charge — The net electric charge is conserved for *all the interactions*. This is related to the gauge invariance of electromagnetic field.

Let us give some examples.

(a) Decay of a free neutron : $n \rightarrow p^+ + e^- + \nu_e$.

(b) Decay of an isolated pion : $\pi^- \rightarrow \mu^- + \bar{\nu}_\mu$

$\pi^+ \rightarrow e^+ + \bar{\nu}_e$

$\pi^- \rightarrow \pi^0 + e^- + \nu_e$

In all the above reactions, the total initial charge is equal to the total final charge.

• If one considers the decay of electron into photons and neutrinos (say), then it would violate the law of conservation of charge. Electron being the *lightest charged particle*, the conservation of charge implies that the **electron must be a stable particle**.

5. Conservation of baryon number — The baryonic charge or the baryon number is an *additive* quantum number. All *baryons* ($p, n, \Lambda^0, \Sigma^+, \Sigma^0, \Sigma^-, \Xi^-, \Xi^0$) are assigned a *baryon quantum number* $B = +1$. *Antibaryons* ($\bar{p}, \bar{n}, \bar{\Lambda}^0, \bar{\Sigma}^+, \bar{\Sigma}^-, \bar{\Xi}^-, \bar{\Xi}^0$) are assigned a baryon quantum number $B = -1$, while the *non-baryons* (photon, leptons and mesons) are assigned a baryon number $B = 0$.

Since the baryon number is an additive quantum number, *the baryon number of a set of particles is the sum of the baryon number of each particle in the set.*

According to this law of conservation, in *any reaction* the initial baryon number is the same as the final baryon number. So, the total number of baryons and antibaryons should remain constant for all the interactions.

Scanned with CamScanner

So, by conservation of strangeness, the reactions (a) and (b) are *allowed*, but (c) is *forbidden*. The reaction (c) might have occurred through weak interaction, but it also violates the selection rule, since $\Delta S = -2$.

Consider the decay of Λ^0. The decay schemes are :

$$\Lambda^0 \rightarrow p + K^-$$
$$\rightarrow n + K^0$$

In each case, the *strangeness* is *conserved*, but *energy* is *not*. The sum of the rest masses of p and K^- is larger than the rest mass of Λ^0. The decay can occur through weak interaction where strangeness *need not* be conserved. The following decay schemes are the possible ones.

$$\Lambda^0 \rightarrow p + \pi^- \quad (\Delta S = -1)$$
$$\rightarrow n + \pi^0 \quad (\Delta S = -1)$$

Other examples of weak decay of semi-stable strange particles obeying the selection rules are :

$$\Sigma^0 \rightarrow \Lambda^0 + \gamma \quad (\Delta S = 0)$$
$$\Xi^0 \rightarrow \Lambda^0 + \pi^0 \quad (\Delta S = +1)$$
$$\Omega^- \rightarrow \Lambda^0 + K^- \quad (\Delta S = +1)$$
$$\Sigma^+ \rightarrow p + \pi^0 \quad (\Delta S = +1)$$

4. Parity — This was discussed earlier in Chapter : *Constituents and General properties of nuclei* and may be consulted again.

Parity is a purely quantum mechanical concept having no classical analogue. It refers to an inherent property that has to do with the *right-handed* and the *left-handedness* in natural phenomena.

When particles like neutrinos are emitted during β-decay, they show a preferred spin direction. If the spin is in the direction at which a *right-handed* screw advances, it is said to possess a *helicity* $+1$; if the spin is in the direction of a *left-handed* screw, the *helicity* is -1 (Fig. 11.4)). As the parity P is related to the spin J, the two quantum numbers are generally combined and is symbolised by J^P. So, $\frac{1}{2}^+$ means $J = \frac{1}{2}$ and

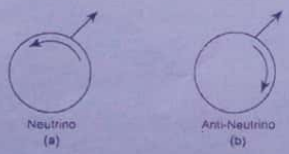

Fig. 11.4 Helicity of neutrino and antineutrino

$P = +1$ (even); $\frac{1}{2}^-$ indicates $J = \frac{1}{2}$, $P = -1$ (odd). Since parity can only be ± 1, the $\pm$ sign over J on the right uniquely determines P.

In *strong nuclear and electromagnetic interactions*, **parity is conserved** but it is *violated in weak interaction*. Since parity is conserved in strong and electromagnetic interactions, it is a good quantum number and an energy eigenstate is also an eigenstate of parity. Non-conservation of parity in weak interaction leads to *charge conjugation*.

5. Charge conjugation — *Charge conjugation means reversal of the signs of all types of charge — electric, baryonic and leptonic — of the particles* (Fig. 11.5). If a physical law holding for a particle also holds for the corresponding antiparticle, then the principle of charge conjugation is said to be valid.

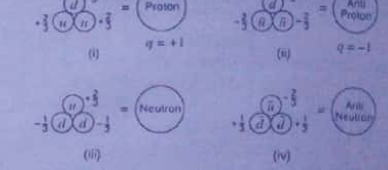

Fig. 11.5 Formation of proton, antiproton and neutron, antineutron by charge conjugation

Consider the following two reactions :

1. $p + \pi^- \rightarrow \Sigma^- + K^+$
2. $\bar{p} + \pi^- \rightarrow \bar{\Sigma}^- + K^+$

where, in the second reaction, all the particles of the first reaction are replaced by their antiparticles. *The principle of charge conjugation implies that the cross-section of both the reactions at a given energy must be the same.*

Charge conjugation applies *not only to charged particles but also to neutral particles*. For instance, neutrino is electrically neutral but its antiparticle anti-neutrino is different from neutrino; their leptonic charges are equal but opposite so that they would interact differently with matter.

But particles like π^0, photons etc. have all their charges zero ($Q = 0$, $B = 0$, $L = 0$) and must therefore be identical with their antiparticles. They are **self-conjugate** and *truly neutral*.

Strong and electromagnetic interactions are invariant under charge conjugation (C)-operation. But the *weak interaction* like β-decay *does not* obey charge conjugation.

• Charge conjugation invariance implies that an event that occurs in *real world* will also occur exactly in the same way in an *anti-world*.

6. Time reversal (T) — The operation T, i.e., *time-reversal* means replacing the time t by $-t$ in all equations of motion, i.e., reflection of time axis at the origin of

Scanned with CamScanner

time coordinate in relativistic space-time continuum. It is thus, like parity operation, a discrete change.

T-operation consists in reversing the signs of momenta ($\vec{p} = d\vec{r}/dt$) and angular momenta ($\vec{L} = \vec{r} \times \vec{p}$). T also transforms the wave function to its *complex conjugate*. If T is conserved i.e., time-reversal invariance occurs, then reversed equation of motion is also a valid equation of motion of the system concerned. All the known fundamental equations of motion are invariant in time-reversal.

Strong and electromagnetic interactions are invariant under time-reversal transformation, but the weak interaction is not.

• One may note that many macroscopic laws do not conform to time-reversal invariance. For instance, the flow of heat from a hot body to a cold one.

11.9 CPT-theorem

This is till now an *exact conservation law*. The CPT-theorem, also called Lüders-Pauli theorem, states that *all interactions in nature are invariant under the joint operations of charge conjugation* (C), *inversion of space coordinates at origin*, i.e., *parity operation* (P) *and the reversal of time* (T). The orders of the three operations are immaterial.

The invariance of CPT-transformation implies that if an interaction is not invariant under any one of the C, P or T-operations, its effect must get *compensated* by the joint effect of the other two.

All evidences so far point to the universal validity of the theorem. But the discovery of a small but definite violation of CP-invarience by Chistensen et al. has opened up the question of the universal validity of CPT-theorem, for if time-reversal invariance holds, then CPT theorem dictates that CP-invariance must also hold. The CPT-violation, if any, can probably be observed in the properties of K^0 and $\bar{K}^0$ mesons.

11.10 Antiparticles : Antinucleon

The existence of an antiparticle was predicted by Dirac in his relativistic quantum mechanical theory of electron. Later, as predicted, antielectron or positron was discovered in cosmic rays (Chapter 10).

The charge conjugation operation C on the wave function of a particle generates its antiparticle. So, all elementary particles existing in nature have their corresponding antiparticles, usually represented by a bar over the symbol.

Definition : *An antiparticle may be defined as a particle having identical mass, spin, decay life time (if unstable) and isospin, but its charge* (if any), *although equal, has opposite sign. The magnetic moment and I_3 also have the same value, but opposite to those of the associated particle.*

The well-known pairs of particle and antiparticle are : (electron e^-, positron e^+), (π^+ and π^- mesons), (proton p, antiproton $\bar{p}$), (neutron n and antineutron $\bar{n}$) and (neutrino ν and antineutrino $\bar{\nu}$).

There are *self-conjugate* particles such as photon (γ^0 particle), neutral pion (π^0) and neutral η-meson (η^0). They act both as particle and their antiparticle.

When a particle combines with its antiparticle, the pair is *annihilated* and an equivalent amount of energy is released in the form of two or more photons :

$$2m_0c^2 + K_+ + K_- = h\nu_1 + h\nu_2 \qquad (11.10.1)$$

where m_0 is the rest mass of the particle (and also of antiparticle), K's their initial kinetic energies and ν's the frequencies of the liberated photons.

In the annihilation process, the total linear momentum is also conserved :

$$m_0\vec{v}_+ + m_0\vec{v}_- = \hbar\vec{k}_1 + \hbar\vec{k}_2 \qquad (11.10.2)$$

where $\vec{v}$'s are the velocity vectors of the particle and the antiparticle and $\vec{k}$'s the propagation constants of the photons related to the corresponding wavelength as

$$\lambda_1 = 2\pi/|\vec{k}_1|; \quad \lambda_2 = 2\pi/|\vec{k}_2| \qquad (11.10.3)$$

In the annihilation of electron-positron pair (both initially at rest) two photons, each of energy 0.511 MeV and wavelength 0.0121 Å are released. Similarly, when a proton and antiproton pair (at rest) combine, two photons each of wavelength 6.61×10^{-9} Å are released.

Discovery of antiproton — The first antinucleon discovered was antiproton in 1956 by Segre and co-workers. As in electron-positron pair production, it was calculated that a γ-ray photon of energy 1850 MeV may produce a proton-antiproton pair. But until 1955, such high energy was only available in cosmic rays. After the commissioning of Bevatron at Berkley, 6.2 BeV protons were available. Since protons and antiprotons are strongly interacting particles, they can produce hadron-antihadron pair by their mutual annihilation. Conversely, p–p collisions at high energies may produce a p-$\bar{p}$ pair. Segre and co-workers, with this idea, bombarded a copper target with 6.2 BeV protons to successfully obtain antiprotons according to the following scheme :

$$p + p \rightarrow p + p + (p + \bar{p})$$

Experimental set-up — The experimental set-up of Chamberlain is shown schematically in Fig. 11.6. A beam of high energy (6.2 BeV) protons from the Bevatron are incident on copper target T. Antiprotons are produced by collisions of incoming protons and the target-protons, according to the above scheme. As the antiprotons are negatively charged, they follow paths having opposite curvature relative to protons in the Bevatron magnetic field and come out of the target, along with negative pions produced in the process.

Scanned with CamScanner

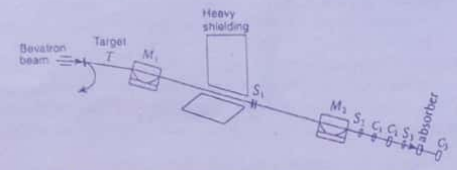

Fig. 11.6 Experimental set-up (schematic) for detection of antiproton

The magnets M_1, M_2 select the particles of a definite momentum to pass through an aperture in the heavy shielding. The speed of pions was of 0.99c while that of antiproton 0.79c. S_1, S_2, S_3 are scintillation counters and C_1, C_2 are two Cerenkov counters. While C_1 detects particles of speed > 0.79c, C_2 detects particles of speed between 0.75c and 0.79c so that only antiprotons are detected by C_2.

The distance between S_1 and S_2 was 12 m and hence the time of flight for pions was 40 ns, while for antiprotons it was 51 ns. S_1, S_2, S_3 and C_2 were *in coincidence* while C_1 *in anticoincidence*. Thus pions, as detected by C_1, produced no coincidence pulse and the arrangement could detect only antiprotons by coincidence. The coincidence pulses were recorded and they provided definite indication for the production of antiproton.

Discovery of antineutron — Cork and co-workers discovered antineutrons, also in 1956. Their experimental set-up is illustrated in Fig. 11.7.

An antiproton beam produced in a Be-target by 6.2 BeV proton beam from the Berkley Bevatron was allowed to enter, *via* the first scintillator S_1, into a large liquid scintillator (LS), scanned by four photomultipliers (P's). S_1 detected the antiproton

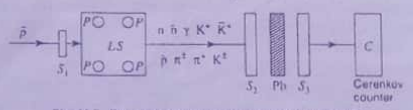

Fig. 11.7 Experimental set-up for detection of antineutron

beam to ensure its proper course. In LS, the antiprotons were *either* (i) annihilated by protons to produce a host of pions and kaons and γ-photons releasing an energy of 1.88 GeV, *or* (ii) produced antineutrons by the charge-exchange reaction :

$$p + \bar{p} \rightarrow \bar{n} + n$$

The photomultiplier in LS registered the strong annihilation pulse of size corresponding to an energy release < 50 MeV. S_2, S_3 are two other scintillation counters that sandwich a lead block Pb and C is a Cerenkov counter. S_2 detects the charged particles produced by annihilation of p in LS, while S_3 detects the associated γ-rays released in the process and converted into charged particles in Pb.

The antineutrons enter C and annihilate. The annihilation pulses in C, without any accompaniment of pulses from S_2, S_3 or large pulses from LS, correspond to antineutrons.

Properties of antiproton and antineutron — The rest mass of antiproton was estimated experimentally by Segre to be $(1824 \pm 51)m_e$, and was equal to that of proton. Its charge is also equal to that of proton but is negative. It is confirmed by the annihilation of proton-antiproton pair. Like the proton, the antiproton is stable and has been used for experiments such as the production of W^+ and Z^0 vector bosons, in p–$\bar{p}$ collider rings.

The $\bar{p}$ and $\bar{n}$ have baryon number, $B = -1$, spin $s = -\frac{1}{2}$ and parity $P = -1$. The mean life for $\bar{n}$ is the same as that of n, the decay scheme being

$$\bar{n} \rightarrow \bar{p} + e^+ + \nu_{e^+}$$

Like n–p doublet, $\bar{n}$ and $\bar{p}$ form an isospin-doublet, so that $I = \frac{1}{2}$ each, but $I_3 = +\frac{1}{2}$ and $-\frac{1}{2}$ respectively, being just the opposite of the corresponding particles.

• ***If a particle is stable, its antiparticle is also stable and conversely.*** Since every particle has an antiparticle, atoms and molecules can be built up out of antiparticles, e.g., ordinary H-atom has a proton in the nucleus and an extranuclear electron. If the proton is replaced by an *antiproton* and the electron by a *positron*, we get what may be called an atom of *antihydrogen*. This has led to the speculation as to the existence of an *anti-world* and the situation in case *world* and *anti-world* come together.

11.11 Resonance particles

So far we have seen that elementary particles are either stable or quasi-stable decaying *via* weak or electromagnetic interacton with mean lives long compared to the *characteristic nuclear time*. The characteristic nuclear time is *defined as the time taken by a pion to travel past a proton* ($\sim 4 \times 10^{-24}$s). For example, neutral pion (π^0) has the shortest life-time of about 10^{-16}s. Particles have been discovered which have mean lives comparable to the characteristic nuclear time and they are called '*particle resonance*'.

The term 'resonance' comes from the fact that these particles are recognised by 'resonance peaks' in the graph showing the variation of cross-section (Fig. 11.8) of different types of events during high energy collisions at certain different energies. The mass of a resonance particle is obtained from the position of the peak, and the mean life from the width of the peak, using the uncertainty relation ($\Delta t = \hbar/\Delta E$).

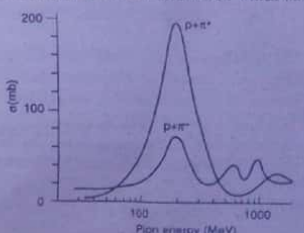

Fig. 11.8 Variation of cross section for pions colliding with protons as a function of energy

Scanned with CamScanner

Table 11.4 shows some resonance particles. They are produced by collisions of high energy hadrons from accelerators.

Table 11.4 : *Some resonance particles*

Family	Particle	Mass (MeV)	Hyper-charge Y	Isospin I	Spin & Parity J^P	Width Γ (MeV)	Principal decay modes
Meson	η	548	0	0	0^-	< 30	3π neutral
	ρ	755	0	1	1^-	120	2π
	ω	783	0	0	1^-	9	3π
	ϕ	1019	0	0	1^-	6	K^+K^-
	f_0	1250	0	0	2^+	75	2π
	K^*	891	+1	$\frac{1}{2}$	1^-	46	$K\pi$
	$K\bar{K}$	1410	0	0	1^+	60	$K\bar{K}\pi$
Nucleon	$N^*_{1/2}$	1512	1	$\frac{1}{2}$	$\frac{3}{2}^-$	125	$N\pi$, $N2\pi$
	$N^*_{1/2}$	1688	1	$\frac{1}{2}$	$\frac{5}{2}^+$	140	$N\pi$, $N2\pi$ and others
	$N^*_{1/2}$	2190	1	$\frac{1}{2}$	$\frac{9}{2}^+$	200	$N\pi$, $N2\pi$, ΣK
	$N^*_{3/2}$	1238	1	$\frac{3}{2}$	$\frac{3}{2}^+$	125	$N\pi$
	$N^*_{3/2}$	1920	1	$\frac{3}{2}$	$\frac{7}{2}^+$	~ 200	$N\pi$, ΣK
	$N^*_{3/2}$	2360	1	$\frac{3}{2}$	$\frac{11}{2}^+$	200	$N\pi$ and others
Hyperon	Y^*_0	1405	0	0	$\frac{1}{2}^-$	50	Σ^-, $\Lambda\, 2\pi$
	Y^*_0	1520	0	0	$\frac{3}{2}^-$	16.4	$\Sigma\pi$, $\bar{K}N$, $\Lambda\, 2\pi$ etc.
	Y^*_0	1815	0	0	$\frac{5}{2}^+$	120	$\Sigma\pi$, KN, $\Lambda 2\pi$
	Y^*_1	1385	0	1	$\frac{3}{2}^+$	47	$\Lambda\pi$, $\Sigma\pi$
	Y^*_1	1600	0	1	$\frac{1}{2}^-$	40	$\Sigma\pi$, $\pi\Lambda$, $\Sigma 2\pi$
	Y^*_1	1765	0	?	?	50	$\Lambda 2\pi$ etc. KN & others
	Ξ^*	1530	−1	—	$\frac{3}{2}^+$	< 7	$\Xi\pi$
	Ξ^*	1770	−1	$\frac{1}{2}$	?	< 80	$\Xi\pi$, $\Xi 2\pi$

11.11.1 Hyperfragment or hypernucleus

A *hyperfragment*, also called *hypernucleus*, is a metastable nucleus whose nucleons (p, n) get replaced by a hyperon. For instance, if one of the two neutrons of ${}^4_2$He be replaced by a Λ^0 (lambda hyperon), we get the hypernucleus ${}^4_\Lambda$He. In 1952, while working with cosmic rays using nuclear emulsion detector, Danysz and Pniewski discovered a hypernucleus ${}^8_\Lambda$Be. This discovery was immediately followed by a large number of other hyperfragments. Of these, one of the heaviest was ${}^{13}_\Lambda$C, obtained by exposing nuclear emission having oxygen nuclei to a beam of high energy K^- mesons. The relevant reaction is

$$K^- + {}^{16}_8\mathrm{O} \rightarrow {}^{13}_\Lambda\mathrm{C} + p + p + n + \pi^-$$

${}^{13}_\Lambda$C decays into nitrogen according to : ${}^{13}_\Lambda\mathrm{C} \rightarrow {}^{14}_7\mathrm{N} + \pi^-$, and from the observed kinetic energies of the particles, the binding energy of Λ^0 in ${}^{13}_\Lambda$C can be computed.

A hypernucleus may have several decay modes. For instance, ${}^4_\Lambda$He may decay as

$$\begin{aligned} {}^4_\Lambda\mathrm{He} &\rightarrow p + p + n + n + \pi^0 \quad (66.7\%) \\ &\rightarrow {}^3\mathrm{He} + p + \pi^- \quad (20\%) \\ &\rightarrow {}^2_1\mathrm{H} + p + n \quad (6.7\%) \\ &\rightarrow {}^2_1\mathrm{H} + {}^2_1\mathrm{H} \quad (20\%) \end{aligned}$$

with relative abundances shown in the bracket against each mode.

11.12 Symmetry classification of elementary particles

We shall give here only a brief reference to this symmetry classification. Any detailed discussion is beyond the scope of the book.

In 1962, M. Gell-Mann and Y. Ne'eman proposed independently an extension of the scheme of classification of elementary particles. The extension is based on the values of I_3 and the hypercharge $Y(= B + S)$ of the particles and is known as SU_3-*symmetry* or the Special Unitary Group of rank 3 symmetry. This is also called the **octet symmetry** or **eight-fold way**.

They proposed, in place of simple isotopic invariance as is assumed in SU_2, the existence of a group of eight baryons, namely $p, n, \Lambda, \Sigma^+, \Sigma^0, \Sigma^-, \Xi^-$, and Ξ^0 in a super-multiplet (octet) in SU_3-scheme. All these baryons have $J^p = \frac{1}{2}^+$. The different baryon groups differ in their values of either the isospin I or the strangeness number S or both. Their masses are also different but the mass-difference does not exceed 15%.

It was therefore assumed that the above eight baryons, formed as a result of a common but very strong interaction, have essentially equal masses (eight-fold degeneracy in strangeness and charge). The octet symmetry however is broken by a moderately strong and strangeness-dependent interaction. And this would remove the strangeness-degeneracy between the groups of different S-values. Again, in each group of a given S-value, the charge degeneracy is removed by the action of an electromagnetic interaction so that the components of same I but with different I_3-values have slightly different masses. The first splitting is of the order of $\Delta M/M \sim 10\%$ to 20%, while the second splitting is of the order of $\Delta M/M \sim 1\%$.

Scanned with CamScanner

This scheme of classification, based on **octet symmetry**, is better visualised if a graphical plot of the baryon octet in the I_3-Y plane is made. This is demonstrated in Fig. 11.9 and is called a *weight diagram*.

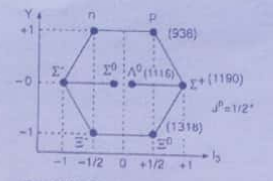

Fig. 11.9 Octet symmetry of baryons

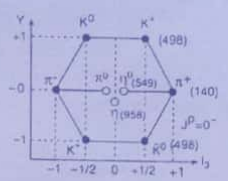

Fig. 11.10 Octet symmetry of mesons

The members of the octet family form a symmetric hexagon (Fig. 11.9) with one member (one baryon) at each corner and two at the centre. The plot shows that the two nucleons — p and n — with $S = 0$ and $I_3 = \pm\frac{1}{2}$ fall on the line $Y = 1$. The three Σ-hyperons with $S = -1$ and $I_3 = \pm 1, 0$ fall on the line $Y = 0$ and the two Ξ-hyperons with $S = -2$ and $I_3 = \pm 1, 0$ fall on the line $Y = -1$. Finally, the single Λ-hyperon with $S = -1$ and $I_3 = 0$ is at the centre of the hexagon, along with Σ^0-hyperon, with $Y = 0$.

A similar super-multiplet for **mesons** can also be arranged in a similar hexagon (Fig. 11.10). The members of this octet family consist of *two kaons* ($S = 1$) with $I_3 = \pm\frac{1}{2}$, the *three pions* ($S = 0$) with $I_3 = \pm 1, 0$, the two *antikaons* ($S = -1$) with $I_3 = \pm\frac{1}{2}$ and the isospin singlet η^0-*meson* ($I_3 = 0, Y = 0$). While the two kaons will be on the line $Y = 1$, the three pions on the line $Y = 0$, the two antikaons on the line $Y = -1$, the η^0 ($I_3 = 0$) is at the centre of the hexagon with $Y = 0$, along with π^0 ($I_3 = 0$). The resonance particle η (958) is also included which makes the *octet* essentially a *nonet*.

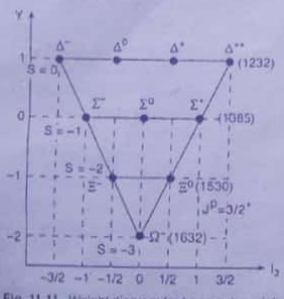

Fig. 11.11 Weight diagram for baryon decuplet

• Similar weight diagrams in Y-I_3 plane can be constructed for resonance particles.

• Apart from octet, the existence of a baryonic (resonance) **decuplet** was also predicted by SU_3-symmetry. Its weight diagram, as shown in Fig. 11.11, is an *equilateral triangle*. The decuplet comprises an isotopic quadruplet, a triplet, a doublet and a singlet. The quadruplet Δ have $S = 0$, $Y = 1$ and $I_3 = \frac{3}{2}, \frac{1}{2}, -\frac{1}{2}, -\frac{3}{2}$; the triplet Σ have $S = -1$, $Y = 0$ and $I_3 = 1, 0, -1$; the doublet Ξ with $S = -2$, $Y = -1$ and $I_3 = \pm\frac{1}{2}$ and the singlet Ω^- with $S = -3$, $Y = -2$ and $I_3 = 0$.

• It is interesting to note that when the prediction of the *decuplet* was made, the particle Ω^- was *not* discovered. The prediction came true only subsequently which

was considered as a triumph for the SU_3-symmetry. Even the properties of Ω^-, as predicted by SU_3-scheme, agreed and have been verified. The discovery of anti-omega ($\bar{\Omega}^-$) particle has also been made.

We shall however not go into the discovery of Ω^- hyperon and the various predictions of SU_3-symmetry. While some of the predictions came true, some were not satisfied, hinting at the fact that Unitary symmetry is much broader in scope than isotopic invariance, based on SU_3-symmetry.

11.13 Quark model

As mentioned earlier, attempts were being made to see if the elementary particles so far described can be understood in terms of still simpler or basic units of particles. One such attempt is the proposition of **Quark model** by Gell-Mann and Zweig in 1964. They analysed certain properties of baryons and mesons, in particular the symmetries involved in the interaction, and proposed the theory that hadrons are made up of still smaller particles called *quarks* each having a charge $\pm\frac{1}{3}$ or $\pm\frac{2}{3}$ of an electronic charge and is assigned specific quantum numbers. The word 'quark' was borrowed by Gell-Mann from an obscure line in a book by James Joyce. All quarks have spin $\frac{1}{2}$ and they are obviously fermions. According to this theory, baryons are composed of *three* quarks each, generated by suitable combinations of the three. Similarly, mesons are composed of appropriate combination of *two* quarks each. Symbolised by u, d and s, *three* different quarks were postulated with the designation '*up*', '*down*' and '*strange*'. For each of these three quarks again, there is also an antiparticle, called *antiquark*.

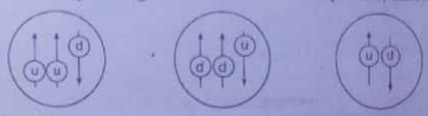

Fig. 11.12 The quark structure of (a) proton, (b) neutron and (c) positive pion

Later, two sub-nuclear particles were discovered that usually have large mass and long half-lives. These particles are named J/psi. Such particles could not be explained only with three quarks. Eventually, therefore, *three more* quarks were added to the list. These are called '*charm*' (c), '*bottom*' (b) and '*top*' (t), having additional quantum numbers. Table 11.5 gives six types of quarks and their antiparticles, with their charge in units of electronic charge, and mass in units of BeV/c^2.

According to the quark model, *mesons* consist of *one quark* and *another antiquark*, e.g. $\pi^+(u\bar{d})$, $K^+(u\bar{s})$, whereas baryons are made of *three quarks* e.g. $p(u\,u\,d)$, $n(u\,d\,d)$, $\Lambda^0(u\,d\,s)$, $\Sigma^0(u\,d\,s)$, $\Xi^-(d\,s\,s)$, $\Omega^-(s\,s\,s)$. A combination of leptons, and u and d quarks forms *stable* particles, while a combination of leptons and s and c quarks form *unstable* particles. In the quark model, there are only two types of particles – *leptons* and *quarks*.

The quark structures of the proton, the neutron and π^+ are shown in Fig. 11.12. The arrows indicate the spins.

Scanned with CamScanner

Table 11.5 : *List of quarks and antiquarks*

Quark	Symbol	Antiquark	Charge	Mass	Strangeness number
1. Down	d	$\bar{d}$	$-\frac{1}{3}e$	Small	0
2. Up	u	$\bar{u}$	$+\frac{2}{3}e$	Small	0
3. Strange	s	$\bar{s}$	$-\frac{1}{3}e$	$0.3\,\text{BeV}/c^2$	-1
4. Charm	c	$\bar{c}$	$+\frac{2}{3}e$	$1.5\,\text{BeV}/c^2$	0
5. Bottom	b	$\bar{b}$	$-\frac{1}{3}e$	$5.2\,\text{BeV}/c^2$	0
6. Top	t	$\bar{t}$	$+\frac{2}{3}e$	$\geq 40\,\text{BeV}/c^2$	0

• The combination of quarks to form mesons and baryons involves a *serious problem* of violation of Pauli's exclusion principle as similar kind of quarks with identical quantum numbers are present in the same particle. Examples are $n(udd)$, $p(uud)$, $\Xi^-(dss)$ etc. To avoid the violation of the exclusion principle, each of six types of quarks are given three distinct colours (flavours) as red, blue and green. Of course, these colours have nothing to do with real colours. This yields 18 types of quarks and 18 types of antiquarks. The similar quarks in a hadron are with different flavours so that the exclusion principle is not violated.

• The quark model derives experimental support from the strong processes in π–N scattering, the electromagnetic process of annihilation of electron-positron pair in hadron and the weak process in the β-decay of neutron. The most convincing support of the model is obtained from the observations on inelastic scattering of high energy electrons by protons.

Table 11.6 shows the quark content of some of the baryons and the mesons.

Table 11.6 : *Quark content of some baryons and mesons*

Baryons (*spin* $\frac{1}{2}$)		Mesons	
Name (symbol)	Quark content	Name (symbol)	Quark content
$N\begin{cases} p \\ n \end{cases}$	uud udd	$\Pi^{\pm}$	$u\bar{d}$, $d\bar{u}$
		Π^0	$u\bar{u}$
Λ	uds	$K^{\pm}$	$u\bar{s}$, $s\bar{u}$
Σ^+	uus	K^0, $\bar{K}^0$	$d\bar{s}$, $s\bar{d}$
Σ^0	uds	$D^{\pm}$	$c\bar{d}$, $d\bar{c}$
Σ^-	dds	D^0, $\bar{D}^0$	$c\bar{u}$, $u\bar{c}$
Ξ^0	uss	$B^{\pm}$	$u\bar{b}$, $b\bar{u}$
Ξ^-	dss	B^0, $\bar{B}^0$	$d\bar{b}$, $b\bar{d}$
Λ_c^+	udc		
Ω^-	sss		

In conformity with the terminology of colour of visible light, the three colours of antiquarks are 'cyan', 'yellow' and 'magenta'. The carrier between the quarks is the *gluon*. Exchange of colour between quarks by gluons provides the binding force between quarks within a hadron (proton, neutron etc.). It is believed that the gluon-grip between the quarks increases rather than decreases with distance and this is the reason why the present accelerators have not been able to isolate quark.

In spite of the best, concerted and world-wide efforts, quarks are yet to be observed in free state. It is almost impossible for quarks to exist as *independent* entities outside hadrons (mesons and baryons). They have *neither* been seen *independently* as they are trapped inside larger particles, *nor* their *charges* have been *confirmed* conclusively. It is estimated that their abundance is $\sim 10^{-27}$ in air, $\sim 10^{-17}$ in meteorites and 10^{-33} in sea water. These are too low abundances to be observed experimentally. Recently, Friendman, Kendall and Taylor have shown the possibility of the existence of quarks in an indirect experiment. They concluded from *electron scattering* that traces of quarks were observed from the scattering of energetic electrons by protons and neutrons. Protons have been shown, with sub-atomic projectiles, to consist of point-like entities similar to quarks linked by gluons. This indicates the possible presence of quarks acting as inelastic scattering centres present in the centre of neutrons.

11.14 Unification of interactions

Particle physicists have been making a conscious effort to unify the four fundamental interactions—the so-called *gauge interactions*—since long. The credit of the first attempt at unification of interactions goes to Maxwell who successfully unified electric and magnetic interactions into a single electromagnetic interaction. This is the story of the nineteenth century. Einstein's attempt to unify gravitational and electromagnetic interaction was unfortunately a failure.

In 1967 Weinberg and Salam developed a unified theory that combined the weak and electromagnetic interactions through intermediate particles called *bosons*. There are *three bosons* : W^+, W^- and Z^0 associated with *three* weak interaction fields. These bosons are fundamental particles transmitting forces produced in interactions and possess finite masses. While W^+ and W^- are charged bosons, Z^0 is neutral with mass $92.2 \pm 1.6\,\text{BeV}/c^2$. The interactions between leptons, electromagnetic and weak fields are unified into the above *electro-weak theory*. The predictions made by this theory is well-confirmed by experiments. It thus establishes that weak and electromagnetic forces are manifestations of one and the same effect.

The strong interaction between quarks is supposed to be due to exchange of eight types of particles. These particles, as already mentioned, are called *gluons*. The neutral gluons have zero rest mass and the strong force between quarks are carried through them. We have seen that weak interaction is produced by W^+, W^- and Z^0, and the photons act as intermediate particles for electromagnetic interaction. On the validity

Scanned with CamScanner